

# Chemical Synthesis to Understand and Influence Biological Systems: Spin Labels, Drug Development, and Biosynthetic Investigations

by

Wayne Vuong

A thesis submitted in partial fulfillment of the requirements for the degree of

Doctor of Philosophy

Department of Chemistry

University of Alberta

© Wayne Vuong, 2022

# Abstract

Spin labels are a useful tool towards the study of protein conformation and enable the mapping of interactions between specific positions within these systems. Synthetic routes towards three different chiral spin-labelled amino acids have been developed. Compared to commercially available spin labelled amino acids, these compounds better replicate the structures found in canonical amino acids. One of the routes involves direct alkylation of an electrophile onto a chiral glycinate, thereby generating the desired natural stereochemistry at the  $\alpha$ -position of the resultant amino acid. The other two routes involve a racemic bond formation reaction between the side chain electrophile and an appropriately protected glycinate nucleophile. This was then followed up with deracemization via dynamic kinetic resolution. While enantioselectivity was not perfect, we demonstrated that two of the three structures produced can be further enantiopurified using D-amino acid oxidase, affording a product with high stereochemical purity as verified through Marfey's assay. Overall, these novel structures aim to be amenable towards incorporation into peptides or proteins through solid phase peptide synthesis or metabolic incorporation via amber codon suppression.

A feline drug, GC376, that originally targets the feline coronavirus FCoV was demonstrated to hold potential as a COVID-19 therapeutic. It was shown to possess nanomolar activity against the main protease of SARS-CoV-2 as well as the original SARS-CoV, exhibiting inhibition in enzymatic assays as well as reducing viral titers in mammalian cells. This inhibitor works by binding to and inhibiting the activity of a catalytic Cys145 in the active site of the main protease, thereby halting its activity as was verified through X-ray crystal structures as well as  $^{13}\text{C}$ -labelled NMR studies. The bisulfite adduct prodrug forms

of these compounds showed greater activity, likely owing to improved solubility in aqueous media.

With the demonstrated activity of GC376 against SARS-CoV-2, improved inhibitors based on this structure were developed. The development of these new inhibitors were concurrently guided by enzymatic assays, mammalian cell assays, and crystallography. This culminated in an SAR study demonstrating that polar groups in the P3 position of the inhibitor or the presence of a nearby chiral methyl group can promote an alternative mode of binding wherein the P3 position (Figure 3.3) preferentially docks in the deeper S4 position of the enzyme (Figure 3.14a), thereby resulting in improved protease inhibition. Studies on the stereochemical characteristics of GC373 and GC376 were also conducted, demonstrating that:

1. Epimerization of the  $\alpha$ -position readily occurs in aqueous media.
2. GC373 exists as a single enantiomer in aprotic solvents but as a mixture of two diastereomers in aqueous media.
3. GC376 exists as a mixture of four diastereomers, and the associated diastereomeric ratios of these species were determined.

Additionally, it was demonstrated that these bisulfite adducts undergo aggregation and appear to form micelles at sufficiently high concentrations, potentiating delivery of these compounds as micellar solutions. Finally, cation replacement of GC376 was demonstrated to significantly increase solubility; up to 90% when a sodium ion is replaced with a choline.

An improved synthetic route to access a building block used to incorporate a  $\gamma$ -lactam ring in numerous antivirals was developed. The improved synthesis of this  $\gamma$ -lactam glutamine analog is scalable, inexpensive, and more than doubles yields when compared to the original synthesis developed by Pfizer. Furthermore, purification is simple, requiring only a quick silica plug in a majority of reactions.

In a tangential direction, work was directed towards overcoming metabolic issues with P450 oxidation. Based on reports of oxidation occurring on the  $\gamma$ -lactam ring of nirmaltrevir

in Paxlovid, it was anticipated that similar reactions would occur with GC376 as well. Attempts were made to replace the metabolically susceptible  $\text{CH}_2$  in the ring with an oxygen, with work in this area still ongoing.

Efforts were also directed towards understanding the biosynthetic programming of polyketide synthases. To test the theory that regulation is a function of reaction kinetics, a series of polyketide substrates and product standards were synthesized. Work is currently ongoing with expression of the polyketide domains required to do kinetic assays.

# Preface

Chapter 2 has been published as Vuong, W.; Mosquera-Guagua, F.; Sanichar, R.; McDonald, T.R.; Ernst, O.P.; Wang, L.; Vederas, J.C. Synthesis of Chiral Spin-Labeled Amino Acids. *Org. Lett.* 21, 10149-10153 (2019). This was a collaborative project primarily between Fabricio Mosquera-Guagua, Randy Sanichar, and myself. In this project I was responsible for designing the target compounds as well as developing the synthetic methodologies required to access them. My focus was primarily situated on development of the synthetic route required to access the extended 6-membered ring spin-labelled amino acid. I also conducted the Marfey's assays required for determination of stereochemical ratios as well as the D-amino acid oxidase assay for enantiopurification.

Chapter 3 has been published as two articles: 1) Vuong, W.; Khan, M.B.; Fischer, C.; Arutyunova, E.; Lamer, T.; Shields, J.; Saffran, H.A.; McKay, R.T.; van Belkum, M.J.; Joyce, M.; Young, H.S.; Tyrrell, D.L.; Vederas, J.C.; Lemieux, M.J. Feline coronavirus drug inhibits the main protease of SARS-CoV-2 and blocks virus replication. *Nature Comm.* 11, Article 4282, 1-8 (2020), and 2) Vuong, W.; Fischer, C.; Khan, M.B.; van Belkum, M. J.; Lamer, T.; Willoughby, K. D.; Lu, J.; Arutyunova, E.; Joyce, M.A.; Saffran, H.A.; Shields, J.A.; Young, H.S.; Nieman, J.A.; Tyrrell, L.D.; Lemieux, M.J.; Vederas, J.C. Improved SARS-CoV-2 M<sup>Pro</sup> inhibitors based on feline antiviral drug GC376: structural enhancements, increased solubility, and micellar studies. *Eur. J. Med. Chem.* 222, 113584, 1-11 (2021). Both papers were highly collaborative in nature. In the first paper I was responsible for the synthesis of all required chemical agents necessary for enzymatic and cellular assays, including inhibitors GC373 and GC376 as well as the substrate required for the FRET

assay. With the help of Dr. Ryan McKay, I also performed the NMR experiments required to demonstrate the mechanism of action of these inhibitors. In the second paper, I was responsible for designing and synthesizing most of the inhibitor analogs that were tested, with additional assistance provided by Dr. Conrad Fischer. Enzymatic purification and FRET assays were primarily done by Dr. Conrad Fischer while cloning and expression of the main protease was conducted by Dr. Marco van Belkum. I was also responsible for the  $^{13}\text{C}$ -labelled NMR studies to look at stereochemical population distributions, the solubility experiments. DOSY experiments were a joint effort between Dr. Conrad Fischer and myself, with technical assistance provided by Mark Miskolzie.

Chapter 4 has been published as Vuong, W.; Vederas, J.C. Improved Synthesis of a Cyclic Glutamine Analog Used in Antiviral Agents Targeting 3C and 3CL Proteases Including SARS-CoV-2 M<sup>pro</sup>. *J. Org. Chem.* 86, 13104-13110 (2021). I was responsible for all aspects of this publication, including experimental design, development of the synthetic route, and compound characterization.

Chapter 5 describes work that is ongoing at the time of this writing. My contributions here pertain to exploration of possible synthetic methodologies required for methylene to oxygen bioisostere exchange.

Chapter 6 also details work that is currently ongoing at the time of this writing. My contributions to this project involve the synthesis and preparation of substrates and product standards required for kinetic assays as well as preliminary attempts to purify the target domains as standalone enzymes.

# Dedication

To my brother, David Vuong. Thank you for inspiring and encouraging me to go beyond and aim higher than I ever thought possible of myself. You have bestowed upon me a world view grounded in reality and rational thought. This academic journey would have never begun without you.

To my mom and dad, Phan Lu and Kien Vuong. Thank you for giving me the opportunity to pursue a career in science. The hard work and sacrifices you have made to build a life in a new and unfamiliar country are not in vain. I hope that this work can begin to validate all that you have done.

# Acknowledgements

I am thrilled to be alive at time when humanity is pushing against the limits of understanding. Even better, we may eventually discover that there are no limits.

---

Richard Dawkins

Science is a collaborative endeavour, and this thesis would not have been possible without the collective contributions of numerous individuals. First and foremost, I am indebted to my mentor, Dr. John C. Vederas. Thank you for having taken a chance on me when I came to you 5 years ago. The knowledge and enthusiasm that you bring to the lab each day is an inspiring example of what it means to be a leader and scientist, and one that I strive to emulate. Furthermore, the mentorship, opportunities, and supportive environment that you have provided through these years have allowed me to grow as a scientist and person in ways that I would never have imagined. You have my deepest gratitude.

Part of what enables the calibre of research that takes place in this department is the tireless effort of the support staff here. My heartfelt thanks goes out to Mark Miskolzie and Dr. Ryan McKay of the NMR facilities; Béla Reiz, Dr. Angie Morales-Izquierdo, and Dr. Randy Whittal of the MS facilities; Jennifer Jones and Dr. Wayne Moffat of the A&I lab; Mike Barteski, Andrew Yeung, and Ryan Lewis of ChemStores; Jason Dibbs of the glass shop; and finally, Paul Crothers, Dieter Starke, Vincent Bizon, and Dirk Kelm of the machine shop. My work would not be possible without all of you.

Additional thanks are owed to collaborators outside the Vederas group, namely from the groups of Dr. M. Joanne Lemieux and Dr. D. Lorne Tyrrell. Their hard work, dedication,



and expertise have enabled project scopes that would otherwise have been impossible.

Further thanks goes to the lab mates that have shaped my time here. To Fabricio Mosquera-Guagua, from whom I cultivated a careful approach to experimental execution and grittiness when reactions inevitably fail. To Alex Ahn, for being so welcoming when I first joined. To Kleinberg Fernandez, for being such a supportive friend both in and out of the lab. To Cameron Pascoe, for his amazing sense of humour and being such a fun benchmate to work beside. To Marco van Belkum, for the rich molecular biology knowledge you bring. To postdocs Dr. Conrad Fischer, for your hard work on the COVID project; Dr. Jon Beadle, for being a bountiful source of synthetic chemistry knowledge; and Dr. Beth Donnelly, for endless enthusiasm, optimism, and positivity when things got tough. Further appreciation goes to Beth and Riley Hsiao for their help in editing this thesis.

I would be remiss to forget the support from friends and family outside of the lab. To Iris Chan, for sparking my interest in climbing and always being down to grab food. To Jeff Wong, for being an amazing friend, scientist, adventurer, and climbing partner outside of the lab. To Boris Wong, Greg Chao, and Carlo Valencia; you guys are like brothers to me, and it is a privilege to be part of the goon squad. To Shirley Lew, for always being there to binge a show or play a game and provide a chance to de-stress from work. To my family in Calgary, particularly my cousin Tina Ho, for the constant encouragement and support. To John Lee and the rest of the climbing group for pushing me to climb hard and get good. To my friends in the chemistry department, who have been there to share in the ups and downs of grad school. At last, to my housemates, who have made my last year in Edmonton an unforgettable one. All of you have greatly enriched my time here.

Finally, financial support in the form of Alberta Innovates, Queen Elizabeth II, Alberta Graduate Excellence, Andrew Steward, and Novartis scholarships is gratefully acknowledged.

# Contents

<b>Abbreviations</b>	<b>xxix</b>
<b>1 Introduction</b>	<b>1</b>
1.1 Background . . . . .	1
1.2 Thesis Overview . . . . .	3
<b>2 Synthesis of Chiral Spin Labelled Amino Acids</b>	<b>7</b>
2.1 Introduction to Spin Labels . . . . .	7
2.2 Synthetic Approach . . . . .	10
2.3 Synthesis of Compound <b>6</b> . . . . .	10
2.4 Synthesis of Compounds <b>7</b> and <b>8</b> . . . . .	12
2.5 Enantiopurification of Amino Acids <b>6</b> , <b>7</b> , and <b>8</b> Using D-amino acid oxidase and Evaluation by Marfey's Assay . . . . .	20
2.6 Conclusion . . . . .	23
<b>3 Development of Peptidomimetic Therapeutics Towards COVID-19</b>	<b>24</b>
3.1 Introduction to severe acute respiratory syndrome coronavirus 2 (SARS-CoV- 2) and coronavirus disease 2019 (COVID-19) . . . . .	24
3.1.1 Coronaviruses - Characteristics and Lifecycle . . . . .	24
3.1.2 Protease Inhibitors as Therapeutic Agents . . . . .	25
3.1.3 Repurposing a Feline Coronavirus Drug . . . . .	27

3.2	Evaluation of GC373 ( <b>62</b> ) and GC376 ( <b>63</b> ) as Potential SARS-CoV-2 main protease (M <sup>pro</sup> ) Inhibitors . . . . .	29
3.2.1	Synthesis of GC373 ( <b>62</b> ) and GC376 ( <b>63</b> ) . . . . .	29
3.2.2	Evaluation of IC <sub>50</sub> Values for GC373 ( <b>62</b> ) and GC376 ( <b>63</b> ) . . . . .	31
3.2.3	Evaluation of EC <sub>50</sub> and CC <sub>50</sub> Values for GC373 ( <b>62</b> ) and GC376 ( <b>63</b> ) . . . . .	36
3.2.4	Co-crystal Structures of GC373 ( <b>62</b> ) and GC376 ( <b>63</b> ) with SARS-CoV-2 M <sup>pro</sup> . . . . .	38
3.2.5	Stereochemical Investigations of GC373 ( <b>62</b> ) and GC376 ( <b>63</b> ) via <sup>13</sup> C- Labelling and nuclear magnetic resonance (NMR) Spectroscopy . . . . .	39
3.3	Development of Improved Inhibitors Against SARS-CoV-2 M <sup>pro</sup> . . . . .	46
3.3.1	Design and Evaluation of Improved Inhibitors . . . . .	46
3.3.2	Structural Analysis of Improved Inhibitors by X-Ray Crystallography . . . . .	53
3.3.3	Examining and Improving Solubility of Bisulfite Adduct Prodrugs . . . . .	56
3.4	Conclusion . . . . .	63
<b>4</b>	<b>Improved Synthesis of a Glutamine Analog</b>	<b>65</b>
4.1	Introduction to a $\gamma$ -Lactam Analog of Glutamine . . . . .	65
4.2	Development of an Improved Synthetic Route Towards a $\gamma$ -Lactam Analog of Glutamine . . . . .	66
4.3	Conclusion . . . . .	71
<b>5</b>	<b>Improving Metabolic Stability of Antivirals Against P450</b>	<b>73</b>
5.1	Introduction to P450 and Metabolic Degradation . . . . .	73
5.2	Methods to Avoid Metabolic Reactions by P450 . . . . .	75
5.3	Synthetic Routes Towards an Oxa-glutamine (Gln) Analog . . . . .	76
5.3.1	Proposed Synthetic Approach 1 - Mitsunobu Reaction . . . . .	77
5.3.2	Proposed Synthetic Approach 2 - Addition via Alkylation . . . . .	78
5.3.3	Proposed Synthetic Approach 3 - Direct N-O Bond Formation . . . . .	80
5.3.4	Proposed Synthetic Approach 4 - Radical Addition . . . . .	83

5.3.5	Proposed Synthetic Approach 5 - <i>N</i> -hydroxyamide Ring Closure . . .	84
5.4	Conclusion and Future Work . . . . .	85
<b>6</b>	<b>Investigations Into Regulation of Polyketide Biosynthesis</b>	<b>87</b>
6.1	Intoduction to Polyketides . . . . .	87
6.2	Polyketide Biosynthetic Process . . . . .	88
6.3	Types of Polyketide Synthases . . . . .	89
6.3.1	Type I Polyketide Synthases . . . . .	90
6.3.2	Type II Polyketide Synthases . . . . .	90
6.3.3	Type III Polyketide Synthases . . . . .	90
6.4	Investigating the Programming of Polyketide Synthesis . . . . .	90
6.5	Synthesis of Probe Substrates and Product Standards . . . . .	92
6.6	Conclusion and Future Work . . . . .	93
<b>7</b>	<b>Experimental Procedures</b>	<b>95</b>
7.1	General Information . . . . .	95
7.1.1	Compound Characterization . . . . .	95
7.1.2	General Synthetic Procedures . . . . .	96
7.1.3	Purification . . . . .	96
7.2	Marfey's Assay for Determination of Amino Acid Enantiomeric Ratios . . . .	97
7.2.1	Marfey's Assay Experimental Procedure . . . . .	97
7.2.2	Marfey's Assay Analysis . . . . .	97
7.3	Synthesis of FRET Substrate for Determination of SARS-CoV-2 M <sup>PRO</sup> Enzyme Kinetics . . . . .	98
7.3.1	General 2-Chlorotrityl Chloride Resin Loading Procedure . . . . .	98
7.3.2	General Automated SPSS Elongation Method . . . . .	98
7.3.3	Synthesis of FRET Peptide Substrate . . . . .	99
7.3.4	General Method for Cleavage of Peptide from Resin . . . . .	99
7.3.5	HPLC Purification Method . . . . .	100

7.4	<sup>13</sup> C-labelled GC373 and GC376 NMR Experiments . . . . .	100
7.4.1	Sample Preparation for NMR Binding Assays . . . . .	100
7.4.2	NMR Spectroscopy Experiments . . . . .	101
7.4.3	Stereochemical Population Distribution Studies . . . . .	102
7.5	Solubility Studies . . . . .	102
7.5.1	Solubility Determination of GC376 Cation Derivatives . . . . .	102
7.5.2	DOSY Experiments . . . . .	103
7.6	Synthetic Procedures and Characterization Data of Compounds . . . . .	104
7.7	Chapter 2 Synthetic Procedures . . . . .	104
	1-Acetyl-2,2,6,6-tetramethylpiperidin-4-one ( <b>10</b> ) . . . . .	104
	<i>N</i> -(2,6-Dimethyl-4-methylenehept-5-en-2-yl)acetamide ( <b>11</b> ) . . . . .	105
	<i>N</i> -Benzyl-L-proline ( <b>14</b> ) . . . . .	106
	( <i>S</i> )- <i>N</i> -(2-Benzoylphenyl)-1-benzylpyrrolidine-2-carboxamide ( <b>16</b> ) . . . . .	107
	Belokon Complex ( <b>18</b> ) . . . . .	108
	3,5-Dibromo-2,2,6,6-tetramethyl-4-oxopiperidin-1-ium bromide ( <b>19</b> ) . . . . .	110
	Methyl 2,2,5,5-tetramethyl-2,5-dihydro-1 <i>H</i> -pyrrole-3-carboxylate ( <b>20</b> ) . . . . .	110
	mCPBA Recrystallization Protocol . . . . .	111
	Methyl 1-oxyl-2,2,5,5-tetramethyl-2,5-dihydro-1 <i>H</i> -pyrrole-3-carboxylate ( <b>21</b> ) . . . . .	112
	3-(Hydroxymethyl)-2,2,5,5-tetramethyl-2,5-dihydro-1 <i>H</i> -pyrrol-1-oxyl ( <b>22</b> ) . . . . .	113
	(1-Oxyl-2,2,5,5-tetramethyl-2,5-dihydro-1 <i>H</i> -pyrrol-3-yl)methyl methanesulfonate ( <b>23</b> ) . . . . .	114
	2,2,2-Trichloroethyl 2,2,6,6-tetramethyl-4-oxo-piperidine-1-carboxylate ( <b>26</b> ) . . . . .	115
	2,2,2-Trichloroethyl 4-hydroxyl-2,2,6,6-tetramethyl-4-piperidine-1- carboxylate ( <b>27</b> ) . . . . .	116
	2,2,2-Trichloroethyl 4-[[[(4-bromophenyl)sulfonyl]oxy}-2,2,6,6- tetramethylpiperidine-1-carboxylate ( <b>29</b> ) . . . . .	117
	Methyltriphenylphosphonium iodide ( <b>30</b> ) . . . . .	118

2,2,2-Trichloroethyl 2,2,6,6-tetramethyl-4-methylenepiperidine-1-carboxylate ( <b>31</b> ) . . . . .	119
2,2,2-Trichloroethyl 4-(hydroxymethyl)-2,2,6,6-tetramethylpiperidine-1- carboxylate ( <b>32</b> ) . . . . .	120
2,2,2-Trichloroethyl 4-(((4-bromophenyl)sulfonyl)oxy)methyl)-2,2,6,6- tetramethylpiperidine-1-carboxylate ( <b>33</b> ) . . . . .	121
Benzyl 2-((diphenylmethylene)amino)acetate ( <b>36</b> ) . . . . .	122
2,2,2-Trichloroethyl 4-(2-amino-3-(benzyloxy)-3-oxopropyl)-2,2,6,6- tetramethylpiperidine-1-carboxylate ( <b>42</b> ) . . . . .	123
2,2,2-Trichloroethyl 4-(3-(benzyloxy)-3-oxo-2-(2,2,2- trifluoroacetamido)propyl)-2,2,6,6-tetramethylpiperidine-1- carboxylate ( <b>43</b> ) . . . . .	125
Benzyl 3-(2,2,6,6-tetramethylpiperidin-4-yl)-2-(2,2,2- trifluoroacetamido)propanoate ( <b>44</b> ) . . . . .	126
Benzyl 3-(1-oxyl-2,2,6,6-tetramethylpiperidin-4-yl)-2-(2,2,2- trifluoroacetamido)propanoate ( <b>45</b> ) . . . . .	127
2-Amino-3-(1-oxyl-2,2,6,6-tetramethylpiperidin-4-yl)propanoic acid ( <b>46</b> ) . . .	128
Soloshonok Ligand ( <b>47</b> ) . . . . .	129
Extended 6-Membered Ring Nickle Complex ( <b>53</b> ) . . . . .	131
( <i>S</i> )-2-Amino-3-(1-oxyl-2,2,6,6-tetramethylpiperidin-4-yl)propanoic acid ( <b>8</b> ) .	132
7.8 Chapter 3 Synthetic Procedures . . . . .	133
Dimethyl ( <i>tert</i> -butoxycarbonyl)-L-glutamate ( <b>65</b> ) . . . . .	133
Methyl ( <i>S</i> )-2-(( <i>tert</i> -butoxycarbonyl)amino)-3-(( <i>S</i> )-2-oxopyrrolidin-3- yl)propanoate ( <b>66</b> ) . . . . .	134
Methyl ( <i>S</i> )-2-(( <i>S</i> )-2-(((benzyloxy)carbonyl)amino)-4-methylpentanamido)-3- (( <i>S</i> )-2-oxopyrrolidin-3-yl)propanoate ( <b>67</b> ) . . . . .	136

Benzyl	(( <i>S</i> )-1-((( <i>S</i> )-1-hydroxy-3-(( <i>S</i> )-2-oxopyrrolidin-3-yl)propan-2-yl)amino)-4-methyl-1-oxopentan-2-yl)carbamate	
	<b>(68)</b>	138
GC373	<b>(62)</b>	139
GC376	<b>(63)</b>	141
<sup>13</sup> C-GC373	<b>(78)</b>	142
<sup>13</sup> C-GC376	<b>(79)</b>	143
Methyl	( <i>S</i> )-2-(( <i>S</i> )-2-(((benzyloxy)carbonyl)amino)-3-cyclopropylpropanamido)-3-(( <i>S</i> )-2-oxopyrrolidin-3-yl)propanoate	
	<b>(167)</b>	143
Methyl	( <i>S</i> )-2-(( <i>S</i> )-2-(((benzyloxy)carbonyl)amino)-3-cyclohexylpropanamido)-3-(( <i>S</i> )-2-oxopyrrolidin-3-yl)propanoate	
	<b>(168)</b>	145
Methyl	( <i>S</i> )-2-(( <i>S</i> )-2-(((benzyloxy)carbonyl)amino)-3-phenylpropanamido)-3-(( <i>S</i> )-2-oxopyrrolidin-3-yl)propanoate	
	<b>(169)</b>	146
Methyl	( <i>S</i> )-2-(( <i>S</i> )-2-(((3-fluorobenzyl)oxy)carbonyl)amino)-4-methylpentanamido)-3-(( <i>S</i> )-2-oxopyrrolidin-3-yl)propanoate	
	<b>(170)</b>	147
Methyl	( <i>S</i> )-2-(( <i>S</i> )-2-(((3-chlorophenoxy)carbonyl)amino)-4-methylpentanamido)-3-(( <i>S</i> )-2-oxopyrrolidin-3-yl)propanoate	
	<b>(171)</b>	148
Methyl	( <i>S</i> )-2-(( <i>S</i> )-2-(4-methoxy-1 <i>H</i> -indole-2-carboxamido)-4-methylpentanamido)-3-(( <i>S</i> )-2-oxopyrrolidin-3-yl)propanoate	
	<b>(172)</b>	149
Methyl	( <i>S</i> )-2-(( <i>S</i> )-4-methyl-2-((( <i>S</i> )-1-phenylethoxy)carbonyl)amino)pentanamido)-3-(( <i>S</i> )-2-oxopyrrolidin-3-yl)propanoate	
	<b>(173)</b>	150

Methyl	( <i>S</i> )-2-(( <i>S</i> )-4-methyl-2-((( <i>R</i> )-1-phenylethoxy)carbonyl)amino)pentanamido)-3-(( <i>S</i> )-2-oxopyrrolidin-3-yl)propanoate ( <b>174</b> ) . . . . .	151
Methyl	( <i>S</i> )-2-(( <i>S</i> )-3-cyclopropyl-2-(((3-fluorobenzyl)oxy)carbonyl)amino)propanamido)-3-(( <i>S</i> )-2-oxopyrrolidin-3-yl)propanoate ( <b>175</b> ) . . . . .	152
Methyl	( <i>S</i> )-2-(( <i>S</i> )-2-(((3-chlorophenethoxy)carbonyl)amino)-3-cyclopropylpropanamido)-3-(( <i>S</i> )-2-oxopyrrolidin-3-yl)propanoate ( <b>176</b> ) . . . . .	153
Methyl	( <i>S</i> )-2-(( <i>S</i> )-3-cyclopropyl-2-(4-methoxy-1 <i>H</i> -indole-2-carboxamido)propanamido)-3-(( <i>S</i> )-2-oxopyrrolidin-3-yl)propanoate ( <b>177</b> ) . . . . .	154
Methyl	( <i>S</i> )-2-(( <i>S</i> )-3-cyclopropyl-2-((( <i>S</i> )-1-phenylethoxy)carbonyl)amino)propanamido)-3-(( <i>S</i> )-2-oxopyrrolidin-3-yl)propanoate ( <b>178</b> ) . . . . .	155
Benzyl	(( <i>S</i> )-3-cyclopropyl-1-((( <i>S</i> )-1-hydroxy-3-(( <i>S</i> )-2-oxopyrrolidin-3-yl)propan-2-yl)amino)-1-oxopropan-2-yl)carbamate ( <b>179</b> ) . . . . .	156
Benzyl	(( <i>S</i> )-3-cyclohexyl-1-((( <i>S</i> )-1-hydroxy-3-(( <i>S</i> )-2-oxopyrrolidin-3-yl)propan-2-yl)amino)-1-oxopropan-2-yl)carbamate ( <b>180</b> ) . . . . .	158
Benzyl	(( <i>S</i> )-1-((( <i>S</i> )-1-hydroxy-3-(( <i>S</i> )-2-oxopyrrolidin-3-yl)propan-2-yl)amino)-1-oxo-3-phenylpropan-2-yl)carbamate ( <b>181</b> ) . . . . .	159
3-Fluorobenzyl	(( <i>S</i> )-1-((( <i>S</i> )-1-hydroxy-3-(( <i>S</i> )-2-oxopyrrolidin-3-yl)propan-2-yl)amino)-4-methyl-1-oxopentan-2-yl)carbamate ( <b>182</b> ) . . . . .	160



3-Chlorophenethyl	(( <i>S</i> )-1-((( <i>S</i> )-1-hydroxy-3-(( <i>S</i> )-2-oxopyrrolidin-3-yl)propan-2-yl)amino)-4-methyl-1-oxopentan-2-yl)carbamate	
(183)		161
<i>N</i> -(( <i>S</i> )-1-((( <i>S</i> )-1-Hydroxy-3-(( <i>S</i> )-2-oxopyrrolidin-3-yl)propan-2-yl)amino)-4-methyl-1-oxopentan-2-yl)-4-methoxy-1 <i>H</i> -indole-2-carboxamide		
(184)		162
( <i>S</i> )-1-Phenylethyl	(( <i>S</i> )-1-((( <i>S</i> )-1-hydroxy-3-(( <i>S</i> )-2-oxopyrrolidin-3-yl)propan-2-yl)amino)-4-methyl-1-oxopentan-2-yl)carbamate	
(185)		163
( <i>R</i> )-1-Phenylethyl	(( <i>S</i> )-1-((( <i>S</i> )-1-hydroxy-3-(( <i>S</i> )-2-oxopyrrolidin-3-yl)propan-2-yl)amino)-4-methyl-1-oxopentan-2-yl)carbamate	
(186)		164
3-Fluorobenzyl	(( <i>S</i> )-3-cyclopropyl-1-((( <i>S</i> )-1-hydroxy-3-(( <i>S</i> )-2-oxopyrrolidin-3-yl)propan-2-yl)amino)-1-oxopropan-2-yl)carbamate	
(187)		165
3-Chlorophenethyl	(( <i>S</i> )-3-cyclopropyl-1-((( <i>S</i> )-1-hydroxy-3-(( <i>S</i> )-2-oxopyrrolidin-3-yl)propan-2-yl)amino)-1-oxopropan-2-yl)carbamate	
(188)		166
<i>N</i> -(( <i>S</i> )-3-Cyclopropyl-1-((( <i>S</i> )-1-hydroxy-3-(( <i>S</i> )-2-oxopyrrolidin-3-yl)propan-2-yl)amino)-1-oxopropan-2-yl)-4-methoxy-1 <i>H</i> -indole-2-carboxamide		
(189)		167
( <i>S</i> )-1-Phenylethyl	(( <i>S</i> )-3-cyclopropyl-1-((( <i>S</i> )-1-hydroxy-3-(( <i>S</i> )-2-oxopyrrolidin-3-yl)propan-2-yl)amino)-1-oxopropan-2-yl)carbamate	
(190)		168
Benzyl	(( <i>S</i> )-3-cyclopropyl-1-oxo-1-((( <i>S</i> )-1-oxo-3-(( <i>S</i> )-2-oxopyrrolidin-3-yl)propan-2-yl)amino)propan-2-yl)carbamate	
(80)		169

Benzyl	(( <i>S</i> )-3-cyclohexyl-1-oxo-1-((( <i>S</i> )-1-oxo-3-(( <i>S</i> )-2-oxopyrrolidin-3-yl)propan-2-yl)amino)propan-2-yl)carbamate	
(81)	.....	170
Benzyl	(( <i>S</i> )-1-oxo-1-((( <i>S</i> )-1-oxo-3-(( <i>S</i> )-2-oxopyrrolidin-3-yl)propan-2-yl)amino)-3-phenylpropan-2-yl)carbamate	
(82)	.....	171
3-Fluorobenzyl	(( <i>S</i> )-4-methyl-1-oxo-1-((( <i>S</i> )-1-oxo-3-(( <i>S</i> )-2-oxopyrrolidin-3-yl)propan-2-yl)amino)pentan-2-yl)carbamate	
(83)	.....	172
3-Chlorophenethyl	(( <i>S</i> )-4-methyl-1-oxo-1-((( <i>S</i> )-1-oxo-3-(( <i>S</i> )-2-oxopyrrolidin-3-yl)propan-2-yl)amino)pentan-2-yl)carbamate (84)	..... 173
4-Methoxy- <i>N</i> -(( <i>S</i> )-4-methyl-1-oxo-1-((( <i>S</i> )-1-oxo-3-(( <i>S</i> )-2-oxopyrrolidin-3-yl)propan-2-yl)amino)pentan-2-yl)-1 <i>H</i> -indole-2-carboxamide		
(85)	.....	174
( <i>S</i> )-1-Phenylethyl	(( <i>S</i> )-4-methyl-1-oxo-1-((( <i>S</i> )-1-oxo-3-(( <i>S</i> )-2-oxopyrrolidin-3-yl)propan-2-yl)amino)pentan-2-yl)carbamate	
(86)	.....	175
( <i>R</i> )-1-Phenylethyl	(( <i>S</i> )-4-methyl-1-oxo-1-((( <i>S</i> )-1-oxo-3-(( <i>S</i> )-2-oxopyrrolidin-3-yl)propan-2-yl)amino)pentan-2-yl)carbamate	
(87)	.....	176
3-Fluorobenzyl	(( <i>S</i> )-3-cyclopropyl-1-oxo-1-((( <i>S</i> )-1-oxo-3-(( <i>S</i> )-2-oxopyrrolidin-3-yl)propan-2-yl)amino)propan-2-yl)carbamate	
(88)	.....	177
3-Chlorophenethyl	(( <i>S</i> )-3-cyclopropyl-1-oxo-1-((( <i>S</i> )-1-oxo-3-(( <i>S</i> )-2-oxopyrrolidin-3-yl)propan-2-yl)amino)propan-2-yl)carbamate	
(89)	.....	178

<i>N</i> -(( <i>S</i> )-3-Cyclopropyl-1-oxo-1-((( <i>S</i> )-1-oxo-3-(( <i>S</i> )-2-oxopyrrolidin-3-yl)propan-2-yl)amino)propan-2-yl)-4-methoxy-1 <i>H</i> -indole-2-carboxamide ( <b>90</b> ) . . . . .	179
( <i>S</i> )-1-Phenylethyl (( <i>S</i> )-3-cyclopropyl-1-oxo-1-((( <i>S</i> )-1-oxo-3-(( <i>S</i> )-2-oxopyrrolidin-3-yl)propan-2-yl)amino)propan-2-yl)carbamate ( <b>91</b> ) . . . . .	180
Sodium (2 <i>S</i> )-2-(( <i>S</i> )-2-(((benzyloxy)carbonyl)amino)-3-cyclopropylpropanamido)-1-hydroxy-3-(( <i>S</i> )-2-oxopyrrolidin-3-yl)propane-1-sulfonate ( <b>92</b> ) . . . . .	181
Sodium (2 <i>S</i> )-1-hydroxy-2-(( <i>S</i> )-2-(4-methoxy-1 <i>H</i> -indole-2-carboxamido)-4-methylpentanamido)-3-(( <i>S</i> )-2-oxopyrrolidin-3-yl)propane-1-sulfonate ( <b>93</b> ) . . . . .	182
Sodium (2 <i>S</i> )-2-(( <i>S</i> )-3-cyclopropyl-2-(((3-fluorobenzyl)oxy)carbonyl)amino)propanamido)-1-hydroxy-3-(( <i>S</i> )-2-oxopyrrolidin-3-yl)propane-1-sulfonate ( <b>94</b> ) . . . . .	183
Sodium (2 <i>S</i> )-2-(( <i>S</i> )-2-(((3-chlorophenethoxy)carbonyl)amino)-3-cyclopropylpropanamido)-1-hydroxy-3-(( <i>S</i> )-2-oxopyrrolidin-3-yl)propane-1-sulfonate ( <b>95</b> ) . . . . .	184
Sodium (2 <i>S</i> )-2-(( <i>S</i> )-3-cyclopropyl-2-(4-methoxy-1 <i>H</i> -indole-2-carboxamido)propanamido)-1-hydroxy-3-(( <i>S</i> )-2-oxopyrrolidin-3-yl)propane-1-sulfonate ( <b>96</b> ) . . . . .	185
Sodium (2 <i>S</i> )-2-(( <i>S</i> )-3-cyclopropyl-2-((( <i>S</i> )-1-phenylethoxy)carbonyl)amino)propanamido)-1-hydroxy-3-(( <i>S</i> )-2-oxopyrrolidin-3-yl)propane-1-sulfonate ( <b>97</b> ) . . . . .	187

Potassium	(2 <i>S</i> )-2-(( <i>S</i> )-2-(((benzyloxy)carbonyl)amino)-4-methylpentanamido)-1-hydroxy-3-(( <i>S</i> )-2-oxopyrrolidin-3-yl)propane-1-sulfonate ( <b>98</b> ) . . . . .	188
Production of Choline Bisulfite . . . . .		189
Production of SO <sub>2</sub> Gas . . . . .		189
Choline (2 <i>S</i> )-2-(( <i>S</i> )-2-(((benzyloxy)carbonyl)amino)-4-methylpentanamido)-1-hydroxy-3-(( <i>S</i> )-2-oxopyrrolidin-3-yl)propane-1-sulfonate ( <b>99</b> ) . . . . .		190
Methyl ( <i>S</i> )-2-(( <i>S</i> )-2-(( <i>tert</i> -butoxycarbonyl)amino)-4-methylpentanamido)-3-(( <i>S</i> )-2-oxopyrrolidin-3-yl)propanoate ( <b>191</b> ) . . . . .		191
Methyl ( <i>S</i> )-2-(( <i>S</i> )-2-(( <i>tert</i> -butoxycarbonyl)amino)-3-cyclopropylpropanamido)-3-(( <i>S</i> )-2-oxopyrrolidin-3-yl)propanoate ( <b>192</b> ) . . . . .		192
7.9 Chapter 4 Synthetic Procedures . . . . .		193
Dimethyl (2 <i>S</i> ,4 <i>S</i> )-2-allyl-4-(( <i>tert</i> -butoxycarbonyl)-amino)pentanedioate ( <b>101</b> )		193
Dimethyl (2 <i>S</i> ,4 <i>S</i> )-2-allyl-4-(bis( <i>tert</i> -butoxycarbonyl)amino)pentanedioate ( <b>102</b> ) . . . . .		195
Dimethyl (2 <i>S</i> ,4 <i>R</i> )-2-(bis( <i>tert</i> -butoxycarbonyl)amino)-4-(2-oxoethyl)pentanedioate ( <b>103</b> ) . . . . .		197
Dimethyl (2 <i>S</i> ,4 <i>R</i> )-2-(bis( <i>tert</i> -butoxycarbonyl)amino)-4-(2-(methoxyimino)ethyl)pentanedioate ( <b>104</b> ) . . . . .		199
Methyl ( <i>S</i> )-2-(bis( <i>tert</i> -butoxycarbonyl)amino)-3-(( <i>S</i> )-2-oxopyrrolidin-3-yl)propanoate ( <b>105</b> ) . . . . .		201
Test reaction utilizing <b>105</b> - formation of compound ( <b>67</b> ) . . . . .		203
7.10 Chapter 5 Synthetic Procedures . . . . .		204
Dimethyl (2 <i>R</i> ,4 <i>S</i> )-2-((benzyloxy)methyl)-4-(( <i>tert</i> -butoxycarbonyl)amino)pentanedioate ( <b>114</b> ) . . . . .		204
Dimethyl ( <i>S</i> )-2-(( <i>tert</i> -butoxycarbonyl)amino)-4-methylenepentanedioate ( <b>119</b> )		205
2-(Chloromethoxy)isoindoline-1,3-dione ( <b>122</b> ) . . . . .		206

2-( <i>tert</i> -Butyl) 3,5-dimethyl (3 <i>S</i> )-1,6-dioxo-3,4,5,6-tetrahydrobenzo[ <i>c</i> ]azocine- 2,3,5(1 <i>H</i> )-tricarboxylate ( <b>123</b> ) . . . . .	207
<i>N,N</i> -Bis(2-nitrobenzyl)hydroxylamine ( <b>125</b> ) . . . . .	209
9 <i>H</i> -Fluoren-9-one <i>O</i> -methylsulfonyl oxime ( <b>127</b> ) . . . . .	210
9 <i>H</i> -Fluoren-9-one <i>O</i> -benzyl oxime ( <b>130</b> ) . . . . .	211
7.11 Chapter 6 Synthetic Procedures . . . . .	212
1-(2-Thioxothiazolidin-3-yl)ethan-1-one ( <b>161</b> ) . . . . .	212
3-Hydroxy-1-(2-thioxothiazolidin-3-yl)hexan-1-one ( <b>162a</b> ) . . . . .	213
3-Hydroxy-1-(2-thioxothiazolidin-3-yl)octan-1-one ( <b>162b</b> ) . . . . .	214
3-Hydroxy-1-(2-thioxothiazolidin-3-yl)decan-1-one ( <b>162c</b> ) . . . . .	215
3-Hydroxy-1-(2-thioxothiazolidin-3-yl)dodecan-1-one ( <b>162d</b> ) . . . . .	215
3-Hydroxy-1-(2-thioxothiazolidin-3-yl)tetradecan-1-one ( <b>162e</b> ) . . . . .	216
<i>S</i> -(2-Acetamidoethyl) 3-hydroxyhexanethioate ( <b>164a</b> ) . . . . .	217
<i>S</i> -(2-Acetamidoethyl) 3-hydroxyoctanethioate ( <b>164b</b> ) . . . . .	218
<i>S</i> -(2-Acetamidoethyl) 3-hydroxydecanethioate ( <b>164c</b> ) . . . . .	219
<i>S</i> -(2-Acetamidoethyl) 3-hydroxydodecanethioate ( <b>164d</b> ) . . . . .	219
<i>S</i> -(2-Acetamidoethyl) 3-hydroxytetradecanethioate ( <b>164e</b> ) . . . . .	220
<i>S</i> -(2-Acetamidoethyl) 3-oxohexanethioate ( <b>165a</b> ) . . . . .	221
<i>S</i> -(2-Acetamidoethyl) 3-oxooctanethioate ( <b>165b</b> ) . . . . .	222
<i>S</i> -(2-Acetamidoethyl) 3-oxodecanethioate ( <b>165c</b> ) . . . . .	223
<i>S</i> -(2-Acetamidoethyl) 3-oxododecanethioate ( <b>165d</b> ) . . . . .	224
<i>S</i> -(2-Acetamidoethyl) 3-oxotetradecanethioate ( <b>165e</b> ) . . . . .	224
<i>S</i> -(2-Acetamidoethyl) 2-methyl-3-oxohexanethioate ( <b>166a</b> ) . . . . .	225
<i>S</i> -(2-Acetamidoethyl) 2-methyl-3-oxooctanethioate ( <b>166b</b> ) . . . . .	226
<i>S</i> -(2-Acetamidoethyl) 2-methyl-3-oxodecanethioate ( <b>166c</b> ) . . . . .	227
<i>S</i> -(2-Acetamidoethyl) 2-methyl-3-oxododecanethioate ( <b>166d</b> ) . . . . .	228
<i>S</i> -(2-Acetamidoethyl) 2-methyl-3-oxotetradecanethioate ( <b>166e</b> ) . . . . .	229



# List of Tables

2.1	Stereochemical ratios of amino acids <b>6</b> , <b>7</b> , and <b>8</b> before and after selective degradation by D-amino acid oxidase (DAAO). . . . .	22
3.1	Catalytic parameters of severe acute respiratory syndrome coronavirus (SARS-CoV) and SARS-CoV-2 M <sup>pro</sup> . . . . .	32
3.2	Inhibition parameters of select reported SARS-CoV-2 M <sup>pro</sup> inhibitors. . . . .	35
3.3	Inhibition parameters of singly modified, first generation inhibitor analogs against SARS-CoV-2 and SARS-CoV-2 M <sup>pro</sup> . . . . .	50
3.3	Inhibition parameters of singly modified, first generation inhibitor analogs against SARS-CoV-2 and SARS-CoV-2 M <sup>pro</sup> . (cont.) . . . . .	51
3.4	Inhibition parameters of doubly modified, second generation inhibitor analogs against SARS-CoV-2 and SARS-CoV-2 M <sup>pro</sup> . . . . .	52
3.5	Inhibition parameters of inhibitor analog bisulfite adducts against SARS-CoV-2 and SARS-CoV-2 M <sup>pro</sup> . . . . .	54
3.5	Inhibition parameters of inhibitor analog bisulfite adducts against SARS-CoV-2 and SARS-CoV-2 M <sup>pro</sup> . (cont.) . . . . .	55
3.6	Diffusion order as a function of concentration for GC376 ( <b>63</b> ) in D <sub>2</sub> O. . . . .	62
4.1	Experimental conditions examined to afford cyclization to $\gamma$ -lactam with minimal epimerization. . . . .	70

# List of Figures

1.1	Chemical structures of the 20 canonical amino acids with charges shown at physiological pH, with three- and one-letter abbreviations shown in brackets.	2
2.1	Examples of compounds used to site-specifically incorporate spin labels into peptides and proteins. . . . .	8
2.2	Chiral spin labelled amino acids for labelling proteins and peptides via solid phase peptide synthesis (SPPS) or genetic incorporation. . . . .	9
2.3	Decomposition of <i>N</i> -acyl protected 2,2,6,6-tetramethyl-4-piperidinone under basic conditions . . . . .	10
2.4	Degradation pathways of 2,2,6,6-tetramethyl-4-piperidinone derived electrophiles and mitigation via brosylate (OBs) utilization. . . . .	13
2.5	Dynamic kinetic resolution process utilizing Soloshonok ligand <b>47</b> to obtain enantiomerically enriched amino acids. . . . .	18
2.6	Selective transformation and degradation of D-amino acids into $\alpha$ -keto acids using D-amino acid oxidase. . . . .	21
3.1	Schematic structure and protease cleavage sites of polyproteins pp1a and pp1ab.	25
3.2	Select examples of protease inhibitors developed for therapeutic use. . . . .	26
3.3	Structures of GC373 ( <b>62</b> ) and GC376 ( <b>63</b> ) and positions within these inhibitors.	28
3.4	Structure of fluorescence resonance energy transfer (FRET) substrate <b>69</b> and mechanism of action. . . . .	33



3.5	Evaluation of half maximal inhibitory concentration ( $IC_{50}$ ) values for GC373 ( <b>62</b> ) and GC376 ( <b>63</b> ) against SARS-CoV and SARS-CoV-2 M <sup>pro</sup> . . . . .	34
3.6	Evaluation of half maximal effective concentration ( $EC_{50}$ ) and half maximal cytotoxic concentration ( $CC_{50}$ ) values for GC373 ( <b>62</b> ) and GC376 ( <b>63</b> ) against SARS-CoV-2. . . . .	36
3.7	Co-crystal structures of GC376 ( <b>63</b> ) with the M <sup>pro</sup> of SARS-CoV-2. . . . .	37
3.8	Possible stereoisomeric forms of GC373 ( <b>62</b> ) resulting from rapid $\alpha$ -carbon isomerization and hydrate formation. . . . .	40
3.9	Possible stereoisomeric forms of GC376 ( <b>63</b> ) resulting from rapid $\alpha$ -carbon isomerization and bisulfite adduct formation. . . . .	41
3.10	Structure of $^{13}C$ -labelled GC373 ( <b>78</b> ) and GC376 ( <b>79</b> ). . . . .	42
3.11	Stereochemical investigations of GC373 ( <b>62</b> ) and GC376 ( <b>63</b> ) via NMR experiments using $^{13}C$ -labelled GC373 ( <b>78</b> ) and $^{13}C$ -labelled GC376 ( <b>79</b> ). . . . .	44
3.11	Stereochemical investigations of GC373 ( <b>62</b> ) and GC376 ( <b>63</b> ) via NMR experiments using $^{13}C$ -labelled GC373 ( <b>78</b> ) and $^{13}C$ -labelled GC376 ( <b>79</b> ). (cont.)	45
3.11	Stereochemical investigations of GC373 ( <b>62</b> ) and GC376 ( <b>63</b> ) via NMR experiments using $^{13}C$ -labelled GC373 ( <b>78</b> ) and $^{13}C$ -labelled GC376 ( <b>79</b> ). (cont.)	46
3.12	Workflow utilized for the development of improved inhibitors of SARS-CoV-2 M <sup>pro</sup> based on GC376 ( <b>63</b> ). . . . .	48
3.13	Chemical structures of <b>94</b> and <b>95</b> identified as lead compounds. . . . .	53
3.14	Co-crystal structures of select inhibitors with SARS-CoV-2 M <sup>pro</sup> . . . . .	57
3.14	Co-crystal structures of select inhibitors with SARS-CoV-2 M <sup>pro</sup> . (cont.) . . . . .	58
3.15	NMR samples of GC376 ( <b>63</b> ) at various concentrations in $D_2O$ . . . . .	60
3.16	DOSY spectra of GC376 ( <b>63</b> ) at concentrations of 440 mM and 5 mM. . . . .	61
3.17	Plotted values of diffusion order as a function of inverse concentration. . . . .	63
4.1	Select examples of viral inhibitors containing a $\gamma$ -lactam Gln analog incorporated using compound <b>66</b> . . . . .	66

5.1	Mechanism of C-H bond oxidation by cytochrome P450 enzymes. . . . .	73
5.2	Constituent compounds of orally active COVID-19 therapeutic Paxlovid. . .	74
5.3	Cytochrome P450 3A4 metabolites of Nirmatrelvir ( <b>106</b> ) as reported by Pfizer. <sup>39</sup>	75
5.4	Methods to mitigate metabolism by cytochrome P450 enzymes . . . . .	75
5.5	Chemical structures of original Gln building block <b>66</b> its oxa-analog <b>113</b> . . .	76
5.6	Proposed Mitsunobu mechanism for the production of alkene byproduct <b>119</b> .	78
5.7	Proposed mustard-like degradation pathway of electrophile <b>126</b> to compound <b>125</b> . . . . .	80
6.1	Structures of various well-known polyketides. . . . .	88
6.2	Biosynthesis of lovastatin precursor dihydromonacolin L by various polyketide domains. . . . .	89
6.3	Structures of lovastatin ( <b>158</b> ) and equisetin ( <b>159</b> ) with backbone and key methyl groups highlighted. . . . .	91

## List of Schemes

2.1	Synthetic route towards Belokon complex ( <b>18</b> ) . . . . .	10
2.2	Synthetic route towards 5-membered ring electrophile ( <b>24</b> ) . . . . .	11
2.3	Alkylation of Belokon complex <b>18</b> to furnish spin labelled amino acid <b>6</b> . . . . .	12
2.4	Protection of 2,2,6,6-tetramethyl-4-piperidinone ( <b>9</b> ) using 2,2,2-trichloroethoxycarbonyl chloride (Troc-Cl). . . . .	14
2.5	Synthesis of 6-membered ring electrophile <b>29</b> . . . . .	14
2.6	Synthesis of extended 6-membered ring electrophile <b>33</b> . . . . .	15
2.7	Synthesis of protected glycine <b>36</b> . . . . .	15
2.8	Synthesis of racemic 6-membered ring amino acid <b>41</b> . . . . .	16
2.9	Synthesis of racemic extended 6-membered ring amino acid <b>46</b> . . . . .	17
2.10	Synthesis of Soloshonok ligand ( <b>47</b> ). . . . .	19
2.11	Deracemization of racemic amino acid <b>41</b> to furnish chiral spin labelled amino acid <b>7</b> . . . . .	19
2.12	Deracemization of racemic amino acid <b>46</b> to furnish extended chiral spin la- belled amino acid <b>8</b> . . . . .	20
3.1	Synthesis of analog <b>66</b> . . . . .	30
3.2	Synthesis of GC373 ( <b>62</b> ) and GC376 ( <b>63</b> ) from glutamine analog <b>66</b> . . . . .	31
3.3	Synthetic route to access first and second generation inhibitors of SARS-CoV- 2 M <sup>Pro</sup> . . . . .	48
3.4	Synthesis of potassium <b>98</b> and choline <b>99</b> analogs of GC376 ( <b>63</b> ) . . . . .	59

4.1	Pfizer’s original synthetic route towards glutamine analog building block <b>66</b> .	67
4.2	Improved synthetic scheme towards glutamine analog building block <b>105</b> . . .	67
4.3	Test reaction using building block <b>105</b> in the formation of known compound <b>67</b> . . . . .	71
5.1	Proposed synthetic path towards oxa-Gln analog <b>113</b> via a Mitsunobu reaction.	77
5.2	Proposed synthetic path towards oxa-Gln analog <b>113</b> via direct alkylation. .	78
5.3	Unexpected formation of 8-membered ring <b>123</b> . . . . .	79
5.4	Attempted methods towards the synthesis of photolabile electrophile <b>126</b> . . .	79
5.5	Proposed synthetic path towards oxa-Gln analog <b>113</b> via direct N-O bond formation using Hassner’s reagent. . . . .	81
5.6	Testing of reagent <b>130</b> using benzyl alcohol and subsequent attempts towards mild removal of 9-fluorenone. . . . .	82
5.7	Attempts at using reagent <b>133</b> for single amino group transfer onto alcohols.	82
5.8	Literature examples of soft nucleophile nitrogen transfer and oxime formation by reagent <b>133</b> . . . . .	83
5.9	Proposed synthetic route to generate oxa-Gln framework via chiral radical addition. . . . .	84
5.10	Attempted synthesis of compound <b>141</b> for use in radical addition. . . . .	84
5.11	Proposed method for the formation of compound <b>113</b> via selective hydrolysis and mesylation. . . . .	84
5.12	Documented use of compound <b>150</b> <sup>118</sup> as an aminotransfer reagent and proposed use for N-O bond formation with compound <b>115</b> . . . . .	86
6.1	General synthetic scheme to access aliphatic polyketide substrates and standards for enzymatic testing. . . . .	93

# Abbreviations

$[\alpha]_{\text{D}}^{26}$  specific rotation at 26 °C. 96

**3CL<sup>pro</sup>** 3-chymotrypsin-like protease. 25

**A549 cells** human alveolar adenocarcinomic basal epithelial cells. 36

**Abz** 2-aminobenzoyl. 32

**ACE** angiotensin converting enzyme. 26

**ACP** acyl carrier protein. 88, 90

**Ala** alanine. 25, 29

**Boc** *tert*-butoxycarbonyl. 65, 68, 69, 71, 77, 136

**Boc<sub>2</sub>O** di-*tert*-butyl dicarbonate. 29

**BsCl** *para*-bromophenylsulfonyl chloride. 14, 15

**Cbz** benzyloxycarbonyl. 30, 38, 47, 49, 56

**CC<sub>50</sub>** half maximal cytotoxic concentration. xi, xxv, 36, 50, 51, 52, 54, 55

**Cha** cyclohexylalanine. 47

**CMC** critical micellar concentration. 62, 63

**CoA** coenzyme A. 88, 90

**CoV** coronavirus. 24, 34

**COVID-19** coronavirus disease 2019. x, xxvi, 4, 5, 24, 29, 46, 74

**CP** CP-100356. 49, 50, 51, 52, 54, 55

**Cpa** cyclopropylalanine. 47

**Cys** cysteine. 37, 38, 57

**DAAO** D-amino acid oxidase. x, xxiii, 20, 21, 22

**Dabcyl** 4-([4-(Dimethylamino)phenyl]azo)benzoic acid. 32

**DCM** dichloromethane. 30

**DEER** double electron-electron resonance. 3, 7

**DH** dehydratase. 88, 89

**DIBAL** diisobutylaluminium hydride. 11, 113

**DIPEA** diisopropylethylamine. 30, 136

**DKR** dynamic kinetic resolution. xxiv, 17, 18, 19

**DMF** dimethylformamide. 12, 19, 143, 144

**DMP** Dess–Martin periodinane. 30, 93

**DOSY** diffusion-ordered spectroscopy. 61

**DPC** dodecyl phosphocholine. 62

**EC<sub>50</sub>** half maximal effective concentration. xi, xxv, 36, 46, 47, 49, 50, 51, 52, 53, 54, 55, 59, 63

**EDANS** 5-[(2-Aminoethyl)amino]naphthalene-1-sulfonic acid. 32

**EPR** electron paramagnetic resonance. 3, 7, 23

**EPS** electron spin resonance. 7

**er** enantiomeric ratio. 11, 12, 20

**ER** enoylreductase. 88, 89

**FCC** flash column chromatography over silica. 29, 93, 205

**FCoV** feline coronavirus. 4, 27, 29, 34

**FDAA** 1-fluoro-2-(4-dinitrophenyl)-5-L-alanine amide. 97

**FIP** feline infectious peritonitis. 27

**FIPV** feline infectious peritonitis virus. 27, 29

**FRET** fluorescence resonance energy transfer. xxiv, 4, 31, 32, 33, 36, 63

**Gln** glutamine. xi, xxv, xxvi, xxviii, 25, 29, 38, 56, 66, 74, 76, 77, 78, 81, 84, 85

**Glu** glutamic acid. 5, 29, 38, 56, 65

**Gly** glycine. 10, 25, 29, 37, 38

**GRAS** generally recognized as safe. 59

**HATU** 1-[*N*-[(dimethylamino)-1*H*-1,2,3-triazolo-[4,5-*b*]pyridin-1-ylmethylene]-*N*-methylethaniminium hexafluorophosphate *N*-oxide. 30,  
143

**His** histidine. 9, 38, 56

**HIV** human immunodeficiency virus. 25

**HMBC** heteronuclear multiple bond correlation. 85

**HOAt** 1-hydroxy-7-azabenzotriazole. 30, 143

**HPLC** high-performance liquid chromatography. 32, 93

**HSQC** heteronuclear single quantum coherence. 42, 43, 44, 45

**IC<sub>50</sub>** half maximal inhibitory concentration. xi, xxv, 31, 32, 34, 35, 46, 47, 50, 51, 52, 53, 54, 55, 59, 63

**Ile** isoleucine. 9

**IR** infrared. 95

**J** coupling constants. 95

**KIE** kinetic isotope effect. 76

**KR** ketoreductase. 88, 89, 91, 92, 93

**KS** ketosynthase. 88, 91

**LC-MS** liquid chromatography–mass spectrometry. 21, 22, 69, 95

**Leu** leucine. 25, 29, 30, 38, 47, 49, 56, 74

**LiHMDS** lithium bis(trimethylsilyl)amide. 16, 17, 30, 77, 134, 193, 194

**M<sup>pro</sup>** main protease. xi, xii, xxiii, xxv, xxvii, 4, 5, 25, 27, 29, 32, 33, 34, 35, 36, 37, 38, 43, 45, 46, 47, 48, 50, 51, 52, 54, 55, 56, 57, 58, 63, 64, 65, 72, 74, 98, 100

**mCPBA** *meta*-chloroperbenzoic acid. 11, 16, 17, 111, 112, 127

**MERS** Middle East respiratory syndrome. 24, 27

**MERS-CoV** Middle East respiratory syndrome-related coronavirus. 5

**mRNA** messenger RNA. 25



**MsCl** methanesulfonyl chloride. 11, 19, 210

**MT** methyltransferase. 88, 89, 91, 92, 93

**NMI** *N*-methylimidazole. 11, 19

**NMR** nuclear magnetic resonance. xi, xxv, 4, 9, 39, 42, 59, 60, 61, 62, 77, 79, 85, 95

**OBs** brosylate. xxiv, 12, 13

**OMs** mesylate. 12

**Phe** phenylalanine. 9, 47

**PKS** polyketide synthase. 5, 6, 88, 89, 90, 92, 94

**PL<sup>pro</sup>** papain-like protease. 25

**RaNi** Raney Nickel. 69

**RNA** ribonucleic acid. 24

**SARS** severe acute respiratory syndrome. 24, 27

**SARS-CoV** severe acute respiratory syndrome coronavirus. xxiii, xxv, 5, 24, 27, 32, 34

**SARS-CoV-2** severe acute respiratory syndrome coronavirus 2. x, xi, xii, xxiii, xxv, xxvii, 4, 5, 24, 27, 29, 32, 34, 35, 36, 37, 38, 43, 45, 46, 47, 48, 50, 51, 52, 54, 55, 56, 57, 58, 63, 64, 65, 74, 98, 100

**Ser** serine. 25, 29, 37, 38

**SNAC** *N*-acetylcysteamine. 92, 93

**SPPS** solid phase peptide synthesis. xxiv, 3, 8, 9, 23, 32, 98, 99, 115

**SUMO** small ubiquitin-like modifier. 32, 34, 36

**TE** thioesterase. 88, 89

**TEMPO** (2,2,6,6-tetramethylpiperidin-1-yl)oxyl. 7

**TFA** trifluoroacetic acid. 30

**TGEV** transmissible gastroenteritis coronavirus. 5

**THF** tetrahydrofuran. 85

**TLC** thin-layer chromatography. 80

**TMS-Cl** trimethylsilyl chloride. 29, 133

**TOAC** 2,2,6,6-tetramethylpiperidine-*N*-oxyl-4-amino-4-carboxylic acid. 8

**Troc** 2,2,2-trichloroethoxycarbonyl. 13, 16

**Troc-Cl** 2,2,2-trichloroethoxycarbonyl chloride. xxvii, 13, 14

**Tyr** tyrosine. 9

**Tyr<sup>NO<sub>2</sub></sup>** 3-nitrotyrosine. 32

**UV** ultraviolet. 21

**Val** valine. 9

**Vero E6 cells** African green monkey epithelial cells. 36, 49

# Chapter 1

## Introduction

### 1.1 Background

Organic chemistry underpins countless aspects in our lives. Evolving from the early dyestuff and pharmaceutical industries in Europe, this field of chemistry has become a vibrant discipline that aims to solve problems including but not limited to energy storage, development of new materials, food production, and the treatment of diseases. Chemical biology, as the sub-discipline of organic chemistry applied to biological systems, aims to understand and rationally influence life processes and biological systems using chemical tools. This thesis encompasses efforts to develop better tools for the understanding of protein structure, creating improved therapeutics for viral infection, and understanding how complex biomolecules are made. The unifying theme of this thesis is the utilization of small molecule chemistry to understand these aforementioned enzymatic systems, with a focus on modified amino acids and peptides, though some attention has also been directed towards polyketides.

Peptides, alongside their constituent amino acid subunits, constitute an incredibly important class of biomolecules. Connected as a repeating backbone of  $-\text{NH}-\text{CHR}-\text{C}(\text{O})-$  with (*S*)-stereochemistry (alongside the exception of L-cysteine which has an (*R*)-stereochemistry as a result of Cahn-Ingold-Prelog rules), peptides are responsible for numerous physiological

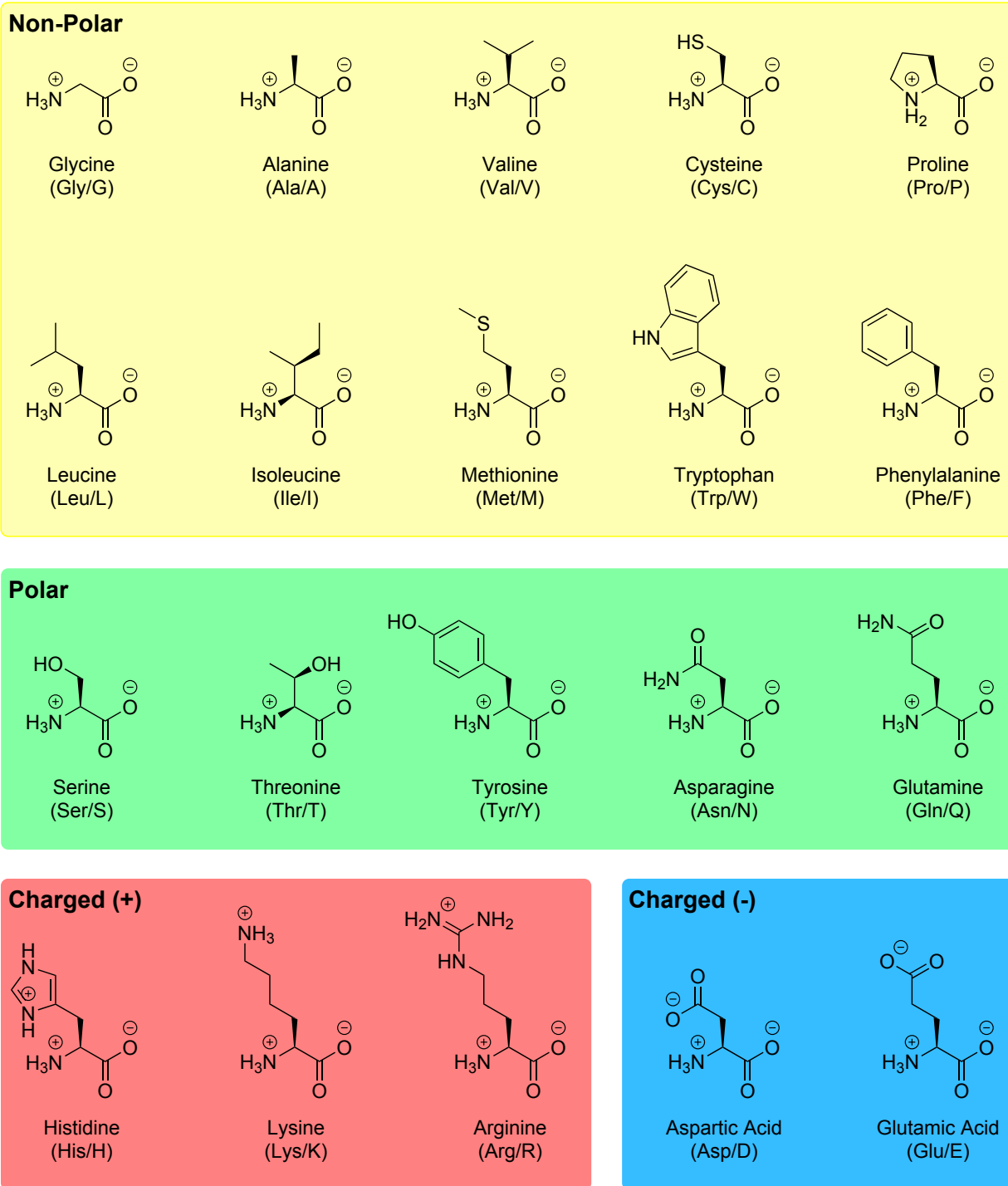


FIGURE 1.1: Chemical structures of the 20 canonical amino acids with charges shown at physiological pH, with three- and one-letter abbreviations shown in brackets.

roles in nature, with functions including but not limited to structural elements,<sup>1</sup> signalling molecules,<sup>2</sup> cellular machinery,<sup>3</sup> antibiotics,<sup>4</sup> toxins,<sup>5,6</sup> and medicines.<sup>7-9</sup> Being comprised of

20 distinct canonical structures with vastly varying steric and electronic properties as a result of differences in the R-group (Figure 1.1) mean that amino acids are a rich source of diversity and function in biological systems. This, coupled with their ubiquity in biology, means that these molecules (alongside their more complex polymeric forms as peptides and proteins) are uniquely poised as versatile handles and starting points in the investigation and manipulation of biological function and biochemical processes. These endeavours can be further expanded through the introduction and utilization of unnatural, modified, or non-canonical amino acids as a method to implement functions and characteristics that are not otherwise accessible. The following chapters detail how these unnatural amino acids are synthesized and utilized with varying goals.

## 1.2 Thesis Overview

Chapter 2 details a number of synthetic routes to access chiral spin labelled amino acids. Spin labels are molecules that contain stable, singly unpaired electrons which can be detected through methods such as electron paramagnetic resonance (EPR).<sup>10-12</sup> Furthermore, this can be extended to doubly spin labelled systems, and the interactions between the two different spin labels can be observed through double electron-electron resonance (DEER).<sup>13-16</sup> Application of this method to biological systems,<sup>17</sup> in particular to proteins, allows for the observation of conformational changes that are paramount to system function. Currently available, commercial spin labelled amino acids are often achiral, may be difficult to incorporate site-specifically in the protein of interest, and have the potential to disrupt the natural conformation of the protein of interest.<sup>18</sup> This chapter outlines our efforts to circumvent these issues by devising synthetic routes with the goal of accessing spin labelled amino acids that are chiral, allow for easier incorporation through SPPS or genetic methods, and aim to better replicate the structures of canonical amino acids found in nature. These routes involve strategies to either chirally form the crucial  $\alpha$ - $\beta$  C-C bond linking the amino acid backbone to the side chain, or to enantiomerically enrich the final products, depending on the spin

labelled side chain being targeted. This is then followed by evaluations of stereochemical purity in the products to determine the effectiveness of the aforementioned synthetic routes in furnishing a chiral product.

Chapter 3 deals with efforts to develop improved inhibitors targeting a key enzyme required in the replication life cycle of SARS-CoV-2. At the time of this work, COVID-19 posed a major health concern and burden on global healthcare systems, and a therapeutic was desperately needed. One of the key enzymatic processes that proved critical to SARS-CoV-2 replication in host cells was the post translational cleavage of long polyproteins that would eventually furnish the active proteins required for viral replication.<sup>19,20</sup> This process is carried out by an enzyme known as SARS-CoV-2 M<sup>pro</sup>, and by inhibiting this enzyme, viral proliferation can be halted. Initial work in this area involved the synthesis and evaluation of an inhibitor that proved to be effective as a therapeutic for a closely related feline coronavirus (FCoV) M<sup>pro</sup>.<sup>21,22</sup> Through enzymatic FRET based assays, cellular assays, and crystallographic studies as a result of extensive collaborative efforts with the groups of Dr. M. Joanne Lemieux (Department of Biochemistry, University of Alberta) and Dr. D. Lorne Tyrrell (Li Ka Shing Institute of Virology, University of Alberta), it was demonstrated that this peptide based inhibitor was both effective and non-toxic. Building upon this, improved peptide based inhibitors were synthesized and evaluated in similar fashion. These improved inhibitors can be induced to bind in the active site of SARS-CoV-2 M<sup>pro</sup> through an alternative mode of binding, resulting in a tighter fit and improved inhibition. Physical chemistry studies were also undertaken, detailing a possible method for administering bisulfite prodrugs of peptide aldehydes that would result in substantially improved solubility and greatly reduced dosing volumes. Additionally, NMR investigations into the stereochemistry of these inhibitors found that they readily interconvert in aqueous media, and that only a single stereoisomer binds in the M<sup>pro</sup> active site.

Chapter 4 provides a method to access a useful  $\gamma$ -lactam glutamine analog building block that is often utilized in the development of numerous antiviral agents.<sup>23-32</sup> A large number of virus families including *Picornaviridae* and *Coronaviridae* are positive strand RNA viruses

that possess proteases that cleave polyproteins required for viral replication at conserved peptide sequences involving a glutamic acid (Glu).<sup>20,23,33–35</sup> Cleavage of these polyproteins then furnishes peptide fragments involved in numerous processes including but not limited to RNA binding, cellular machinery for genetic replication, and RNA transcription.<sup>36</sup> A number of well known diseases are the result of viruses belonging to the picornavirus family such as foot and mouth disease, human rhinoviruses, and poliovirus.<sup>33</sup> In contrast, the coronavirus family contains within it a large number of diseases which affect both animals and humans such as transmissible gastroenteritis coronavirus (TGEV) which infects pigs, and SARS-CoV, Middle East respiratory syndrome-related coronavirus (MERS-CoV), and more recently, SARS-CoV-2 which causes COVID-19. The development of this improved synthetic route features scalability, improved yields, and inexpensive reagents as the main goals, alongside the requirement that the product be enantiomerically pure and functionally equivalent to that of the original.

Chapter 5 recounts efforts to circumvent predicted metabolic degradation of inhibitors investigated in Chapter 3 by cytochrome P450 enzymes. These enzymes work by using a heme-centered iron-oxo radical to cleave C–H bonds and install oxygen(s) in order to facilitate the degradation and expulsion of xenobiotic compounds.<sup>37,38</sup> At the time of this work, the orally active COVID-19 therapeutic Paxlovid<sup>™</sup> unveiled by Pfizer involved the coadministration of an active SARS-CoV-2 M<sup>pro</sup> inhibitor in combination with a P450 inhibitor.<sup>39</sup> As noted by Pfizer, one of the main sites of metabolic oxidation by P450 enzymes is at the methylene positions in the aforementioned  $\gamma$ -lactam ring,<sup>39</sup> a structure that is shared with our inhibitors. The aim of this project was to investigate methods to circumvent this oxidation, with possibilities involving deuterium, fluorine, or oxygen atom replacement at these methylene positions. Work in this chapter primarily focuses on oxygen replacement, which involved investigating synthetic methods in an attempt to incorporate the desired oxygen atom at the appropriate position. Work in this area remains ongoing.

Chapter 6 details investigations into the mechanisms of biosynthetic regulation in polyketide synthases (PKSs). The biosynthesis of polyketides relies on the repetitive processes of

acetate subunit condensation, substrate elongation, methylation, and reduction in a selective manner by PKSs containing numerous domains.<sup>40</sup> As a result, enzymatic control of when and if a particular chemical transformation occurs is of utmost importance in producing the correct natural product. At the moment, our hypothesis is that regulation of these complex biosynthetic systems is dictated by reaction kinetics. Essentially, at each stage of the biosynthetic process, the correct chemical transformation also happens to be the quickest to occur, resulting in the incorrect transformation being "outcompeted" and consequently not occurring. To investigate this hypothesis, the appropriate polyketide substrates and product standards used for feeding studies are synthesized. Additionally, select standalone domains from PKSs will be expressed. Kinetic assays will then be done in order to determine the effects that substrate variation has on reaction rates. Work in this area also remains ongoing.



## Chapter 2

# Synthesis of Chiral Spin Labelled Amino Acids

### 2.1 Introduction to Spin Labels

Spin labels are chemical moieties that contain stable unpaired electrons, often used in EPR experiments.<sup>10-12</sup> This technique, also known as electron spin resonance (EPS),<sup>10</sup> is a spectroscopic method to study paramagnetic compounds and has been extended to investigate biological systems,<sup>17</sup> particularly protein conformations,<sup>13,41,42</sup> via the pulsed-EPR technique known as DEER.<sup>13-16</sup> This technique works via measuring the interspin distances between two electrons, often by way of installing two spin labels at different positions,<sup>14,15,18,42,43</sup> and is effective in measuring distances ranging from 15 to  $>100$  Å.<sup>13,41,42</sup> In the case of proteins, this often involves the site-specific incorporation of spin labelled amino acids installed at various site-specific positions,<sup>18,42,44</sup> the triangulation of which allows for the measurement of three-dimensional conformational changes.<sup>45</sup> Another example of EPR being utilized in the study of biological systems are investigations into protein-ligand binding and interactions.<sup>46,47</sup> This application involves the use of a spin label pair, with one label situated on the protein itself and the other being a part of the ligand, revealing information regarding binding site positions and number, induced conformational changes, and binding affinity.<sup>46-48</sup>

Biological spin labels often involve the use of a (2,2,6,6-tetramethylpiperidin-1-yl)oxyl

(TEMPO) motif or derivatives thereof<sup>17,18,49</sup> and are commonly incorporated by selectively modifying, or using, modified amino acids. Examples of such include using cysteine residues as reactive handles for direct covalent attachment via alkylation (using spin label **1**) or disulfide bond formation (using spin label **2**) (Figure 2.1). While this is a viable method, a number of drawbacks remain. Firstly, the site-specific labelling of cysteine residues naturally becomes more difficult as the size and complexity of the protein target increases due to the greater likelihood of multiple cysteines being present. Additionally, this strategy may not be amenable for investigating enzyme-substrate interactions where the target protein contains a catalytic cysteine in the active site. Furthermore, the formation or disruption of native disulfide bonds required for the incorporation of spin labels such as **2** may result in deleterious effects on protein conformation and function. Finally, attachment of these spin labels results in the formation of lengthy and flexible side chains that may have a large degree of conformation freedom, an aspect that could lead to misrepresentations of interspin distances when compared to the native protein of interest.

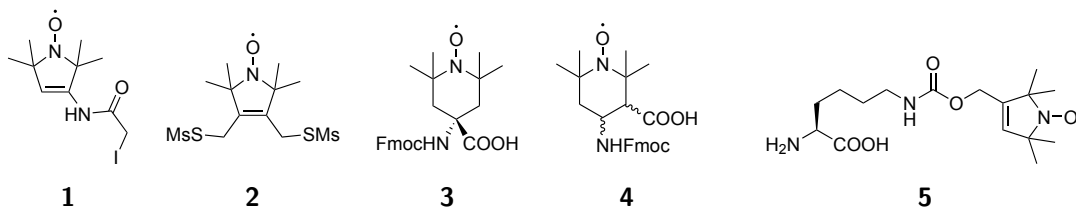


FIGURE 2.1: Examples of compounds used to site-specifically incorporate spin labels into peptides and proteins.

In light of this limitation, direct incorporation of unnatural amino acids onto the protein backbone presents an attractive alternative. Methods by which this is achieved involve utilizing amino acids amenable for SPPS, such as **3** and **4**, or genetic incorporation, such as **5**. Yet each of these also present their own difficulties. Commercially available 2,2,6,6-tetramethylpiperidine-*N*-oxyl-4-amino-4-carboxylic acid (TOAC) **3**, being  $\alpha,\alpha$ -disubstituted, is very rigid and therefore prone to inducing changes in protein conformation<sup>18</sup> while the  $\beta$ -amino acid **4** is stereochemically undefined. Unnatural amino acids can also be

incorporated by utilizing non-canonical tRNA/aminoacyl-tRNA synthetase pairs obtained from directed evolution,<sup>50-52</sup> as was done in the case of **5**.<sup>53</sup> However, all three examples (**3**, **4**, and **5**) lack resemblance to canonical amino acids, and in the case of **3** and **4**, the difficulty associated with generating the appropriate tRNA/aminoacyl-tRNA synthase pairs is increased.

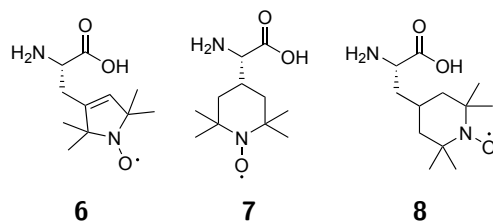


FIGURE 2.2: Chiral spin labelled amino acids for labelling proteins and peptides via SPPS or genetic incorporation.

In an attempt to alleviate these issues, three amino acids (Figure 2.2) were synthesized with the goal of better resembling canonical amino acids, with compounds **6**, **7**, and **8** corresponding to histidine (His), valine (Val), and isoleucine (Ile)/phenylalanine (Phe)/tyrosine (Tyr) respectively. While the synthesis of chiral  $\alpha$ -amino acids is well documented,<sup>54-56</sup> the synthesis of these target compounds presents unique challenges. Firstly, the presence of a nitroxyl radical significantly broadens NMR signals, rendering the acquisition of structural information difficult. The readily available starting material 2,2,6,6-tetramethyl-4-piperidinone (**9**) is tetrasubstituted on the carbons adjacent to the nitrogen (Figure 2.3), readily enabling protonation of nitrogen and consequent cation formation and ring opening through elimination reactions. This nitrogen atom can be protected through *N*-acylation (providing compound **10**). However, these derivatives are prone to deprotonation at the  $\alpha$ -position under basic conditions, consequently leading to elimination of the *N*-acyl functionality, generating compounds such as **11**. As such, the syntheses of these compounds must be done under relatively mild conditions.

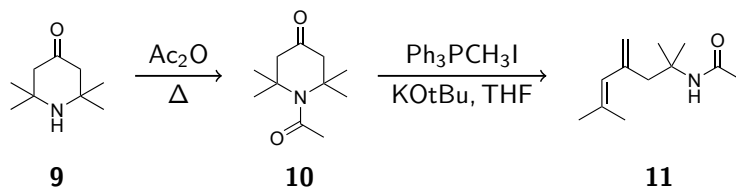
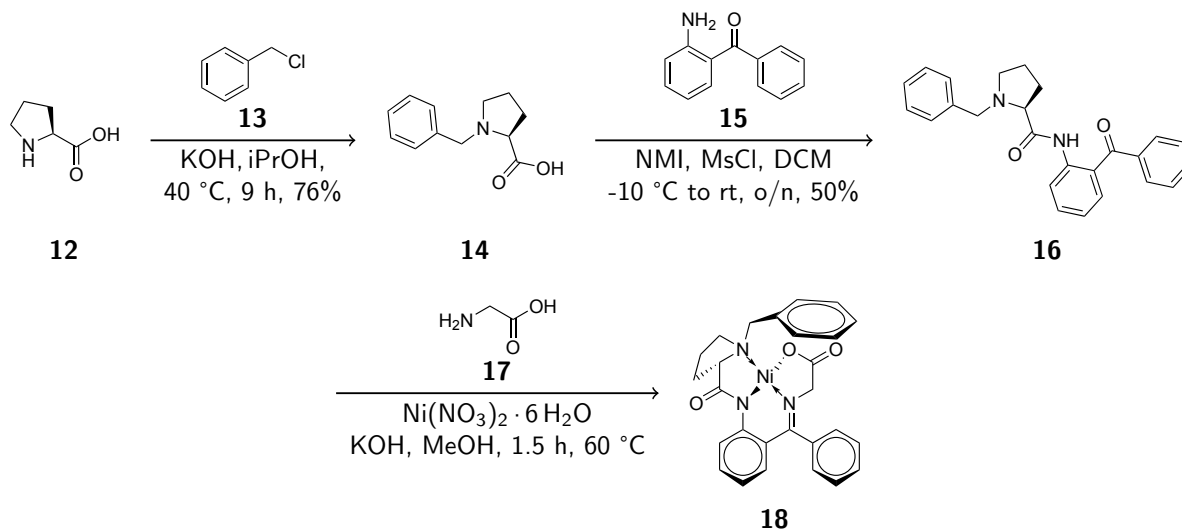


FIGURE 2.3: Decomposition of *N*-acetyl protected 2,2,6,6-tetramethyl-4-piperidinone under basic conditions

## 2.2 Synthetic Approach

The general synthetic approach taken towards the target compounds **6**, **7**, and **8** involve the attachment of an electrophilic side chain to the nucleophilic  $\alpha$ -carbon of a glycine (Gly) derivative. The method of attaching the electrophile to generate compound **6** was stereoselective, while the generation of compounds **7** and **8** was accomplished by an achiral bond formation between the  $\alpha$ - and  $\beta$ -carbons followed by a deracemization procedure.

## 2.3 Synthesis of Compound 6

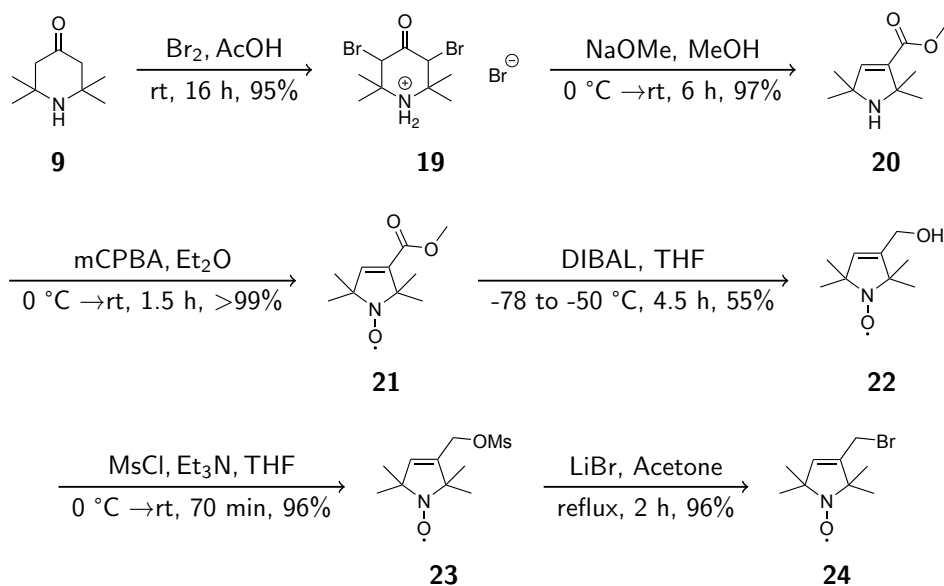


SCHEME 2.1: Synthetic route towards Belokon complex (**18**)

The synthetic route towards compound **6** began with the synthesis of Belokon complex (**18**), which functions as a chiral glycinate. Synthesis of Belokon complex (**18**) was initially

achieved by *N*-benzylation of **12** using benzyl chloride (**13**) to furnish **14**. This intermediate was then further conjugated to 2-aminobenzophenone (**15**) through mesyl chloride mediated amination in the presence of *N*-methylimidazole (NMI) to furnish compound **16**. Subsequent incubation of **16** with glycine (**17**) and Ni(NO<sub>3</sub>)<sub>2</sub> · 6 H<sub>2</sub>O in the presence of base and methanol then yielded the desired Belokon complex (**18**) (Scheme 2.1).

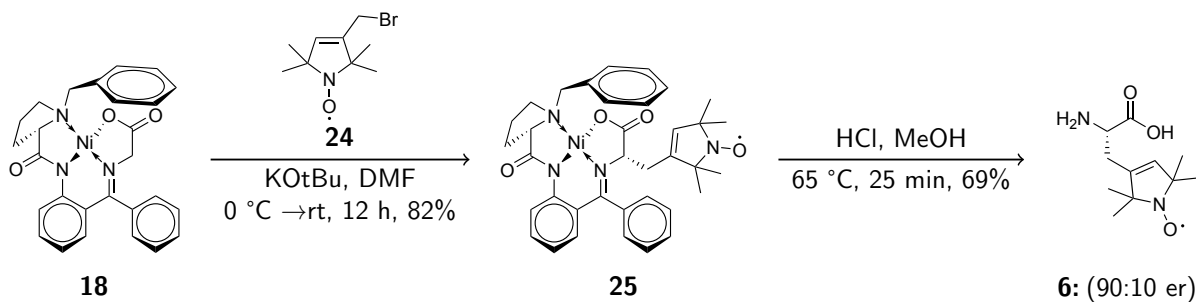
Next, the appropriate electrophile was synthesized starting from commercially available 2,2,6,6-tetramethyl-4-piperidinone (**9**), which was dibrominated to furnish **19**. This compound was then subjected to a Favorskii rearrangement, yielding compound **20**. Following this with *N*-oxidation using *meta*-chloroperbenzoic acid (mCPBA) then provides nitroxide radical **21**, which was reduced to alcohol **22** using diisobutylaluminium hydride (DIBAL). Mesylation with methanesulfonyl chloride (MsCl) then furnished compound **23** (Scheme 2.2).



SCHEME 2.2: Synthetic route towards 5-membered ring electrophile (**24**)

At this point, both the Belokon complex (**18**) and mesylate **23** were handed over to Dr. Randy Sanichar. Compound **23** was subjected to bromide substitution which then provides the desired electrophile **24** ready for alkylation onto **18**. The final alkylation procedure as well as determining the enantiomeric ratio (er) of the resultant amino acid **6** were also performed by Dr. Randy Sanichar. This key step was then done by first deprotonating a

solution of **18** in dimethylformamide (DMF) using KOtBu followed by dropwise addition of **24** as a DMF solution, furnishing **25**. Hydrolysis of the imine bond in **25** then releases the desired chiral spin labelled amino acid **6** in an er of 90:10 (Scheme 2.3), as determined by Marfey's assay<sup>57</sup> (see Table 2.1 in Section 2.5).



SCHEME 2.3: Alkylation of Belokon complex **18** to furnish spin labelled amino acid **6**.

## 2.4 Synthesis of Compounds **7** and **8**

The initial synthetic approach towards spin labelled amino acids **7** and **8** was largely the same. However, direct alkylation of various 2,2,6,6-tetramethyl-4-piperidinone derived electrophiles onto **18** did not give the desired products. Instead, it was observed that the acidic conditions required for cleavage of the alkylated Belokon complexes yielded a number of degradation products involving protonation of the piperidinone nitrogen followed by subsequent cation formation at the adjacent carbon and ring opening (Figure 2.4a). This is slightly mitigated by acylating the nitrogen, however derivatives containing a small leaving group (e.g. mesylate (OMs) or bromide) at the 4-position in the ring are subject to elimination upon exposure to the basic conditions required for alkylation (Figure 2.4b). It was eventually found that this issue could be eliminated by installing a large leaving group at the 4-position in the form of a OBs. As a result of its large steric bulk, the OBs leaving group would be forced to remain in an equatorial position, therefore diminishing the possibility of elimination reactions as the requisite adjacent anti-periplanar hydrogens would no longer be as available (Figure 2.4c).

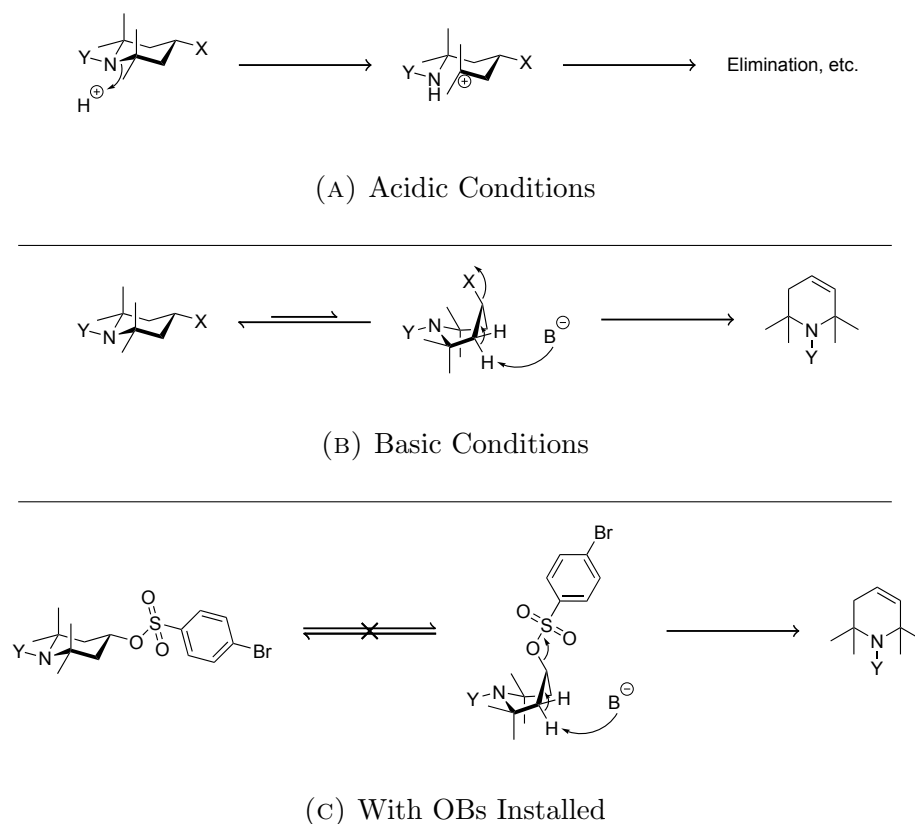
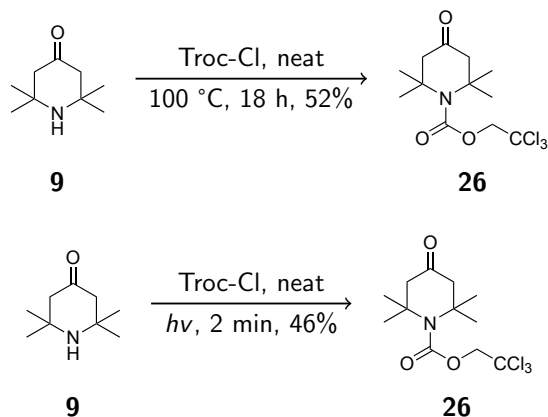


FIGURE 2.4: Degradation pathways of 2,2,6,6-tetramethyl-4-piperidinone derived electrophiles and mitigation via OBs utilization.

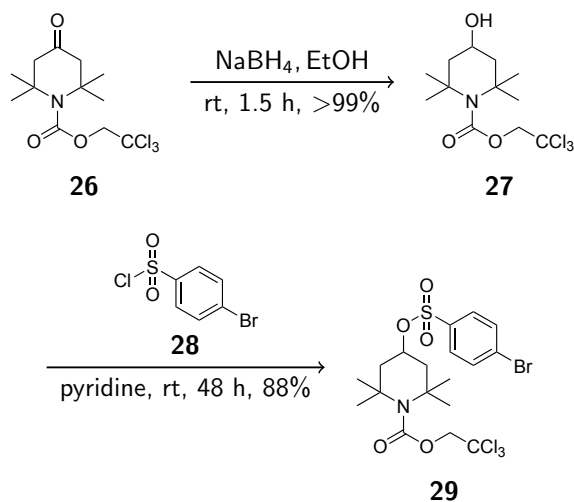
Moving forward, the nitrogen atom was protected using a 2,2,2-trichloroethoxycarbonyl (Troc) group, as it is amenable to removal under mild reducing conditions (Zn/AcOH) without the need for direct attack of the hindered *N*-acyl carbonyl carbon. With these major issues resolved, we went about synthesizing the appropriate electrophiles required for forming the two 6-membered ring side chains. Synthesis of both electrophiles began with the Troc protection of 2,2,6,6-tetramethyl-4-piperidinone (**9**) with Troc-Cl to furnish Troc-protected piperidinone **26**. This is accomplished via two different methods: 1) 2,2,6,6-tetramethyl-4-piperidinone (**9**) can be dissolved in neat Troc-Cl and heated at 100 °C for 18 hours (Scheme 2.4, Top); or 2) A mixture of 2,2,6,6-tetramethyl-4-piperidinone (**9**) and Troc-Cl can be subjected to microwave irradiation for 2 minutes (Scheme 2.4, Bottom), with both methods providing the desired product **26** in comparable yields.

Next, the two different 6-membered ring electrophiles were synthesized. The synthetic



SCHEME 2.4: Protection of 2,2,6,6-tetramethyl-4-piperidinone (**9**) using Troc-Cl.

route towards the 6-membered ring electrophile **29** was developed with the help of Fabricio Mosquera-Guagua, while I developed the route towards and synthesized the extended 6-membered ring electrophile **33**.

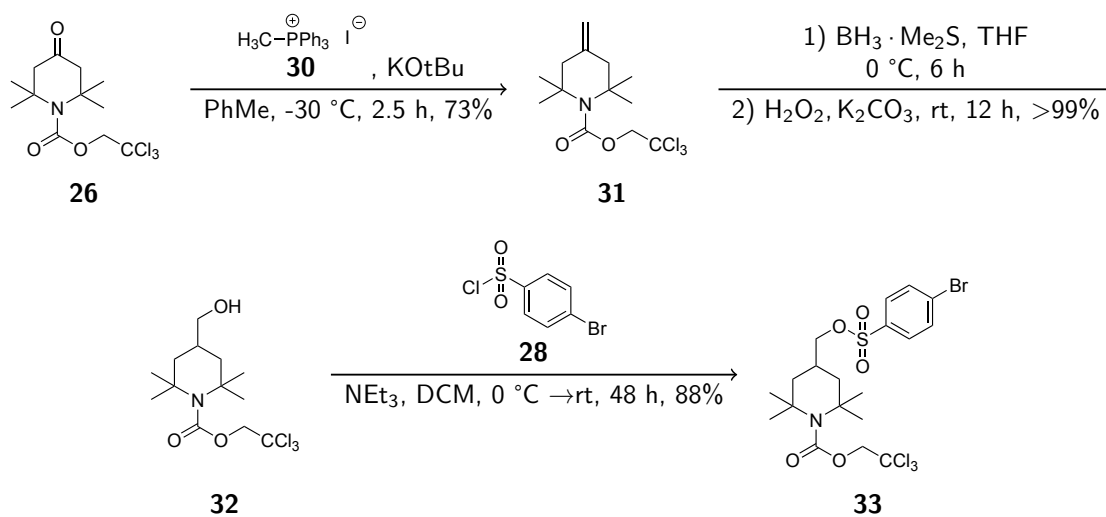


SCHEME 2.5: Synthesis of 6-membered ring electrophile **29**.

Electrophile **29** was obtained by reducing the ketone in compound **26** to produce alcohol **27**. This was then brosylated using *para*-bromophenylsulfonyl chloride (BsCl) to provide electrophile **29** (Scheme 2.5). Electrophile **33** was synthesized by homologating ketone **26** by a Wittig reaction using **30** to obtain alkene **31**. This step was performed with very careful control of reaction times, addition rates, and temperatures, otherwise significant

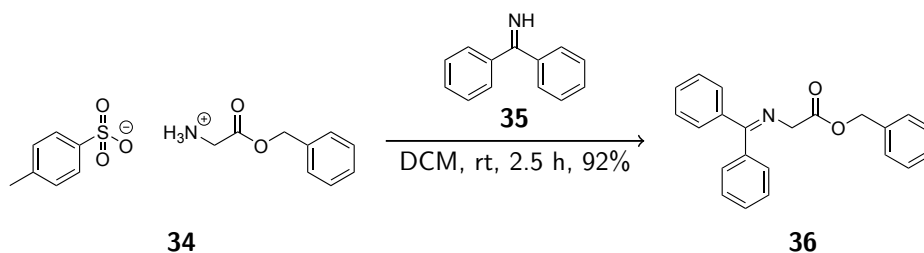


decomposition and ring opening of the product occurs, resulting in harshly diminished yields. Alkene **31** was then hydroborated to give the primary alcohol **32**, which was then brosylated using BsCl to give the extended 6-membered ring electrophile **33** (Scheme 2.6).



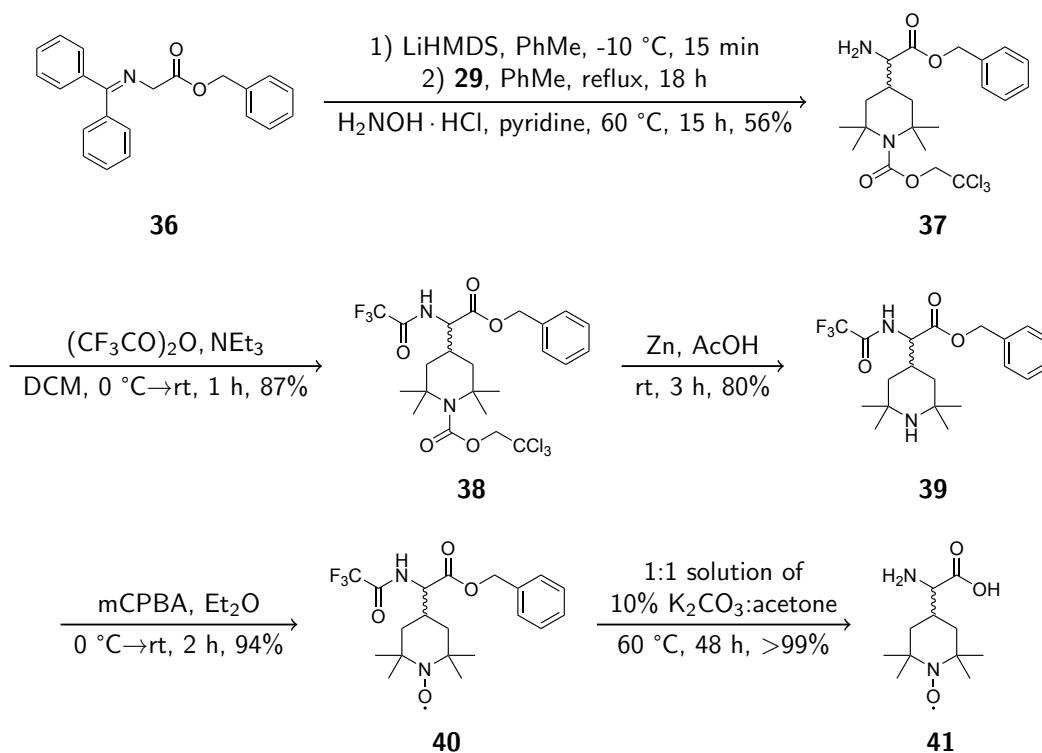
SCHEME 2.6: Synthesis of extended 6-membered ring electrophile **33**.

With both electrophiles now synthesized, we attempted to alkylate Belokon complex **18** as was previously done using electrophile **24**, however none of the desired product was obtained. It was hypothesized that this was due to the large amount of steric bulk on both the nucleophile and electrophiles. As a result, we opted to form the  $\alpha$ - $\beta$  carbon bond in the final amino acids via a less sterically hindered but non-stereospecific alkylation procedure followed by a deracemization protocol using a ligand developed by Soloshonok and coworkers<sup>58</sup> to furnish the desired chiral amino acids. In order to do this, the protected glycine **36** was synthesized by protecting **34** using benzophenone imine (**35**)<sup>59</sup> (Scheme 2.7).



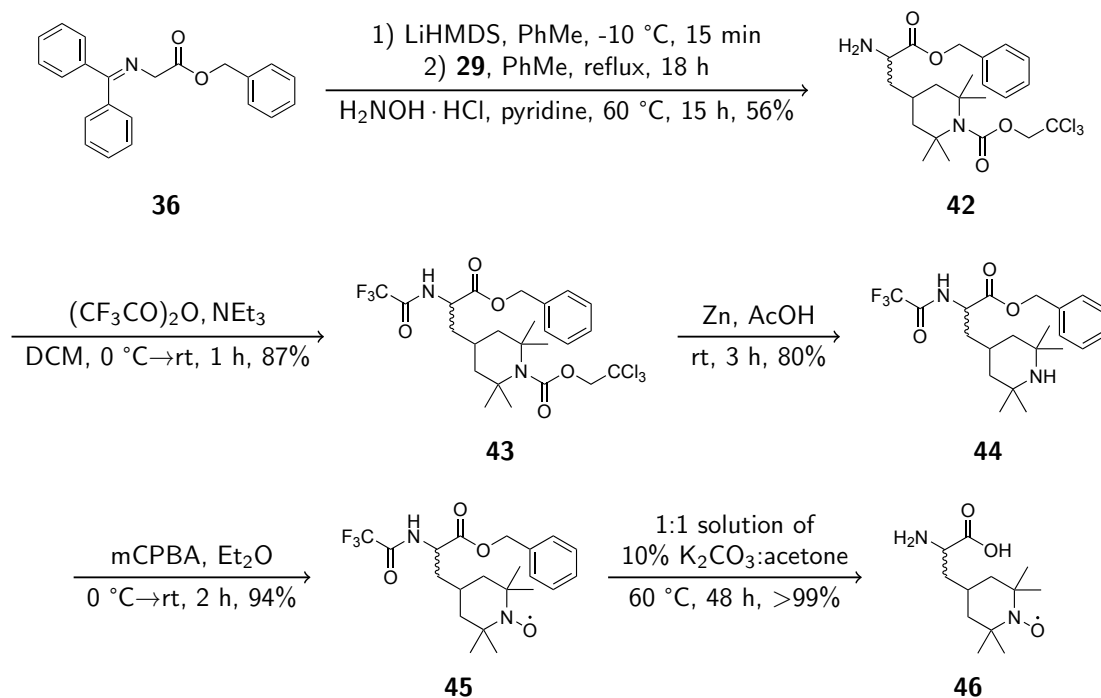
SCHEME 2.7: Synthesis of protected glycine **36**.

Protected glycine **36** was then utilized in an alkylation reaction with electrophile **29** facilitated by lithium bis(trimethylsilyl)amide (LiHMDS), followed by removal of the benzophenone imine protecting group via transimination to facilitate protecting group exchange, providing the benzyl ester protected amino acid **37** as a racemic mixture. The free nitrogen was then reprotected using trifluoroacetic anhydride to provide compound **38**. This protecting group exchange is necessary as the upcoming nitrogen oxidation step adds oxygens to electron rich amines, and the trifluoroacetyl group prevents *N*-oxidation from occurring at the incorrect position by way of its electron withdrawing effect while still being relatively easy to remove under mild hydrolysis conditions. The Troc group on **38** was then removed under mildly reductive conditions to provide **39**, which was then oxidized to the nitroxide radical **40** using mCPBA. Finally, gentle hydrolysis under basic conditions furnishes the racemic spin labelled amino acid **41** (Scheme 2.8).



SCHEME 2.8: Synthesis of racemic 6-membered ring amino acid **41**.

Synthesis of extended 6-membered amino acid **46** was done in an identical fashion (Scheme 2.9).



SCHEME 2.9: Synthesis of racemic extended 6-membered ring amino acid **46**.

Next, the synthesis of a kinetic resolution ligand developed by Soloshonok and coworkers<sup>58</sup> was done. This method works by forming a nickel complex akin to Belokon complex **18** which then undergoes repeated protonation-deprotonation cycles, with the reprotonation step happening selectively onto a single face. Over time, this process results in the favoured formation of a single stereoisomer in a process known as dynamic kinetic resolution (DKR). Consequently this allows for the formation of an amino acid with a desired chirality from an initially racemic form (Figure 2.5).

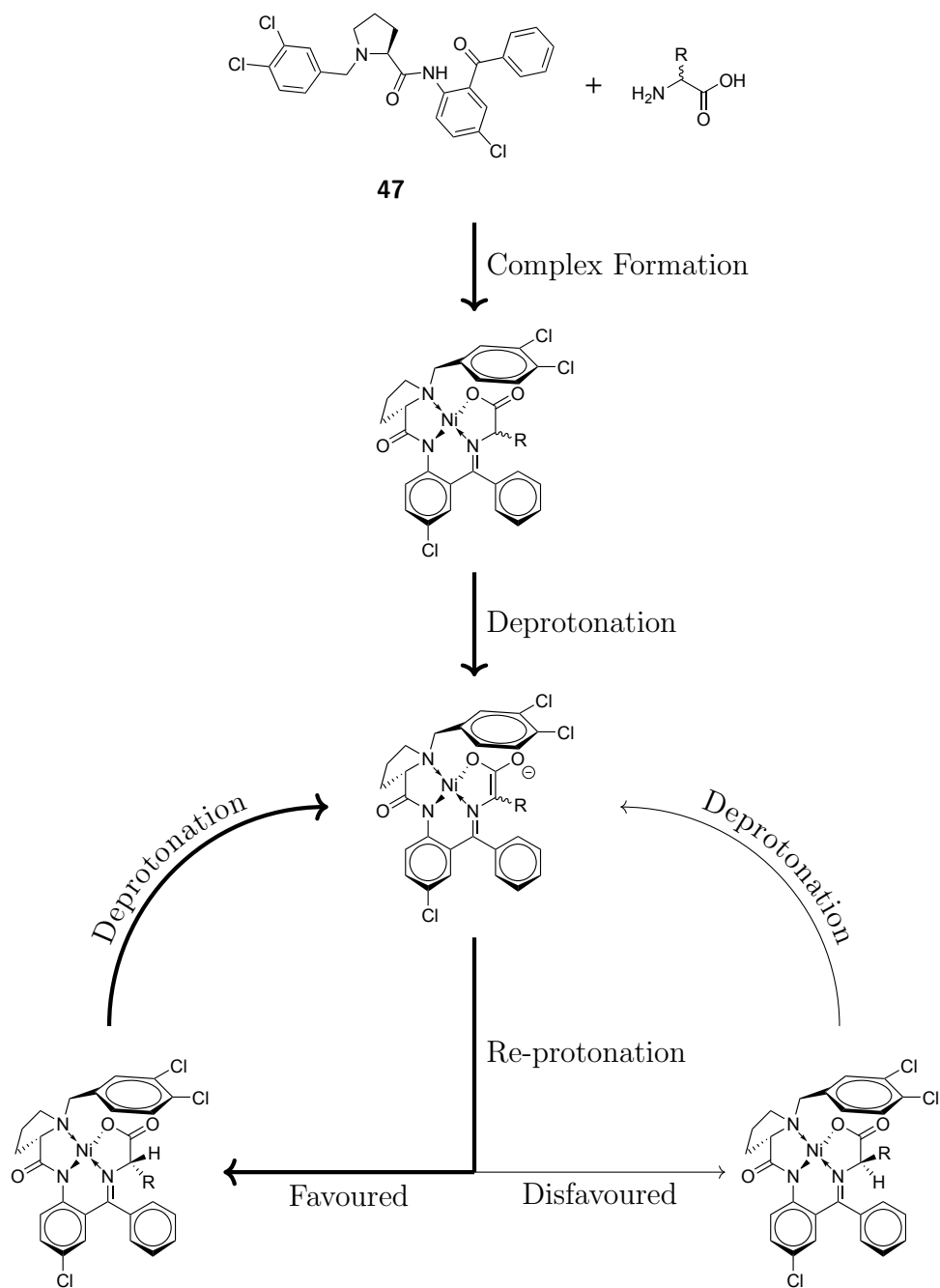
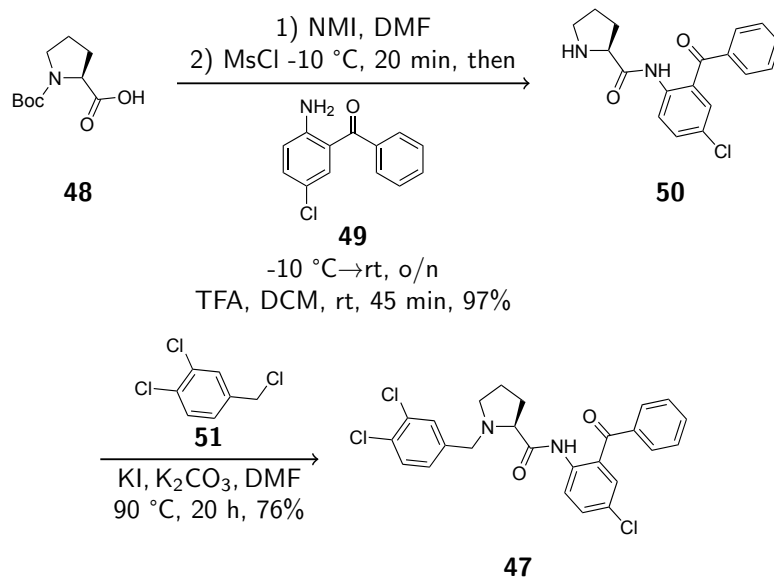


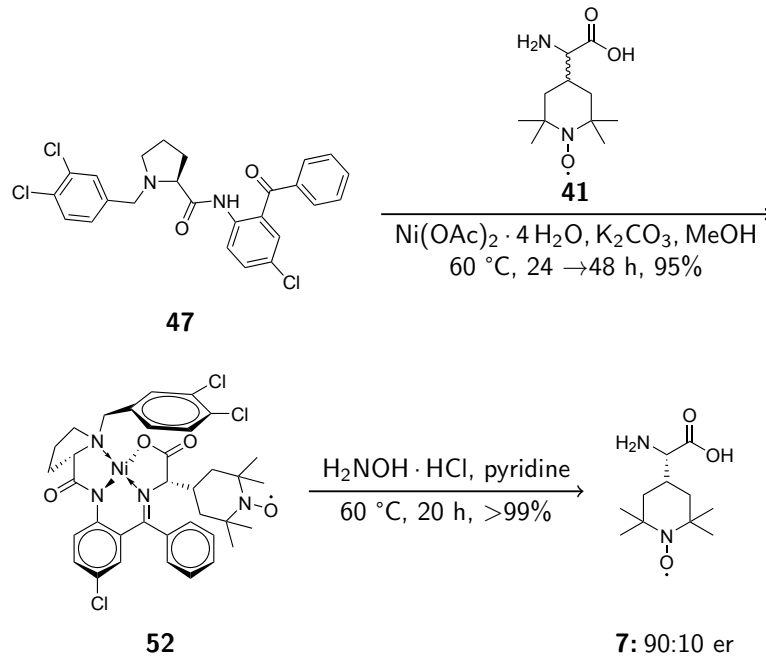
FIGURE 2.5: Dynamic kinetic resolution process utilizing Soloshonok ligand **47** to obtain enantiomerically enriched amino acids.

The synthesis of the Soloshonok ligand **47** is accomplished using similar reactions as those used for the synthesis of compound **16**, albeit in a different order, which was found to increase yields (Scheme 2.10).

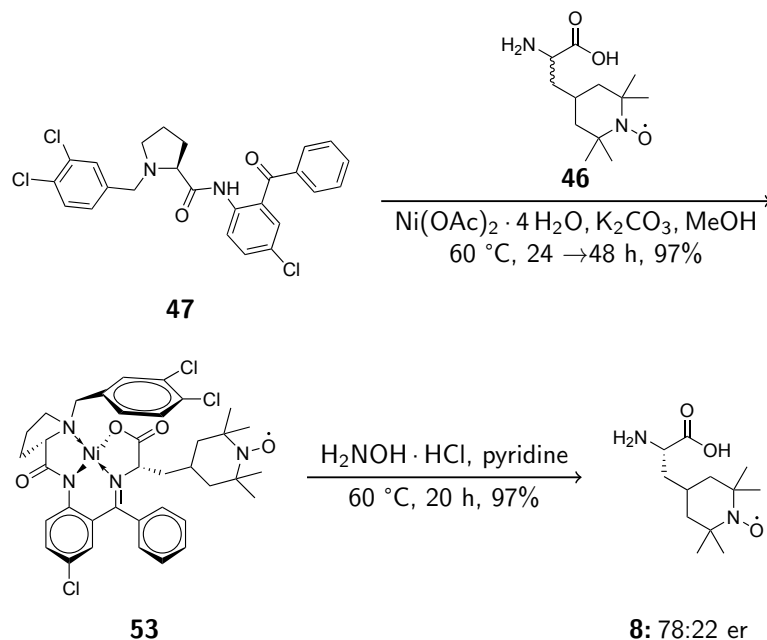


SCHEME 2.10: Synthesis of Soloshonok ligand (**47**).

With the required Soloshonok ligand **47** synthesized, both amino acids **41** and **46** were deracemized via DKR as shown in Schemes 2.11 and 2.12.



SCHEME 2.11: Deracemization of racemic amino acid **41** to furnish chiral spin labelled amino acid **7**.



SCHEME 2.12: Deracemization of racemic amino acid **46** to furnish extended chiral spin labelled amino acid **8**.

Deracemization times for the complex ranged from 24 to 48 hours, however stereochemical enrichment appeared to experience diminishing returns after 24 hours, with better enantiomeric ratios at the cost of slightly reduced yields for longer reactions. Near-quantitative disassembly of the Soloshonok nickel complexes **52** and **53** was accomplished using  $\text{H}_2\text{NOH} \cdot \text{HCl}$  via a transimination reaction, yielding amino acids with S:R er values of 90:10 and 78:22 for **41** and **46**, respectively, as determined by Marfey's assay<sup>57</sup> (see Table 2.1 in Section 2.5).

## 2.5 Enantiopurification of Amino Acids **6**, **7**, and **8** Using

### D-amino acid oxidase and Evaluation by Marfey's Assay

With all three chiral spin labelled amino acids (**6**, **7**, and **8**) in hand, we wanted to see if it is possible to further improve the enantiomeric ratio of these compounds, as while the er values were quite good, they were not perfect. In order to accomplish this, compounds **6**, **7**, and **8** were subjected to reaction with D-amino acid oxidase (DAAO). This involves an

enzyme catalyzed process that enables the separation of D- and L-amino acids by selectively transforming D-amino acids into  $\alpha$ -keto amino acids<sup>60,61</sup> (Figure 2.6).

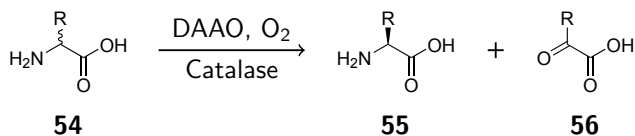
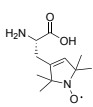
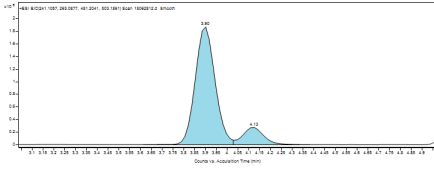
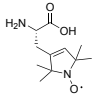
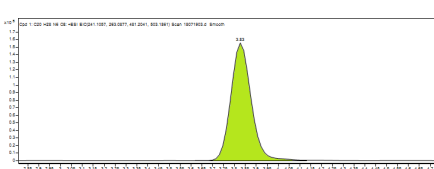
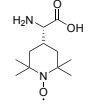
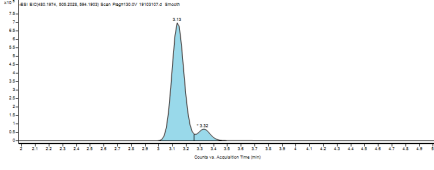
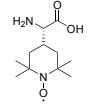
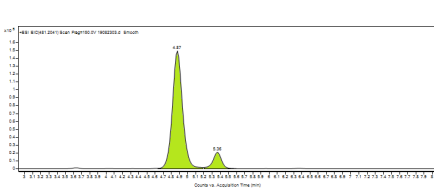
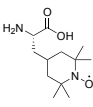
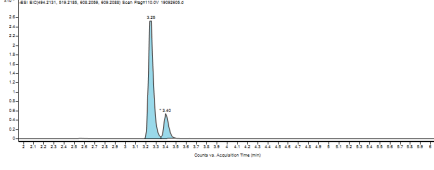
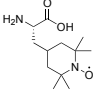
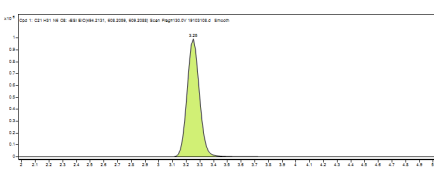
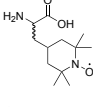
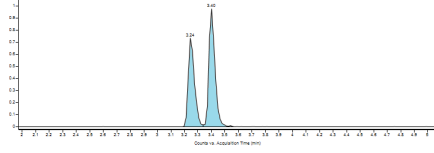


FIGURE 2.6: Selective transformation and degradation of D-amino acids into  $\alpha$ -keto acids using D-amino acid oxidase.

This procedure furnished enantiomerically pure samples for **6** and **8**, however failed to transform **7**. A possible reason for this outcome is that **7** failed to fit into the enzyme active site of DAAO, as the the side chain of this amino acid is quite bulky and somewhat rigid. All samples before and after exposure to D-amino acid oxidase (DAAO) were subjected to Marfey's assay<sup>57</sup> to determine enantiomeric purity of the resultant compounds and verify that the DAAO purification procedure had worked as intended. The assay was analyzed by liquid chromatography–mass spectrometry (LC-MS) analysis to determine said ratios via ultraviolet (UV) absorbance (Table 2.1).

TABLE 2.1: Stereochemical ratios of amino acids **6**, **7**, and **8** before and after selective degradation by DAAO.

Compound	LC-MS Spectra	Ratio (L/D)
 <b>6</b>		90/10
 <b>6: Post-DAAO</b>		>99/1
 <b>7</b>		90/10
 <b>7: Post-DAAO</b>		90/10
 <b>8</b>		78/22
 <b>8: Post-DAAO</b>		>99/1
 <b>46: Control</b>		44/56



## 2.6 Conclusion

In conclusion, a synthetic route towards chiral spin labelled amino acids **6**, **7**, and **8** was developed. This route furnishes amino acids **6** and **8** that better resemble canonical structures found in nature, with the additional goal of being amenable towards incorporation via SPPS or genetic incorporation. Compound **7** may be amenable towards genetic incorporation but would likely require further enantiopurification via chiral chromatography or stereoselective co-crystallization with a chiral salt prior to use in SPPS. In all, these amino acids more closely resemble the steric bulk and natural conformations of amino acids found in nature, facilitating more accurate EPR measurements and better replication of structural dynamics once incorporated into proteins. At the time of this writing, these spin labels have been sent to collaborators (Oliver Ernst, University of Toronto, and Lei Wang, University of California San Francisco) for genetic incorporation into proteins of interest.

## Chapter 3

# Development of Peptidomimetic Therapeutics Towards COVID-19

### 3.1 Introduction to SARS-CoV-2 and COVID-19

The end of 2019 and beginning of 2020 marked the beginning of the global COVID-19 pandemic, with over 521 million confirmed cases and 6.3 million deaths at the time of this writing.<sup>62</sup> The causative agent, SARS-CoV-2 contrasts the more deadly but less virulent SARS-CoV responsible for the initial severe acute respiratory syndrome (SARS) outbreak of 2002-2003 with 8000 cases and 774 deaths worldwide.<sup>63</sup> Common between both diseases is that the causative agents both belong to the coronavirus family of viruses.

#### 3.1.1 Coronaviruses - Characteristics and Lifecycle

Coronaviruses (CoVs) are a family of viruses responsible for a number of diseases in mammalian and avian species including but not limited to diarrhea, common cold, respiratory illness, and demyelinating encephalitis that range in severity from mild to lethal.<sup>20,64-66</sup> In regards to humans, diseases known to be caused by coronaviruses include SARS, Middle East respiratory syndrome (MERS), and COVID-19.<sup>25,34,67-69</sup> These viruses contain a single strand of positive-sense ribonucleic acid (RNA) as the genome and are contained within a viral envelope.<sup>70,71</sup> This positive-sense RNA strand is responsible for encoding two overlapping

polyproteins: pp1a and pp1ab (Figure 3.1).

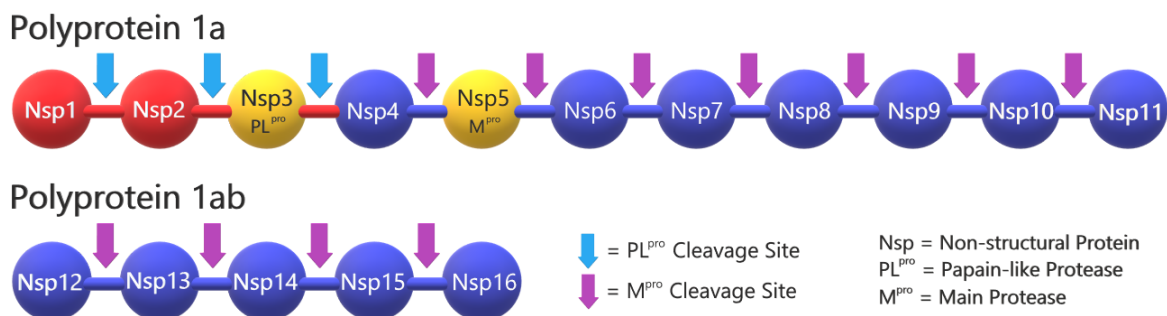


FIGURE 3.1: Schematic structure and protease cleavage sites of polyproteins pp1a and pp1ab.

Both are translated from the same viral messenger RNA (mRNA) sequence, with a ribosomal frameshift during the production of pp1a resulting in translation proceeding through the whole length of the mRNA and consequent production of the elongated polyprotein pp1ab instead.<sup>19</sup> These polyproteins need to undergo cleavage by an appropriate protease in order to release the individual functional proteins necessary for viral replication.<sup>20</sup> In particular, two proteases are responsible for cleaving the aforementioned polyproteins: the papain-like protease (PL<sup>pro</sup>) and the M<sup>pro</sup> (alternatively known as the 3-chymotrypsin-like protease (3CL<sup>pro</sup>)), responsible for cleavage at 3 and 11 positions respectively.<sup>20</sup> In particular, M<sup>pro</sup> cleaves at a known and conserved M recognition sequence: Leu-Gln↑Ser-Ala-Gly, with the cleavage occurring between the Gln and serine (Ser) residues as denoted by ↑.<sup>20</sup> Due to the critical importance of M<sup>pro</sup> in the viral replication cycle, it presents a prominent role as a target in the development of antiviral therapeutics.<sup>20,26,33,66,72–78</sup>

### 3.1.2 Protease Inhibitors as Therapeutic Agents

Examples of protease inhibitors as therapeutic agents are not limited to antivirals, as numerous compounds are now or have been used in clinical settings to treat conditions and diseases both inside and outside of viral infections. Select examples include Tipranavir for the treatment of human immunodeficiency virus (HIV), Boceprevir for hepatitis C, Captop-

pril (an angiotensin converting enzyme (ACE) inhibitor) for hypertension, Ximelagatran for thrombosis, and Rupintrivir for rhinoviruses (Figure 3.2).<sup>20,79–82</sup>

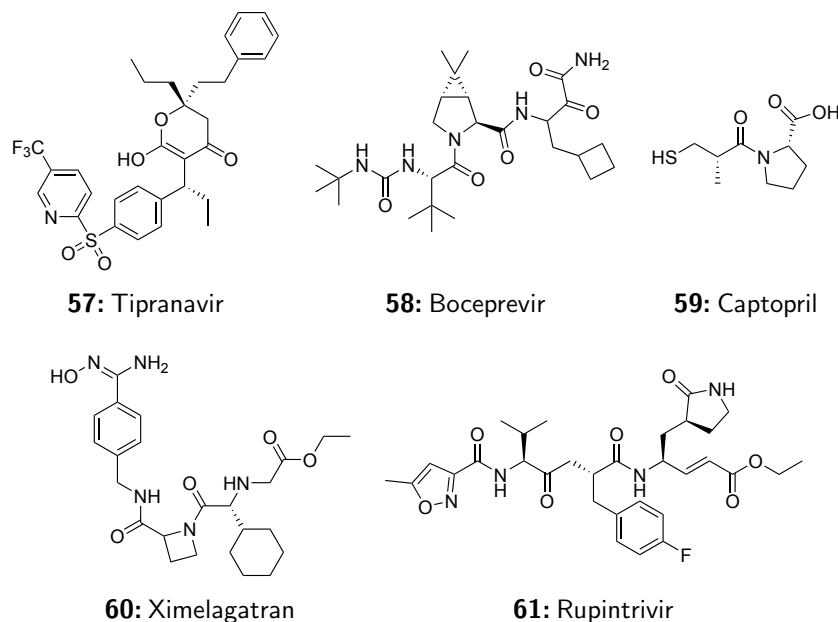


FIGURE 3.2: Select examples of protease inhibitors developed for therapeutic use.

There are a number of considerations when developing protease inhibitors, particularly in that they should have low toxicity, be adequately soluble for administration, and be reversible in nature.<sup>8</sup> Of particular importance is the need for reversibility, with a distinct example being **61** (an irreversible Michael acceptor of reactive sulfhydryls in cysteine proteases) failing to pass clinical trials as a consequence of limited efficacy.<sup>20</sup> Irreversible inhibitors have numerous drawbacks including off-target reaction with numerous mammalian thiols (e.g. glutathione) leading to destruction or premature excretion of the inhibitor. Additionally, errant reactions with host proteins also leads to the potential for build up of toxic byproducts or the undesired triggering of host immune responses. A possible solution for this issue is the use of covalent inhibitors that are reversible in nature, such as those containing aldehyde warheads. Upon binding to the active site cysteine in a protease, aldehydes can form reversible hemithioacetal moieties that are preferentially stabilized by the enzyme active site, in contrast to instances of off-target binding where the resultant hemithioacetal

is far less stable.<sup>73</sup> An additional advantage of aldehyde based inhibitors is the potential to reversibly derivatize them to bisulfite adducts which possess substantially higher water solubility. These bisulfite adducts can then be administered as prodrugs which spontaneously revert to the active aldehyde form under physiological conditions.<sup>76</sup>

### 3.1.3 Repurposing a Feline Coronavirus Drug

A number of years ago, the Vederas lab was involved in the development of peptide based antiviral inhibitors that targeted cysteine proteases using an aldehyde warhead.<sup>73</sup> Later on, these compounds were investigated as possible inhibitors against the M<sup>pro</sup> of SARS-CoV during the initial SARS outbreak of 2003.<sup>72</sup> Following these investigations, Groutas and coworkers subsequently investigated the use of peptide aldehydes in 2012 as protease inhibitors against FCoV, in particular against feline infectious peritonitis virus (FIPV).<sup>33</sup> In felines, FCoVs generally causes only mild illness, but FIPV in particular can lead to feline infectious peritonitis (FIP), a disease state that often presents itself in kittens and carries with it a near absolute fatality rate.<sup>33</sup> This disease led to the development of the peptide aldehyde inhibitor GC373 (**62**) and its bisulfite prodrug GC376 (**63**) (Figure 3.3) by Groutas and coworkers,<sup>21</sup> which was shown to inhibit FIPV replication and successfully treat FIP while being well tolerated in cats.<sup>22</sup> Further studies demonstrated that it also possessed broad spectrum activity and was effective inhibiting feline, ferret, and mink coronaviruses.<sup>22,66,83</sup>

Precedence of broad spectrum effectiveness was extended to human coronaviruses when in 2018 a co-crystal structure of GC376 **63** in the active site of MERS was published, showcasing the formation of a covalent bond between the active site cysteine of the MERS M<sup>pro</sup> and the acyl carbon of the aldehyde warhead.<sup>84</sup> More recently, reports of the M<sup>pro</sup> of SARS-CoV-2 co-crystallized with a number of peptide-based  $\alpha$ -ketoamide inhibitors have surfaced,<sup>24</sup> along with related reports of repurposing other compounds such as anticancer agents as M<sup>pro</sup> inhibitors. While holding promise as potential inhibitors, these reports failed to demonstrate the use of these compounds as coronavirus inhibitors in animal models. In response to this, we surmised that it would be possible to repurpose GC376 (**63**) as an inhibitor of the

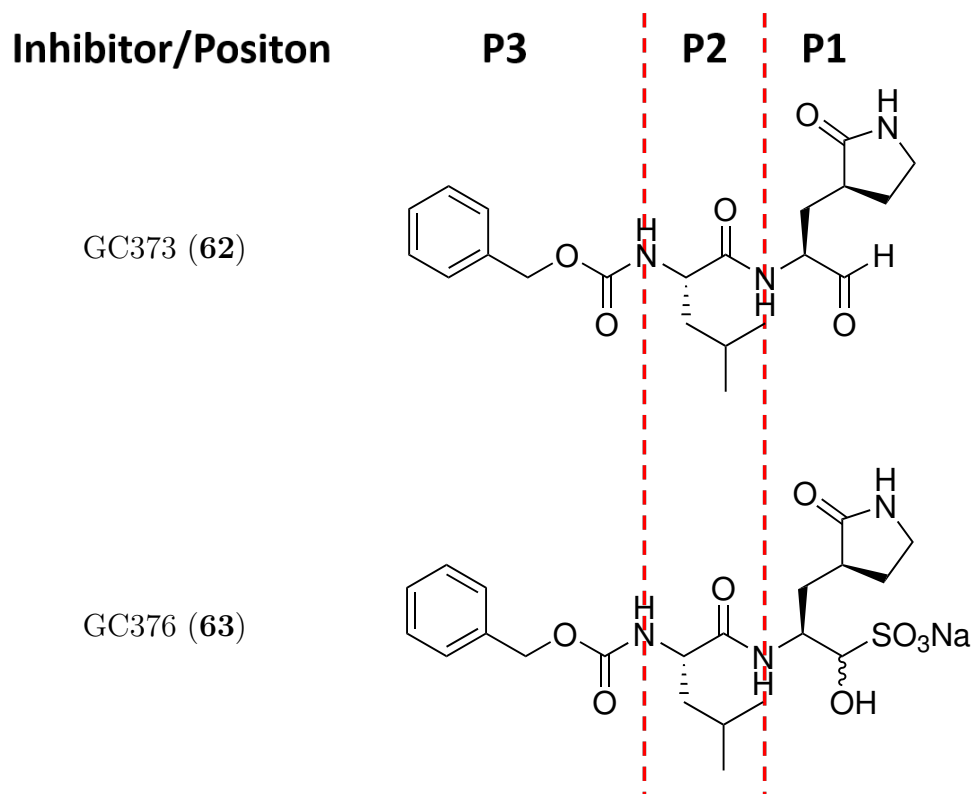


FIGURE 3.3: Structures of GC373 (**62**) and GC376 (**63**) and positions within these inhibitors.

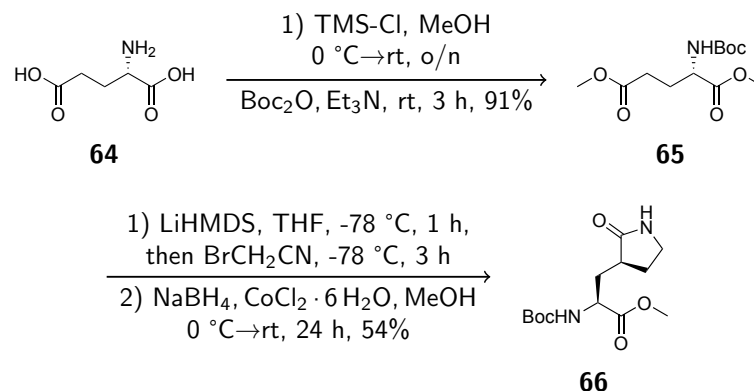
SARS-CoV-2 M<sup>pro</sup> owing to a number of factors: 1) The M<sup>pro</sup> of FIPV and SARS-CoV-2 share a high degree of structural and sequence similarity; 2) GC376 (**63**) has been shown to be well tolerated in a number of animal models;<sup>22,66,83</sup> 3) A number of irreversible M<sup>pro</sup> inhibitors possess intense side effects when administered to human cells, but GC376 (**63**) (being reversible in nature) ought to be able to circumvent this issue; and 4) The SARS-CoV-2 M<sup>pro</sup> cuts at a conserved Leu-Gln↑Ser-Ala-Gly sequence, meaning that targeting it should selectively inhibit the virus with minimal detrimental effects toward healthy host cellular function. All of these characteristics in tandem position GC376 (**63**) for rapid advancement into clinical trials at the time of this work, and so we set out to investigate the potential repurposing of this FCoV drug as a therapeutic agent against COVID-19.

## 3.2 Evaluation of GC373 (**62**) and GC376 (**63**) as Potential SARS-CoV-2 M<sup>pro</sup> Inhibitors

### 3.2.1 Synthesis of GC373 (**62**) and GC376 (**63**)

Investigations began with the synthesis of GC373 (**62**) and GC376 (**63**), which first required the synthesis of the core  $\gamma$ -lactam glutamine analog required for recognition by the SARS-CoV-2 M<sup>pro</sup>. Synthesis of this glutamine analog was accomplished based on a literature procedure.<sup>32</sup> This began with the protection of free Glu using trimethylsilyl chloride (TMS-Cl) and methanol to form the dimethyl ester, which was further protected using di-*tert*-butyl dicarbonate (Boc<sub>2</sub>O) to give protected Glu **65**. Next, a stereoselective alkylation procedure developed by Hanessian and coworkers<sup>85,86</sup> was used along with bromoacetonitrile to alkylate compound **65**, followed by subsequent reduction using a NaBH<sub>4</sub>-CoCl<sub>2</sub> mixture to selectively reduce the nitrile group to a primary amine. Under these basic conditions, the amine spontaneously cyclizes onto the methyl ester to form  $\gamma$ -lactam **66** with defined stereochemistry. In our time working with this reaction, we observed that the intermediate nitrile formed after the alkylation reaction was difficult to isolate by flash column chromatog-

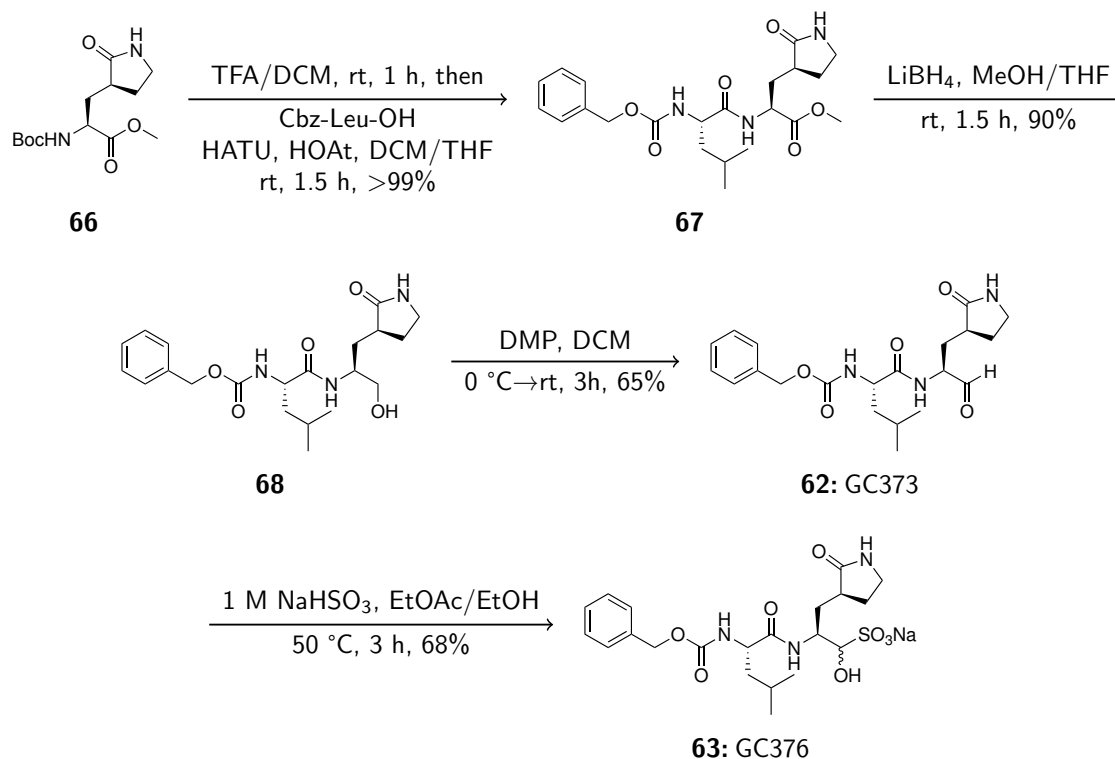
raphy over silica (FCC), often resulting in lowered yields when this was attempted. Instead, we observed that quickly subjecting the crude intermediate material to the subsequent reduction step after work up afforded increased yields. An alternative method to reduce the intermediate nitrile to the desired primary amine also exists in the form of PtO<sub>2</sub> catalysed hydrogenation at 50 psi. This is then followed up with Na<sub>2</sub>CO<sub>3</sub> mediated cyclization to afford the desired  $\gamma$ -lactam **66**. In our case we opted to proceed via the borohydride mediated approach as both the reduction and cyclization proceeds in a single step (Scheme 3.1).



SCHEME 3.1: Synthesis of analog **66**.

Next, compound **66** was deprotected using a trifluoroacetic acid (TFA)/dichloromethane (DCM) mixture and coupled to Cbz-Leu-OH using 1-[*N*-[(dimethylamino)-1*H*-1,2,3-triazolo-[4,5-*b*]pyridin-1-ylmethylene]-*N*-methylmethanaminium hexafluorophosphate *N*-oxide (HATU), 1-hydroxy-7-azabenzotriazole (HOAt), and diisopropylethylamine (DIPEA) under standard coupling conditions to afford methyl ester **67**. This compound was then reduced to the alcohol using LiBH<sub>4</sub> to furnish compound **68**. Subsequent oxidation of the hydroxyl group using Dess–Martin periodinane (DMP) then provides the aldehyde drug GC373 (**62**), with further derivatization using NaHSO<sub>3</sub> giving the prodrug GC376 (**63**) (Scheme 3.2).





SCHEME 3.2: Synthesis of GC373 (**62**) and GC376 (**63**) from glutamine analog **66**.

### 3.2.2 Evaluation of $\text{IC}_{50}$ Values for GC373 (**62**) and GC376 (**63**)

Afterwards, the  $\text{IC}_{50}$  values of GC373 (**62**) and GC376 (**63**) were measured via FRET assays. FRET is a mechanism by which energy is transferred between two chromophores, or light-sensitive molecules.<sup>87</sup> As depicted in Figure 3.4, this process involves the use of a chromophore pair, where the selective irradiation of the donor chromophore at a particular excitation wavelength ( $\text{Wavelength}_1$ ) then results in a non-radiative transfer of energy to an acceptor chromophore, which then fluoresces at its own emission wavelength ( $\text{Wavelength}_3$ ) (Figure 3.4b). Though this process is non-radiative in nature (i.e. there is no photon emission by the donor with subsequent photon absorption by the acceptor), it is paramount that there exists ample spectral overlap between the chromophore pair (i.e. the emission wavelength of the donor should closely match that of the acceptor).<sup>87</sup> Upon cleavage of the FRET substrate, the donor and acceptor pair experiences a subsequent increase in distance between them, and the non-radiative energy transfer event can no longer take place. This

results in the fluorescent emission of photons by the donor at its own emission wavelength (Wavelength<sub>2</sub>) instead (Figure 3.4c). Cleavage of the FRET substrate can be easily detected as the efficiency of the energy transfer phenomenon is inversely proportional to the sixth power of the distance between the chromophore pair; consequently this technique is extremely sensitive to even small changes in distance.<sup>87</sup>

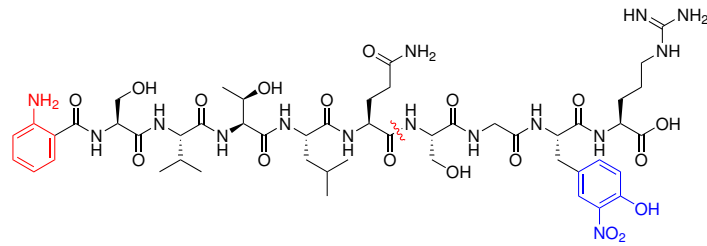
FRET substrate **69** (Figure 3.4a) was synthesized by myself using automated SPPS on a commercial peptide synthesizer and purified using high-performance liquid chromatography (HPLC) by Tess Lamer, a graduate student from our group. This amino acid sequence was chosen as it was identified via screening efforts by Blanchard et al. to be an excellent substrate mimic for the original SARS-CoV M<sup>Pro</sup> and additionally uses an Abz-Tyr<sup>NO2</sup> chromophore pair, which has been shown to be >10-fold more sensitive than the more commonly encountered EDANS-Dabcyl pairing.<sup>88</sup> Next, the M<sup>Pro</sup>s from both SARS-CoV and SARS-CoV-2 were expressed and purified by Dr. Marco van Belkum of our group as a small ubiquitin-like modifier (SUMO)-tagged fusion protein, as this allowed for the generation of native N- and C-termini along with being high-yielding and stabilizing in nature. Additional enzyme purification and IC<sub>50</sub> determination via FRET assays were accomplished by Dr. Conrad Fischer, also from our group. Starting off, various kinetic and catalytic parameters were determined for both M<sup>Pro</sup>s via FRET assays performed by Dr. Conrad Fischer. The results are tabulated in Table 3.1.

TABLE 3.1: Catalytic parameters of SARS-CoV and SARS-CoV-2 M<sup>Pro</sup>.

Protease	K <sub>0.5</sub> (μM)	k <sub>cat</sub> (min <sup>-1</sup> )	k <sub>cat</sub> /K <sub>0.5</sub> (min <sup>-1</sup> μM <sup>-1</sup> )	Hill Coefficient
SARS-CoV-2 M <sup>Pro</sup>	70 ± 10	135 ± 6	1.8 ± 0.4	2.2
SARS-CoV M <sup>Pro</sup>	52 ± 17	30 ± 2	0.6 ± 0.2	1.9

From the IC<sub>50</sub> experiments we found that both GC373 (**62**) and GC376 (**63**) inhibited the M<sup>Pro</sup> from both SARS-CoV and SARS-CoV-2 at nanomolar concentrations, with the compounds showing slightly greater effectiveness towards the SARS-CoV M<sup>Pro</sup> (Figure 3.5). Additionally, it was also observed that the bisulfite adduct form appeared to possess greater activity than that of the aldehyde, possibly owing to greater aqueous solubility. We observed

(A) Chemical structure of FRET substrate **69**

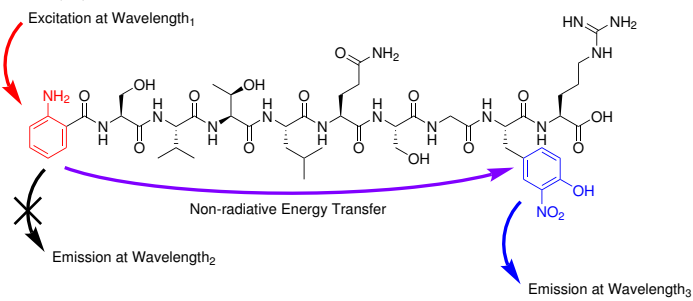


**69**

Red squiggle denotes cut site of M<sup>pro</sup>.

Legend: Fluorophore/Donor Quencher/Acceptor

(B) FRET substrate prior to cleavage by M<sup>pro</sup>



(C) FRET substrate after cleavage by M<sup>pro</sup>

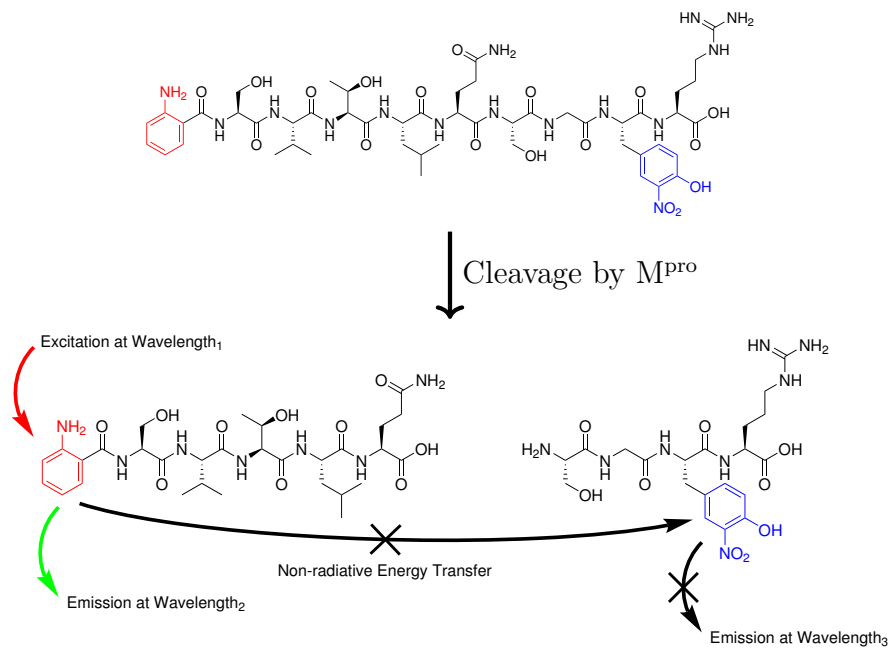


FIGURE 3.4: Structure of FRET substrate **69** and mechanism of action.

that the  $IC_{50}$  values for the SARS-CoV-2  $M^{pro}$  were  $0.40 \pm 0.05 \mu M$  and  $0.19 \pm 0.04 \mu M$  for GC373 (**62**) and GC376 (**63**), respectively. This outcome is in line with the values for broad-spectrum activity of these compounds against a number of other viruses. For reference, GC376 (**63**) has an  $IC_{50}$  value of  $0.49 \pm 0.07 \mu M$  against FCoV,  $1.33 \pm 0.19 \mu M$  against the ferret coronavirus (CoV), and  $1.44 \pm 0.38 \mu M$  against the mink CoV.<sup>66</sup> The  $IC_{50}$  values observed against the original SARS-CoV  $M^{pro}$  were  $0.07 \pm 0.02 \mu M$  and  $0.05 \pm 0.01 \mu M$  for GC373 (**62**) and GC376 (**63**), respectively, demonstrating slightly greater binding affinity. In comparison to other inhibitors being investigated at the time of this work, GC373 (**62**) and GC376 (**63**) were the most potent reversible compounds available. Examples of inhibitors being investigated at the time included ebselen **72**,<sup>89</sup> tideglusib **73**,<sup>89</sup> carmofur **74**,<sup>89</sup> disulfiram **75**,<sup>89</sup> shikonin **76**,<sup>89</sup> PX-12 **77**,<sup>89</sup> and an  $\alpha$ -ketoamide inhibitor **71** developed by Hilgenfeld and coworkers.<sup>67</sup> Liu and coworkers also reported an inhibitor containing an indole at the P3 position and an aldehyde warhead with  $IC_{50}$  values of  $0.053 \pm 0.005 \mu M$ , but contrasting GC376 (**63**), this compound was not yet demonstrated to be therapeutic in animals (Table 3.2).<sup>27</sup>

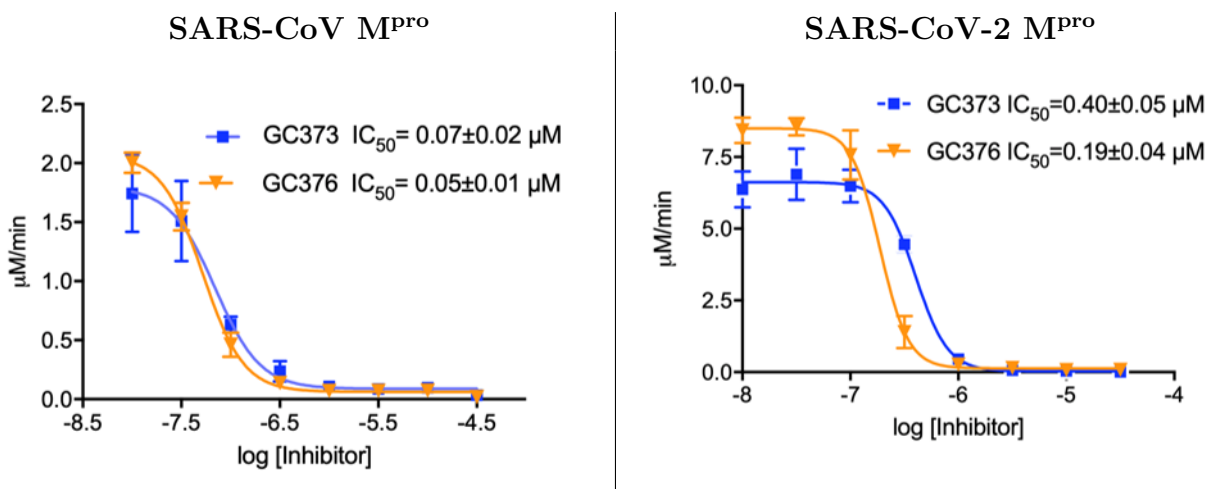
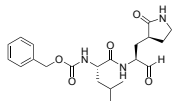
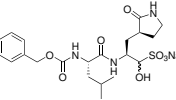
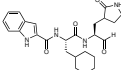
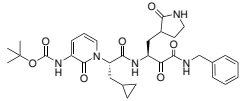
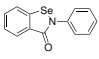
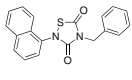
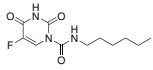
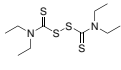
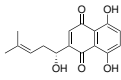
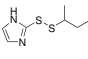


FIGURE 3.5: Evaluation of  $IC_{50}$  values for GC373 (**62**) and GC376 (**63**) against SARS-CoV and SARS-CoV-2  $M^{pro}$ .

Finally, it was found that dimerization of two  $M^{pro}$  monomers was required for activity, and that dimerization is prevented prior to SUMO tag cleavage as demonstrated by a lack

TABLE 3.2: Inhibition parameters of select reported SARS-CoV-2 M<sup>pro</sup> inhibitors.

Inhibitor	IC <sub>50</sub> (μM)	Cellular Assays (Cell Type)	Efficacy in Animals
 <b>62: GC373</b>	0.40 ± 0.05	Vero E6 (monkey) and A549 (human) <sup>25</sup>	No
 <b>63: GC376</b>	0.19 ± 0.04	Vero E6 (monkey) and A549 (human) <sup>25</sup>	Yes (mouse, cat, mink, ferret) <sup>21,66</sup>
 <b>70: Dai Inhibitor</b>	0.053 ± 0.005 <sup>27</sup>	Vero E6 (monkey) <sup>27</sup>	Yes (rat, dog) <sup>27</sup>
 <b>71: Hilgenfeld Inhibitor</b>	0.67 ± 0.18 <sup>67</sup>	Calu-3 (human) <sup>67</sup>	Yes (mouse) <sup>67</sup>
 <b>72: Ebselen</b>	0.67 ± 0.09 <sup>89</sup>	Vero E6 (monkey) <sup>89</sup>	No
 <b>73: Tideglusib</b>	1.55 ± 0.30 <sup>89</sup>	Vero E6 (monkey) <sup>89</sup>	No
 <b>74: Carmofur</b>	1.82 ± 0.06 <sup>89</sup>	Vero E6 (monkey) <sup>89</sup>	No
 <b>75: Disulfiram</b>	9.35 ± 0.18 <sup>89</sup>	Vero E6 (monkey) <sup>89</sup>	No
 <b>76: Shikonin</b>	15.75 ± 8.22 <sup>89</sup>	Vero E6 (monkey) <sup>89</sup>	No
 <b>77: PX-12</b>	21.39 ± 7.06 <sup>89</sup>	Vero E6 (monkey) <sup>89</sup>	No

of activity when utilizing SUMO-tagged M<sup>Pro</sup> in the FRET assays.

### 3.2.3 Evaluation of EC<sub>50</sub> and CC<sub>50</sub> Values for GC373 (**62**) and GC376 (**63**)

In collaboration with the group of Dr. D. Lorne Tyrrell, EC<sub>50</sub> and CC<sub>50</sub> values for these compounds were also determined. Plaque reductions assays were done by the Tyrrell group on African green monkey epithelial cells (Vero E6 cells), examining the number of plaque-forming units as a function of absence, presence, and concentration of GC373 (**62**) and GC376 (**63**). The EC<sub>50</sub> values determined for GC373 (**62**) and GC376 (**63**) were 1.5  $\mu$ M and 0.92  $\mu$ M respectively, as shown by the **hollow blue** circles in Figure 3.6. Cytotoxicity of these two compounds were also measured using both Vero E6 cells and human alveolar adenocarcinomic basal epithelial cells (A549 cells) and determined to be >200  $\mu$ M. These results are plotted in Figure 3.6 as well, with **filled blue** circles representing Vero E6 cells and **filled orange** circles representing A549 cells. Consideration of the determined EC<sub>50</sub> and CC<sub>50</sub> values provides a very favourable therapeutic index (CC<sub>50</sub>/EC<sub>50</sub>) of >200.

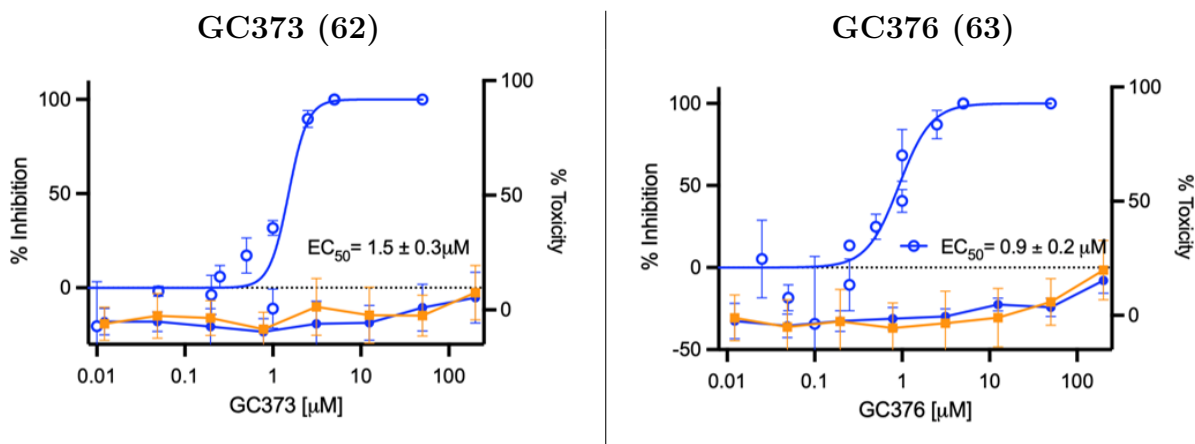
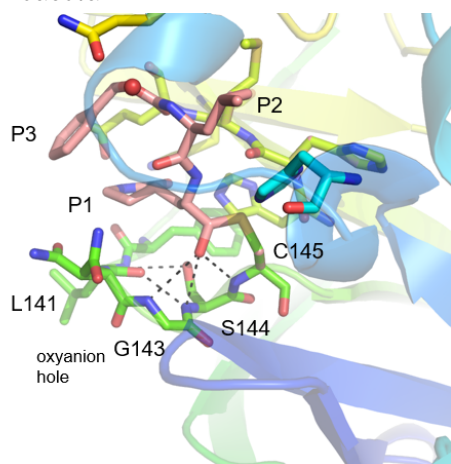


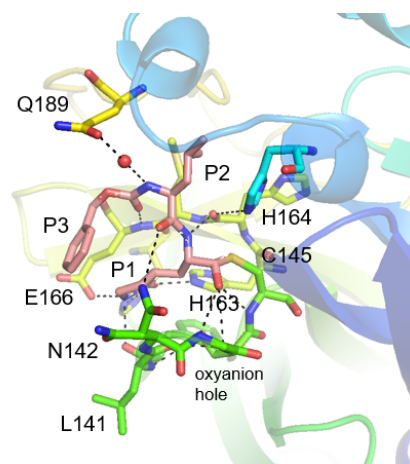
FIGURE 3.6: Evaluation of EC<sub>50</sub> and CC<sub>50</sub> values for GC373 (**62**) and GC376 (**63**) against SARS-CoV-2.

(A) Oxy-Anion Hole Stabilization of Hemithioacetal



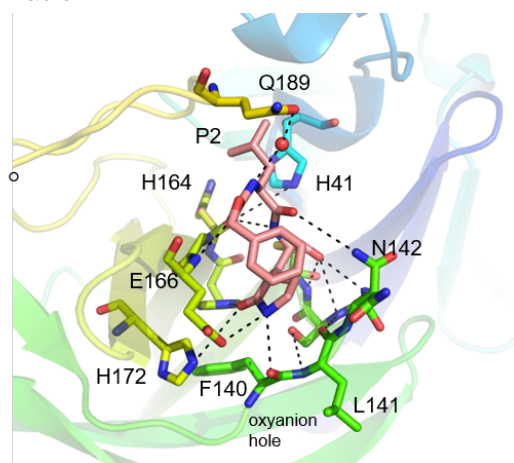
The hemithioacetal formed upon attack of the aldehyde warhead by cysteine (Cys)145 is stabilized by interactions between the oxygen and nearby backbone heteroatoms of Gly143, Ser144, and Cys145.

(B) Stabilization of Inhibitor P1, P2, and P3 Positions



The P1, P2, and P3 positions of the inhibitor are stabilized by a combination of hydrophilic and hydrophobic interactions with the S1 and S2 binding pockets as well as the S3 surface depression respectively.

(c) Alternative View of P1, P2, and P3 Stabilization



An alternative view (after a 90° eastward rotation) of interactions involved in inhibitor binding and stabilization is presented.

FIGURE 3.7: Co-crystal structures of GC376 (**63**) with the M<sup>pro</sup> of SARS-CoV-2.

### 3.2.4 Co-crystal Structures of GC373 (**62**) and GC376 (**63**) with SARS-CoV-2 M<sup>pro</sup>

Crystal structures were obtained by our collaborators in the lab of Dr. M. Joanne Lemieux. These structures further support the requirement of dimerization for full SARS-CoV-2 M<sup>pro</sup> activity. This was done by separately co-crystallizing both GC373 (**62**) and GC376 (**63**) with the M<sup>pro</sup> of SARS-CoV-2. From the crystal structures, we were able to observe that the crystal structures involving GC373 (**62**) were identical to that involving GC376 (**63**), demonstrating that the prodrug form does indeed spontaneously revert to the active aldehyde form prior to binding to the M<sup>pro</sup> active site in an (*S*)-configuration at both the aldehyde and adjacent  $\alpha$ -carbon. In regards to the enzyme, the active site consisted of a catalytic dyad involving Cys145 and His41, with the Cys being the nucleophile that attacks the aldehyde carbonyl to form the aforementioned hemithioacetal, and the His acting as a general base. Upon formation of the hemithioacetal, the oxygen is stabilized by an oxy-anion hole involving the enzyme backbone of the M<sup>pro</sup> at positions Gly143, Ser144, and Cys145 (Figure 3.7a). The Gln analog at the P1 position of the inhibitor was found to form hydrogen bonds with the side chains of His163 and Glu166 (Figure 3.7b) and hydrophobic interactions with His172 (Figure 3.7c), binding to the S1 position of the enzyme. The leucine (Leu) side chain at the P2 position of the inhibitor was found to bind to the S2 pocket of the enzyme (Figure 3.7b), while the benzyloxycarbonyl (Cbz) moiety in the P3 position of the inhibitor was found to form a hydrogen bond between the carbonyl and the nearby backbone amide of Glu166 (Figure 3.7c). Conversely, the aryl group of the Cbz was found to interact with a shallow surface depression of the M<sup>pro</sup>, dubbed the S3 position (Figure 3.7b). Of note is the nearby proximity of a significantly deeper binding pocket dubbed S4, which represents opportunities for further inhibitor development (Figure 3.7).



### 3.2.5 Stereochemical Investigations of GC373 (**62**) and GC376 (**63**) via <sup>13</sup>C-Labeling and NMR Spectroscopy

With promising inhibitory parameters determined for GC373 (**62**) and GC376 (**63**) we aimed to advance these compounds into clinical trials. In order to do this, regulatory bodies often require information regarding the stereochemical nature of the proposed therapeutic compounds. GC373 (**62**) and GC376 (**63**) are special in that we hypothesize that they exist in multiple stereoisomeric forms. In the case of GC373 (**62**), as it is a peptide aldehyde, it is hypothesized to form hydrates in aqueous media as well as epimerize at the  $\alpha$ -position adjacent to the aldehyde, as is known to be the case for other peptide aldehydes (Figure 3.8).<sup>73,90</sup> For GC376 (**63**), as the derivitization to the prodrug form from GC373 (**62**) is done in aqueous media, there should exist four different stereoisomers resulting from the epimeric position at the  $\alpha$ -carbon as well as the resultant hemithioacetal depending on which face of the aldehyde the bisulfite anion attacks during the formation step (Figure 3.9).

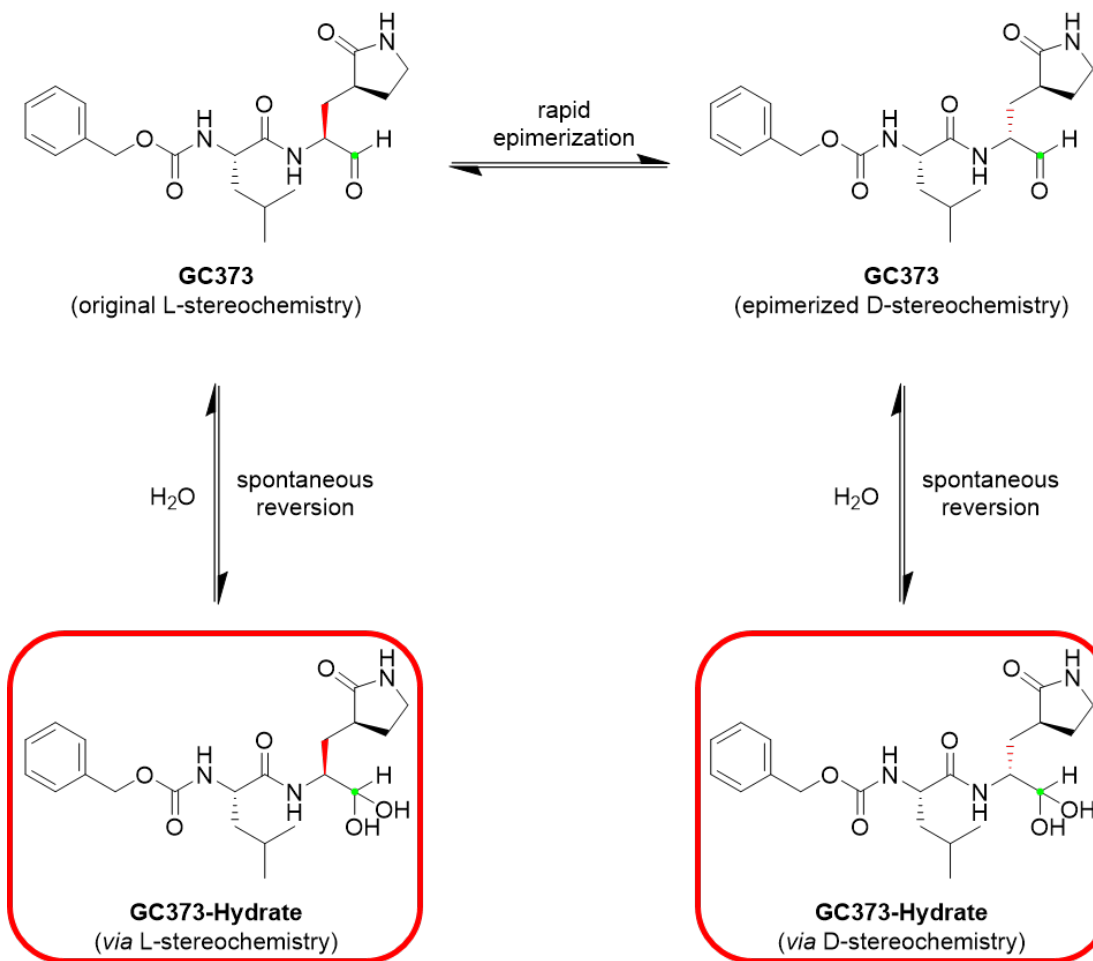


FIGURE 3.8: Possible stereoisomeric forms of GC373 (**62**) resulting from rapid  $\alpha$ -carbon isomerization and hydrate formation.

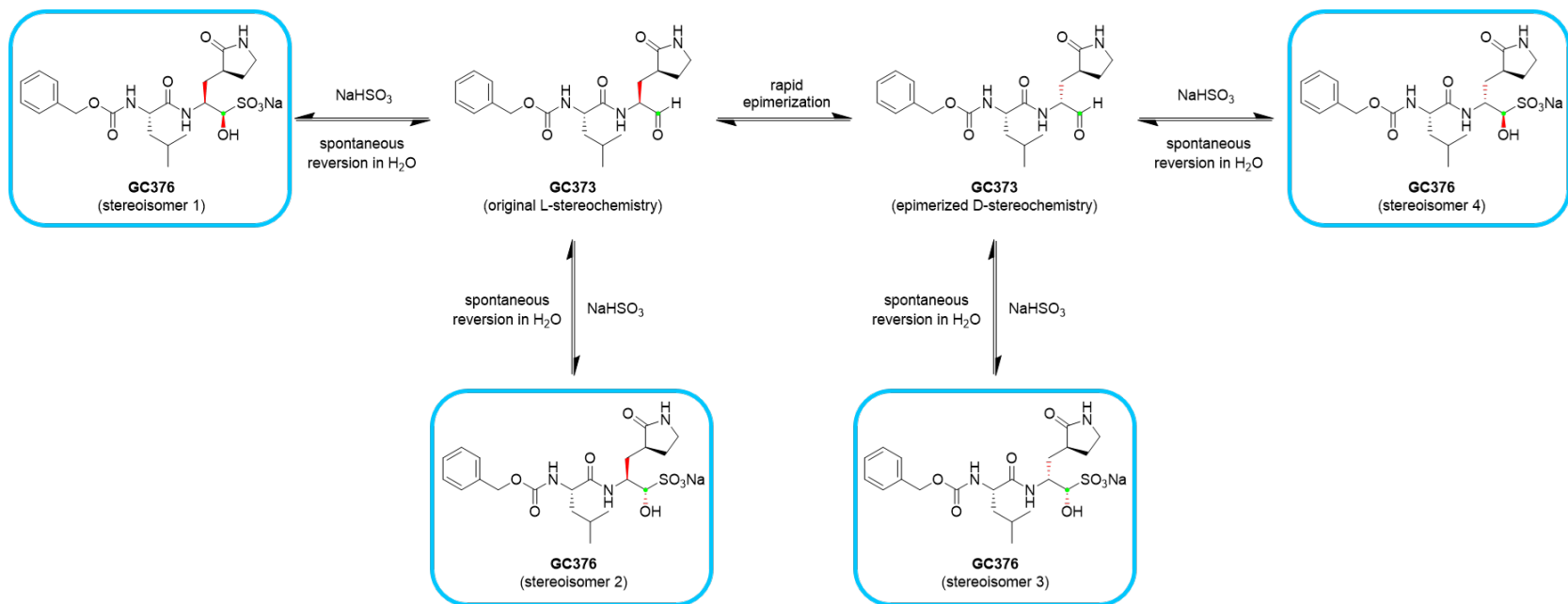


FIGURE 3.9: Possible stereoisomeric forms of GC376 (**63**) resulting from rapid  $\alpha$ -carbon isomerization and bisulfite adduct formation.

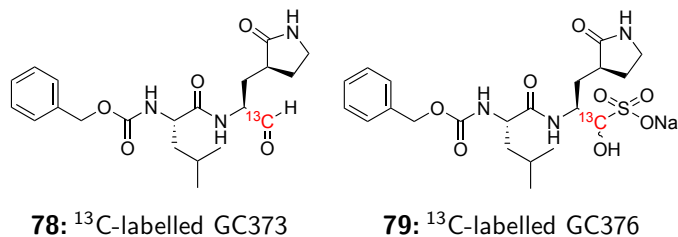


FIGURE 3.10: Structure of  $^{13}\text{C}$ -labelled GC373 (**78**) and GC376 (**79**).

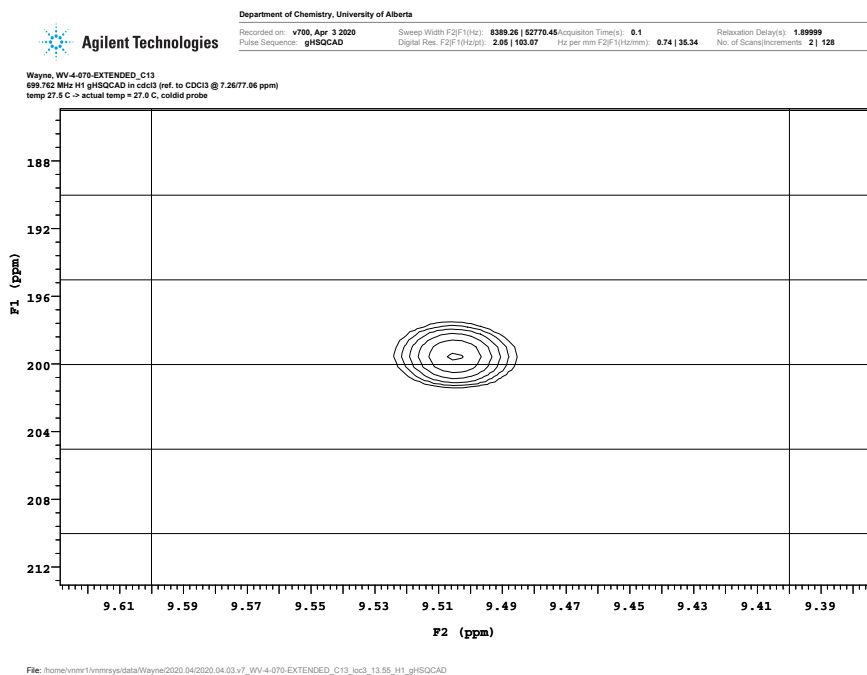
To verify this hypothesis, we sought to accomplish a number of goals via NMR spectroscopy using  $^{13}\text{C}$ -labelled versions of these two compounds:

1. Determine the number of diastereomers corresponding to the aldehyde hydrates
2. Determine the number of diastereomers for the bisulfite adducts
3. Confirm the stereospecific binding of a single diastereomer to the enzyme active site
4. Determine stereochemical ratios of GC373 (**62**) and GC376 (**63**) in solution
5. Investigate whether the compounds are subject to dynamic stereochemical inversion

The structure and position of  $^{13}\text{C}$ -labelling is shown in Figure 3.10. These compounds were synthesized using identical methods as those used for the synthesis of unlabelled GC373 (**62**) and GC376 (**63**), then utilized in heteronuclear single quantum coherence (HSQC) NMR experiments conducted with the assistance of Dr. Ryan McKay (Figure 3.11). Beginning in Figure 3.11a, an HSQC control experiment of  $^{13}\text{C}$ -labelled GC373 **78** in  $\text{CDCl}_3$  was conducted. As expected, only a single signal corresponding to the aldehyde proton is observed (with chemical shift values in agreement as well), resulting from all the preparatory reactions up to this point being stereocontrolled or achiral in nature. In contrast, when the same experiment was conducted using  $\text{D}_2\text{O}$  as the solvent (Figure 3.11b), two distinct peaks corresponding to aldehyde hydrates were observed. This is evidence of epimerization occurring at the  $\alpha$ -position adjacent to the  $^{13}\text{C}$  label, with the diastereomeric ratio being approximately 71:29 as determined via integration of the HSQC signal peaks. Next, this experiment was

repeated in Figure 3.11c but with the additional presence of SARS-CoV-2 M<sup>Pro</sup>. A single new signal appeared, with chemical shift values corresponding to those expected of hemithioacetals.<sup>73</sup> Additionally, the ratios of the hydrate signals were found to remain the same as in Figure 3.11b, indicating that: 1) Only a single stereoisomer binds to the active site of M<sup>Pro</sup>, and 2) The stereochemical interconversion occurring at the  $\alpha$ -position adjacent to the <sup>13</sup>C-label is dynamic, with the stereoisomers continuously interconverting and the "correct" form binding to the M<sup>Pro</sup>. Following this, an HSQC experiment was conducted using <sup>13</sup>C-labelled GC376 **79** in D<sub>2</sub>O (Figure 3.11d). Surprisingly, only three signals were observed with a ratio of 36:46:18, as opposed to the four that were expected for the bisulfite adduct. This is rectified upon closer examination of the one-dimensional <sup>13</sup>C spectra of this experiment (Figure 3.11e). It can be observed that one of three HSQC signals is actually an overlap of signals arising from two different diastereomers, as evidenced by the left shoulder present on the <sup>13</sup>C signal centered at 84.96 ppm, thus totalling four different distinct stereoisomers that correspond to <sup>13</sup>C-labelled GC376 (**79**). Taken altogether, this study demonstrates that GC373 (**62**) and GC376 (**63**) exists in dynamic stereochemical equilibrium, with all four of the bisulfite adduct stereoisomers dissociating in aqueous media to form the active aldehyde which then epimerizes at the  $\alpha$ -position, of which a single isomer then goes on to bind into the active site of M<sup>Pro</sup>. Understanding the stereochemical properties of these compounds is an important step towards implementation in clinical trials.

(A) HSQC spectra of  $^{13}\text{C}$ -labelled GC373 (**78**) in  $\text{CDCl}_3$



(B) HSQC spectra of  $^{13}\text{C}$ -labelled GC373 (**78**) in  $\text{D}_2\text{O}$

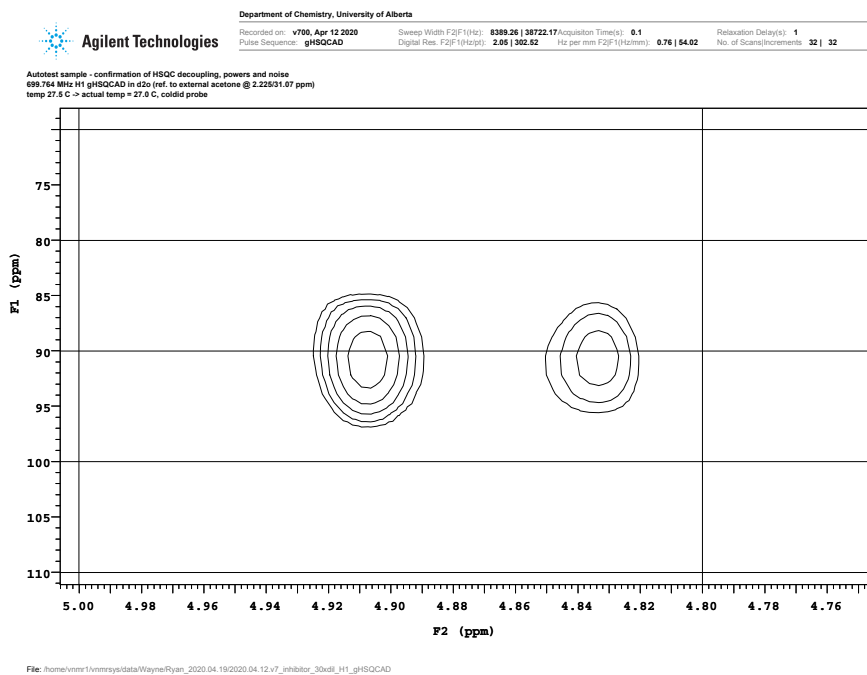
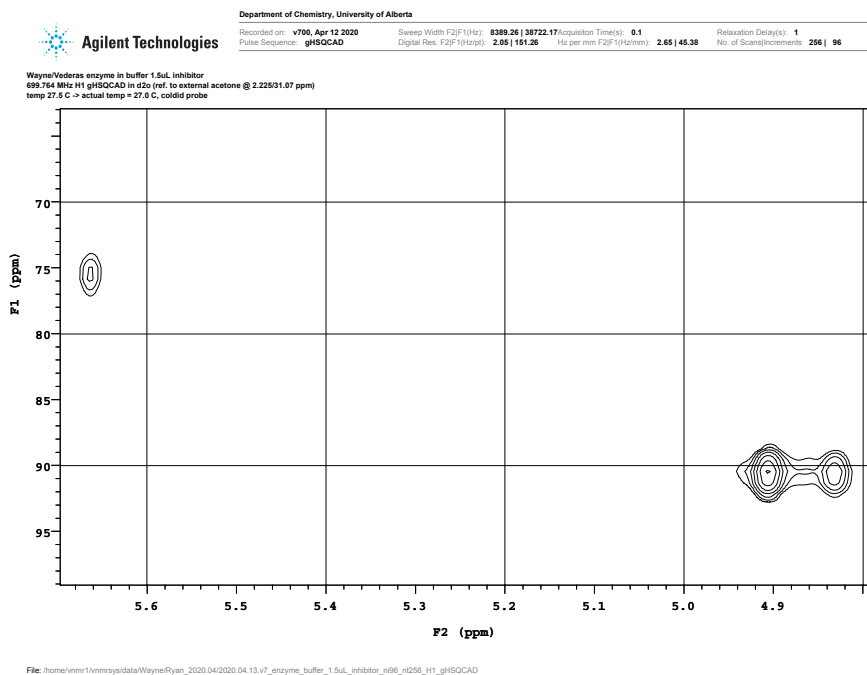


FIGURE 3.11: Stereochemical investigations of GC373 (**62**) and GC376 (**63**) via NMR experiments using  $^{13}\text{C}$ -labelled GC373 (**78**) and  $^{13}\text{C}$ -labelled GC376 (**79**).

(c) HSQC spectra of  $^{13}\text{C}$ -labelled GC373 (**78**) in  $\text{D}_2\text{O}$  with SARS-CoV-2 M<sup>Pro</sup>



(D) HSQC spectra of  $^{13}\text{C}$ -labelled GC376 (**79**) in  $\text{D}_2\text{O}$

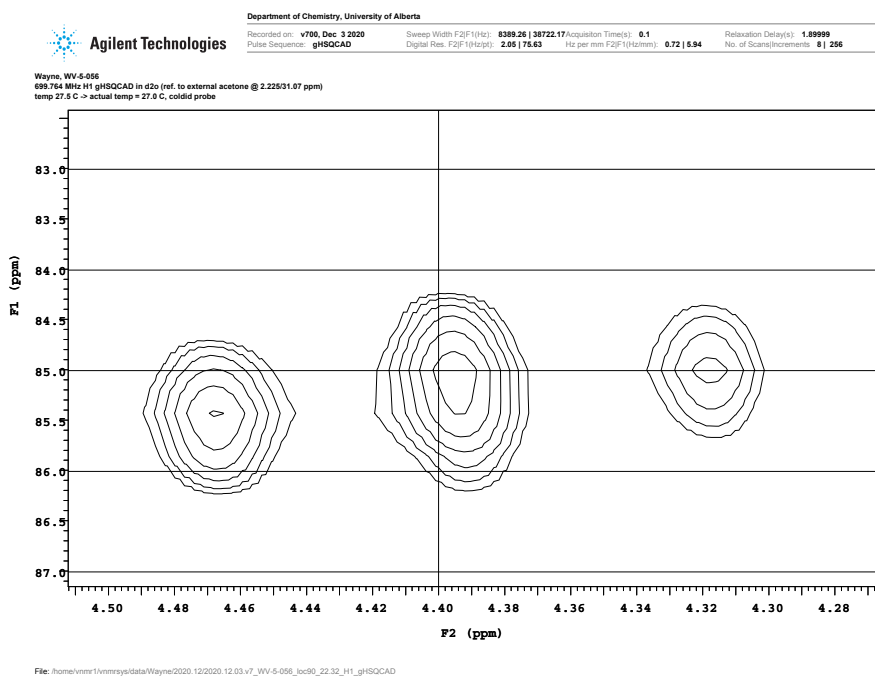


FIGURE 3.11: Stereochemical investigations of GC373 (**62**) and GC376 (**63**) via NMR experiments using  $^{13}\text{C}$ -labelled GC373 (**78**) and  $^{13}\text{C}$ -labelled GC376 (**79**). (cont.)

(E) 1D  $^{13}\text{C}$ -NMR spectra of  $^{13}\text{C}$ -labelled GC373 (**79**) in  $\text{D}_2\text{O}$

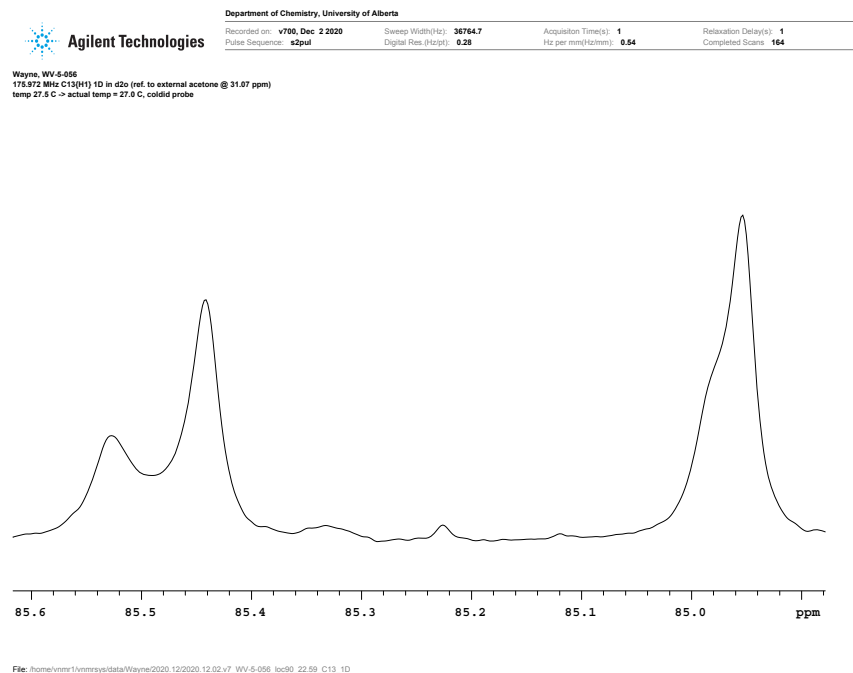


FIGURE 3.11: Stereochemical investigations of GC373 (**62**) and GC376 (**63**) via NMR experiments using  $^{13}\text{C}$ -labelled GC373 (**78**) and  $^{13}\text{C}$ -labelled GC376 (**79**). (cont.)

### 3.3 Development of Improved Inhibitors Against SARS-CoV-2

#### $\text{M}^{\text{pro}}$

Our next focus was the development of improved inhibitors against SARS-CoV-2  $\text{M}^{\text{pro}}$  as potential therapeutics against COVID-19. Although the  $\text{IC}_{50}$  and  $\text{EC}_{50}$  numbers displayed by GC373 (**62**) and GC376 (**63**) were quite good (and at the time of this work the best that was known in literature), we believed that there was room for improvement.

#### 3.3.1 Design and Evaluation of Improved Inhibitors

We began by considering which position in the original inhibitor framework we would be able to make modifications, namely the P1, P2, and P3 positions (Figure 3.3). In our initial work,<sup>25</sup> it was found that the  $\gamma$ -lactam ring at the P1 position was involved in extensive



stabilization with nearby residues in the active site of M<sup>Pro</sup>, particularly in regards to the formation of hydrogen bonding networks. For this reason, in addition to the established  $\gamma$ -lactam amino acid building block **66** being readily available and on hand, it was decided that the P1 residue would be kept with no alteration. In contrast, the P2 and P3 positions were ripe for experimentation and modifications owing to the large degree of variation at these positions found in literature for related M<sup>Pro</sup>s.<sup>66–68,73</sup> In co-crystal structures<sup>25</sup> of the original inhibitors (GC373 (**62**) and GC376 (**63**)) with SARS-CoV-2 M<sup>Pro</sup> it was noted that the S2 pocket within the M<sup>Pro</sup> to which the Leu side chain was bound appeared to have some extra room for alternative aliphatic functionalities. In response, inhibitor analogs with the amino acids Phe, cyclohexylalanine (Cha), and cyclopropylalanine (Cpa) at the P2 position were synthesized, while maintaining the Cbz benzyl structure at P3. Another set of inhibitors were also synthesized, this time focusing on possible modifications at the P3 position. Replacement of structures for the Cbz benzyl group at this position included 3-fluorobenzyl, 3-chloroethyl, 4-methoxyindole, as well as the installation of (*R*)- and (*S*)-methyl groups on the benzyl methylene of the original compound. These singly modified, first generation inhibitors were then evaluated via IC<sub>50</sub>, EC<sub>50</sub>, and crystal structure studies to better understand how different modifications affected binding affinity towards the M<sup>Pro</sup>. Following this, the best modifications at the P2 and P3 positions were combined to furnish doubly modified second generation inhibitors, which were then reevaluated via the aforementioned methods. Additional work was directed towards the synthesis of bisulfite adducts with salt variations to increase solubility, which is further described in Section 3.3.3. The overall workflow for these analogs is shown in Figure 3.12, with the synthetic scheme to access them described in Scheme 3.3.

Evaluation of the inhibitors was performed by Dr. Conrad Fischer (IC<sub>50</sub>) and the team of Dr. Lorne Tyrrell (EC<sub>50</sub>) concurrently with the synthesis of various inhibitor analogs performed by myself with the aid of Dr. Conrad Fischer. This workflow resulted in the simultaneous determination of inhibition parameters throughout the development process, beginning with the first generation all the way through to the second generation. At the time

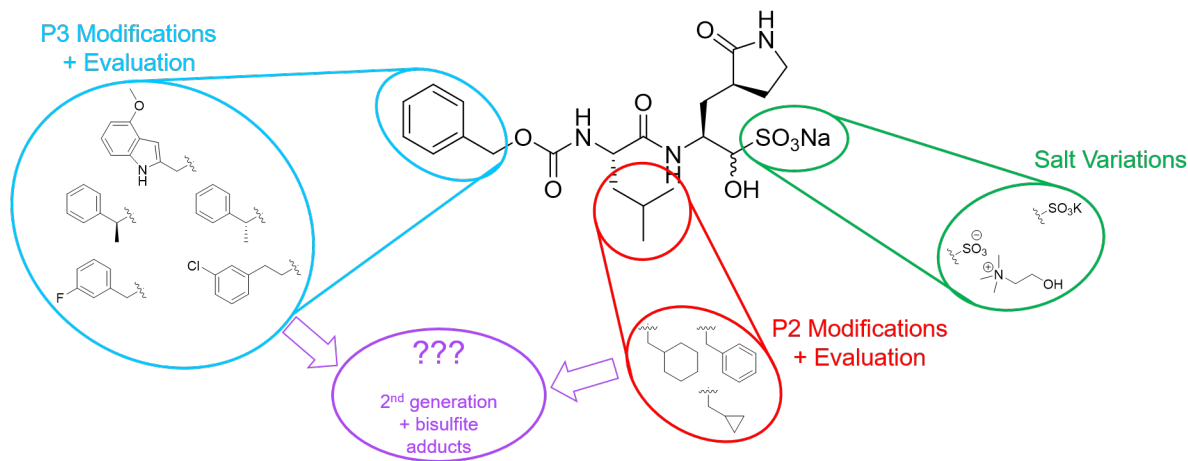
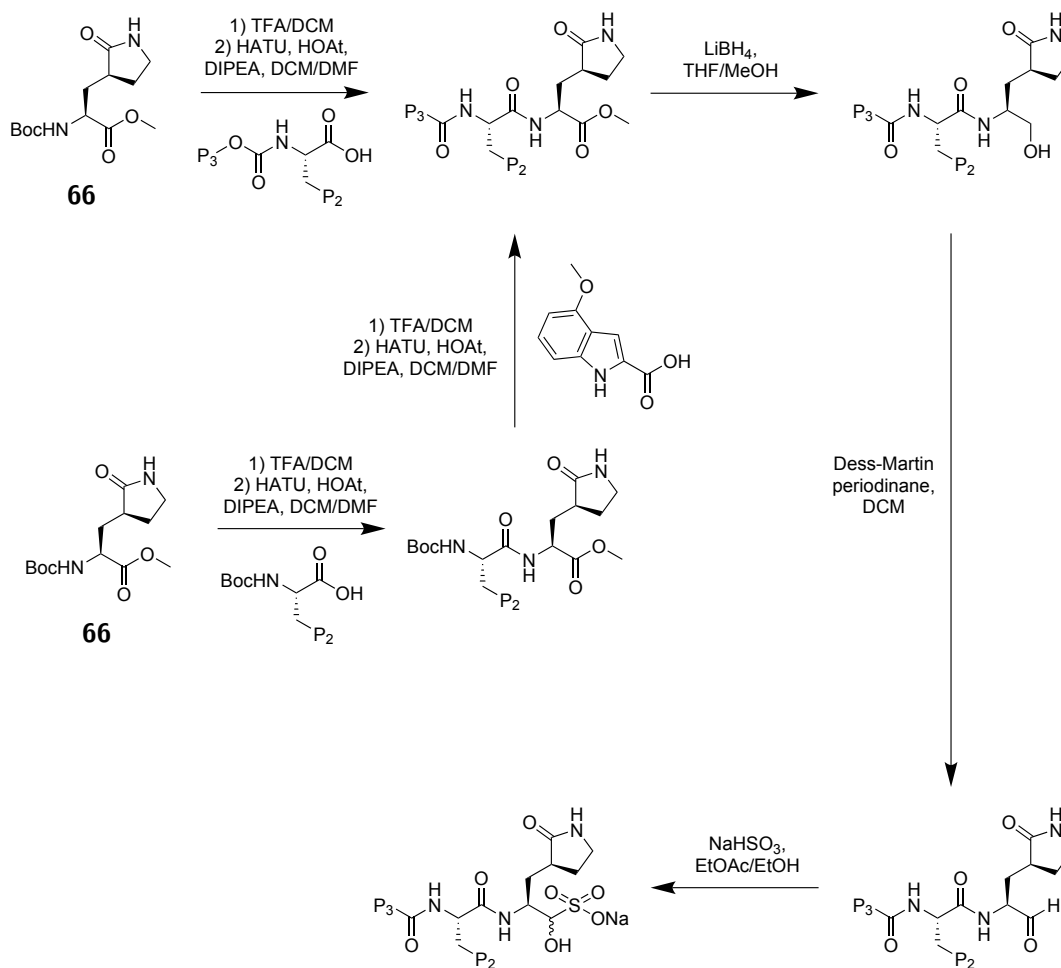


FIGURE 3.12: Workflow utilized for the development of improved inhibitors of SARS-CoV-2 M<sup>pro</sup> based on GC376 (**63**).



SCHEME 3.3: Synthetic route to access first and second generation inhibitors of SARS-CoV-2 M<sup>pro</sup>.

of this work, it was noted by Boras et al. in a preprint article<sup>91</sup> that cellular efflux in Vero E6 cells was an issue of note, so EC<sub>50</sub> experiments were also conducted in the presence of an efflux inhibitor CP-100356 (CP) for certain compounds showing especially good inhibition parameters. The results pertaining to the first generation, singly modified inhibitors are shown below in Table 3.3.

It appears that while the Leu side chain in the original inhibitor was bound to a largely hydrophobic pocket, this pocket is only limited in size. This was evidenced by the installation of a phenyl or cyclohexyl group leading to a decrease in binding affinity of the resultant inhibitor. Conversely, the utilization of a cyclopropyl group enabled deeper insertion of the P2 functionality into the binding pocket, resulting in significantly better binding. Examining the P3 modifications demonstrated alternative factors that influence binding at this position. As previously mentioned, when consulting the original crystal structures shown in Figure 3.7, the Cbz benzyl group of the original inhibitor appeared to bind only to a shallow surface depression denoted as S3, with the possibility of alternative modes of binding to the nearby S4 binding pocket. The improved binding upon the installation of groups that increased dipole interactions as is the case for **83**, **84**, and **85** demonstrates that polar interactions play a significant role into facilitating this alternative binding mode. As an alternative, this secondary mode of binding can also be encouraged via the stereospecific installation of a methyl group. The fact that both **86** and **87** out perform the native GC373 (**62**) suggests that steric interactions may be able to induce binding into the S4 pocket, while the difference in binding affinity between the two compounds demonstrates that the degree of effectiveness for this process is also chirally dependent. Both proposed methods (polar as well as steric interactions) for improved binding are further supported by crystal structures (see Section 3.3.2).

The most potent inhibitors from Table 3.3, namely compounds **80**, **83**, **84**, **85**, and **86** were taken, and their modifications were combined to furnish the four second generation inhibitors shown in Table 3.4. A cyclopropyl moiety at the P2 position was chosen as it was the best performer of all the modifications at that position tested, while the selected

TABLE 3.3: Inhibition parameters of singly modified, first generation inhibitor analogs against SARS-CoV-2 and SARS-CoV-2 M<sup>pro</sup>.

Co-administration of efflux inhibitor CP-100356 is denoted with +CP. In all cases, CC<sub>50</sub> values were found to be >200 μM. ND indicates that the value was not determined.

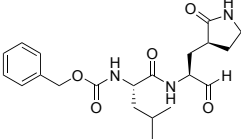
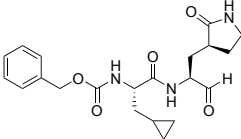
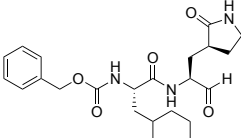
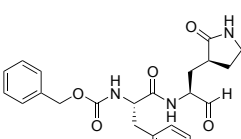
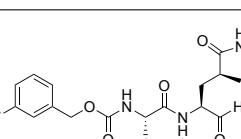
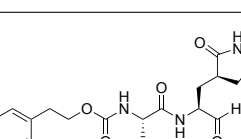
Inhibitor	IC <sub>50</sub> (μM)	EC <sub>50</sub> (μM)	EC <sub>50</sub> (μM) +CP
 <p><b>62: GC373</b></p>	0.40 ± 0.05	1.5 ± 0.3	0.32 ± 0.05
 <p><b>80</b></p>	0.05 ± 0.01	1.1 ± 0.1	0.32 ± 0.09
 <p><b>81</b></p>	0.61 ± 0.15	1.2 ± 0.4	ND
 <p><b>82</b></p>	0.23 ± 0.10	>10	ND
 <p><b>83</b></p>	0.13 ± 0.04	1.4 ± 0.5	ND
 <p><b>84</b></p>	0.15 ± 0.05	1.47 ± 0.8	ND

TABLE 3.3: Inhibition parameters of singly modified, first generation inhibitor analogs against SARS-CoV-2 and SARS-CoV-2 M<sup>PRO</sup>. (cont.)

Co-administration of efflux inhibitor CP-100356 is denoted with +CP. In all cases, CC<sub>50</sub> values were found to be >200 μM. ND indicates that the value was not determined.

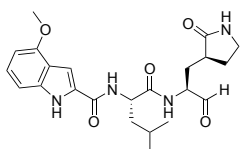
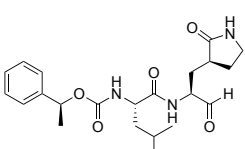
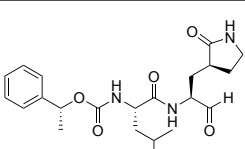
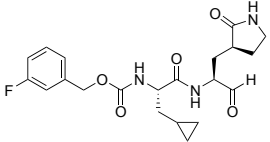
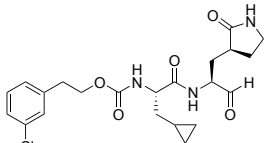
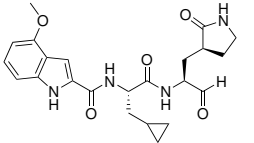
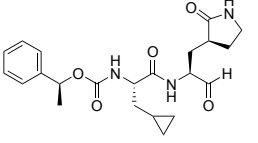
Inhibitor	IC <sub>50</sub> (μM)	EC <sub>50</sub> (μM)	EC <sub>50</sub> (μM) +CP
 <p><b>85</b></p>	0.06 ± 0.01	0.9 ± 0.1	0.25 ± 0.01
 <p><b>86</b></p>	0.27 ± 0.09	1.1 ± 0.5	ND
 <p><b>87</b></p>	0.35 ± 0.11	1.4 ± 0.7	ND

TABLE 3.4: Inhibition parameters of doubly modified, second generation inhibitor analogs against SARS-CoV-2 and SARS-CoV-2 M<sup>PRO</sup>.

Co-administration of efflux inhibitor CP-100356 is denoted with +CP. In all cases, CC<sub>50</sub> values were found to be >200  $\mu$ M.

Inhibitor	IC <sub>50</sub> ( $\mu$ M)	EC <sub>50</sub> ( $\mu$ M)	EC <sub>50</sub> ( $\mu$ M) +CP
 <p><b>88</b></p>	0.14 $\pm$ 0.04	1.1 $\pm$ 0.2	0.25 $\pm$ 0.01
 <p><b>89</b></p>	0.24 $\pm$ 0.09	0.8 $\pm$ 0.2	0.28 $\pm$ 0.02
 <p><b>90</b></p>	0.35 $\pm$ 0.11	0.7 $\pm$ 0.1	0.27 $\pm$ 0.4
 <p><b>91</b></p>	0.35 $\pm$ 0.11	2.0 $\pm$ 0.5	0.25 $\pm$ 0.01

P3 modifications were chosen as a good representation of the two methods of inducing S4 pocket binding. These new inhibitors were then evaluated via the same methods as used previously.

Unexpectedly, these second generation analogs seem to exhibit little improvement over their singly modified counterparts. In our previous work<sup>25</sup> it was observed that bisulfite adduct derivatives outperformed their aldehyde counterparts, possibly as a result of improved solubility. As such, the best singular P2 and P3 modifications (compounds **80** and **85**) along with the four second generation analogs (compounds **88**, **89**, **90**, and **91**) were then

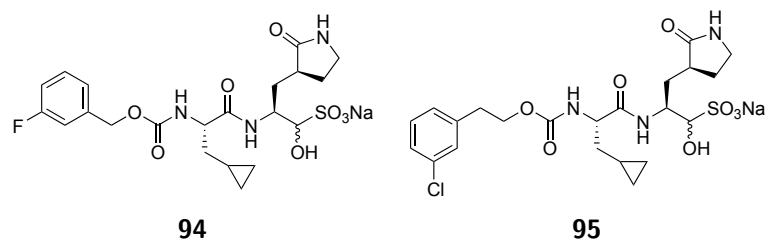


FIGURE 3.13: Chemical structures of **94** and **95** identified as lead compounds.

transformed to their bisulfite adduct forms and evaluated. Additionally, as part of our work on improving the solubility of these inhibitors (discussed further in Section 3.3.3), GC376 (**63**) analogs with the sodium counter ion replaced with either potassium or choline were also synthesized and evaluated (Table 3.5).

While the singly modified bisulfite adducts **92** and **93** did not display substantial decreases in  $IC_{50}$  values compared to their parent aldehyde forms, the doubly modified inhibitors **94**, **95**, **96**, and **97** did. Compared to the parent GC376 (**63**), these second generation bisulfite adducts experienced a 2.5-5.0 fold improvement in  $IC_{50}$  values. A further note is that changing the positive counter ion in GC376 (**63**) did not result in any significant changes in either  $IC_{50}$  or  $EC_{50}$  values. Of all the tested inhibitors, compounds **94** and **95** present themselves as the most promising lead compounds (Figure 3.13) owing to a favourable combination of good  $IC_{50}$  and  $EC_{50}$  values as well as ease of preparation with high yields.

### 3.3.2 Structural Analysis of Improved Inhibitors by X-Ray Crystallography

In order to better understand the physical implications of structural modifications of our compounds and guide development, they were concurrently co-crystallized by the group of Dr. M. Joanne Lemieux in the Department of Biochemistry at the University of Alberta. As was previously the case, all of these crystal structures demonstrate that the mode of action of the aldehyde warhead is retained, forming the same hemithioacetal structure and stabilizing interactions as previously noted upon GC373 (**62**) binding to the active site. The

TABLE 3.5: Inhibition parameters of inhibitor analog bisulfite adducts against SARS-CoV-2 and SARS-CoV-2 M<sup>pro</sup>.

Co-administration of efflux inhibitor CP-100356 is denoted with +CP. In all cases, CC<sub>50</sub> values were found to be >200  $\mu$ M. ND indicates that the value was not determined.

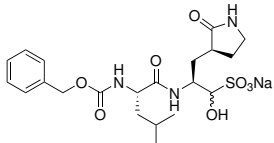
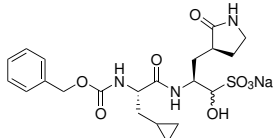
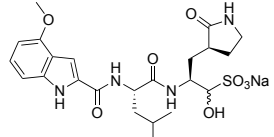
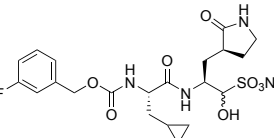
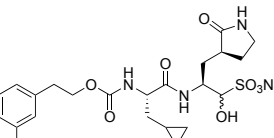
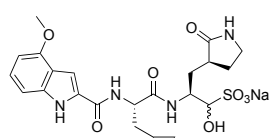
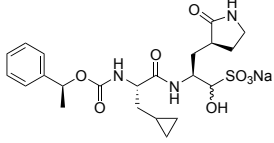
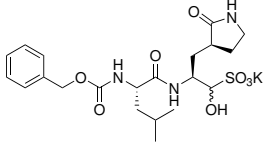
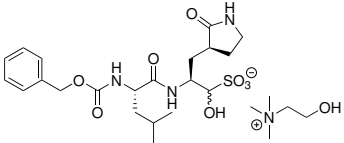
Inhibitor	IC <sub>50</sub> ( $\mu$ M)	EC <sub>50</sub> ( $\mu$ M)	EC <sub>50</sub> ( $\mu$ M) +CP
 <p><b>63: GC376</b></p>	0.19 $\pm$ 0.04	0.9 $\pm$ 0.2	0.25 $\pm$ 0.02
 <p><b>92</b></p>	0.08 $\pm$ 0.03	0.9 $\pm$ 0.3	0.27 $\pm$ 0.2
 <p><b>93</b></p>	0.07 $\pm$ 0.02	1.7 $\pm$ 0.3	0.32 $\pm$ 0.04
 <p><b>94</b></p>	0.07 $\pm$ 0.01	0.57 $\pm$ 0.07	0.19 $\pm$ 0.06
 <p><b>95</b></p>	0.08 $\pm$ 0.02	0.7 $\pm$ 0.2	0.18 $\pm$ 0.04
 <p><b>96</b></p>	0.04 $\pm$ 0.01	1.8 $\pm$ 0.4	0.29 $\pm$ 0.03



TABLE 3.5: Inhibition parameters of inhibitor analog bisulfite adducts against SARS-CoV-2 and SARS-CoV-2 M<sup>Pro</sup>. (cont.)

Co-administration of efflux inhibitor CP-100356 is denoted with +CP. In all cases, CC<sub>50</sub> values were found to be >200 μM. ND indicates that the value was not determined.

Inhibitor	IC <sub>50</sub> (μM)	EC <sub>50</sub> (μM)	EC <sub>50</sub> (μM) +CP
 <p><b>97</b></p>	0.05 ± 0.03	1.2 ± 0.2	0.5 ± 0.1
 <p><b>98</b></p>	0.20 ± 0.04	0.8 ± 0.3	ND
 <p><b>99</b></p>	0.18 ± 0.04	1.2 ± 0.2	ND

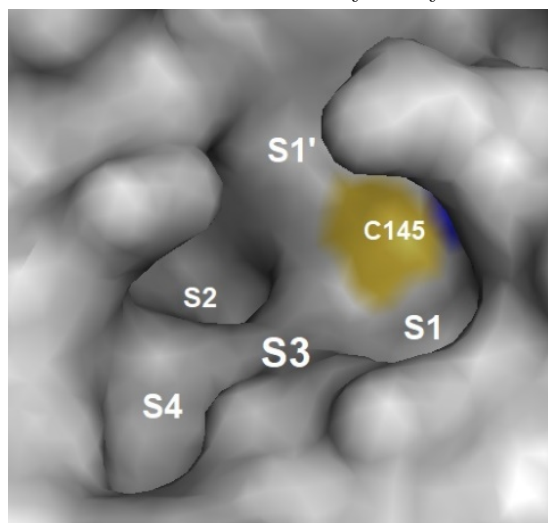
structure of the empty active site as well as the crystal structures of **80**, **88**, **85**, and **86** are shown in Figure 3.14.

In all cases the lactam carbonyl of the Gln analog at the P1 position forms a strong hydrogen bond with the side chain of His163, while the lactam NH is shown to be hydrogen bonding with the side chain carbonyl of Glu166, supporting the decision to retain the  $\gamma$ -lactam ring. In the crystal structures of compounds **80** and **88**, the cyclopropyl group at the P2 position was shown to fill the S2 pocket of the M<sup>pro</sup> in a more compact fashion as compared to the parent Leu side chain found in the crystal structures of compounds **85** and **86**. When examining the modes of binding that the P3 position of the various inhibitors take on, the Cbz benzyl ring of compound **80** was found to lay against the shallow S3 surface depression analogous to what was originally observed for GC373 (**62**). In contrast, when a 3-fluorobenzyl (compound **88**, Figure 3.14c) or a 4-methoxyindole (compound **85**, Figure 3.14d) group is installed at the P3 position, the alternative mode of binding involving the S4 pocket can be observed, suggesting that the presence of polar bonds induced by the presence of a fluoro or methoxy group can enable this conformational change. Examining Figure 3.14e shows that the installation of a (*S*)-methyl group in compound **86** causes the methyl group to lay on the S3 depression while the phenyl ring is rotated into the S4 pocket. This method of using a nearby stereogenic methyl group to improve binding has not yet been reported and represents an attractive approach for sealing off the entrance of the M<sup>pro</sup> catalytic cleft using hydrophobic groups. Overall, these crystal structures demonstrate that in the case of SARS-CoV-2, inhibitors targeting the M<sup>pro</sup> S4 position seem to function better as a result of the deeper binding pocket.

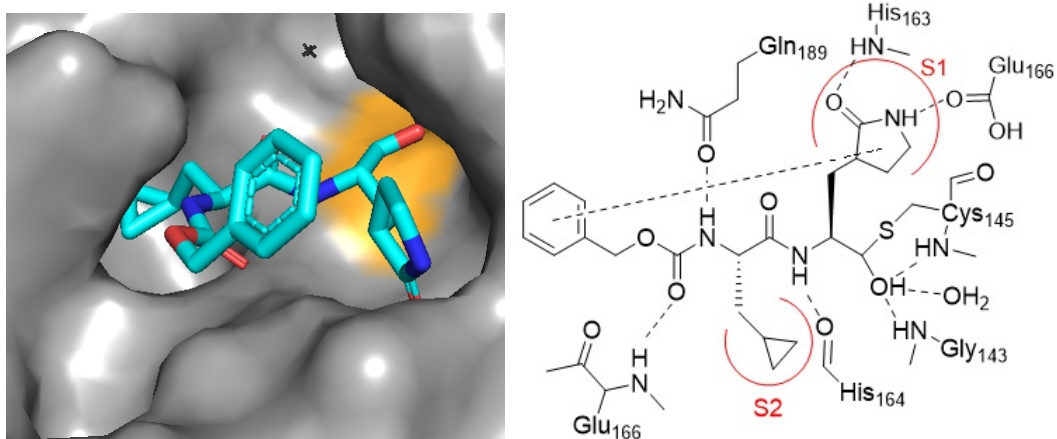
### 3.3.3 Examining and Improving Solubility of Bisulfite Adduct Prodrugs

We next turned our attention towards improving the solubility of these inhibitors with a goal of enabling them for use with humans in a clinical setting. It was hypothesized that by increasing the atomic radii of the positive counter ion in GC376 (**63**) it would be possible to also increase solubility as a result of improved cation solvation. To that end, two

(A) Empty active site of SARS-CoV-2 M<sup>Pro</sup> with catalytic Cys145 and binding sites S1-S4 labelled



(B) SARS-CoV-2 M<sup>Pro</sup> with inhibitor **80** bound in the active site



(c) SARS-CoV-2 M<sup>Pro</sup> with inhibitor **88** bound in the active site

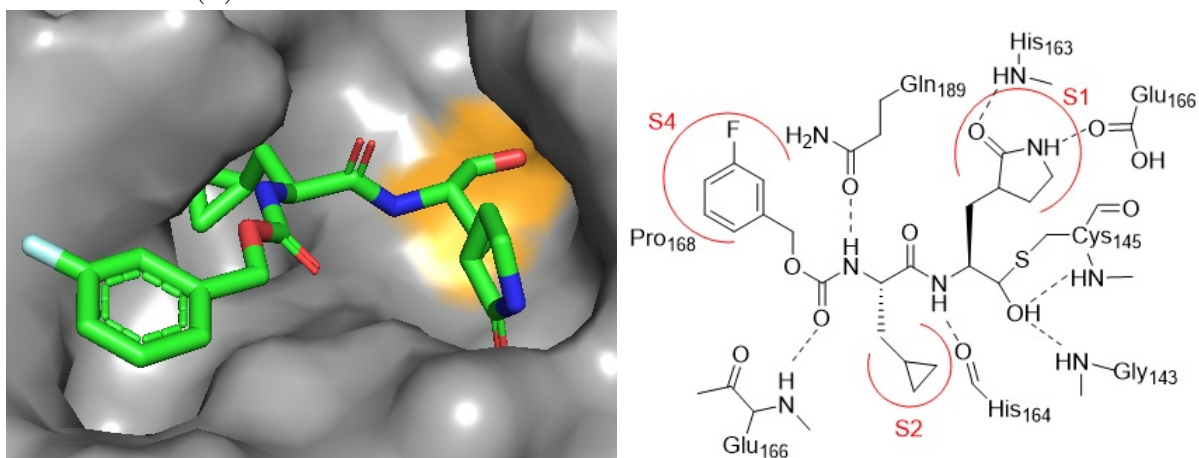
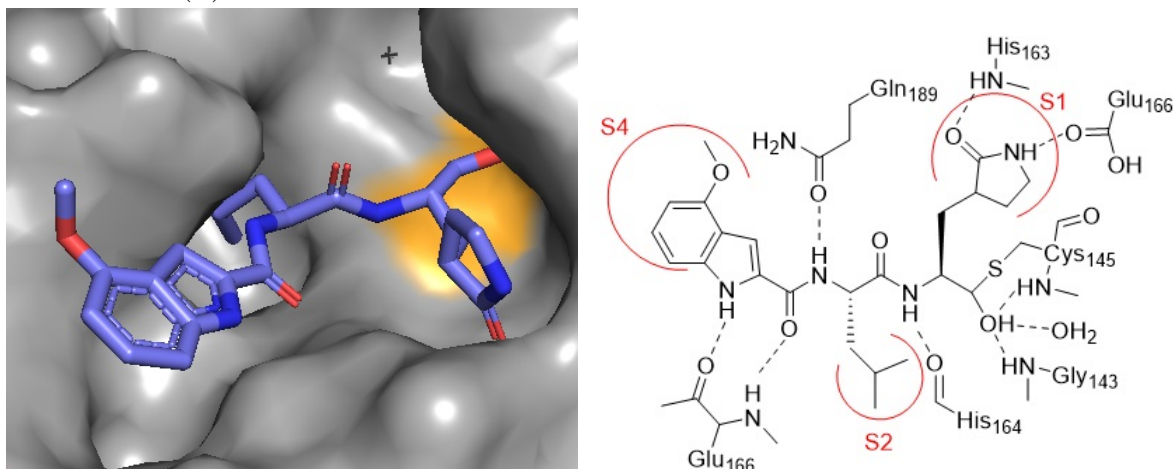


FIGURE 3.14: Co-crystal structures of select inhibitors with SARS-CoV-2 M<sup>Pro</sup>.

(D) SARS-CoV-2 M<sup>Pro</sup> with inhibitor **85** bound in the active site



(E) SARS-CoV-2 M<sup>Pro</sup> with inhibitor **86** bound in the active site

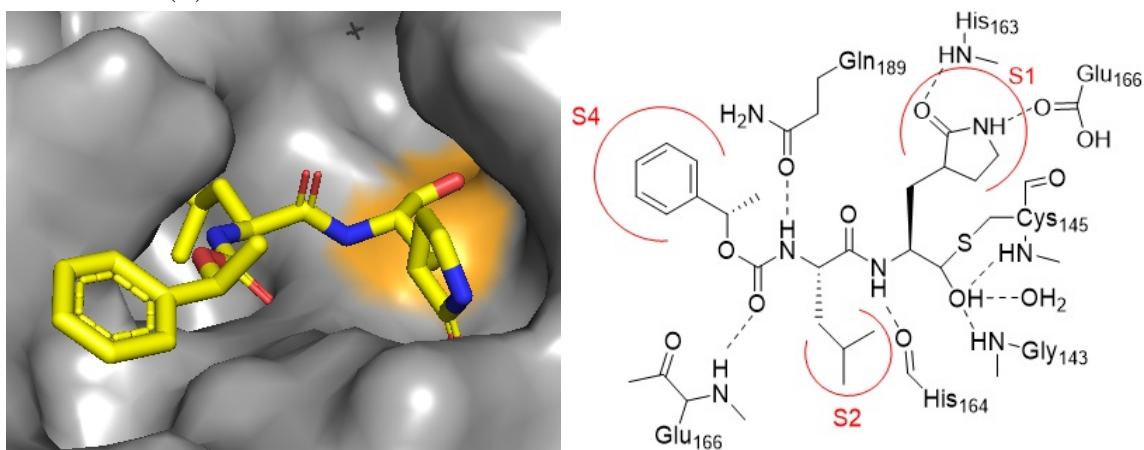
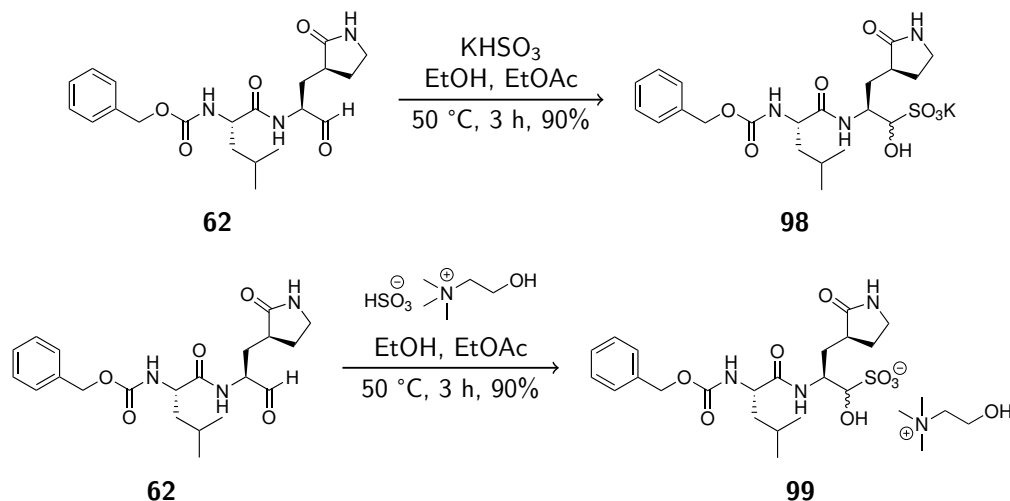


FIGURE 3.14: Co-crystal structures of select inhibitors with SARS-CoV-2 M<sup>Pro</sup>. (cont.)

additional compounds were synthesized, where the original sodium cation was replaced by potassium (GC376-K (**98**)) or choline (GC376-Cho (**99**)) due to the generally recognized as safe (GRAS) nature of these counter ions. These compounds were synthesized from GC373 (**62**) using solutions of potassium or choline bisulfite respectively (Scheme 3.4)



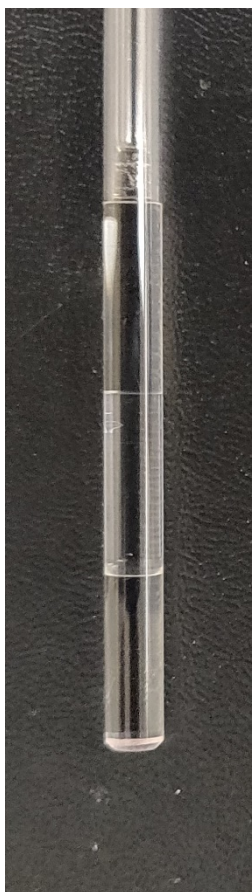
SCHEME 3.4: Synthesis of potassium **98** and choline **99** analogs of GC376 (**63**)

Replacement of the sodium cation in both cases resulted in significantly increased solubility in  $\text{H}_2\text{O}$ , with GC376-K (**98**) and GC376-Cho (**99**) demonstrating an increase in solubility of 30% and >90% respectively. Efficacy testing of these compounds (Table 3.5) demonstrated no observable loss in inhibitory activity, in terms of both  $\text{IC}_{50}$  and  $\text{EC}_{50}$  values. As such, this approach presents a possible avenue towards solving solubility issues of salt- or ion-based therapeutics.

Over the course of characterizing these bisulfite adducts by NMR in  $\text{D}_2\text{O}$  it was noted that at either very high (440 mM, Figure 3.15a) or very low (5 mM, Figure 3.15c) concentrations a clear solution was formed, however at medium concentrations (50 mM, Figure 3.15b) the NMR solution appeared cloudy and turbid instead (Figure 3.15).

This was hypothesized to be a result of self-aggregation between the bisulfite adducts akin to that of fatty acids. In this manner, the charged bisulfite oxyanion functions as a polar head group while the rest of the aliphatic side chains of the peptide functions as a fatty

(A) 440 mM Sample in 5 mM Shigemi Tube



(B) 50 mM in Standard 5 mM NMR Tube



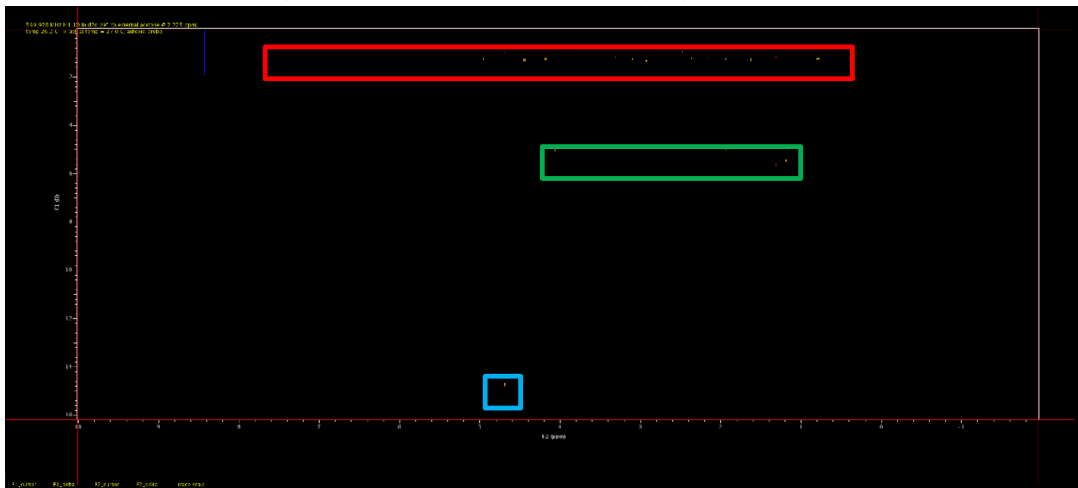
(C) 5 mM in Standard 5 mM NMR Tube



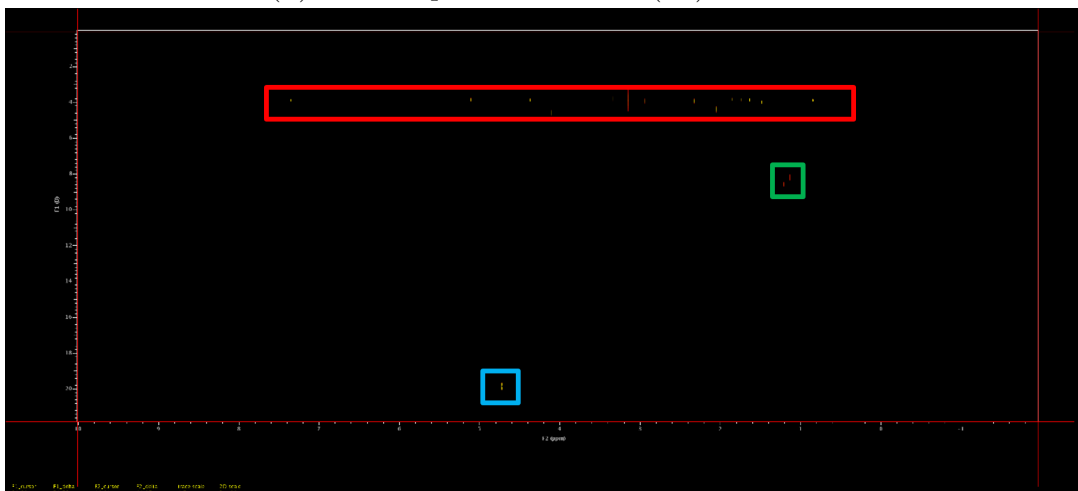
FIGURE 3.15: NMR samples of GC376 (**63**) at various concentrations in D<sub>2</sub>O

acid tail. In order to determine whether this was the case, we conducted diffusion-ordered spectroscopy (DOSY) NMR studies on GC376 (**63**) in D<sub>2</sub>O to determine diffusion order as a function of concentration. Select examples of DOSY spectra at two different concentrations (440 mM, Figure 3.16a; 5 mM, Figure 3.16b) are shown in Figure 3.16, with the full data set of diffusion order as a function of concentration shown in Table 3.6.

(A) DOSY Spectra of GC376 (**63**) at 440 mM



(B) DOSY Spectra of GC376 (**63**) at 5 mM



Red = GC376 (**63**) — Green = Trace Ethyl Acetate — Blue = D<sub>2</sub>O

FIGURE 3.16: DOSY spectra of GC376 (**63**) at concentrations of 440 mM and 5 mM.

Taking the data shown in Table 3.6 and plotting diffusion order as a function of inverse concentration (Figure 3.17) reveals an inflection point. By graphing two lines of best fit

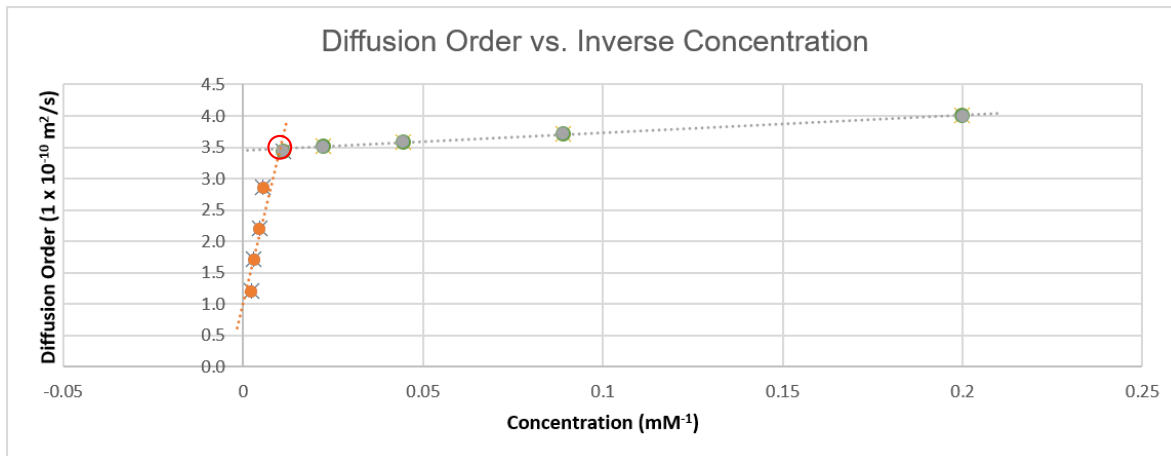
TABLE 3.6: Diffusion order as a function of concentration for GC376 (**63**) in D<sub>2</sub>O.

Concentration (mM)	Diffusion Order ( $1 \times 10^{-10} \text{ m}^2/\text{s}$ )	Appearance
440.0	1.20	Clear
330.0	1.71	Clear
220.0	2.20	Slightly Turbid
180.0	2.86	Milky
90.0	3.44	Milky
45.0	3.51	Milky
22.5	3.59	Turbid
11.3	3.72	Clear
5.0	4.00	Clear

before and after the inflection and examining the intersecting point, it is possible to determine a critical micellar concentration (CMC) value.<sup>92</sup> In the case of GC376 (**63**), the CMC was determined to be 96.7 mM. When examining the diffusion order at the highest ( $1.2 \times 10^{-10} \text{ m}^2/\text{s}$  at 440 mM) and lowest ( $4.0 \times 10^{-10} \text{ m}^2/\text{s}$  at 5 mM) concentrations, we can calculate corresponding hydrodynamic radii of 20.6 Å and 6.2 Å (41.2 Å and 12.4 Å in diameter) respectively,<sup>93</sup> a significant difference that suggests the formation of colloidal or micellar bodies in solution. For reference, reported hydrodynamic diameters for dodecyl phosphocholine (DPC) micelles in water range from 64 Å to 72 Å in size.<sup>94</sup> Similar experiments were conducted using a version of GC373 with choline (GC373-Cho (**99**)), yielding similar results and a CMC value of 91.1 mM. Details of such as well as additional 1D <sup>1</sup>H-NMR experiments providing evidence for colloidal properties of bisulfite adducts can be found in a pertinent publication.<sup>26</sup>

The presence of a CMC concentration coupled with a change in diffusion order as a function of concentration for GC376 (**63**) strongly suggests the presence of a self-aggregation phenomena. As the administration of GC376 (**63**) is subcutaneous in nature, the significance of this discovery lays in the possibility of administering this therapeutic as a colloidal mixture. Considering the fact that previously established dosing for felines is an estimated 5-10 mg/kg body-weight/day, twice daily<sup>21</sup> and that the general upper volume limit of subcutaneous injections for humans is an estimated 1.5 mL,<sup>95</sup> colloidal administration may allow





Red circle denotes CMC (96.7 mM)

FIGURE 3.17: Plotted values of diffusion order as a function of inverse concentration.

for injection volumes as low as 0.11 mL per injection (as calculated for a 62 kg human), significantly increasing patient compliance. In theory, this technique could be expanded as an additional method for the administration of other drugs that exhibit similar micellar properties in order to circumvent solubility issues that stand in the way of gaining regulatory approval.

### 3.4 Conclusion

In conclusion, GC376 (**63**) (an established feline therapeutic) was demonstrated to be effective in inhibiting the functionality of SARS-CoV-2 M<sup>pro</sup> and halt viral replication. Binding of this compound to the active site was demonstrated by crystallographic studies, while efficacy demonstrated by FRET assays as well as plaque reduction assays. These methods were used to determine IC<sub>50</sub> and EC<sub>50</sub> values for both GC373 (**62**) and GC376 (**63**) (Table 3.2 and Figure 3.6). In an attempt to expedite advancement of GC376 (**63**) into clinical trials, <sup>13</sup>C-labelled NMR experiments were conducted to gain insight into the stereochemical properties of these compounds. The stereochemistry of both GC373 (**62**) and GC376 (**63**) was found to be dynamic in aqueous media, with epimerization readily occurring at the  $\alpha$ -carbon of the P1 position. Work was then done on the development of more potent in-

hibitors, a process which was guided by a combination of crystallography, enzymatic testing, and mammalian cell assays. These new inhibitors were found to be more potent than the parent compounds, owing to differences in their mode of binding, with the P3 position of the inhibitors docking into a nearby S4 pocket instead of the shallow surface depression of S3, as supported by co-crystal structures with SARS-CoV-2 M<sup>pro</sup>. Finally, cation analogs and colloidal properties of GC376 (**63**) were investigated, leading to two possible methods for circumventing solubility issues with these bisulfite prodrugs. Additional avenues of work on this project would be to advance these compounds into animal testing and eventually clinical trials.

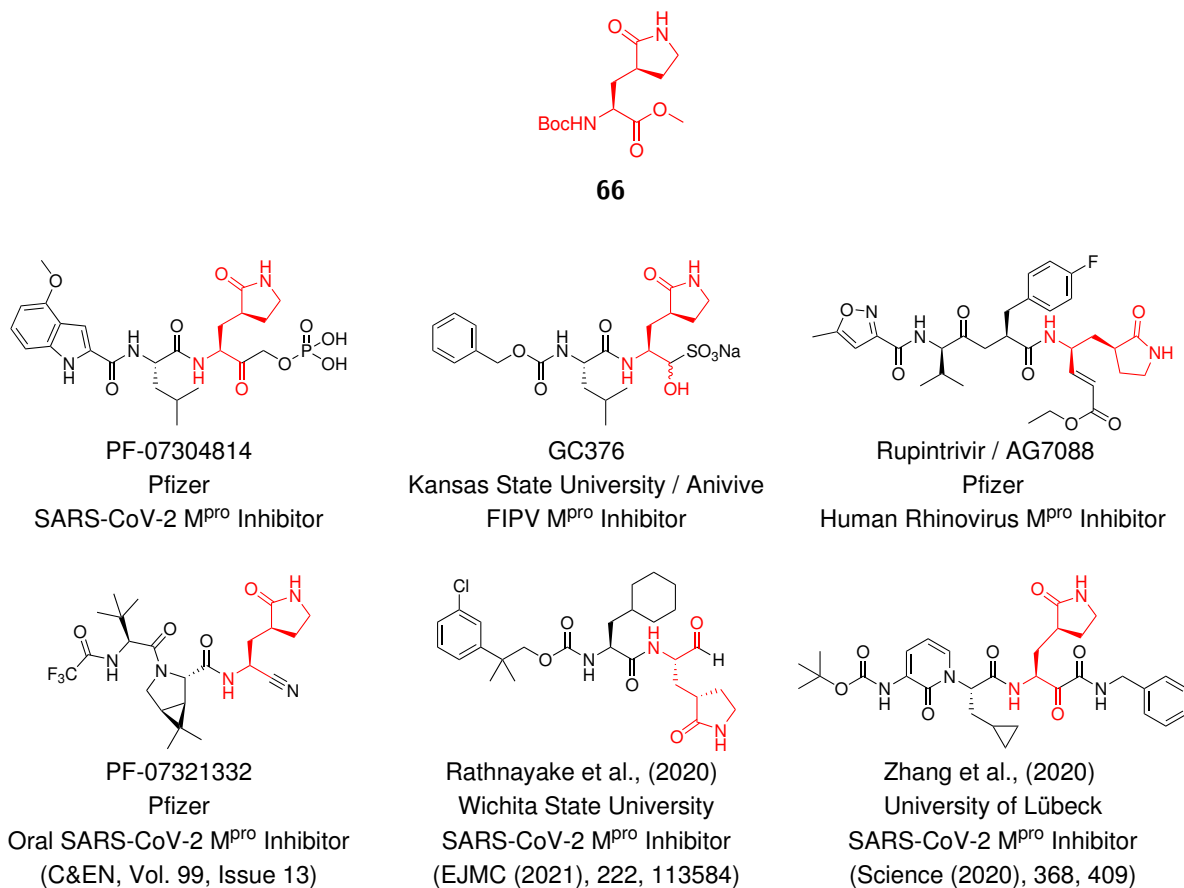
## Chapter 4

# Improved Synthesis of a Glutamine Analog

### 4.1 Introduction to a $\gamma$ -Lactam Analog of Glutamine

As the life cycle of SARS-CoV-2 is dependent upon the function of M<sup>Pro</sup> (see Chapter 3, Section 3.1), a significant portion of antiviral development efforts are targeted towards the inhibition of this protease.<sup>23,25–31,67,76,89,96,97</sup> Central to many of these compounds (Figure 4.1) is the cyclic glutamine analog with a (3*S*)-pyrrolid-2-one-3-yl-L-alanine structure, installed using the *tert*-butoxycarbonyl (Boc) and methyl ester protected building block **66**.<sup>23–32</sup>

This substructure is often utilized as it binds well to viral proteases and enables a large number of stabilizing interactions in the binding pocket.<sup>25,26</sup> As an added bonus, this also hinders the interaction of the side chain amide nitrogen from interacting with any electrophilic warheads meant to bind to the reactive cysteine thiol present in the active site. Throughout our previous work, we noticed that the synthesis of building block **66** was generally low yielding, with literature yields ranging from 27% to 66% overall yield when starting from Boc-glutamic acid dimethyl ester.<sup>24,32,98–101</sup> A further testament to the difficulty of this synthesis comes from the original kilogram-scale synthesis reported by Pfizer Global Research and Development, wherein the reported yield was only 40% over three steps.<sup>32</sup> Despite reports of higher yields,<sup>101</sup> 40% was also generally a maximum in our experience. While building block **66** is commercially available as a fine chemical from suppliers providing cus-



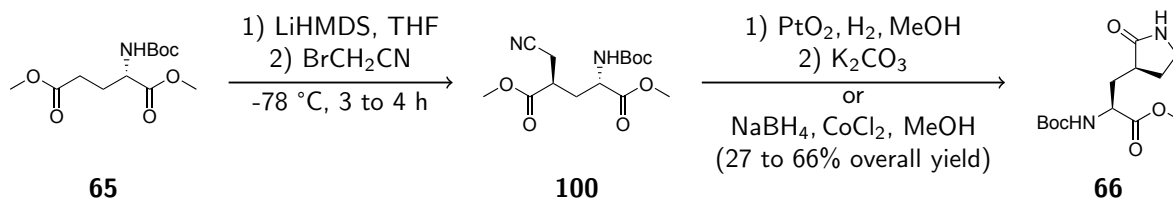
Inhibitor substructures derived from building block **66** are highlighted in red.

FIGURE 4.1: Select examples of viral inhibitors containing a  $\gamma$ -lactam Gln analog incorporated using compound **66**.

tom synthesis services, the cost is quite high - typically around \$150 for 50 mg, making it cost-prohibitive for some research efforts. We aimed to remedy this by developing a synthetic route that is affordable, higher yielding, scalable, and requires only minimal purification in order to gain access to larger quantities of this useful building block.

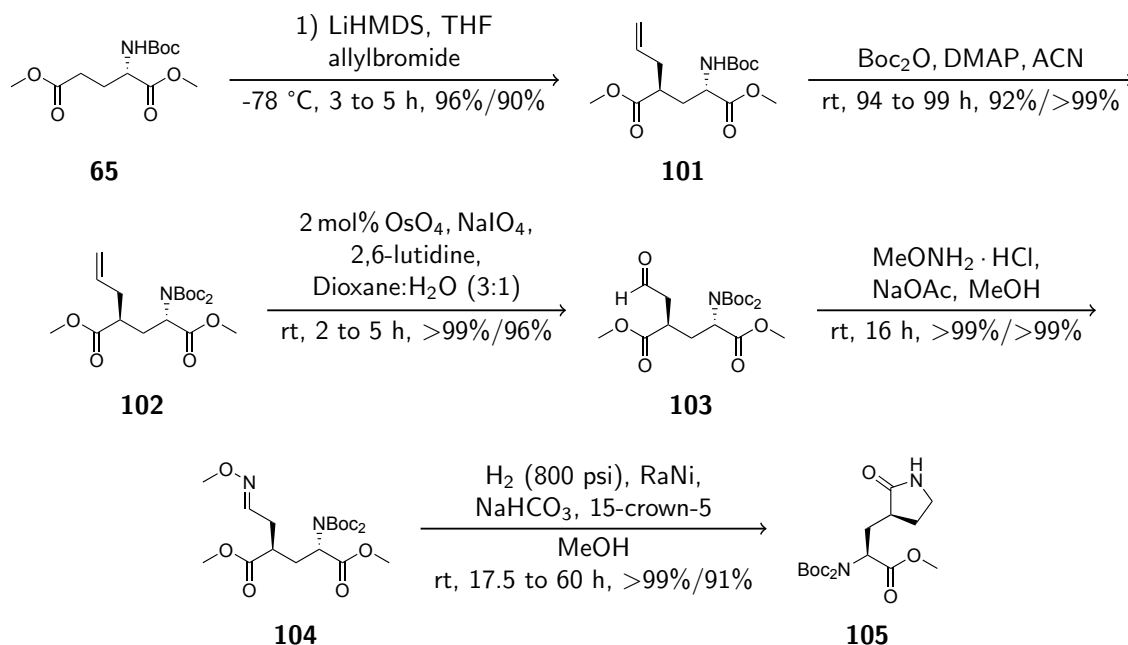
## 4.2 Development of an Improved Synthetic Route Towards a $\gamma$ -Lactam Analog of Glutamine

The original synthesis developed and reported by Pfizer involved the stereoselective alkylation of the distal  $\alpha$ -carbon using bromoacetonitrile via a method originally reported by



SCHEME 4.1: Pfizer's original synthetic route towards glutamine analog building block **66**.

Hanessian and coworkers.<sup>85,86</sup> The newly introduced cyano group was then reduced to a primary amine and subsequently cyclized onto the nearby methyl ester in one of two ways: 1) hydrogenation at medium pressures over a  $\text{PtO}_2$  catalyst followed by basic cyclization using  $\text{K}_2\text{CO}_3$ , or 2) reduction using  $\text{NaBH}_4$  in the presence of  $\text{CoCl}_2$  to furnish building block **66** (Scheme 4.1).<sup>32</sup> In our experience of this synthetic route, we noted that the major hindrance towards higher yields was the initial alkylation step. Upon examination of Hanessian's original work, we noted that when utilizing electrophiles such as allyl bromide the isolated yields of the resultant products were upwards of 90%.<sup>85</sup>



**Note:** Yields presented as <small scale %>/<large scale %>

SCHEME 4.2: Improved synthetic scheme towards glutamine analog building block **105**.

As such, we began developing our alternative synthesis via small scale reactions as de-

picted in Scheme 4.2. This alternative route began with a stereoselective alkylation using allyl bromide in place of bromoacetonitrile as the electrophile. This carbon-carbon bond formation step utilizing an allylic electrophile resulted in substantially increased yields, allowing access to alkene **101** at yields equal to or greater than 90%. At this point, we attempted to subject **101** to ozonolysis directly, but it appeared that the product does not fare well in the presence of the carbamate NH of the Boc group, resulting in substantially diminished yields and a host of undesired byproducts. This hypothesis is generally supported by prior experience in our group.<sup>102</sup> To remedy this, we opted to further protect the NH with a second Boc group to furnish the di-protected compound **102**. This compound was then re-subjected to a number of methods in an attempt to cleave the alkene and form the aldehyde. Both ozonolysis and Lemieux-Johnson oxidation were tried, with the latter generally performing better and forming product **103** at nearly quantitative yields. At this point, the aldehyde oxygen of **103** needed to be replaced by a nitrogen in order to generate the required framework and bond connectivities prior to cyclization. Several approaches were examined, including reductive amination using either ammonia or benzylamine, as well as oxime/oxime ether formation followed by N-O bond cleavage and reduction using hydroxylamine or derivatives thereof. In our attempts, oxime ether formation proved to be the best, forming the resultant products with generally higher yields. Initial attempts using hydroxylamine hydrochloride provided the resultant oxime in only modest yields (70%), concomitant with the formation of side products and rendering this approach unfeasible for large scale synthesis. We then turned to investigating the formation of oxime ethers using either *O*-benzylhydroxylamine or *O*-methylhydroxylamine. The product formed using *O*-benzylhydroxylamine was isolated in 89% yield, while the use of *O*-methylhydroxylamine afforded quantitative conversion to compound **104**. It should be noted that throughout the development process of this step in the synthesis, the basic species used to catalyze addition of the hydroxylamine nitrogen to the aldehyde has an effect on the stereochemical purity of the product. Initial approaches using NaHCO<sub>3</sub> as the base were found to epimerize the nearby  $\alpha$ -position, necessitating a switch to NaOAc instead. This is likely because while NaHCO<sub>3</sub> is a relatively weak base in

aqueous media, the lack of solvation results in it being unexpectedly basic when used in an alcoholic solvent like methanol. With **104** now in hand, the final tasks were to: 1) Cleave the N-O bond of the oxime ether, 2) reduce the C=N double bond to a C-N single bond, and 3) cyclize the resultant primary amine onto the nearby methyl ester carbonyl.

This final step proved to be the most technically complicated step in the synthesis and required the most effort to optimize. As the goal of this synthetic route was to facilitate ease of execution and scale-up, we aimed to do this step as a one-pot reaction. At first, a number of methods were tried such as borane reduction, as well as hydrogenation using a number of different catalysts such as PtO<sub>2</sub>, various ruthenium catalysts, Pd/C, and Raney Nickel (RaNi). A number of difficulties were faced in this process. Reduction using borane prove ineffective in this case, while hydrogenation using PtO<sub>2</sub> and the various ruthenium catalysts were found to be equally futile. Hydrogenation using Pd/C for similar transformations has been reported in literature, however yields are inconsistent and many protocols utilize hydrochloric acid, rendering the method incompatible in the presence of Boc groups. Equally incompatible were reports of using LiAlH<sub>4</sub> for reduction of oxime ethers to primary amines, as this would reduce the distal methyl ester of **104** as well. Only the reduction by RaNi proved effective, furnishing the uncyclized primary amine. Throughout the optimization process, reaction monitoring by LC-MS demonstrated that higher H<sub>2</sub> pressures appeared to afford cleaner transformations. We hypothesize that higher pressures may lead to a more rapid and quantitative reduction to the primary amine, minimizing the duration and chances of dimerization as a result of an intermediate imine species being present. Additionally, it was found that cleaner transformations can also be facilitated by performing the reaction at higher dilutions, further supporting the theory that dimerization products may be forming due to the presence of reduction intermediates.

At this point, we aimed to couple the reduction and cyclization steps together to simplify reaction execution. The difficulty in this step lays in finding a balance between having the reaction environment basic enough to afford cyclization while avoiding epimerization (Table 4.1).

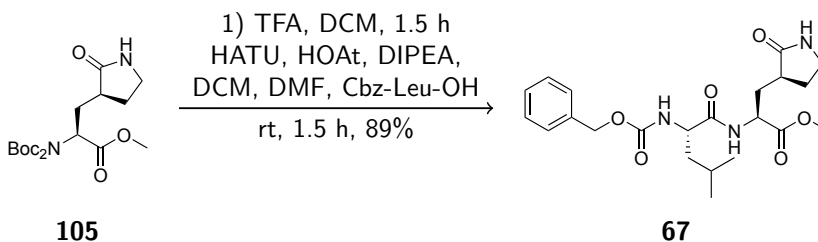
TABLE 4.1: Experimental conditions examined to afford cyclization to  $\gamma$ -lactam with minimal epimerization.

Trial	Base	Additional Parameters	Result
1	NaHCO <sub>3</sub>	4 mol eq.	Cyclization with epimerization
2	NaOAc	N/A	No reaction
3	Et <sub>3</sub> N	N/A	No reaction
4	NaHCO <sub>3</sub>	50/50 (v/v) H <sub>2</sub> O in MeOH	No reaction
5	NaHCO <sub>3</sub>	3 mol eq.	Cyclization with epimerization
6	NaHCO <sub>3</sub>	2 mol eq.	Cyclization with epimerization
7	NaHCO <sub>3</sub>	1 mol eq.	Cyclization with epimerization
8	NaHCO <sub>3</sub>	0.5 mol eq.	No reaction
9	NaHCO <sub>3</sub> as a saturated solution	1 mol eq.	Cyclization with lessened epimerization
10	NaHCO <sub>3</sub> as a saturated solution	1 mol eq. with 15-crown-5	Cyclization with no observable epimerization

In the process of optimizing this reaction, it was found that Na<sub>2</sub>CO<sub>3</sub> was too basic to afford cyclization without epimerization, while NaOAc and other organic bases such as Et<sub>3</sub>N were altogether ineffective in facilitating this transformation. NaHCO<sub>3</sub> was found to initially also lead to epimerization as a result of its lack of solvation in methanol. Conversely, when this reaction was run with a larger amount of water, the cyclization event did not happen. Directly varying amounts of NaHCO<sub>3</sub> also led to either cyclization with epimerization or no cyclization at all. Next, it was thought that since the base used was heterogeneous with the reaction environment, perhaps a lower amount of NaHCO<sub>3</sub> could be used if the reaction surface of the base was kept high. To afford this increased surface area, NaHCO<sub>3</sub> was added instead as a saturated solution in water, keeping aqueous volumes to a minimum. This was successful in increasing the surface area of the base, with very fine NaHCO<sub>3</sub> particulates forming upon addition of the saturated solution to the methanolic mixture, however a small amount of epimerization could still be seen in the cyclized product. Finally, it was thought



that partial solubilization of the  $\text{NaHCO}_3$  could be encouraged by chelation of the sodium ion by a crown ether. With this, it was found that addition of 15-crown-5 to the reaction mixture provided an environment that was basic enough to afford cyclization while avoiding epimerization, finally furnishing the desired di-Boc-protected building block **105** as a single enantiomer in 86% overall yield. A repeat of all of these reactions up to 10 gram scale provided the compound in 79% overall yield (Scheme 4.2), demonstrating the feasibility of scaling up this synthetic route.



SCHEME 4.3: Test reaction using building block **105** in the formation of known compound **67**.

With building block **105** in hand, it was used in a test reaction to synthesize compound **67**, which had been made a number of times before, in order to demonstrate that building block **105** is functionally equivalent to **66** (Scheme 4.3). Pleasantly, it was found that all characterization data for this test product matched previously reported literature values.

### 4.3 Conclusion

In conclusion, an improved synthesis towards a building block used to introduce (3*S*)-pyrrolid-2-one-3-yl-L-alanine into medicinal targets was developed. This method more than doubled the original ca. 40% overall yield reported by Pfizer<sup>32</sup> and requires chromatographic purification at only two steps: during the formation of **101** and **105**. This method was demonstrated to be scalable in nature and furnishes the product as a single enantiomer. Furthermore, it utilizes inexpensive and commercially available reagents, and employs the use of expensive transition metals in only catalytic amounts. At present, limits associated

with this route include the required use of OsO<sub>4</sub> in addition to the use of expensive 15-crown-5 ether, though it may be possible to circumvent this requirement by utilizing KHCO<sub>3</sub> instead, an aspect which presents itself as a point of possible future optimization efforts. Finally, while this route is much higher yielding than the previous route established and documented by Pfizer, it has the drawback of requiring a greater number of synthetic steps. With established widespread utilization of this structure in numerous pharmaceutical compounds and antiviral inhibitors, this route represents an attractive avenue to access this popular pharmacophore, facilitating and expediting the development of M<sup>Pro</sup> inhibitors and other antivirals.

## Chapter 5

# Improving Metabolic Stability of Antivirals Against P450

### 5.1 Introduction to P450 and Metabolic Degradation

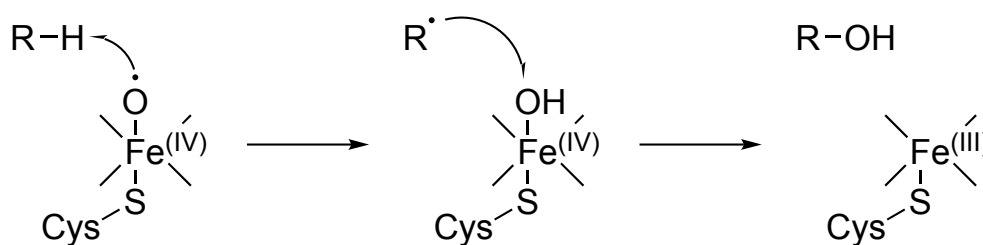


FIGURE 5.1: Mechanism of C-H bond oxidation by cytochrome P450 enzymes.

A major hurdle regarding the advancement of pharmaceuticals through clinical trials is overcoming unwanted metabolic degradation and excretion by patients.<sup>103,104</sup> Oftentimes this is done by a class of enzymes known as cytochrome P450s. In humans, the main enzyme involved in drug metabolism is cytochrome P450 3A4, located in the liver.<sup>104-106</sup> These enzymes work by generating a reactive iron(IV)-oxo radical using a heme group that is subsequently able to cleave C-H bonds and generate an iron-bound hydroxyl species along with a carbon-centered radical (Figure 5.1). Transfer of this iron-bound hydroxyl to the carbon radical then results in reduction of the heme-centered iron to iron(III) and concomitant formation of an alcohol group on the substrate.<sup>37,38</sup> Metabolizing a large variety of substrates,

metabolism by this type of enzyme has proven difficult to circumvent, and in the case of Pfizer's newly released orally active SARS-CoV-2 drug, requires the co-administration of a P450 inhibitor.<sup>39</sup>

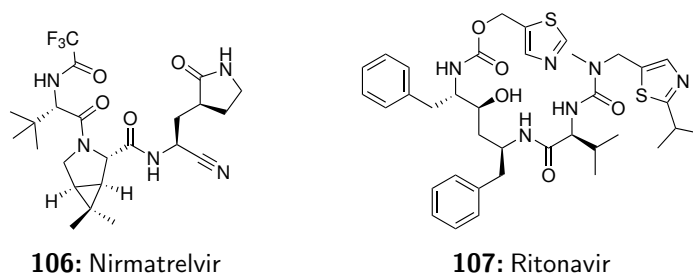


FIGURE 5.2: Constituent compounds of orally active COVID-19 therapeutic Paxlovid.

Known as Paxlovid<sup>™</sup>, this drug is actually a combination of two different compounds - nirmatrelvir (**106**) and ritonavir (**107**) (Figure 5.2). The actual SARS-CoV-2 M<sup>PRO</sup> inhibitor is nirmatrelvir (also referred to as PF-07321332), while ritonavir is included as a P450 inhibitor to prevent unwanted metabolic degradation of nirmatrelvir.<sup>39</sup> In a report released by Pfizer,<sup>39</sup> it was found that P450 3A4 oxidized a number of aliphatic positions in nirmatrelvir (Figure 5.3), namely at various methyl groups (metabolites **108**, **109**, and **110**) and more importantly in the  $\gamma$ -lactam ring of the Gln analog (metabolites **111** and **112**). Seeing this, we thought that GC376 (**93**), which contains an identical  $\gamma$ -lactam ring at the P1 position as well as methyl groups in the form of an isopropyl group as part of Leu at position P2 would also be susceptible towards similar forms of metabolic reactions.

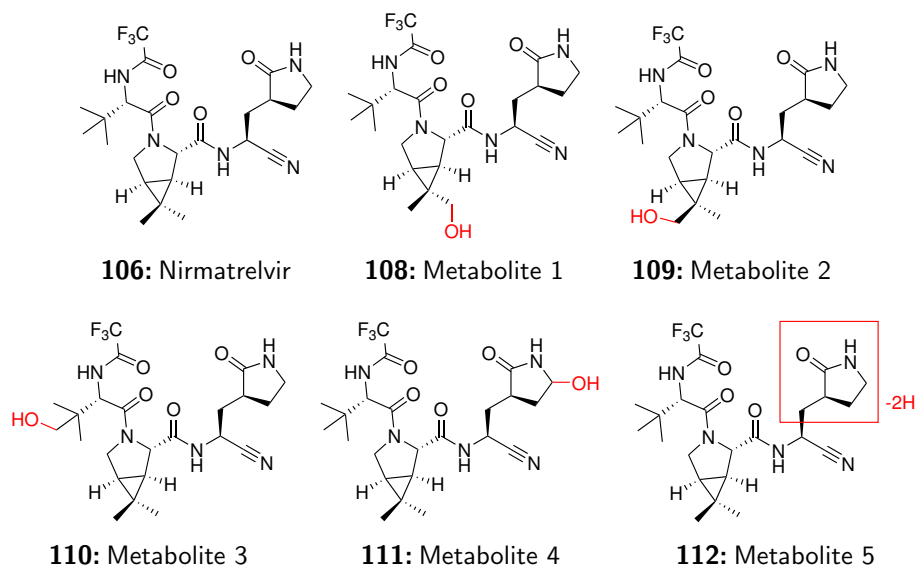


FIGURE 5.3: Cytochrome P450 3A4 metabolites of Nirmatrelvir (**106**) as reported by Pfizer.<sup>39</sup>

## 5.2 Methods to Avoid Metabolic Reactions by P450

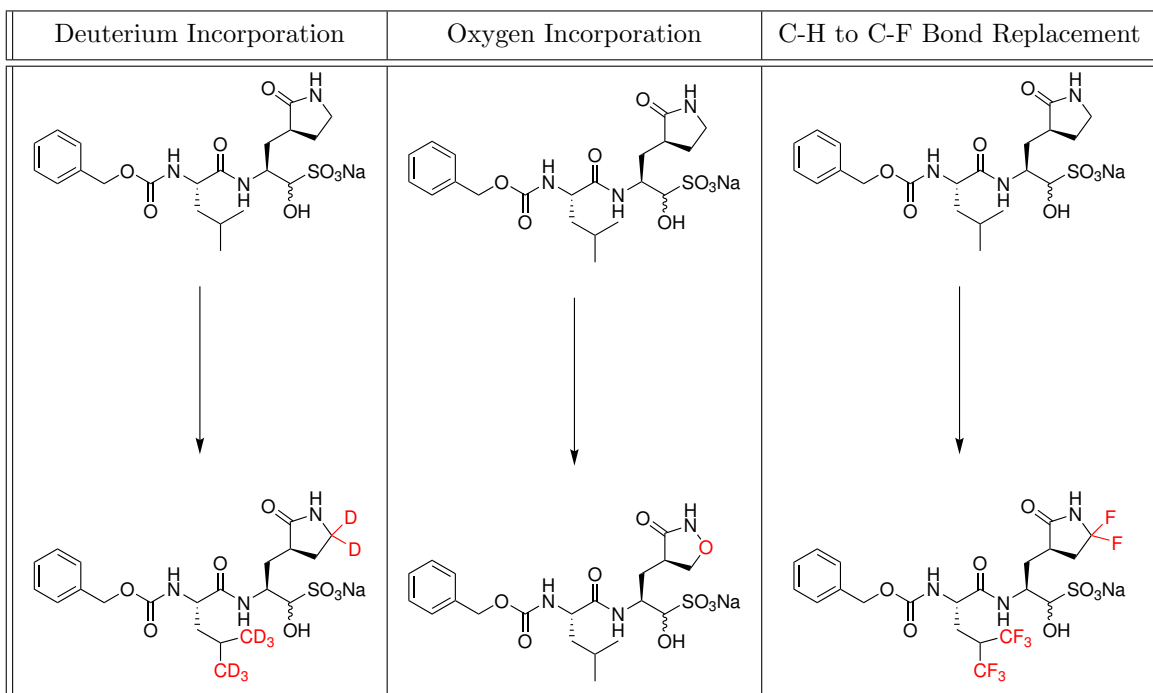


FIGURE 5.4: Methods to mitigate metabolism by cytochrome P450 enzymes

A number of methods exist to overcome oxidation by P450, with three possible options

being deuterium incorporation,<sup>103</sup> oxygen incorporation, and fluorine replacement<sup>107</sup> (Figure 5.4). Deuterium incorporation reduces the capacity for oxidation as a result of the kinetic isotope effect (KIE), wherein a heavier isotope requires greater energy input before a bond dissociation event can occur.<sup>108</sup> Consequently, this results in slower reaction kinetics at that position and reduced rates of metabolic degradation. Installation of an oxygen atom functions by eliminating a possible site of oxidation altogether while maintaining similar bond angles in the case of methylenes, with the added benefit of possibly increasing solubility of the resultant compound in aqueous environments due to increased hydrogen bonding. Finally, C-H to C-F replacement functions by replacing a comparatively weaker C-H bond with a much stronger C-F bond.<sup>107</sup> Additionally, as fluorine has a bond length to carbon similar to that of hydrogen, the replacement should be expected to result in the product maintaining similar steric characteristics as the parent compound.<sup>109</sup> In this project, my work has been focused on the oxygen incorporation method in order to mitigate oxidation of the  $\gamma$ -lactam ring.

### 5.3 Synthetic Routes Towards an Oxa-Gln Analog

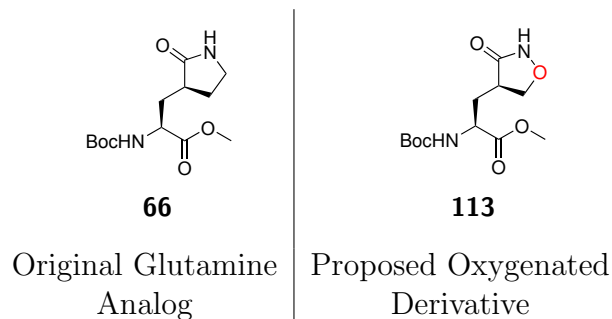
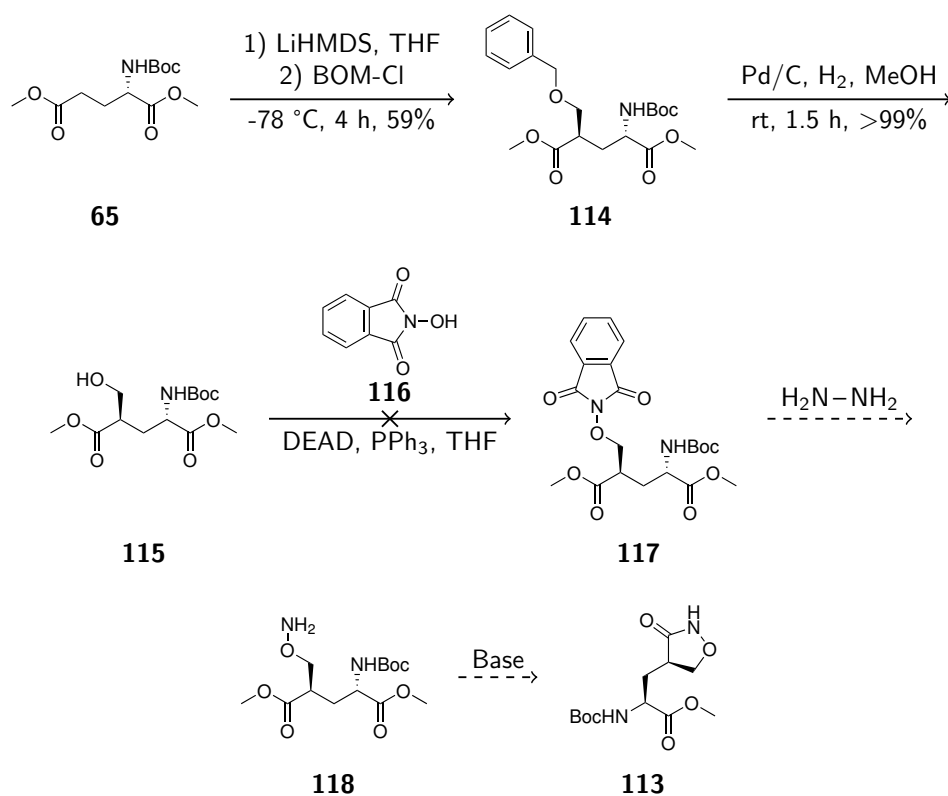


FIGURE 5.5: Chemical structures of original Gln building block **66** its oxa-analog **113**.

The following subsections depict a number of proposed synthetic paths towards the oxa-Gln analog depicted in Figure 5.5. Precedent for the formation of this 3-isoxazolidinone ring system came in the form of cycloserine and the numerous methods available for its synthesis.

### 5.3.1 Proposed Synthetic Approach 1 - Mitsunobu Reaction



SCHEME 5.1: Proposed synthetic path towards oxa-Gln analog **113** via a Mitsunobu reaction.

This pathway began with the stereoselective alkylation of Boc-protected glutamic acid dimethyl ester (**65**) using LiHMDS and benzyloxymethyl chloride. The reaction proceeded smoothly, albeit in moderate yield, furnishing product **114** in 59% yield (Scheme 5.1). Following this, a standard hydrogenolysis reaction over palladium to remove the benzyl group reveals a free hydroxyl in compound **115**. We attempted to couple this to *N*-hydroxyphthalimide using Mitsunobu conditions to provide compound **117**, which could potentially be subsequently reacted with hydrazine to afford product **118** containing a hydroxyl amine with a free nitrogen. Cyclization onto the nearby methyl ester would furnish the desired oxa-Gln analog **113**. Unfortunately, it was found that the Mitsunobu reaction produces alkene **119** instead, as confirmed by NMR data. This is hypothesized to be a consequence of triphenylphosphine oxide functioning as a leaving group during the reaction

resulting from a relatively acidic  $\alpha$ -hydrogen being present at the adjacent position (Figure 5.6). We attempted to add the *N*-hydroxyphthalimide to the alkene byproduct via a Michael addition. However, no reaction was observed to take place. Consequently, this synthetic approach was deemed a failure.

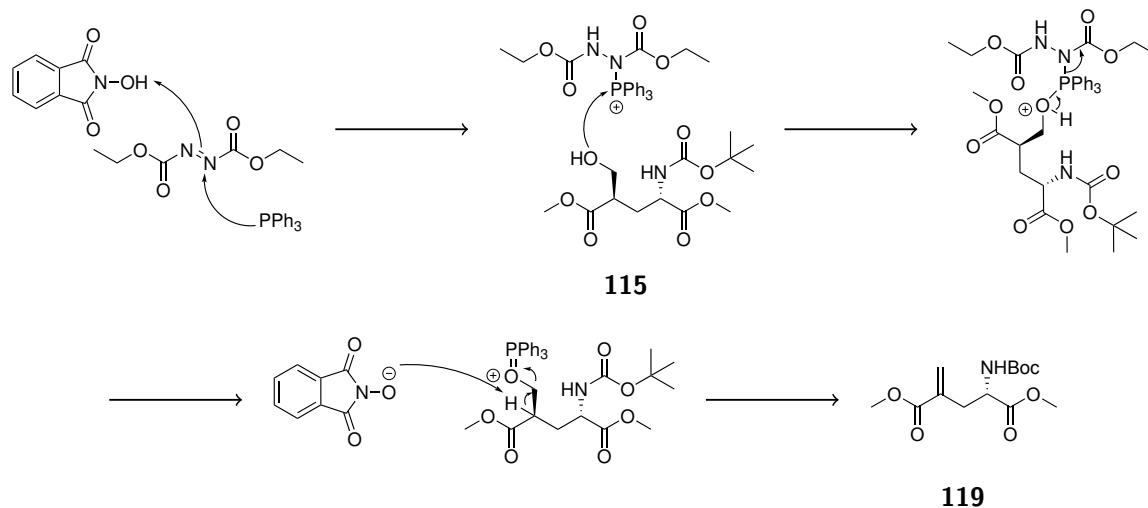
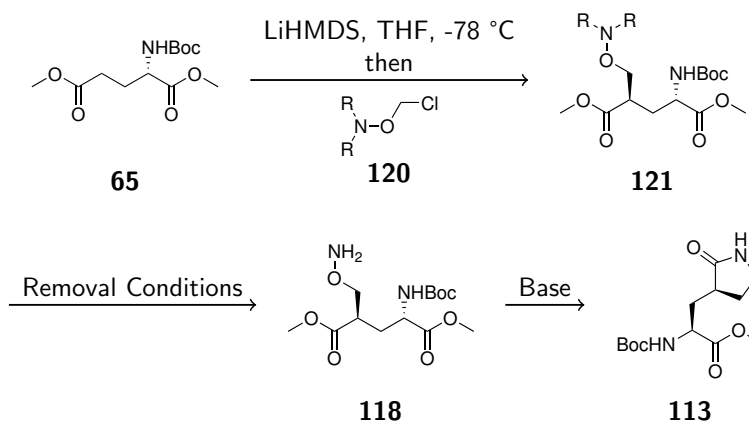


FIGURE 5.6: Proposed Mitsunobu mechanism for the production of alkene byproduct **119**.

### 5.3.2 Proposed Synthetic Approach 2 - Addition via Alkylation

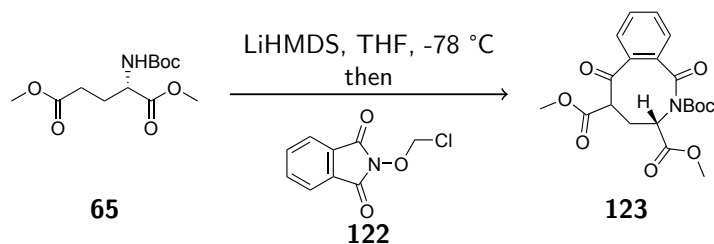


SCHEME 5.2: Proposed synthetic path towards oxa-Gln analog **113** via direct alkylation.

As an alternative, it was thought that an electrophilic synthon containing the required  $-\text{CH}_2-\text{O}-\text{N}-$  connectivity could be directly added to compound **65**, with the nitrogen

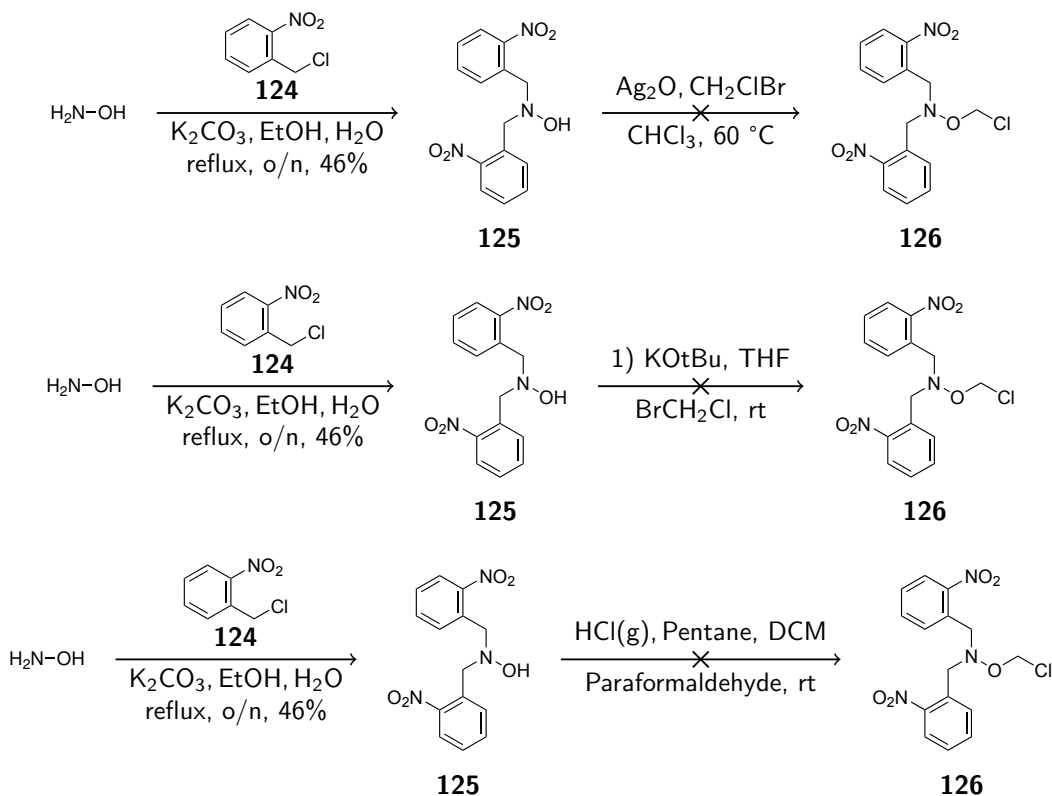


atom protected in some way, followed by deprotection and cyclization as depicted in Scheme 5.2.



SCHEME 5.3: Unexpected formation of 8-membered ring **123**.

The initial iteration of this pathway involved the alkylation of **65** with **122**. However, preliminary NMR data suggests that instead of the desired product forming, an 8-membered ring was formed instead (Scheme 5.3). While unexpected, limited examples could be found in literature.<sup>110,111</sup>



SCHEME 5.4: Attempted methods towards the synthesis of photolabile electrophile **126**.

Moving on from this, it was thought that the protecting groups on the nitrogen depicted

in Scheme 5.2 could be photolabile in nature, allowing them to be more robust during the alkylation step. Towards this goal, we sought to synthesize compound **126**. However, none of the reactions employed in an attempt to produce this compound were successful. During aqueous workup for the third reaction depicted in Scheme 5.4, it was observed that a spot on thin-layer chromatography (TLC) that had previously appeared in the reaction mixture had disappeared. It was hypothesized that a mustard-like decomposition pathway had contributed to the degradation of this compound, as depicted in Figure 5.7.

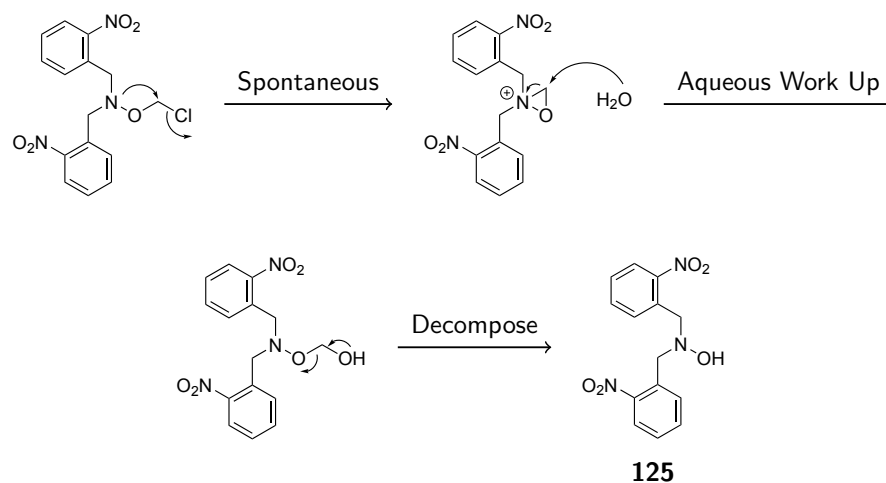
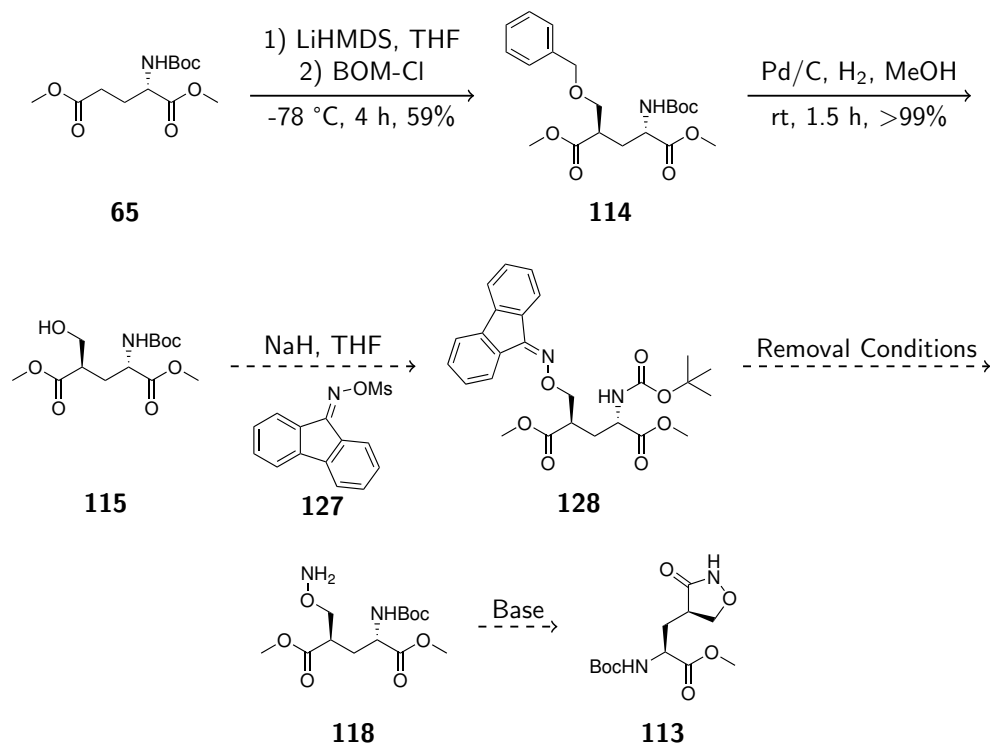


FIGURE 5.7: Proposed mustard-like degradation pathway of electrophile **126** to compound **125**.

### 5.3.3 Proposed Synthetic Approach 3 - Direct N-O Bond Formation

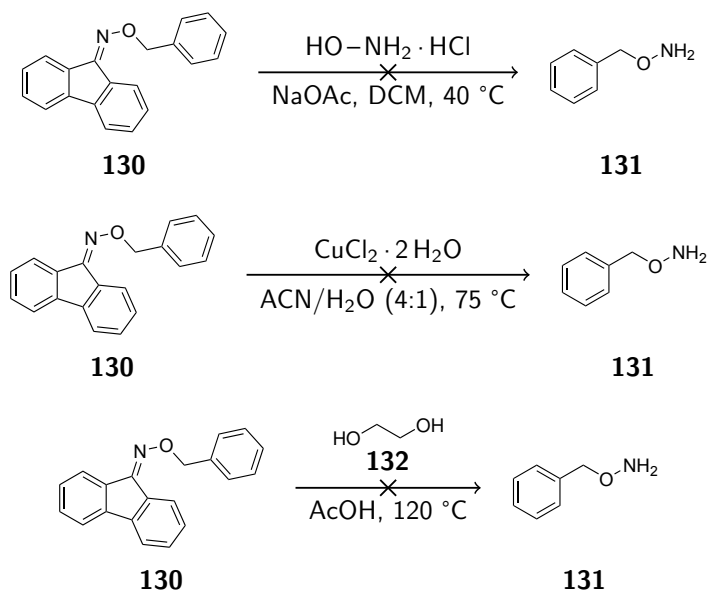
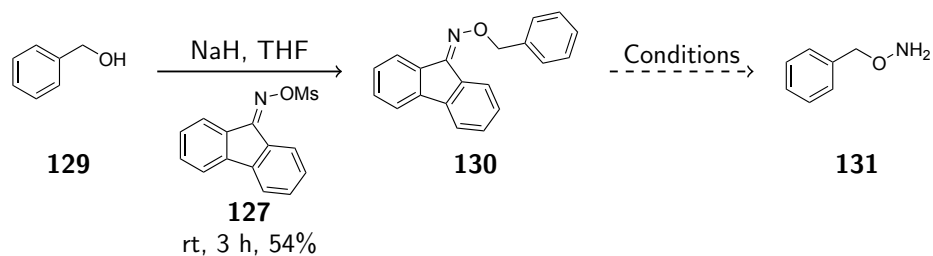
A third synthetic method that was tried involved the direct formation of an N-O bond using Hassner's reagent (Scheme 5.5). It was reported by Hassner and coworkers that having an appropriate leaving group on nitrogen could allow for displacement by a deprotonated alcohol.<sup>112</sup> We tested this reagent by utilizing benzyl alcohol as the nucleophile (Scheme 5.6). Unfortunately, comparatively harsh acidic conditions (6 M HCl in AcOH with heating) were required for removal of the 9-fluorenone group,<sup>112</sup> with none of the milder deprotection conditions (including one reported by Quan et al. involving CuCl<sub>2</sub><sup>113</sup>) being successful, this method was rendered incompatible with our goals.



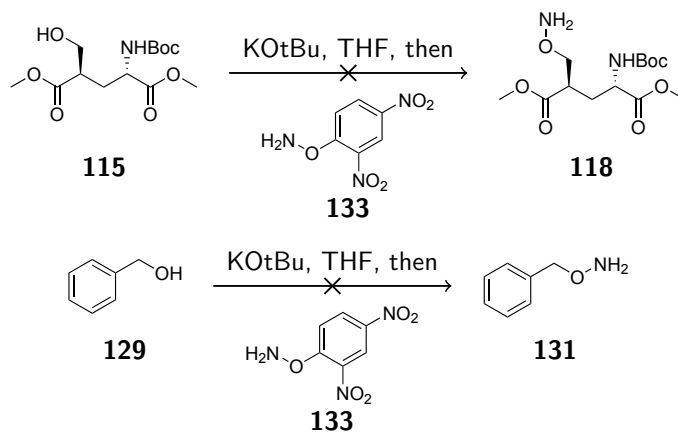
SCHEME 5.5: Proposed synthetic path towards oxa-Gln analog **113** via direct N-O bond formation using Hassner's reagent.

Examining the literature, we found reagent **133** reported by Legault and Charette<sup>114</sup> that was capable of electrophilically transferring a single amino group, however when trying to use the reagent with either compound **65** or benzyl alcohol, no reaction was found to occur (Scheme 5.7).

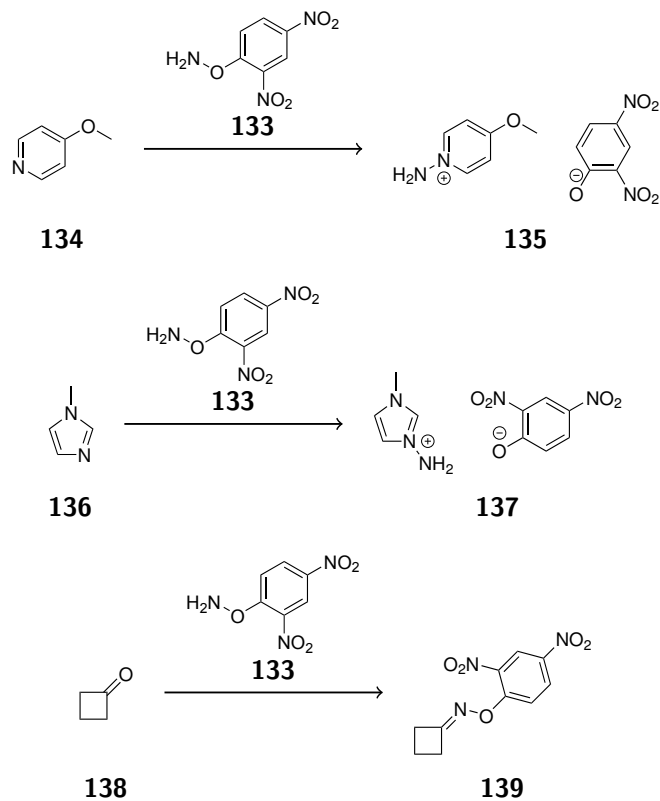
Further exploration of reports<sup>115,116</sup> using compound **133** demonstrated that it was largely effective only for transferring an amino group onto generally soft nucleophiles, while in the presence of electrophilic carbonyls such as ketones, functions as a nucleophile to form oximes instead<sup>117</sup> (Scheme 5.8).



SCHEME 5.6: Testing of reagent **130** using benzyl alcohol and subsequent attempts towards mild removal of 9-fluorenone.



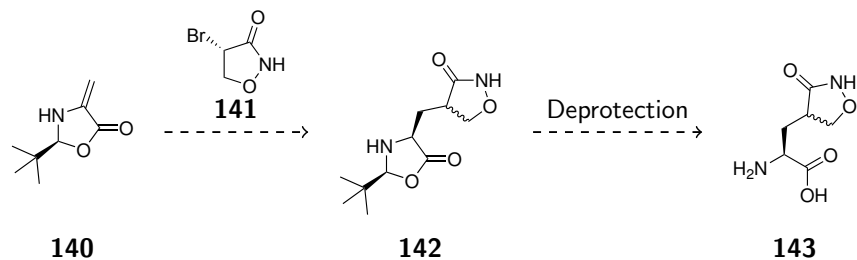
SCHEME 5.7: Attempts at using reagent **133** for single amino group transfer onto alcohols.



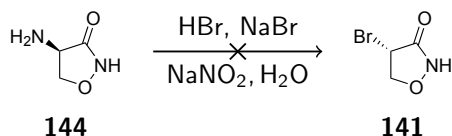
SCHEME 5.8: Literature examples of soft nucleophile nitrogen transfer and oxime formation by reagent **133**.

#### 5.3.4 Proposed Synthetic Approach 4 - Radical Addition

Another idea was to perform a chiral radical addition reaction onto chiral dehydroalanine **140** using a brominated derivative of cycloserine **141**. Subsequent removal of the pivaloyl group would then furnish diastereomers with the correct bond connectivity framework, differing at only one stereogenic center (Scheme 5.9). Unfortunately, it appears that the synthesis of **141** starting from D-cycloserine (**144**) results in degradation of the compound to unrecognizable polar byproducts (Scheme 5.10).

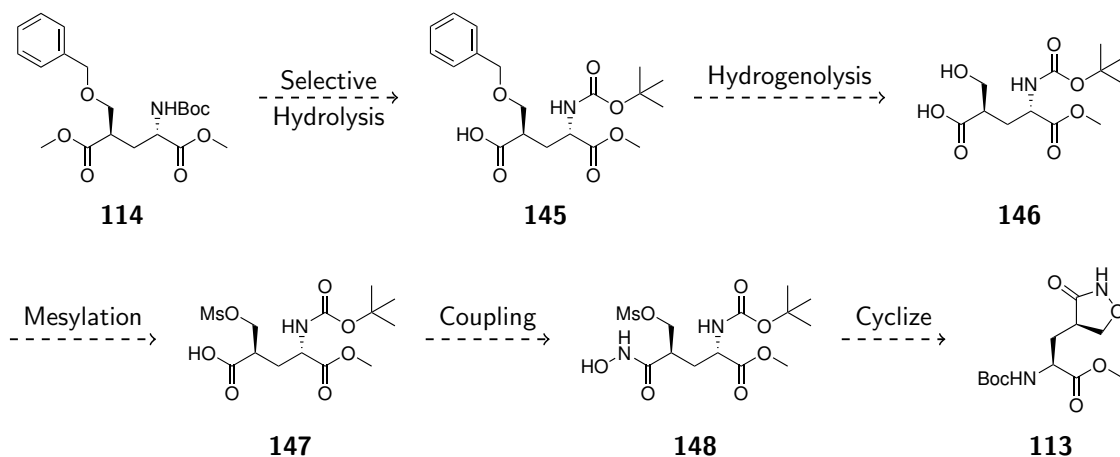


SCHEME 5.9: Proposed synthetic route to generate oxa-Gln framework via chiral radical addition.



SCHEME 5.10: Attempted synthesis of compound **141** for use in radical addition.

### 5.3.5 Proposed Synthetic Approach 5 - *N*-hydroxyamide Ring Closure



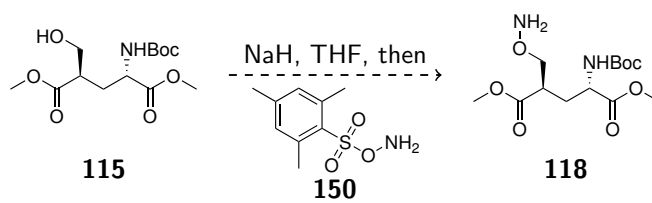
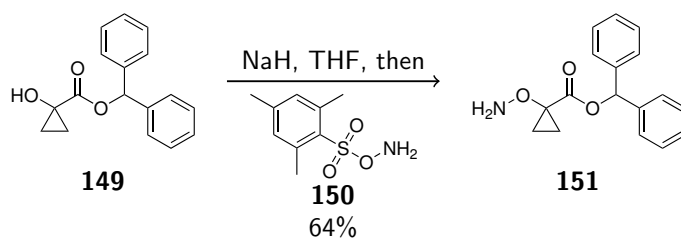
SCHEME 5.11: Proposed method for the formation of compound **113** via selective hydrolysis and mesylation.

The fifth method (Scheme 5.11) that is currently under investigation is the selective hydrolysis of one of the methyl esters in **114** to furnish the free acid **145**. This would then be subjected to removal of the benzyl group to provide hydroxy acid **146**, followed by subsequent mesylation of the alcohol to give mesylate **147**. Unlike the Mitsunobu intermediate containing the triphenylphosphine oxide group discussed in Section 5.3.1, elimination of the

mesyl group in compound **147** would likely not occur, as preferential deprotonation of the nearby free carboxylate and consequent anion formation should prevent further deprotonation at the  $\alpha$ -position adjacent to the mesyl group. Hydroxylamine protected on the oxygen can then be coupled to the free acid and subsequently deprotected to provide compound **148**. Finally, cyclization via nucleophilic attack of the hydroxyamide oxygen onto the mesylate methylene should in theory afford the desired oxa-Gln analog **113**. At present, the main challenge is to determine whether selective hydrolysis of one methyl ester over the other in compound **114** is feasible. Preliminary NMR studies using LiOH/D<sub>2</sub>O/tetrahydrofuran (THF) mixtures to hydrolyze compound **114** have so far proved inconclusive as the residual THF-d<sub>8</sub> signal overlaps with that of the ester methyl groups, though it appears that one of the signals is indeed decreasing. This will likely need to be further investigated using 2D heteronuclear multiple bond correlation (HMBC) NMR experiments in order to truly determine whether one methyl group is being selectively hydrolyzed, and if so, which one.

## 5.4 Conclusion and Future Work

Efforts towards a synthetic route to furnish the proposed oxa-Gln analog **113**, if successful, should find widespread use in the medicinal chemistry community as it would allow for bypassing metabolic reactions on a widely used  $\gamma$ -lactam Gln analog (see Chapter 4). Furthermore, proposed compound **113** also has a further benefit of possibly increasing solubility of therapeutics that it is employed in. The work presented in this chapter is currently ongoing. Aside from further investigations associated with evaluating the feasibility of the synthetic approach discussed in Section 5.3.5, another reagent (compound **150**) reported by Yamawaki et al. demonstrates direct transfer of an amino group onto a hard oxyanion nucleophile<sup>118</sup> (Scheme 5.12). This represents a promising avenue towards formation of the desired N-O bond and warrants further investigation.



SCHEME 5.12: Documented use of compound **150**<sup>118</sup> as an aminotransfer reagent and proposed use for N-O bond formation with compound **115**.



## Chapter 6

# Investigations Into Regulation of Polyketide Biosynthesis

### 6.1 Introduction to Polyketides

Polyketides are natural products found in fungi, bacteria, and plants. Comprising one of the largest classes of natural products, these secondary metabolites are noted for exhibiting bioactivity with surprising regularity.<sup>40,119–122</sup> With >7000 known structures and >20 of them currently utilized as commercial drugs,<sup>121</sup> better understanding how these compounds are synthesized is instrumental towards a number of pursuits with impact in both industry and academia. These include but are not limited to discovering potential new therapeutics through genome mining, modifying current scaffolds for increased therapeutic potential, and the design of completely novel structures.<sup>123,124</sup> Prominent examples of polyketides with biological activity include erythromycin (**152**) (antibiotic), aflatoxin B1 (**153**) (carcinogen), rapamycin (**154**) (immunosuppressant), curvularin (**155**) (anti-inflammatory), doxorubicin (**156**) (anticancer), cladosporin (**157**) (antimalarial), lovastatin (**158**) (anti-cholesterol), and equisetin (**159**) (toxin)<sup>119,121,125–128</sup> (Figure 6.1). With such a broad range of biological activities associated with this single class of natural products, it is hardly surprising to know that according to a report published in 2005, polyketides constitute 20% of the top selling drugs globally with an estimated economic impact of >20 billion USD.<sup>121</sup>

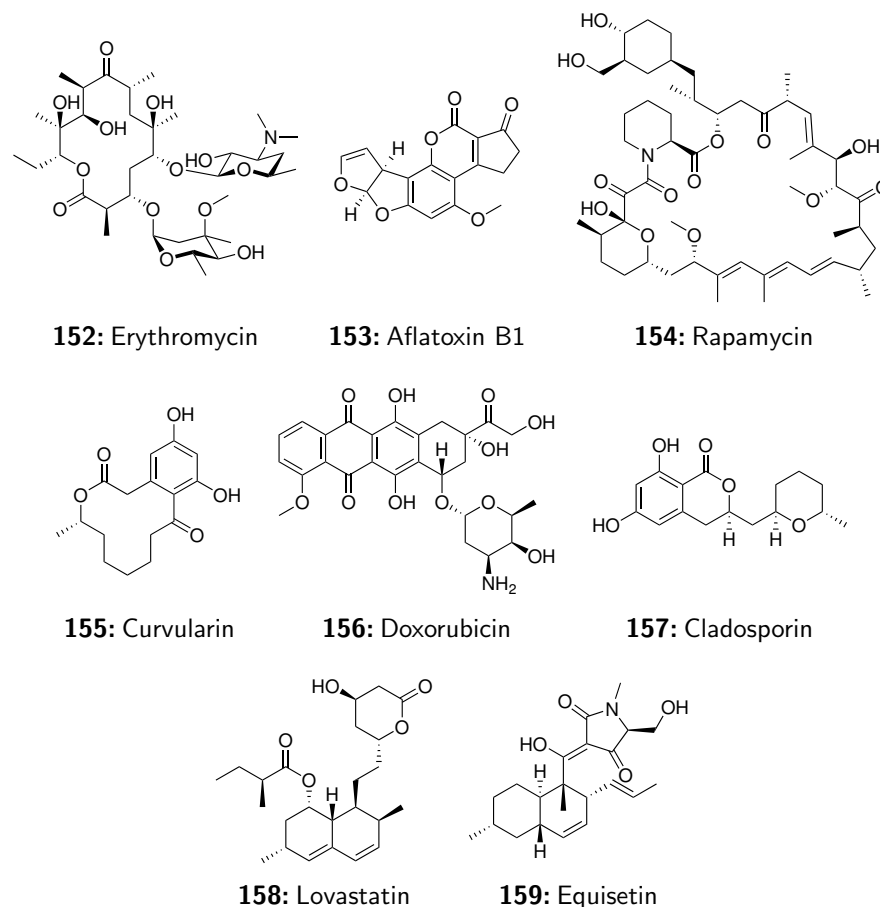


FIGURE 6.1: Structures of various well-known polyketides.

## 6.2 Polyketide Biosynthetic Process

Polyketides are biosynthesized through the repeated condensation, elongation, and modification of acetate subunits in a process analogous to fatty acid production.<sup>40</sup> A representative schematic depicting the biosynthesis of lovastatin precursor dihydromonacolin L is shown in Figure 6.2. Contained within the PKS megaenzyme are a number domains or modules that carry out specific biochemical transformations on the substrate.<sup>40,128,129</sup> Included amongst these are acyl carrier protein (ACP), ketosynthase (KS), methyltransferase (MT), ketoreductase (KR), dehydratase (DH), enoylreductase (ER), and thioesterase (TE) domains. The ACP works in tandem with the KS domain to elongate the substrate through decarboxylative condensation reactions using malonyl coenzyme A (CoA). At this point, the

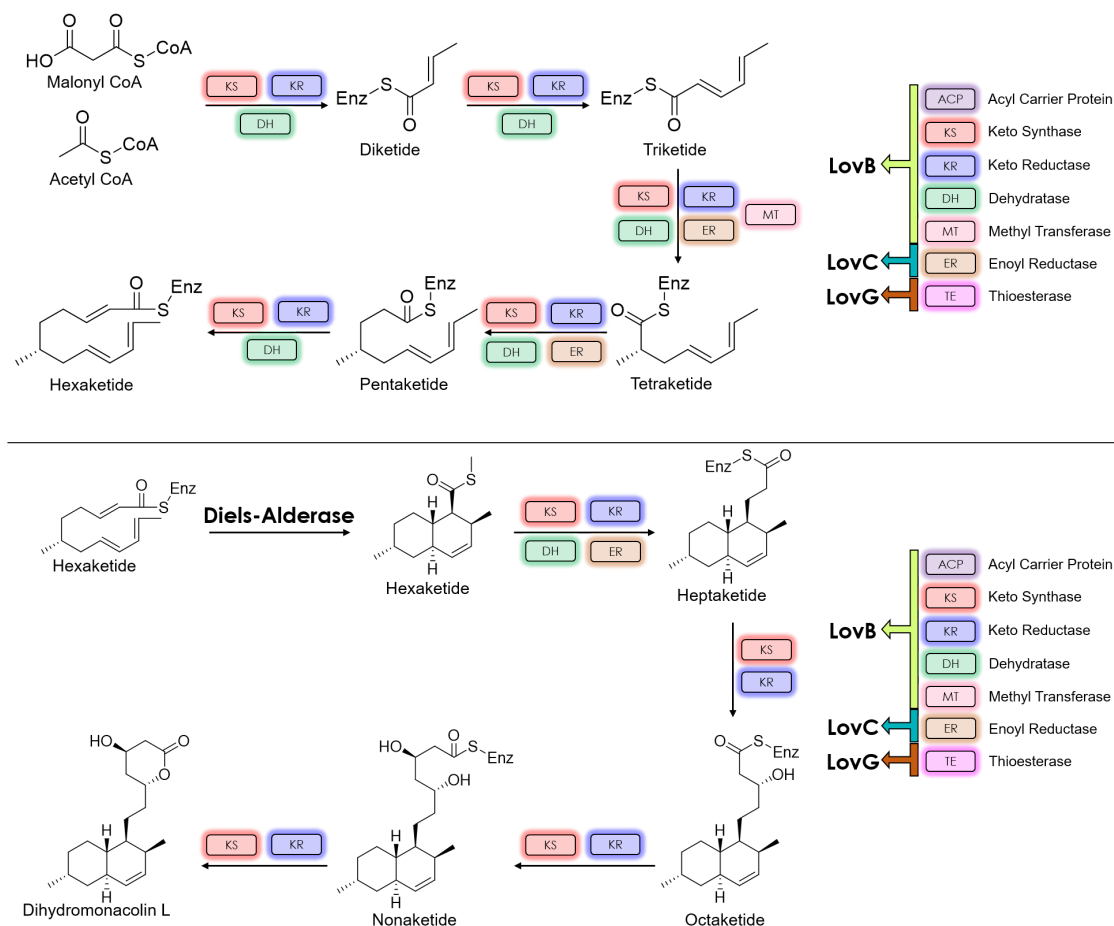


FIGURE 6.2: Biosynthesis of lovastatin precursor dihydromonacolin L by various polyketide domains.

MT domain optionally engages in the addition of a methyl group to a the  $\beta$ -keto thioester while the KR domain reduces the ketone to an alcohol. This can proceed further by a DH to give an alkene which may be reduced once more by an ER domain. At any point in this process the substrate may be subjected to another cycle of elongation, or be terminated and released from the enzyme by a TE domain.<sup>40</sup>

### 6.3 Types of Polyketide Synthases

There exists a number of different PKSs, and they can be classified into types I,<sup>130–132</sup> II,<sup>133</sup> and III.<sup>134</sup>

### 6.3.1 Type I Polyketide Synthases

Type I PKS can be further subdivided into iterative<sup>130</sup> and modular<sup>132</sup> types. Modular PKS systems are comprised of multiple sub-units or modules that do a single chain elongation and tailoring cycle. Conversely, iterative PKSs contain domains which are used repetitively throughout each round of chain elongation and modification, and are primarily found in fungi.<sup>130</sup> Overall, type I PKS systems are multimeric complexes made up of large multifunctional sub-units with domains required to fully carry out each constructive cycle of substrate synthesis.<sup>128,130</sup>

### 6.3.2 Type II Polyketide Synthases

Type II PKS are comprised of generally small dissociable domains and are primarily found in bacteria.<sup>135</sup> They are also responsible for the synthesis of a number of aromatic products such as doxorubicin.<sup>136</sup>

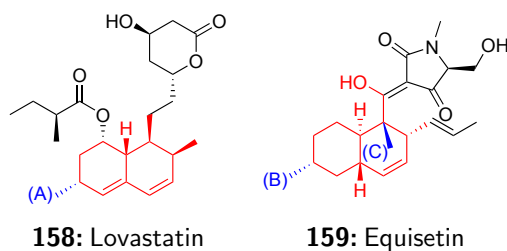
### 6.3.3 Type III Polyketide Synthases

Type III PKS are the rarest of the three types and are generally found in plants.<sup>134,137</sup> This type of PKS lacks an ACP component, and freely use CoA thioesters, both aliphatic and aromatic in nature, as feedstock for the biosynthesis of many plant-derived natural products and metabolites.<sup>137,138</sup>

## 6.4 Investigating the Programming of Polyketide Synthesis

Focus in the Vederas lab has traditionally been on type I iterative PKS systems.<sup>128,129,139,140</sup> While each domain responsible for completing a particular transformation on the growing substrate is used repeatedly in these systems, they are not used in every single elongation cycle. At times, the substrate is fully reduced before the next elongation cycle occurs, while in other cases the substrate is only partially reduced, retaining either a double bond or an alcohol, or perhaps not reduced at all, retaining

the nascent keto group formed after the initial activity of the KS domain. In other instances, the MT domain appears to function only when the substrate is at certain lengths, remaining largely inactive in all other cases.<sup>139</sup> The method by which this type of complex programming is accomplished with such precision in the enzyme is not yet well understood. Our hypothesis is that whether a particular transformation is utilized or not is dependent upon substrate-enzyme compatibility and reaction rate, i.e. the naturally observed modification is the fastest reaction at a particular instance, and is the one that occurs. A secondary caveat that this hypothesis introduces is that in the event that the expected modification at a particular step cannot happen (e.g. the required domain is not present or is inactivated, or the appropriate cofactors are absent), the next fastest reaction will take place, leading to unnatural substrates being produced, albeit at a much slower rate, and in fact this has been observed previously.<sup>128,139</sup> This facilitates the introduction of seemingly limitless combinations of complexity in the final products, ranging from aromatic ring systems to reactive handles for subsequent post-synthetic modifications. Better understanding of this regulatory mechanism could hypothetically allow access to designer polyketides and facilitate precise, directed modifications of currently known structures.



Red denotes core structure of polyketide.

Blue denotes methyl groups installed by MT domains.

FIGURE 6.3: Structures of lovastatin (**158**) and equisetin (**159**) with backbone and key methyl groups highlighted.

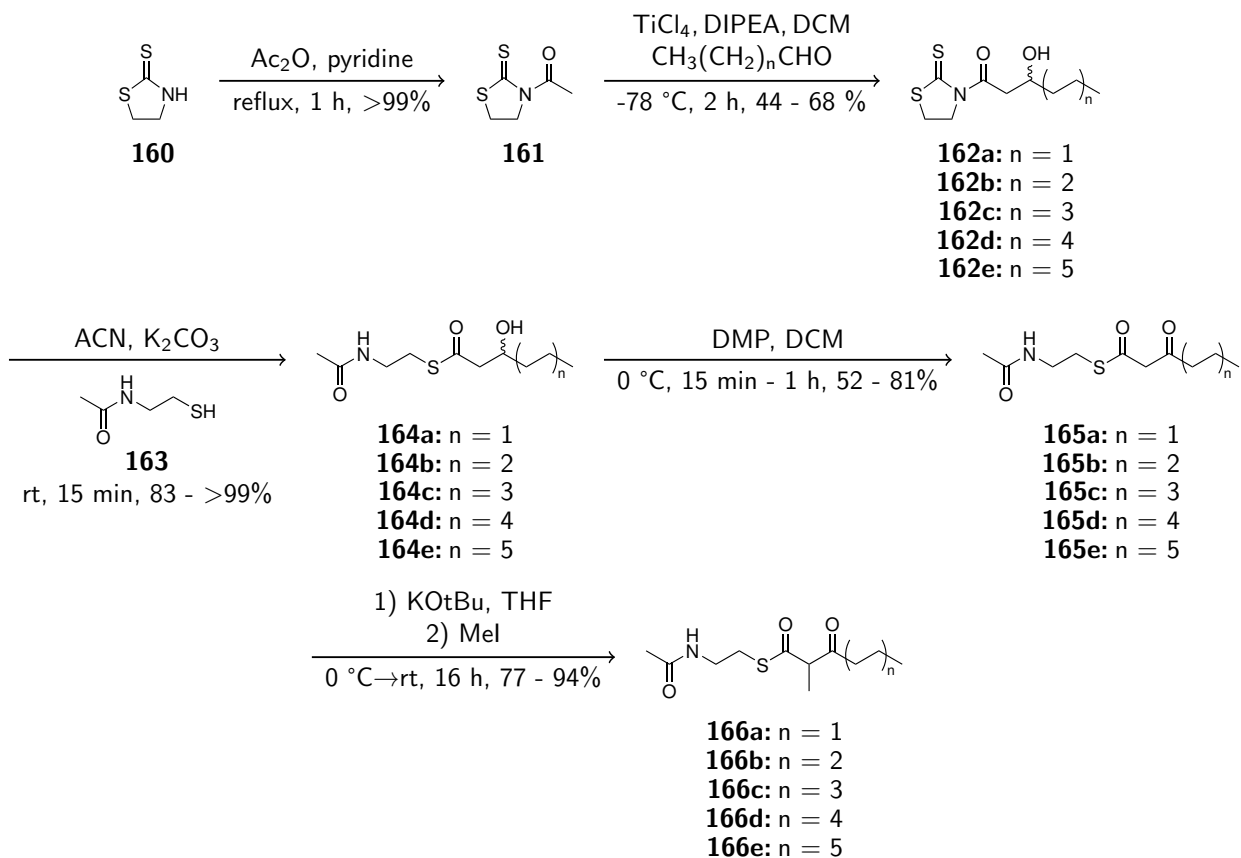
To test our hypothesis of kinetically-controlled biosynthesis, we began our efforts by simplifying this system down to two domains: MT and KR. These were chosen as they represented the very first domains to act after chain elongation by KS and in theory should

possess the fastest inherent kinetics. Additionally, the activity of MT is gated by KR, as MT can only function prior to reduction of the keto group by KR. Next, we chose two polyketide products to examine, namely lovastatin (anti-cholesterol, produced by *Aspergillus terreus*) and equisetin (toxin, produced by *Fusarium heterosporum*), as while their core structures are quite similar, they differ significantly in biological activity. As shown in Figure 6.3, while the backbones (highlighted in red) of these two polyketides are very similar, methyl groups (highlighted in blue) installed by the MT domain of each PKS system are located at different positions and installed during different stages of polyketide synthesis. For comparison, the methyl group in lovastatin ((A), Figure 6.3) is installed during the tetraketide stage, while those in equisetin ((B) and (C), Figure 6.3) are installed during the pentaketide and heptaketide stages.

The experimental setup would involve the synthesis of various model polyketides and product standards as *N*-acetylcysteamine (SNAC) thioesters differing initially in chain length, and in the future, functional groups. These would then be individually assayed against isolated MT and KR domains from both *A. terreus* and *F. heterosporum* to determine baseline reaction kinetics for each domain as a function of chain length. As a further follow up, competition experiments where the MT of *A. terreus* and the KR of *F. heterosporum* (and vice-versa) are both in the presence a single substrate would be conducted to see which one would act faster and whether baseline reaction kinetics would hold true. If successful, this would prove to be a key experiment in demonstrating that substrate specificity and PKS programming is indeed a function of reaction kinetics.

## 6.5 Synthesis of Probe Substrates and Product Standards

Synthesis of the required substrates began with synthesis of the achiral Crimmins auxiliary **161** starting from 2-thiazoline-2-thione (**160**) via a simple acylation reaction with Ac<sub>2</sub>O in pyridine. Next, an aldol condensation onto an appropriate aldehyde provides the  $\beta$ -hydroxyamides **162**. The Crimmins auxiliary of these compounds were then removed via



SCHEME 6.1: General synthetic scheme to access aliphatic polyketide substrates and standards for enzymatic testing.

displacement with SNAC to furnish compounds **164**. Following this, oxidation using DMP then provides the KR and MT substrates **165**. Finally, KOtBu mediated alkylation using methyl iodide then produces the MT products **166** as a mixture of mono- and di-alkylated compounds (Scheme 6.1). At the time of this writing, they will require a final HPLC purification prior to use as product standards as these are inseparable via standard FCC on silica.

## 6.6 Conclusion and Future Work

With the substrates and product standards for both the MT and KR domains now in hand, the next step is to purify the domains as standalone enzymes to perform the required assays and determine the aforementioned baseline kinetic rates of each substrate-domain

permutation. The major hurdle here is expression, ideally in a heterologous fashion, of domains that remain functional as standalone enzymes. An alternative is the expression of the PKS system as a whole accompanied by site-directed mutagenesis to selectively disable domains that are outside of experimental scope.<sup>139</sup> Should this be successful, the subsequent experiment is a mixed-domain assay for each substrate to examine and compare relative rates between the domains. This will open the door to a number of additional experiments examining the effects of different functional groups, as well as substrate compatibility with other domains. The ultimate goal is to expand this platform in an attempt to undertake mix-and-match synthesis using numerous domains from a variety of organisms. Developing this platform for designer polyketides will facilitate access to structures not found in nature and promote drug discovery efforts not otherwise available.



## Chapter 7

# Experimental Procedures

**Note:** Significant portions of the experimental data presented herein have been published<sup>25,26,141,142</sup> at the time of this writing and are reprinted below for the reader's convenience.

### 7.1 General Information

#### 7.1.1 Compound Characterization

NMR spectra and coupling constants (J) were obtained using an Agilent VNMRS 700 MHz, Agilent/Varian VNMRS 600 MHz, Agilent/Varian VNMRS 500 MHz, Agilent/Varian Inova 500 MHz, Agilent/Varian Inova 400 MHz, or Agilent/Varian DD2 MR 400 MHz spectrometer. For <sup>1</sup>H (700, 600, 500, 400 MHz) spectra,  $\delta$  values were referenced to CDCl<sub>3</sub> (7.26 ppm), CD<sub>3</sub>OD (3.31 ppm), or (CD<sub>3</sub>)<sub>2</sub>SO (2.50 ppm), and for <sup>13</sup>C (175, 150, 125, 100 MHz) spectra,  $\delta$  values were referenced to CDCl<sub>3</sub> (77.16 ppm), CD<sub>3</sub>OD (49.00 ppm), or (CD<sub>3</sub>)<sub>2</sub>SO (39.52 ppm) as the solvents. Samples containing a radical are quenched with a small amount of phenylhydrazine prior to NMR spectra acquisition. Infrared (IR) spectra were recorded on a Nicolet Magna 750 or a 20SX FT-IR spectrometer. Cast film and thin film refers to the evaporation of a solution on a NaCl plate. Mass spectra were recorded on a ZabSpec IsoMass VG (high resolution electrospray (ES)). LC-MS analysis was performed on an Agilent Tech-

nologies 6220 orthogonal acceleration TOF instrument equipped with +ve and -ve ion ESI ionization, and full-scan MS (high resolution analysis) with two-point lock mass correction operating mode. The instrument inlet was an Agilent Technologies 1200 SL HPLC system. specific rotation at 26 °C ( $[\alpha]_D^{26}$ ) was measured using a Perkin Elmer 241 Polarimeter.

### 7.1.2 General Synthetic Procedures

All commercially available reagents and protected amino acids were purchased and used without further purification unless otherwise noted. All the solvents used for reactions were used without further purification unless otherwise noted. Dry solvents refer to solvents freshly distilled over appropriate drying reagents prior to use. Drying over a drying agent refers to drying the organic solution using said agent followed by filtration to remove the solid particulate matter. Commercially available ACS grade solvents (>99.0% purity) were used for column chromatography without any further purification. Heating of reactions was achieved via oil baths unless otherwise noted.

### 7.1.3 Purification

All reactions and fractions from column chromatography were monitored by thin layer chromatography (TLC) using glass plates (5 × 2.5 cm) pre-coated (0.25 mm) with silica gel (normal SiO<sub>2</sub>, Merck 60 F254). Visualization of TLC plates was performed by UV fluorescence at 254 nm in addition to staining by KMnO<sub>4</sub>, ninhydrin, or phosphomolybdic acid (PMA) solutions. Flash chromatography was performed using Merck type 60, 230-400 mesh silica gel at elevated pressures.

## 7.2 Marfey's Assay for Determination of Amino Acid Enantiomeric Ratios

### 7.2.1 Marfey's Assay Experimental Procedure

Marfey's assay works by derivitizing an enantiomeric mixture of amino acids using 1-fluoro-2-4-dinitrophenyl-5-L-alanine amide (FDAA), forming a diastereomeric mixture that can be separated using achiral chromatographic methods. Subsequent analysis can then determine relative proportions of the initial enantiomeric mixture. The general procedure for stereochemical analysis by Marfey's assay is as follows: Spin-labeled amino acid (1 mg, 0.0041 mmol, 1.0 equiv) and 1-fluoro-2-4-dinitrophenyl-5-L-alanine amide (FDAA, Marfey's Reagent) (5.5 mg, 0.0205 mmol, 5.0 equiv) was dissolved in 2.0 mL of acetonitrile. To this was added  $\text{NEt}_3$  (5.7  $\mu\text{L}$ , 0.0411 mmol, 10.0 equiv). The reaction mixture was then capped and allowed to stir overnight at 40 °C. An LCMS sample was then prepared by diluting 15  $\mu\text{L}$  of reaction mixture in 1.5 mL of acetonitrile and the sample was sent for analysis.

### 7.2.2 Marfey's Assay Analysis

RP-HPLC-MS was performed using an Agilent 1200 SL HPLC System with a Kinetex C8 reverse-phase analytical column (2.1x50 mm, 1.7  $\mu\text{m}$  particle size, 100 Å) (Phenomenex, Torrance, CA, USA), thermostated at 50 °C followed by mass spectrometric detection. An aliquot of 2  $\mu\text{L}$  was loaded onto the column at a flow rate of 0.50 mL/min and an initial buffer composition of 2% mobile phase A (0.1% formic acid in  $\text{H}_2\text{O}$ ) and 98% mobile phase B (0.1% formic acid in acetonitrile). Analytes were eluted using a linear gradient from 2% to 95% mobile phase B over a period of 5.5 minutes, held at 95% mobile phase B for 2 minutes to remove all analytes from the column and 95% to 2% mobile phase B over a period of 0.5 minutes. Mass spectra were acquired in negative mode of ionization using an Agilent 6220 Accurate-Mass TOF HPLC/MS system (Santa Clara, CA, USA) equipped with a dual sprayer electrospray ionization source with the second sprayer providing a reference

mass solution. Mass spectrometric conditions were drying gas 10 L/min at 325°C, nebulizer 30 psi, mass range 100-1100 Da, acquisition rate of  $\sim 1.03$  spectra/sec, fragmentor 110V, skimmer 65 V, capillary 3500 V, instrument state 4 GHz High Resolution. Mass correction was performed for every individual spectrum using peaks at  $m/z$  112.9856 and 1033.9881 from the reference solution. Data acquisition was performed using the Mass Hunter software package (ver. B.04.00.). Analysis of the HPLC-UV-MS data was done using the Agilent Mass Hunter Qualitative Analysis software (ver. B.07.00 SP2).

## **7.3 Synthesis of FRET Substrate for Determination of SARS-CoV-2 M<sup>Pro</sup> Enzyme Kinetics**

### **7.3.1 General 2-Chlorotrityl Chloride Resin Loading Procedure**

2-Chlorotrityl chloride resin was transferred to a SPPS vessel and washed with dry DCM ( $2 \times 10$  mL) and then dry DMF ( $2 \times 10$  mL) for 1 min each, and then bubbled under argon in dry DMF (10 mL) for 10 min. The desired Fmoc-protected amino acid (1.0 equiv, based on desired resin loading) and DIPEA (5.0 equiv) were suspended in 10 mL of a 50/50 mixture of dry  $\text{CH}_2\text{Cl}_2$ /DMF. This solution was bubbled under argon for 2.5 h to load the desired amino acid onto the solid support, continually topping up the DCM to maintain an approximately 10 mL volume. To end cap any remaining trityl groups, dry MeOH was added to the vessel (0.8 mL per gram of resin) and bubbled under Ar for 15 min. After draining, the resin was washed with dry DMF ( $3 \times 10$  mL), dry DCM ( $3 \times 10$  mL), and then with dry MeOH ( $3 \times 10$  mL) for one min each. The resin was dried thoroughly and then stored at  $-20$  °C under argon.

### **7.3.2 General Automated SPPS Elongation Method**

All peptides were synthesized on a PreludeX (Gyros protein technologies). SPPS was carried out on a 0.1 mmol scale using Fmoc chemistry on 2-chlorotrityl resin (0.8 mmol/g).

Commercially available Fmoc-protected amino acids were loaded on the peptide synthesizer as 0.2 M solutions in DMF. All amino acids were coupled using 1- [Bis(dimethylamino)-methylene]-1*H*-1,2,3-triazolo[4,5-*b*]pyridinium 3-oxide hexafluorophosphate (HATU) as the activating agent with a coupling time of 1 h. Fmoc residues were deprotected using a 20% solution of piperidine in DMF.

### 7.3.3 Synthesis of FRET Peptide Substrate

Fmoc-L-Arg(Pmc)-OH was loaded onto 2-chlorotrityl chloride resin (0.18 mmol/g) using the aforementioned general procedure. The resin was elongated using automated SPPS, introducing amino acids in the following order: Fmoc-Tyr(NO<sub>2</sub>)-OH, Fmoc-Gly-OH, Fmoc-Ser(*O**t*Bu)-OH, Fmoc-Gln(*Trt*)-OH, Fmoc-Leu-OH, Fmoc-Thr(*t*Bu)-OH, Fmoc-Val-OH, Fmoc-Ser(*O**t*Bu)-OH, and Boc-Abz-OH with the final N-terminal Boc group being left on the peptide. The peptide was then cleaved off the resin using the following documented procedure (see Subsection 7.3.4), and purified using a Vydac Si C18 RP-HPLC semipreparative column (300 Å, 5 μM, 10 × 250 mm) (see Subsection 7.3.5), with the desired peptide eluting at 16.2 minutes. The HPLC fractions were pooled and lyophilized to produce the peptide as a yellow powder. The peptide was analyzed using HRMS (ESI) calcd for C<sub>50</sub>H<sub>77</sub>N<sub>15</sub>O<sub>18</sub> [M + 2H]<sup>2+</sup> 587.7780, found 587.7781.

### 7.3.4 General Method for Cleavage of Peptide from Resin

Resin-bound analogue was suspended in 95/2.5/2.5 TFA/TIPS/H<sub>2</sub>O with shaking for 2-3 h. The resin was removed via filtration through glass wool, rinsed with TFA, and the solution concentrated *in vacuo*. Cold Et<sub>2</sub>O (2 × 5 mL) was added to triturate the crude residue. The Et<sub>2</sub>O was decanted and briefly centrifuged for 3 min at 13000 rpm to pellet any residual peptide. The Et<sub>2</sub>O was removed and the peptide pellet was then dried thoroughly by centrifugation in a vacuum centrifuge for 5 min. The pellet and triturated crude residue were combined and dissolved in 0.1% aqueous TFA.

### 7.3.5 HPLC Purification Method

Purification of the FRET peptide substrate was carried out by Tess Lamer. The FRET peptide substrate was purified using a C<sub>18</sub> RP-HPLC column with aqueous 0.1% TFA (solvent A) and 0.1% TFA in acetonitrile (solvent B) as eluents. The analytical purification method used was: 0 – 3 min 10% B, 3 – 4.5 min 10% – 25% B, 4.5 – 14.5 min 25% – 40% B, 14.5 – 17 min 40% – 90% B, 17 – 19.5 min 95% B, 19.5 – 20.5 min 95% – 10% B, 20.5 – 30 min 10% B.

## 7.4 <sup>13</sup>C-labelled GC373 and GC376 NMR Experiments

### 7.4.1 Sample Preparation for NMR Binding Assays

NMR samples were first prepared by dialyzing SARS-CoV-2 M<sup>pro</sup> enzyme to exchange buffers (target buffer: D<sub>2</sub>O, 50 mM phosphate, pD 7.5 with 20 mM DTT) by spin filtration (Amicon micro-spinfilter, 10 kDa cutoff). A 50  $\mu$ L solution of 2.6 mg/mL enzyme was added to the spin filter and diluted to 300  $\mu$ L, then spun at 6600 g for 18 min. This was repeated an additional 2 times, and the sample was then made up to 300  $\mu$ L in volume and transferred to the NMR tube. Samples of enzyme in the presence of inhibitor were prepared by administering an additional 1.5  $\mu$ L of <sup>13</sup>C labelled GC373 solution (20 mM in DMSO) to the aforementioned enzyme sample. Sample data was acquired in 5 mm Varian specific D<sub>2</sub>O susceptibility matched microcell (i.e. BMS-00V) Shigemi NMR tubes purchased from Wilmad Lab-glass Inc. All NMR solvents were purchased from Sigma Aldrich. NMR tubes were washed between runs using 5 rinses of D<sub>2</sub>O, and then inverted to air dry overnight. Small volume additions (e.g. inhibitor added to enzyme) to samples in Shigemi NMR tubes were done by adding to the top of the outer NMR tube with the inner plunger removed, and then carefully tapping the sample tube in an almost horizontal position while rotating to break the surface tension and allow sample liquid to flow up the tube. The sample volume was allowed to travel up until making contact with the additional material. The tube was

then repeatedly whipped downward to move the material to the bottom. This was repeated several times so that additions were rinsed down into the microcell ensuring proper mixing.

#### 7.4.2 NMR Spectroscopy Experiments

NMR experiments were collected at 16.45 T (i.e. 700 MHz) using a 4-channel ‘VNMR5’ (Varian/Agilent) NMR spectrometer (VNMRJ 4.2 patch110 software) with an Agilent 7620 automatic sample handling system. A 5 mm triple resonance cryogenically cooled (20 K)  $^1\text{H}$  direct-detection (i.e. with  $^{13}\text{C}^{15}\text{N}$  on the outer coil) probe was utilized for all experiments. The probe had cooled preamplifiers on the  $^1\text{H}$  and  $^{13}\text{C}$  detection channels. The sample temperature was calibrated to 27 °C using methanol.<sup>143</sup> All spectra were run “locked” on the  $^2\text{H}$  resonance signal and chemical shifts were referenced using the residual proton  $^1\text{HOD}$  signal position<sup>144</sup> (i.e. 4.7 ppm) prior to saturation. One dimensional  $^1\text{H}$  data were acquired using presaturation<sup>145,146</sup> for residual  $^1\text{HOD}$  solvent suppression, followed by a 90° excitation pulse and data acquisition. The saturation carrier position amplitudes were manually optimized using a position sweep array and based on the calibrated high-power pulse, respectively. Saturation was applied directly on the water resonance (i.e. depending on water suppression efficacy and the ability to avoid analog to digital and/or receiver overloads with sufficient gain for data acquisition). The saturation was applied with a gammaB1 induced field strength of 80 Hz,<sup>147</sup> and a duration of 2 seconds. The 90° pulse width was determined after tuning and matching each sample, using one-pulse nutation optimization.<sup>148</sup> Other specific 1D acquisition parameter settings were: sweep width of 14044 Hz, acquisition time 2.5 seconds, with 70224 total (i.e. real plus imaginary) data points. A gradient-selected phase-sensitive two dimensional  $^1\text{H},^{13}\text{C}$ -heteronuclear single quantum correlation (HSQC)<sup>149–151</sup> with adiabatic inversion, refocusing and decoupling  $^{13}\text{C}$  pulses (i.e. gHSQ-CAD Varian/Agilent “ChemPack”, Krish Krishnamurthy) was used for all experiments. The HSQC spectra were acquired with  $^1\text{H}$  and  $^{13}\text{C}$  sweep widths (and recorded points) of 8389 Hz (12 ppm) and 38722 Hz (220 ppm), respectively (1678 total directly detected and 32 complex indirectly detected points, also respectively). A gradient stabilization delay of 500

$\mu\text{s}$  was used and 146 Hz JHC applied for INEPT transfers. Adiabatic inversion/recovery  $^{13}\text{C}$  pulses were applied at a 13.1 kHz induced field with a 600  $\mu\text{s}$  duration covering 400 ppm. Adiabatic decoupling was applied at 2.6 kHz induced field during the entire 100ms acquisition period. Carbon chemical shift referencing and carrier position (100 ppm) was based on indirect IUPAC  $^1\text{H}$  referencing.<sup>152</sup> The carbon carrier position was moved (e.g. 80, 90, or 100 ppm) to eliminate the possibility of peaks of interest near the carrier position being artifactual (i.e. quadrature “glitch”). For processing of NMR data, all dimensions were zero-filled to twice the number of acquired points. A line-broadening apodization function of 0.25 Hz was applied for  $^1\text{H}$ -1D spectra while a  $\pi/2$  squared sine-bell weighting function was utilized for the 2D HSQC (both dimensions). No linear prediction was applied nor was non-linear/nonuniform data acquisition utilized to avoid any possible artifacts in the resulting data. The final spectra were manually phased and baseline corrected.

### 7.4.3 Stereochemical Population Distribution Studies

NMR samples of GC373 were prepared by dissolving the sample in  $\text{CDCl}_3$  or in the case of  $\text{D}_2\text{O}$ , as a solution in DMSO- $d_6$  that was subsequently diluted to a final concentration of 1% DMSO- $d_6$  in  $\text{D}_2\text{O}$ . Preparation of GC376 samples omitted the use of DMSO- $d_6$  as a co-solvent. Additional information and protocols for samples containing  $\text{M}^{\text{pro}}$  enzyme can be found previously documented in literature.<sup>25</sup> Experiments were executed on a 700 MHz Agilent VNMRs spectrometer equipped with a cryo-cooled HCN triple resonance Z-gradient probe.

## 7.5 Solubility Studies

### 7.5.1 Solubility Determination of GC376 Cation Derivatives

Solubility studies were carried out by depositing 10 mg of bisulfite prodrug (differing in cation - Na, K, or choline) in a small conical vial and sequentially adding  $\text{H}_2\text{O}$  in 0.5  $\mu\text{L}$  increments at 25  $^\circ\text{C}$ . These mixtures were then alternately vortexed using a desktop



instrument (30 s) and sonicated in a water bath (30 s) 3 × each. The mixtures were then observed to see if and solids remained. Additional volumes of H<sub>2</sub>O (in 0.5 mL increments) were added followed by vortexing and sonication steps until a clear, transparent mixture was obtained. Back calculation then allowed for determination of upper solubility limits for each variant of bisulfite salt.

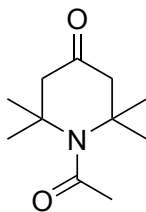
### 7.5.2 DOSY Experiments

Diffusion Ordered Spectroscopy (DOSY) measurements were performed on a 600 MHz four-channel Varian VNMRS spectrometer equipped with an HCN Z-gradient probe using OpenVNMRJ 2.1A as the acquisition and processing software. The Oneshot45 DOSY pulse sequence<sup>153,154</sup> was used for all diffusion measurements. All experiments were done at 27 °C. The 90 ° pulse was optimized for each sample using a simple pulse acquire NMR experiment with presaturation of the residual HOD during the relaxation delay. The diffusion delay was optimized for each sample using the Oneshot45 pulse sequence using 5 different pulsed field gradient strengths from 2.4 G/cm to 59.5 G/cm. Based on the optimized diffusion delay, for GC376 (**63**) and compound **99** diffusion delays of 50-200 ms were used, the final DOSY experiment was acquired using 15 different pulsed field gradient strengths from 2 G/cm to 59.5 G/cm with 12 scans for each value of gradient strength. The DOSY data were baseline corrected and then processed using a two component fit, were corrected for non-uniform pulsed field gradient shapes and plotted using the DOSY module in OpenVNMRJ 2.1A.

## 7.6 Synthetic Procedures and Characterization Data of Compounds

### 7.7 Chapter 2 Synthetic Procedures

#### 1-Acetyl-2,2,6,6-tetramethylpiperidin-4-one (10)



10

Under an argon atmosphere was added  $\text{Ac}_2\text{O}$  (40 mL, 420 mmol, 6.52 equiv) and 2,2,6,6-tetramethyl-4-piperidinone. The reaction mixture was then heated to 100 °C and stirred overnight, turning black during this time. Upon reaction completion, excess  $\text{Ac}_2\text{O}$  was removed *in vacuo*. The oily material was quenched and diluted with 10% NaOH (250 mL) and DCM (250 mL). The layers were then separated and the aqueous phase was further extracted using DCM ( $2 \times 250$  mL). The organic layers were combined and dried over  $\text{Na}_2\text{SO}_4$  before concentration *in vacuo* to furnish a dark brown solid. This crude material was then purified by flash column chromatography using an eluent system of 10/90  $\rightarrow$ 60/40 EtOAc/Hexane as a slow gradient. Product elution was monitored by TLC and  $\text{KMnO}_4$  staining ( $R_f = 0.46$ , 75/25 EtOAc/Hexane). Concentration of product fractions furnished a pale yellow solid as the desired material (9.0 g, 45.6 mmol, 71%).

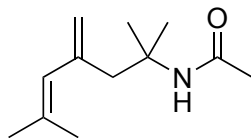
IR (thin film,  $\nu_{\text{max}}$  /  $\text{cm}^{-1}$ ) 3412, 3247, 3032, 2984, 2916, 2895, 1719, 1630, 1392, 1245

$^1\text{H}$  NMR (600 MHz,  $\text{CDCl}_3$ )  $\delta$ H 2.60 (4H, s), 2.24 (3H, s), 1.54 (12H, s)

$^{13}\text{C}$  NMR (125 MHz,  $\text{CDCl}_3$ )  $\delta$ C 208.0, 173.9, 57.0, 54.3, 30.5, 28.6

HRMS (ESI) Calcd for  $\text{C}_{11}\text{H}_{20}\text{NO}_2$   $[\text{M} + \text{H}]^+$  198.1489, found 198.1487

***N*-(2,6-Dimethyl-4-methylenehept-5-en-2-yl)acetamide (11)**



**11**

KOtBu (0.854 g, 7.61 mmol, 1.5 equiv) and **30** (2.71 g, 7.61 mmol, 1.5 equiv) was dissolved in dry THF (93.5 mL), under argon at -15 °C. The reaction mixture was then warmed to 0 °C and allowed to stir for 30 min. Afterwards, a solution of **10** (1.00 g, 5.07 mmol, 1.0 equiv) dissolved in dry THF (10 mL) was added. The reaction mixture was then allowed to warm to room temperature and stirred overnight. At this point, the reaction mixture was yellow in colour. Afterwards, a small amount of H<sub>2</sub>O was added until the reaction mixture became transparent. Subsequently, the reaction mixture was concentrated *in vacuo* to remove THF and the resultant aqueous phase was extracted with Et<sub>2</sub>O (3 × 100 mL). The combined organic layers were then dried over Na<sub>2</sub>SO<sub>4</sub> and concentrated to yield a crude solid. The crude material was then purified by flash column chromatography using an eluent gradient of 30/70 → 60/40 EtOAc/Hexane. Product elution was monitored by TLC and KMnO<sub>4</sub> staining (R<sub>f</sub> = 0.47, 60/40 EtOAc/Hexane). Concentration of product fractions furnished a white solid (0.68 g, 3.47 mmol, 69%).

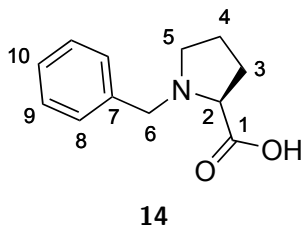
IR (thin film,  $\nu_{\text{max}}$  / cm<sup>-1</sup>) 3307, 3081, 2970, 2929, 2878, 1652, 1555, 1445, 1371, 1305

<sup>1</sup>H NMR (600 MHz, CDCl<sub>3</sub>)  $\delta$ H 5.60 (1H, s), 5.32 (1H, br s), 5.01 (1H, d, *J* = 2.6 Hz), 4.93-4.92 (1H, m), 2.42 (2H, s), 1.85 (3H, s), 1.81 (3H, d, *J* = 1.2 Hz), 1.78 (3H, d, *J* = 1.2 Hz), 1.32 (6H, s)

<sup>13</sup>C NMR (125 MHz, CDCl<sub>3</sub>)  $\delta$ C 169.4, 142.6, 134.3, 127.8, 117.4, 53.5, 47.6, 27.3, 26.4, 24.4, 19.5

HRMS (ESI) Calcd for C<sub>12</sub>H<sub>22</sub>NO [M + H]<sup>+</sup> 196.1696, found 196.1694

## *N*-Benzyl-L-proline (**14**)



This known compound was synthesized based on a literature procedure.<sup>155</sup> To 600 mL of isopropanol was added (*S*)-proline (100 g, 868 mmol, 1.00 equiv). The solution was then stirred at 40 °C, with KOH (187 g, 3334 mmol, 3.85 equiv) subsequently added. As soon as the solution started becoming transparent, benzyl chloride (130 mL, 1133 mmol, 1.54 equiv) was added dropwise by addition funnel over a span of 3 hours. At the end of 3 hours, the solution went from clear and light yellow to slightly cloudy and orange. The reaction mixture was then left to stir for an additional 6 hours at 40 °C. The reaction mixture was subsequently removed from heat and allowed to cool to room temperature before quenching with concentrated HCl (approximately 120 mL). CHCl<sub>3</sub> (280 mL) was then added to the reaction vessel and allowed to stir overnight. The resultant precipitate was then removed by filtration and the filtrate concentrated by vacuum to yield a yellow solid. This solid was then mechanically broken down in the presence of acetone and filtered. The solid was then washed with more acetone until most of the yellow color had dissipated and was then transferred to a vacuum oven to be dried over P<sub>2</sub>O<sub>5</sub> overnight at room temperature to yield the product **14** as a white powder (136 g, 663 mmol, 76%) without need for further purification.

IR (thin film,  $\nu_{\text{max}}$  / cm<sup>-1</sup>) 3449, 3374, 3289, 3086, 2998, 2914, 2872, 1657, 1624, 1595, 1499  
<sup>1</sup>H NMR (700 MHz, CDCl<sub>3</sub>)  $\delta$ H 9.36 (1H, br s, COOH), 7.44—7.41 (2H, m, H9), 7.38—7.35 (3H, m, H8, H10), 4.33 (1H, d,  $J$  = 12.9 Hz, H6), 4.15 (1H, d,  $J$  = 12.9 Hz, H6), 3.79 (1H, dd,  $J$  = 9.5, 6.3 Hz, H2), 3.63 (1H, ddd,  $J$  = 11.2, 7.7, 4.2 Hz, H5), 2.85 (1H, ddd,  $J$  = 11.2, 9.5, 7.7 Hz, H5), 2.34—2.21 (2H, m, H3), 1.99 (1H, m, H4), 1.90 (1H, m, H4)

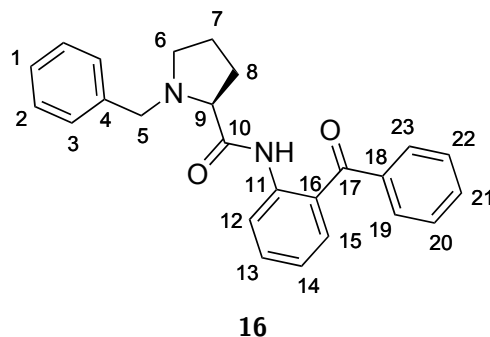
<sup>13</sup>C NMR (175 MHz, CDCl<sub>3</sub>)  $\delta$ C 206.1 (C1), 131.3 (Ar-C), 130.3 (Ar-C), 129.3 (Ar-C), 129.1

(Ar-C), 67.5 (C2), 58.0 (C6), 53.4 (C5), 29.0 (C3), 23.1 (C4)

OR:  $[\alpha]_D^{26} = -2.54$  ( $c = 0.488$ , DCM)

HRMS (ESI) Calcd for  $C_{12}H_{15}NO_2$   $[M]^{*+}$  205.1103, found 205.1101

**(S)-N-(2-Benzoylphenyl)-1-benzylpyrrolidine-2-carboxamide (16)**



This known compound was synthesized based on a literature procedure.<sup>155</sup> **14** (70.0 g, 341 mmol, 1.00 equiv) was dissolved in 525 mL of DMF at 0 °C with stirring. To this solution was added 1-methylimidazole (70.7 mL, 888 mmol, 2.60 equiv), followed by stirring for 10 minutes. At this point the reaction mixture turned from cloudy and white to slightly yellow and clear. After 10 minutes, the reaction vessel was cooled to -10 °C followed by addition of methanesulfonyl chloride (26.6 mL, 341 mmol, 1.00 equiv) and left to stir for an additional 20 minutes. 2-Aminobenzophenone (60.6 g, 307 mmol, 0.90 equiv) was then added and the reaction mixture allowed to warm to room temperature with stirring overnight. The reaction had turned dark brown at this point. Afterwards, the reaction was concentrated by vacuum to yield a slurry, which was then dissolved in ethyl acetate (1.5 L) and 1 M HCl (1 L) and separated in a separatory funnel. The organic portion was additionally washed with 1 M HCl (1 × 1 L), H<sub>2</sub>O (2 × 1 L), and brine (2 × 1 L). Throughout this process, the product forms as a yellowish solid in the separatory funnel. The ethyl acetate was removed while keeping the solid in the separatory funnel, with 1 L of H<sub>2</sub>O and 1 L of DCM added. After draining the DCM layer, the solid was washed with an additional 500 mL of DCM. The solid was filtered and dried to yield pure product with no additional purification required. The

DCM washings also contained a substantial amount of product along with a small amount of impurities, which was concentrated by vacuum to yield a solid. The product **16** was obtained as a yellow solid (66.0 g, 172 mmol, 50%).

IR (thin film,  $\nu_{\max}$  /  $\text{cm}^{-1}$ ) 3363, 3164, 2958, 1689, 1663, 1606, 1544, 1449, 1352, 1316, 1291, 1265, 1180

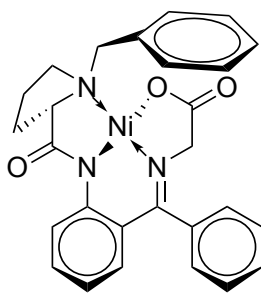
$^1\text{H}$  NMR (600 MHz,  $\text{CD}_3\text{OD}$ )  $\delta$ H 7.76 (2H, dd,  $J = 7.8, 0.6$  Hz, Ar-H), 7.62 (1H, tt,  $J = 9.1, 1.4$  Hz, Ar-H), 7.58 (1H, td,  $J = 7.8, 1.2$  Hz, Ar-H), 7.51—7.42 (5H, m, Ar-H), 7.40—7.37 (4H, m, Ar-H), 7.35 (1H, td,  $J = 7.8, 0.6$  Hz, Ar-H), 4.35—4.24 (3H, m, H5, H6), 3.54 (1H, ddd,  $J = 10.8, 7.2, 3.6$  Hz, H6), 3.36-3.27 (1H, m, H9, overlap with  $\text{CD}_3\text{OD}$ ), 2.38 (1H, app dq,  $J = 13.8, 8.4$  Hz, H8), 2.16—2.08 (1H, m, H8), 1.91—1.81 (1H, m, H7), 1.63 (1H, tdd,  $J = 13.8, 8.4, 6.0$  Hz, H7)

$^{13}\text{C}$  NMR-APT (150 MHz,  $\text{CD}_3\text{OD}$ )  $\delta$ C 132.9 (Ar-C), 131.7 (Ar-C), 130.6 (Ar-C), 130.2 (Ar-C), 129.8 (Ar-C), 129.7 (Ar-C), 128.8 (Ar-C), 128.1 (Ar-C), 125.4 (Ar-C), 124.2 (Ar-C), 66.6 (C9), 57.9 (C5), 54.4 (C6), 28.1 (C9), 22.3 (C7)

OR:  $[\alpha]_{\text{D}}^{26} = -48.62$  ( $c = 1.81$ , MeOH)

HRMS (ESI) Calcd for  $\text{C}_{25}\text{H}_{25}\text{N}_2\text{O}_2$   $[\text{M} + \text{H}]^+$  385.1911, found 385.1907

### Belokon Complex (**18**)



**18**

This known compound was synthesized based on a literature procedure.<sup>155</sup> **16** (20.0 g, 52.0 mmol, 1.00 equiv),  $\text{Ni}(\text{NO}_3) \cdot 6 \text{H}_2\text{O}$  (30.2 g, 104 mmol, 2.00 equiv), and L-glycine (19.6 g, 260 mmol, 5.00 equiv) was dissolved in 182 mL of dry methanol under argon at 45 °C. To this

solution was added a solution of KOH (20.4 g, 364 mmol, 7.00 equiv) dissolved in 78 mL of dry methanol under argon, transferred by cannula. The temperature of the reaction mixture was then raised to 60 °C. Upon addition of the KOH solution, the reaction mixture quickly turned from a transparent green to an opaque red-orange. After 1.5 hours, 20 mL of glacial acetic acid was added, followed by addition of 500 mL of H<sub>2</sub>O. The reaction mixture was then stirred overnight at room temperature. The solid that had formed was then filtered off and washed twice with H<sub>2</sub>O. The solid was then purified by column chromatography (SiO<sub>2</sub>, 1.15 kg) using an elution of gradient of 1:19 to 3:19 of MeOH:EtOAc. The product possesses an R<sub>f</sub> = 0.31 on TLC using an elution system of 1:9 MeOH:EtOAc and can be visualized as a red spot as well as by UV. The product **18** was isolated as a dark red solid (13.6 g, 27.2 mmol, 52%).

IR (thin film,  $\nu_{\max}$  / cm<sup>-1</sup>) 3524, 3054, 2975, 2872, 1676, 1639, 1590, 1545, 1495, 1471, 1441, 1363, 1336, 1310, 1259, 1166

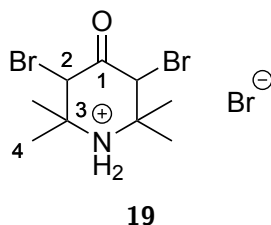
<sup>1</sup>H NMR (500 MHz, CDCl<sub>3</sub>)  $\delta$ H 8.32 (1H, dd,  $J$  = 9.0, 1.0 Hz), 8.08 (2H, dd,  $J$  = 8.0, 1.0 Hz), 7.57—7.48 (3H, m), 7.43 (2H, app t,  $J$  = 7.5 Hz), 7.32 (1H, tt,  $J$  = 7.5, 1.0 Hz), 7.22 (1H, ddd,  $J$  = 9.0, 7.0, 2.0 Hz), 7.11 (1H, d,  $J$  = 7.5 Hz), 7.01—6.97 (1H, m), 6.81 (1H, dd,  $J$  = 8.5, 2.0 Hz), 6.71 (1H, ddd,  $J$  = 8.5, 7.0, 1.5 Hz), 4.50 (1H, d,  $J$  = 12.5 Hz), 3.82—3.65 (4H, m), 3.48 (1H, dd,  $J$  = 11.0, 5.5 Hz), 3.41—3.30 (1H, m), 2.62—2.54 (1H, m), 2.48—2.38 (1H, m), 2.16 (1H, td,  $J$  = 11.0, 6.0 Hz), 2.12—2.04 (1H, m);

<sup>13</sup>C NMR (125 MHz, CDCl<sub>3</sub>)  $\delta$ C 181.3, 177.2, 171.6, 142.5, 134.6, 133.3, 133.1, 132.2, 131.7, 129.7, 129.6, 129.3, 129.1, 128.9, 126.2, 125.7, 125.1, 124.2, 120.8, 69.9, 63.1, 61.3, 57.5, 30.7, 23.7

OR:  $[\alpha]_{\text{D}}^{26} = 1895.30$  ( $c = 0.500$ , MeOH)

HRMS (ESI) Calcd for C<sub>27</sub>H<sub>26</sub>N<sub>3</sub>NiO<sub>3</sub> [M + H]<sup>+</sup> 498.1322, found 498.1329

### 3,5-Dibromo-2,2,6,6-tetramethyl-4-oxopiperidin-1-ium bromide (19)



This known compound was synthesized based on a literature procedure.<sup>156</sup> 2,2,6,6-Tetramethyl-4-piperidinone (40.0 g, 257 mmol, 1.00 equiv) was dissolved in 125 mL of glacial acetic acid at room temperature, giving a dark yellow solution. A solution of Br<sub>2</sub> (206 g, 1288 mmol, 5.00 equiv) in 95 mL of glacial acetic acid was then added in a dropwise fashion. The reaction mixture was then stirred at room temperature for 16 hours. The precipitate that had formed was then isolated by filtration and washed using glacial acetic acid followed by diethyl ether, which had gradually removed the yellow/orange colour. A white powder **19** was obtained as the product (76.2 g, 245 mmol, 95%) as a mixture of 2 isomers (2.7/1.0 ratio based on NMR).

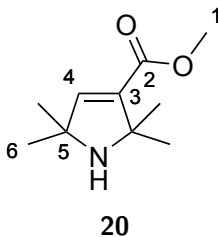
IR (thin film,  $\nu_{\max}$  / cm<sup>-1</sup>) 2890, 2694, 1751, 1741, 1719, 1557, 1543, 1397, 1270, 1253

<sup>1</sup>H NMR (600 MHz, DMSO-d<sub>6</sub>) (major isomer)  $\delta$ H 9.41 (1H, br s, NH), 5.49 (2H, s, H2), 1.71 (6H, s, H4), 1.36 (6H, s, H4)

<sup>13</sup>C NMR (150 MHz, DMSO-d<sub>6</sub>)  $\delta$ C 188.7 (C1), 64.3 (C3), 60.2 (C2), 27.7 (C4), 22.0 (C4)

HRMS (ESI) Calcd for C<sub>9</sub>H<sub>16</sub>Br<sub>2</sub>NO [M + H]<sup>+</sup> 311.9593, found 311.9593

### Methyl 2,2,5,5-tetramethyl-2,5-dihydro-1H-pyrrole-3-carboxylate (20)





This known compound was synthesized based on a literature procedure.<sup>156</sup> To a flame dried round-bottom flask under an atmosphere of Ar, NaOMe (19.6 g, 363 mmol, 7.0 equiv) was suspended in 250 mL of anhydrous MeOH. This solution was cooled to 0 °C, followed by the addition of a suspension of **19** (20.4 g, 51.8 mmol, 1.0 equiv) in 100 mL of anhydrous MeOH. The solution was brought up to room temperature and stirred for 6 h. The solution was concentrated *in vacuo*, suspended in 10% aqueous K<sub>2</sub>CO<sub>3</sub>, and extracted with Et<sub>2</sub>O (3 x 100 mL). The organic layers were combined, washed with brine (2 x 50 mL), dried over Na<sub>2</sub>SO<sub>4</sub>, and then concentrated *in vacuo* yielding methyl 2,2,5,5-tetramethyl-2,5-dihydro-1H-pyrrole-3-carboxylate **20** as an off yellow, nearly colorless oil. No purification was required (9.18 g, 50.0 mmol, 97%).

IR (thin film,  $\nu_{\max}$  / cm<sup>-1</sup>) 3357, 2967, 2928, 2868, 1720, 1634, 1436, 1374, 1360, 1328, 1280, 1255, 1210

<sup>1</sup>H NMR (600 MHz, CDCl<sub>3</sub>)  $\delta$ H 6.52 (1H, d,  $J$  = 3.6 Hz, H4), 3.63 (3H, d,  $J$  = 4.2 Hz H1), 1.75 (1H, br s, NH), 1.30 (6H, d,  $J$  = 4.2 Hz, H6), 1.18 (6H, d,  $J$  = 3.6 Hz, H6)

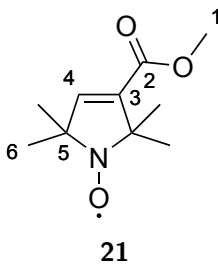
<sup>13</sup>C NMR (150 MHz, CDCl<sub>3</sub>)  $\delta$ C 164.4 (C2), 149.0 (C4), 139.0 (C3), 65.8 (C5), 63.3 (C5), 51.2 (C1), 29.9 (C6), 29.8 (C6)

HRMS (ESI) Calcd for C<sub>10</sub>H<sub>18</sub>NO<sub>2</sub> [M + H]<sup>+</sup> 184.1332, found 184.1332

### mCPBA Recrystallization Protocol

mCPBA was purified before use following a known procedure.<sup>157</sup> 30.0 g of mCPBA (Sigma Aldrich, 57 – 86%) was dissolved in 250 mL of Et<sub>2</sub>O and washed using 3 x 150 mL of buffer. Buffer composition was a mix of 410 mL of 0.1 M NaOH and 250 mL of 0.2 M KH<sub>2</sub>PO<sub>4</sub> made up to 1L, pH = 7.5. The washed organic layer was then dried over MgSO<sub>4</sub> and the solvent removed by rotary evaporation to yield 22.3 g of pure mCPBA.

Methyl 1-oxyl-2,2,5,5-tetramethyl-2,5-dihydro-1*H*-pyrrole-3-carboxylate (**21**)



This known compound was synthesized based on a literature procedure.<sup>156</sup> **20** (0.800 g, 4.37 mmol, 1.00 equiv) was dissolved in dry Et<sub>2</sub>O (16 mL) under argon at 0 °C. To this was added dropwise a solution of freshly recrystallized mCPBA (1.51 g, 8.74 mmol, 2.00 equiv) in dry Et<sub>2</sub>O (16 mL) under argon. After addition, the reaction mixture was removed from the ice bath and allowed to warm to room temperature. After 1.5 hours, the reaction mixture was transferred to a separatory funnel containing 160 mL of 10% Na<sub>2</sub>CO<sub>3</sub> and extracted using 3 x 320 mL of Et<sub>2</sub>O before being dried over Na<sub>2</sub>SO<sub>4</sub>. Removal of the solvent by rotary evaporation yielded a yellow crystalline solid **21** (0.88 g, 4.44 mmol, 100%).

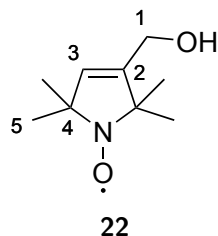
IR (thin film,  $\nu_{\max}$  / cm<sup>-1</sup>) 3071, 3004, 2987, 2976, 2953, 2933, 2872, 1717, 1628, 1477, 1462, 1441, 1292

<sup>1</sup>H NMR (600 MHz, CDCl<sub>3</sub>)  $\delta$ H 6.50 (1H, s, H4), 3.65 (3H, s, H1), 1.33 (6H, s, H6), 1.21 (6H, s, H6)

<sup>13</sup>C NMR (150 MHz, CDCl<sub>3</sub>)  $\delta$ C 164.0 (C2), 145.7 (C4), 136.5 (C3), 70.6 (C5), 68.6 (C5), 51.6 (C1), 24.8 (C6), 24.5 (C6)

HRMS (ESI) Calcd for C<sub>10</sub>H<sub>17</sub>NO<sub>3</sub> [M + H]<sup>+</sup> 199.1203, found 199.1205

### 3-(Hydroxymethyl)-2,2,5,5-tetramethyl-2,5-dihydro-1*H*-pyrrol-1-oxyl (**22**)



This known compound was synthesized based on a literature procedure.<sup>156</sup> **21** (3.00 g, 15.14 mmol, 1.0 equiv) was dissolved in 30 mL of anhydrous THF and cooled to  $-78$  °C. To this solution was added dropwise DIBAL as a 1 M solution in hexane (37.85 mL, 37.85 mmol, 2.5 equiv). The reaction mixture was then allowed to slowly warm up to  $-50$  °C with stirring. After 4.5 h, the reaction mixture was quenched by addition of 120 mL of 2 M NaOH at 0 °C. The mixture was then further diluted with 100 mL of brine and extracted with 3 x 200 mL EtOAc. The combined organic fractions were dried over Na<sub>2</sub>SO<sub>4</sub> and concentrated to furnish a crude yellow solid. This solid was subjected to further purification by flash chromatography on silica using an eluent system of 1/1 EtOAc/Petroleum ether. Product elution was monitored by TLC and staining with KMnO<sub>4</sub> using an eluent of 1/1 EtOAc/Petroleum ether ( $R_f = 0.31$ ). Concentration of fractions yielded a solid product **22** (1.40 g, 8.34 mmol, 55%).

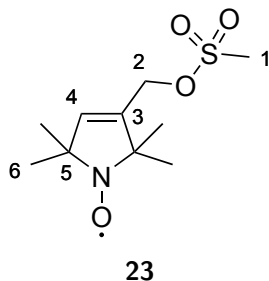
IR (thin film,  $\nu_{\max}$  / cm<sup>-1</sup>) 3367, 2978, 2930, 2857, 2828, 2727, 1654, 1443, 1428, 1386, 1375, 1359, 1284

<sup>1</sup>H NMR (600 MHz, CDCl<sub>3</sub>)  $\delta$ H 5.47 (1H, s, H3), 4.08 (2H, s, H1), 1.25 (6H, s, H5), 1.23 (6H, s, H5)

<sup>13</sup>C NMR-APT (150 MHz, CDCl<sub>3</sub>)  $\delta$ C 128.4 (C3), 59.3 (C1), 25.3 (C5), 24.3 (C5)

HRMS (EI) Calcd for C<sub>9</sub>H<sub>16</sub>O<sub>2</sub>N [M + H]<sup>+</sup> 170.1181, found 170.1181

(1-Oxyl-2,2,5,5-tetramethyl-2,5-dihydro-1*H*-pyrrol-3-yl)methyl  
methanesulfonate (**23**)



This known compound was synthesized based on a literature procedure.<sup>156</sup> **22** (0.100 g, 0.596 mmol, 1.00 equiv) and Et<sub>3</sub>N (99.0  $\mu$ L, 0.715 mmol, 1.20 equiv) was dissolved in 1.5 mL of dry THF at 0 °C. To this solution was added methanesulfonyl chloride (55.0  $\mu$ L, 0.715 mmol, 1.20 equiv). Stirring was continued at 0 °C for 40 minutes before allowing the reaction mixture to warm to room temperature over an additional period of 30 minutes. The reaction mixture was then quenched with 1 mL of H<sub>2</sub>O followed by dilution with 4 mL of DCM. The aqueous layer was additionally extracted with 3 x 3 mL of DCM and the combined organic layers were dried over MgSO<sub>4</sub> and concentrated in vacuo to obtain the product as a dark yellow solid with no further purification required (0.135 g, 0.544 mmol, 96%).

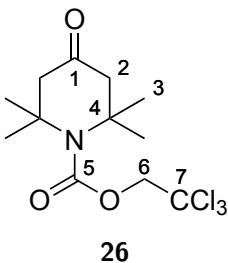
IR (thin film,  $\nu_{\max}$  / cm<sup>-1</sup>) 2978, 2933, 2871, 1725, 1655, 1468, 1428, 1357, 1285, 1226, 1176, 1100, 1056

<sup>1</sup>H NMR (600 MHz, CDCl<sub>3</sub>)  $\delta$ H 5.65 (1H, s, H4), 4.62 (2H, s, H2), 2.92 (3H, s, H1), 1.18 (6H, s, H6), 1.15 (6H, s, H6)

<sup>13</sup>C NMR-APT (150 MHz, CDCl<sub>3</sub>)  $\delta$ C 128.5 (C4), 65.6 (C2), 38.2 (C1), 25.4 (C6), 28.6 (C6)

HRMS (EI) Calcd for C<sub>10</sub>H<sub>18</sub>NO<sub>4</sub>S [M]<sup>+</sup> 248.0957, found 248.0951

## 2,2,2-Trichloroethyl 2,2,6,6-tetramethyl-4-oxo-piperidine-1-carboxylate (**26**)



**Method A.** 2,2,6,6-tetramethyl-4-piperidinone (5.007 g, 6.44 mmol, 1.0 equiv) was dissolved in trichloroethyl chloroformate (20 mL, 145 mmol, 22.5 equiv). The solution was heated to 100 °C and stirred for 18 hours. The reaction was cooled down to room temperature and quenched with a 10% NaOH solution (100 mL). This mixture was let to stir at ambient temperature for 1 hour. This biphasic mixture was then separated and the aqueous layer extracted with EtOAc (3 x 100 mL). The organic phases were combined, washed with brine (300 mL), dried over Na<sub>2</sub>SO<sub>4</sub>, filtered and the solvent evaporated in vacuo affording a crude yellow thick oil. The residue was purified using flash column chromatography (10% EtOAc in hexanes) affording the product 2,2,2-trichloroethyl 2,2,6,6-tetramethyl-4-oxo-piperidine-1-carboxylate (**26**) as a white solid, R<sub>f</sub> = 0.67 (33/67 EtOAc/Hexane), (5.066 g, 3.35 mmol, 52%).

IR (DCM cast film,  $\nu_{\max}$  / cm<sup>-1</sup>) 2970, 2943, 1706, 1378, 1336, 1294, 1116, 1056 cm<sup>-1</sup>.

<sup>1</sup>H NMR (700 MHz, CDCl<sub>3</sub>)  $\delta$ H 4.81 (2H, s, H6), 2.62 (4H, s, H2), 1.55 (12H, s, H4).

<sup>13</sup>C NMR (175 MHz, CDCl<sub>3</sub>)  $\delta$ C 207.3 (C1), 154.2 (C5), 95.3 (C7), 74.9 (C6), 57.2 (C4), 29.9 (C3);

HRMS (ESI) Calcd for C<sub>12</sub>H<sub>18</sub>Cl<sub>3</sub>NNaO<sub>3</sub> [M + Na]<sup>+</sup> 352.0244, found 352.0241.

**Method B.** In a fritted column equipped with a 3-way stopcock (glass SPPS vessel) was deposited commercially available 2,2,6,6-tetramethyl-4-piperidinone (30.0 g, 193.25 mmol, 1.0 equiv) and 30 mL of DCM. The solution was then bubbled with argon and 2,2,2-trichloroethoxycarbonyl chloride (37.5 mL, 272.36 mmol, 1.4 equiv) was added. The so-

lution was then bubbled with argon for 5 h until most of the DCM had evaporated. The viscous slurry was then microwaved in a Danby Junior model DMW654 microwave set to the defrost setting for  $5 \times 20$  sec rounds of irradiation. The slurry then largely became a solid and was subjected to filtration using 5/95 EtOAc/Hexane solution to extract the crude product. The filtrate was then concentrated to yield a yellow oil which was then subjected to flash chromatography on silica using an elution gradient system of 5/95  $\rightarrow$  20/80 EtOAc/Hexane. Concentration of fractions yields **26** as white, chunky solids ( $R_f = 0.40$ , 20/80 EtOAc/Hexane) (29.3 g, 89.1 mmol, 46%).

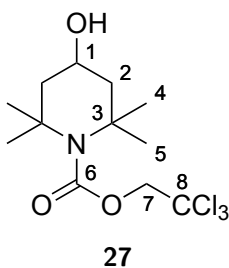
IR (thin film,  $\nu_{\max}$  /  $\text{cm}^{-1}$ ) 3032, 2993, 2974, 2949, 2903, 1698, 1453, 1379, 1340, 1299

$^1\text{H}$  NMR (500 MHz,  $\text{CDCl}_3$ )  $\delta$ H 4.82 (2H, s, H6), 2.63 (4H, s, H2), 1.55 (12H, s, H3);

$^{13}\text{C}$  NMR (125 MHz,  $\text{CDCl}_3$ )  $\delta$ C 207.3 (C1), 154.3 (C5), 95.4 (C7), 75.0 (C6), 57.3 (C4), 53.3 (C2), 30.0 (C3)

HRMS (EI) Calcd for  $\text{C}_{12}\text{H}_{18}\text{Cl}_3\text{NO}_3$   $[\text{M} + \text{H}]^+$  329.0352, found 329.0354

**2,2,2-Trichloroethyl 4-hydroxyl-2,2,6,6-tetramethyl-4-piperidine-1-carboxylate**  
(**27**)



**26** (2.511 g, 7.59 mmol, 1.0 equiv) was suspended in EtOH (20 mL). To this mixture  $\text{NaBH}_4$  (0.144 g, 3.80 mmol, 0.5 equiv) was carefully added at ambient temperature. The reaction was then allowed to proceed for 90 min. Upon completion, the reaction was quenched with brine (30 mL) and the product extracted with DCM ( $3 \times 40$  mL). The organic fractions were combined, dried over  $\text{Na}_2\text{SO}_4$ , filtered and the solvent evaporated in vacuo to afford a pale yellow oil. The product 2,2,2-trichloroethyl 4-hydroxyl-2,2,6,6-tetramethyl-4-piperidine-

1-carboxylate (**27**) was used without further purification,  $R_f = 0.55$  (33/67 EtOAc/Hexane), (1.586 g, quantitative yield).

IR (DCM cast film,  $\nu_{\max}$  /  $\text{cm}^{-1}$ ) 3453, 2969, 2945, 1703, 1373, 1318, 1111, 1062

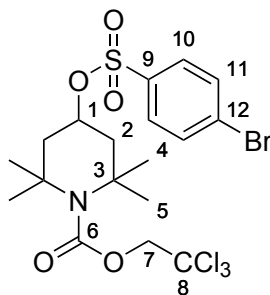
$^1\text{H}$  NMR (400 MHz,  $\text{CDCl}_3$ )  $\delta$ H 4.78 (2H, s, H7), 4.13-4.09 (1H, m, H1), 2.08 (2H, dd,  $J = 13.9, 5.8$  Hz, H2), 1.74 (2H, dd,  $J = 13.9, 8.7$  Hz, H2), 1.61 (6H, s, H4), 1.46 (6H, s, H5)

$^{13}\text{C}$  NMR (175 MHz,  $\text{CDCl}_3$ )  $\delta$ C 154.7 (C6), 95.5 (C8), 75.0 (C7), 62.2 (C1), 58.0 (C3), 49.2 (C2), 32.2 (C4), 28.2 (C5)

HRMS (ESI) Calcd for  $\text{C}_{12}\text{H}_{21}\text{Cl}_3\text{NO}_3$   $[\text{M} + \text{H}]^+$  332.0582, found 332.0579

## 2,2,2-Trichloroethyl

### 4-[[[(4-bromophenyl)sulfonyl]oxy]-2,2,6,6-tetramethylpiperidine-1-carboxylate (**29**)



**29**

**27** (10.091 g, 30.3 mmol, 1.0 equiv) was dissolved in dry pyridine (100 mL) and cooled down to 0 °C in an ice bath. *p*-Bromobenzenesulfonyl chloride (9.303 g, 36.4 mmol, 1.2 equiv) was added and the mixture was stirred at 0 °C for 5 minutes. The reaction vessel was quickly purged with argon and the resulting solution was removed from the ice bath, cooled to room temperature, and stirred for 48 hours. After the reaction time was completed, pyridine was co-evaporated *in vacuo* using toluene (3 × 100 mL). The resulting residue was partitioned between  $\text{CHCl}_3$  (200 mL) and saturated  $\text{NaHCO}_3$  (200 mL) and the phases separated. The aqueous phase was extracted with  $\text{CHCl}_3$  (3 × 200 mL). The organic fractions were combined, dried over  $\text{Na}_2\text{SO}_4$ , filtered and the solvent evaporated

in vacuo to afford a crude off-yellow solid. The crude mixture was purified using flash column chromatography (5/95 EtOAc/Hexane) affording the product 2,2,2-trichloroethyl 4-(((4-bromophenyl)sulfonyl)oxy)-2,2,6,6-tetramethylpiperidine-1-carboxylate (**27**) as a white solid,  $R_f = 0.48$  (20/80 EtOAc/Hexane), (14.743 g, 26.7 mmol, 88%).

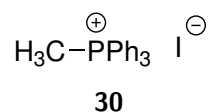
IR (DCM cast film,  $\nu_{\max}$  /  $\text{cm}^{-1}$ ) 3091, 2973, 2945, 1703, 1577, 1473, 1370, 1188  $\text{cm}^{-1}$ .

$^1\text{H}$  NMR (400 MHz,  $\text{CDCl}_3$ )  $\delta$ H 7.79 (2H, d,  $J = 8.7$  Hz, H10), 7.72 (2H, d,  $J = 8.7$  Hz, H11), 4.91 (1H, m, H1), 4.76 (2H, s, H7), 2.15 (2H, dd,  $J = 14.8, 6.8$  Hz, H2), 2.01 (2H, dd,  $J = 14.8, 7.1$  Hz, H2), 1.54 (6H, s, H4), 1.42 (6H, s, H5).

$^{13}\text{C}$  NMR (176 MHz,  $\text{CDCl}_3$ )  $\delta$ C 154.3 (C6), 136.3 (C9), 132.7 (C11), 129.0 (C10), 95.4 (C8) 74.9 (C7), 74.8 (C1), 56.8 (C3), 44.4 (C2), 31.0 (C4), 28.7 (C5).

HRMS (ESI) Calcd for  $\text{C}_{18}\text{H}_{23}\text{BrCl}_3\text{NNaO}_5\text{S}$   $[\text{M} + \text{Na}]^+$  548.9543, found 548.9546.

### Methyltriphenylphosphonium iodide (**30**)



This known compound was synthesized based on a literature procedure.<sup>158</sup> To a flame-dried round bottom flask under argon was added triphenylphosphine (30.0 g, 114 mmol, 1.0 equiv) and 75 mL of dry DCM. Reaction mixture was then cooled to 0 °C and iodomethane (9.0 mL, 144.0 mmol, 1.2 equiv) was added dropwise. The reaction mixture was then removed from the ice bath and allowed to warm to room temperature, stirring overnight. The reaction mixture was then concentrated to yield a white solid. This solid was then washed using  $\text{Et}_2\text{O}$  on filter and dried. The product was obtained as a white solid with no further purification required (46.2 g, 114 mmol, >99%).

IR (thin film,  $\nu_{\max}$  /  $\text{cm}^{-1}$ ) 3052, 3009, 2989, 2935, 2874, 1587, 1484, 1437

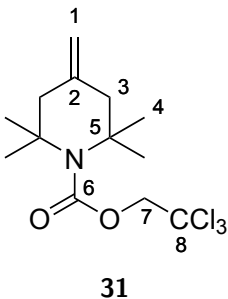
$^1\text{H}$  NMR (500 MHz,  $\text{CDCl}_3$ )  $\delta$ H 7.82—7.65 (15H, m, Ph-H), 3.19 (3H, d,  $J = 13.3$  Hz,  $\text{CH}_3$ )

$^{13}\text{C}$  NMR (125 MHz,  $\text{CDCl}_3$ )  $\delta$ C 135.3 (d,  $J = 3.0$  Hz, Ph-C), 133.4 (d,  $J = 10.5$  Hz, Ph-C), 130.6 (d,  $J = 12.9$  Hz, Ph-C), 118.9 (d,  $J = 88.8$  Hz, Ph-C), 11.7 (d,  $J = 57.5$  Hz,  $\text{CH}_3$ )



HRMS (ESI) Calcd for C<sub>19</sub>H<sub>18</sub>P [M]<sup>\*+</sup> 277.1146, found 277.1146

**2,2,2-Trichloroethyl 2,2,6,6-tetramethyl-4-methylenepiperidine-1-carboxylate**  
**(31)**



To a flame dried 1 L addition funnel was added **30** (40.0 g, 99 mmol, 2.5 equiv) and KOtBu (11.1 g, 99.0 mmol, 2.5 equiv) under argon. To the solids was added 500 mL of dry toluene and the mixture was stirred at room temperature for 1.5 h until a bright yellow homogenous solution was obtained. The solution was then added to a previously prepared solution of **26** (13.0 g, 39.6 mmol, 1.0 equiv) dissolved in 250 mL of dry toluene in a flame dried round-bottom flask under argon. The addition was performed as multiple small streams over a period of 40 min at -30 °C. After addition was completed, the reaction mixture was stirred at -30 °C for an additional 1 h 50 min, total reaction time is 2.5 h. The reaction mixture turned from bright yellow to orange during this time. 500 mL of H<sub>2</sub>O was then used to quench the reaction, followed by dilution using DCM. The layers were then separated and further extractions performed using 2 × 200 mL of DCM. The combined organic layers were then dried over Na<sub>2</sub>SO<sub>4</sub> and concentrated to yield a light brown solid. The crude material was purified by column chromatography on silica using 2/98 Diisopropyl Ether/Pentane as the eluent. Elution of product material was monitored by TLC and staining with KMnO<sub>4</sub> (R<sub>f</sub> = 0.44, 5/95 Diisopropyl Ether/Pentane). Concentration of fractions furnished a light yellow oil **31** as the final product (9.55 g, 29.0 mmol, 73%).

IR (DCM cast film,  $\nu_{\max}$  / cm<sup>-1</sup>) 3076, 2970, 2938, 1707, 1651, 1456

<sup>1</sup>H NMR (600 MHz, CDCl<sub>3</sub>)  $\delta$ H 4.86 (2H, app quint,  $J$  = 1.7 Hz, H1), 4.78 (2H, s, H7), 2.50

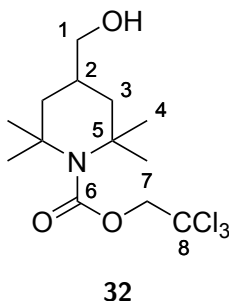
(4H, t,  $J = 1.7$  Hz, H3), 1.47 (12H, s, H4)

$^{13}\text{C}$  NMR (125 MHz,  $\text{CDCl}_3$ )  $\delta$  154.8 (C6), 140.4 (C2), 111.0 (C1), 95.8 (C5), 75.0 (C8), 57.5 (C7), 46.3 (C3), 29.9 (C4)

HRMS (EI) Calcd for  $\text{C}_{13}\text{H}_{20}\text{Cl}_3\text{NO}_2$   $[\text{M}]^{*+}$  327.0560, found 327.0556

## 2,2,2-Trichloroethyl

### 4-(hydroxymethyl)-2,2,6,6-tetramethylpiperidine-1-carboxylate (**32**)



In a flame-dried round-bottom flask under argon was dissolved **31** (9.55 g, 29.0 mmol, 1.0 equiv) in 300 mL of dry THF at  $-30$  °C. To this solution was then added borane dimethyl sulfide complex as a 2.0 M solution in THF (17.4 mL, 34.8 mmol, 1.2 equiv). Reaction mixture was then allowed to stir for 6 h at  $0$  °C. After 6 h, to the reaction mixture was added dropwise a solution of  $\text{K}_2\text{CO}_3$  (10.0 g, 72.6 mmol, 2.5 equiv) and 30% (w/w)  $\text{H}_2\text{O}_2$  (7.26 mL, 72.6 mmol, 2.5 equiv) in 100 mL of  $\text{H}_2\text{O}$ . Gas evolution occurred and the reaction mixture was then allowed to stir at  $0$  °C for an additional 17 h. Afterwards, the reaction was diluted by addition of 400 mL of 0.05 M, pH 7 phosphate buffer, 400 mL of brine, 250 mL of  $\text{H}_2\text{O}$ , and 400 mL of DCM. The layers were separated and further extractions performed using  $3 \times 250$  mL of DCM. The organic layers were combined and dried over  $\text{Na}_2\text{SO}_4$  before concentrating to yield a crude oil. The material was then purified by flash chromatography on silica using an eluent system of 30/70 EtOAc/Hexane. Elution of product material was monitored by TLC and staining with  $\text{KMnO}_4$  ( $R_f = 0.25$ , 30/70 EtOAc/Hexane). Concentration of the fractions yielded a clear, colourless oil (**32**) that solidified to a white solid (7.80 g, 22.6 mmol, 78%).

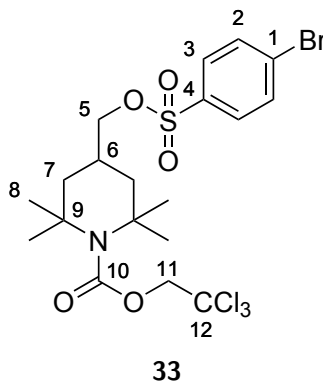
IR (thin film,  $\nu_{\max}$  /  $\text{cm}^{-1}$ ) 3454, 3023, 2968, 2936, 2870, 1698, 1472, 1397, 1379 1317

$^1\text{H}$  NMR (600 MHz,  $\text{CDCl}_3$ )  $\delta$ H 4.79 (2H, s, H7), 3.53 (2H, d,  $J = 6.7$  Hz, H1), 2.00 (1H, ttt,  $J = 11.1, 6.7, 4.6$  Hz, H2), 1.78 (2H, dd,  $J = 13.3, 4.6$  Hz, H3), 1.59 (6H, s, H4), 1.45 (6H, s, H4), 1.42 (2H, dd,  $J = 11.1, 13.3$  Hz, H3);

$^{13}\text{C}$  NMR (125 MHz,  $\text{CDCl}_3$ )  $\delta$ C 155.2 (C6, assigned by HMBC), 95.8 (C8, assigned by HMBC), 75.1 (C7), 67.8 (C1), 57.7 (C5), 44.4 (C3), 33.0 (C4), 30.2 (C2), 27.4 (C4)

HRMS (EI) Calcd for  $\text{C}_{13}\text{H}_{22}\text{Cl}_3\text{NO}_3$   $[\text{M}]^{*+}$  345.0665, found 345.0661

**2,2,2-Trichloroethyl 4-(((4-bromophenyl)sulfonyl)oxy)methyl)-2,2,6,6-tetramethylpiperidine-1-carboxylate (33)**



**32** (7.00 g, 20.25 mmol, 1.0 equiv) and 4-bromobenzene sulfonyl chloride (6.21 g, 24.3 mmol, 1.2 equiv) was deposited in a flame-dried round-bottom flask under an argon atmosphere. To this was then added 140 mL of DCM and the solution was cooled to 0 °C. Triethylamine (11.0 mL, 101 mmol, 5.0 equiv) was then added and stirring continued at 0 °C for 30 min. Afterwards, the reaction was removed from the cooling bath and allowed to warm to room temperature, stirring overnight. The reaction mixture was then diluted using 500 mL of  $\text{H}_2\text{O}$ . The layers were separated and further extractions were performed using DCM (3  $\times$  150 mL). Combined organic layers were then dried over  $\text{Na}_2\text{SO}_4$  and concentration furnished a crude white solid. The crude material was then purified by flash chromatography on silica using an eluent system of 10/90 EtOAc/Hexane. Elution of product material was

monitored by TLC and staining with  $\text{KMnO}_4$  ( $R_f = 0.32$ , 10/90 EtOAc/Hexane). Concentration of product fractions furnished a white solid **33** (10.4 g, 18.4 mmol, 91%).

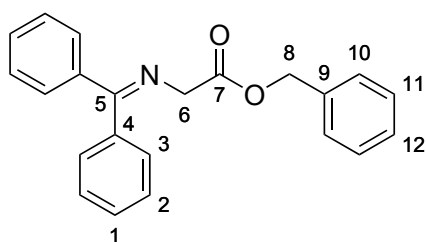
IR (thin film,  $\nu_{\text{max}} / \text{cm}^{-1}$ ) 3093, 3025, 2968, 2946, 1700, 1577, 1473, 1392, 1370, 1317, 1298, 1189

$^1\text{H}$  NMR (600 MHz,  $\text{CDCl}_3$ )  $\delta$ H 7.78 (2H, d,  $J = 8.7$  Hz, H3), 7.72 (2H, d,  $J = 8.7$  Hz, H2), 4.77 (2H, s, H11), 3.91 (2H, d,  $J = 6.7$  Hz, H5), 2.17 (1H, m, H6), 2.07 (2H, dd,  $J = 13.5$ , 4.9 Hz, H7), 1.55 (6H, s, H8), 1.40 (6H, s, H8), 1.38 (2H, dd,  $J = 13.5$ , 11.4 Hz, H7);

$^{13}\text{C}$  NMR (125 MHz,  $\text{CDCl}_3$ )  $\delta$ C 155.1 (C10), 135.1 (C1), 132.8 (C3), 129.5 (C2), 129.3 (C4), 95.6 (C12), 75.1 (C11), 74.7 (C5), 57.5 (C9), 43.7 (C7), 33.1 (C8), 27.8 (C6), 27.4 (C8)

HRMS (EI) Calcd for  $\text{C}_{19}\text{H}_{25}\text{BrCl}_3\text{NNaO}_5\text{S}$   $[\text{M}]^{*+}$  562.9702, found 562.9695

### Benzyl 2-((diphenylmethylene)amino)acetate (**36**)



**36**

This known compound was synthesized based on a modified literature procedure.<sup>159</sup> In a flame dried round-bottom flask under argon was deposited glycine benzyl ester *para*-toluenesulfonic acid salt (51.2 g, 151.8 mmol, 1.0 equiv) and 200 mL of DCM. Following this, the mixture was stirred, forming a suspension to which benzophenone imine (25.5 mL, 151.8 mmol, 1.0 equiv) was added. The reaction mixture turned bright white at this point. The reaction mixture was then allowed to stir at room temperature for 2.5 h. After, the mixture was diluted with 500 mL of  $\text{H}_2\text{O}$  and washed with 3 x 500 mL of  $\text{H}_2\text{O}$  followed by 500 mL of brine. The organic layer was dried over  $\text{MgSO}_4$  and concentrated to give a white solid with no further purification required (46.0 g, 139.65 mmol, 92%). Product was visualized on TLC with  $\text{KMnO}_4$  staining using an eluent system of 15/85 EtOAc/Hexane with 0.1%

NEt<sub>3</sub> as a two spots (R<sub>f</sub> = 0.24 and 0.35) corresponding to the product and benzophenone (product degrades on silica) respectively.

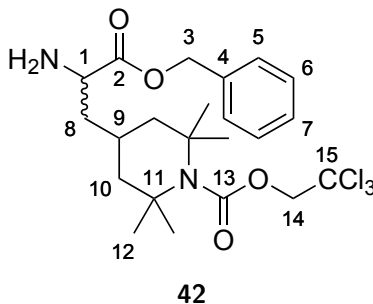
IR (thin film,  $\nu_{\max}$  / cm<sup>-1</sup>) 3055, 2953, 2895, 1748, 1660, 1624, 1575, 1491, 1459, 1445, 1220, 1189, 1177

<sup>1</sup>H NMR (600 MHz, CDCl<sub>3</sub>)  $\delta$ H 7.69-7.66 (2H, m, Ar-H), 7.46-7.42 (3H, m, Ar-H), 7.42-7.39 (1H, m, Ar-H), 7.37-7.31 (7H, m, Ar-H), 7.18-7.15 (2H, m, Ar-H), 5.20 (2H, s, H8), 4.27 (2H, s, H6)

<sup>13</sup>C NMR (150 MHz, CDCl<sub>3</sub>) 172.2 (C7), 170.6 (C5), 139.4 (Ar-C), 136.1 (Ar-C), 135.9 (Ar-C), 130.6 (Ar-C), 129.0 (Ar-C), 128.9 (Ar-C), 128.8 (Ar-C), 128.7 (Ar-C), 128.5 (Ar-C), 128.4 (Ar-C), 128.2 (Ar-C), 127.8 (Ar-C), 66.7 (C8), 55.8 (C6)

HRMS (EI) Calcd for C<sub>22</sub>H<sub>20</sub>NO<sub>2</sub> [M]<sup>+</sup> 329.1416, found 329.1416

### 2,2,2-Trichloroethyl 4-(2-amino-3-(benzyloxy)-3-oxopropyl)-2,2,6,6-tetramethylpiperidine-1-carboxylate (**42**)



In a flame-dried round-bottom flask under argon was deposited **36** (11.67 g, 35.41 mmol, 4.0 equiv). The flask was then charged with 250 mL of toluene and cooled to 0 °C. To this solution was then added LiHMDS as a 1 M solution in THF (35.41 mL, 35.41 mmol, 4.0 equiv) dropwise over a period of 25 min. The reaction mixture transitioned from clear and colourless to yellow, orange, and back to yellow again. Mixture was allowed to stir at 0 °C for 15 min. Afterwards, a solution of **33** (5.00 g, 8.85 mmol, 1.0 equiv) dissolved in 30 mL of toluene was added by cannula, with an additional 20 mL of toluene used to ensure quantitative transfer. The reaction mixture was removed from the cooling bath and heated

to reflux with an attached condenser overnight. The reaction mixture slowly turned dark brown as temperature was increased. The mixture was then quenched with 500 mL H<sub>2</sub>O and extractions were performed with DCM (3 × 250 mL). The combined organic layers were dried over Na<sub>2</sub>SO<sub>4</sub> and concentrated to furnish a dark brown oil. To this oil was added 200 mL of pyridine and hydroxylamine hydrochloride (9.84 g, 141.64 mmol, 16.0 equiv). The reaction mixture was then heated to 60 °C for 4 h and subsequently concentrated by coevaporation with toluene on a rotary evaporator. Next, the material was washed with 200 mL of saturated NaHCO<sub>3</sub> and extractions were performed with CHCl<sub>3</sub> (3 x 150 mL). The combined organic layers were dried over Na<sub>2</sub>SO<sub>4</sub> and concentrated to furnish a dark brown oil. This material was then purified on silica column using an eluent system of 40/60 EtOAc/Hexane with 0.1% NEt<sub>3</sub>. Elution of material was monitored by TLC using an elution system of 70/30 EtOAc/Hexane (R<sub>f</sub> = 0.22) and is slow, streaky, and takes many fractions. Concentration of fractions furnishes a light yellow oil **42** (3.30 g, 6.68 mmol, 76%).

IR (thin film,  $\nu_{\max}$  / cm<sup>-1</sup>) 3373, 3307, 3093, 3064, 3032, 2966, 2938, 2854, 1736, 1698, 1455, 1316, 1293

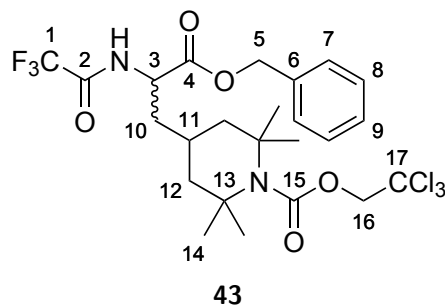
<sup>1</sup>H NMR (700 MHz, CDCl<sub>3</sub>)  $\delta$ H 7.38—7.30 (5H, m, Ar-H), 5.17 (2H, d,  $J$  = 2.1 Hz, H3), 4.77 (2H, s, H14), 3.52 (1H, dd,  $J$  = 8.1, 6.1 Hz, H1), 1.93 (1H, m, H9), 1.72—1.67 (2H, m, H10), 1.66—1.61 (1H, m, H8), 1.55 (3H, s, H12), 1.54 (3H, s, H12), 1.49—1.44 (1H, m, H8), 1.36 (3H, s, H12), 1.34 (3H, s, H12), 1.34—1.29 (2H, m, H10)

<sup>13</sup>C NMR (175 MHz, CDCl<sub>3</sub>)  $\delta$ C 176.2 (C2), 155.1 (C13), 135.6 (C4), 128.7 (C6), 128.5 (C7), 128.4 (C5), 95.6 (C15), 75.1 (C14), 66.8 (C3), 57.9 (C11), 57.9 (C11), 52.3 (C1), 48.6 (C12), 48.1 (C12), 41.8 (C8), 33.1 (C12), 27.1 (C12), 27.0 (C12), 23.9 (C9)

HRMS (ESI) Calcd for C<sub>22</sub>H<sub>23</sub>Cl<sub>3</sub>N<sub>2</sub>O<sub>4</sub> [M]<sup>\*+</sup> 492.1349, found 492.1350

**2,2,2-Trichloroethyl 4-(3-(benzyloxy)-3-oxo-2-(2,2,2-trifluoroacetamido)propyl)-  
2,2,6,6-tetramethylpiperidine-1-carboxylate**

(43)



Compound **42** (2.80 g, 5.67 mmol, 1.0 equiv) was dissolved in 56.7 mL of dry DCM under argon. The solution was then cooled to 0 °C and trifluoroacetic anhydride (1.40 mL, 8.50 mmol, 1.5 equiv) was added dropwise. This was followed by dropwise addition of NEt<sub>3</sub> (1.97 mL, 14.17 mmol, 2.5 equiv). The reaction mixture was then allowed to warm to room temperature, stirring for 1 h. The reaction mixture was then diluted with CHCl<sub>3</sub> (150 mL) and washed twice with saturated NH<sub>4</sub>Cl(aq) (150 mL), followed by an additional washing with brine. The organic layer was then dried over Na<sub>2</sub>SO<sub>4</sub> and concentrated to furnish a dark brown oil. The crude material was purified by flash chromatography on silica using an eluent of 10/90 EtOAc/Hexane. Product elution monitored by TLC using an eluent system of 10/90 EtOAc/Hexane (R<sub>f</sub> = 0.23). Concentration of fractions furnished an oil **43** as the final product (2.64 g, 4.48 mmol, 79%).

IR (thin film,  $\nu_{\max}$  / cm<sup>-1</sup>) 3307, 3090, 3034, 2968, 2937, 1747, 1709, 1553, 1499, 1456, 1398

<sup>1</sup>H NMR (600 MHz, CDCl<sub>3</sub>)  $\delta$ H 7.41—7.33 (5H, m, Ar-H), 5.26 (1H, dd, *J* = 11.9, 5.3 Hz, H5), 5.18 (1H, dd, *J* = 11.9, 3.4 Hz, H5), 4.77 (2H, s, H16), 4.77—4.71 (1H, m, H3), 1.87—1.72 (3H, m, H10, H11). 1.71—1.62 (2H, m, H12), 1.56 (3H, s, H13), 1.54 (3H, s, H13), 1.41—1.33 (2H, m, H12), 1.32 (3H, s, H13), 1.31 (3H, s, H13)

<sup>13</sup>C NMR (150 MHz, CDCl<sub>3</sub>)  $\delta$ C 171.0 (C4), 156.8 (q, *J* = 37.3 Hz, C2), 155.0 (C15), 129.0 (C6), 128.9 (C9), 128.8 (C7), 128.7 (C8), 115.6 (q, *J* = 285.3 Hz, C1), 95.6 (C17), 75.2

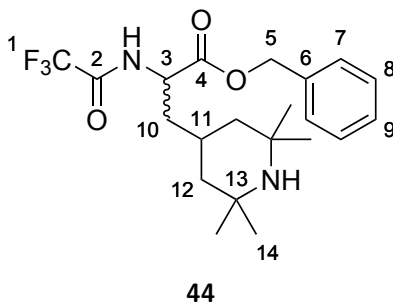
(C16), 68.1 (C5), 57.9 (C13), 57.8 (C13), 50.4 (C3), 48.5 (C12), 48.0 (C12), 39.2 (C10), 33.2 (C14), 33.2 (C14), 26.8 (C14), 26.7 (C14), 24.0 (C11)

HRMS (ESI) Calcd for C<sub>24</sub>H<sub>30</sub>Cl<sub>3</sub>F<sub>3</sub>N<sub>2</sub>NaO<sub>5</sub> [M]<sup>\*+</sup> 588.1172, found 588.1176

## Benzyl

### 3-(2,2,6,6-tetramethylpiperidin-4-yl)-2-(2,2,2-trifluoroacetamido)propanoate

(44)



Zn dust (33.27 g, 508.8 mmol, 120.0 equiv) was suspended in 200 mL of AcOH at room temperature. To this was added a solution of **43** (2.50 g, 4.24 mmol, 1.0 equiv) dissolved in 50 mL of AcOH. The reaction mixture was then allowed to stir at room temperature for 3 h. The reaction mixture was then filtered through Celite to remove the suspended zinc. Filtrate was then concentrated on rotovap to yield an oily crude. The material was then partitioned between 5% EDTA<sub>(aq)</sub> pH 8, brine, and EtOAc. Further extractions were made using EtOAc and the combined organic layers was washed once with saturated NaHCO<sub>3</sub>(aq). The organic layer was then dried over Na<sub>2</sub>SO<sub>4</sub> and concentrated to yield a crude. Purification was performed by flash column chromatography on silica using an eluent of 10/90 MeOH/EtOAc with 0.1% NEt<sub>3</sub>. Product elution was monitored by TLC with an eluent system of 20/80 MeOH/EtOAc and PMA stain (R<sub>f</sub> = 0.52). Concentration of fractions yields a solid product **44** (1.50 g, 3.62 mmol, 85%).

IR (thin film,  $\nu_{\max}$  / cm<sup>-1</sup>) 3311, 3068, 3038, 2959, 2920, 2840, 1747, 1716, 1557, 1499, 1456, 1215, 1183

<sup>1</sup>H NMR (400 MHz, CDCl<sub>3</sub>)  $\delta$ H 7.43—7.33 (5H, m, Ar-H), 5.26 (1H, d, *J* = 11.9 Hz, H5),



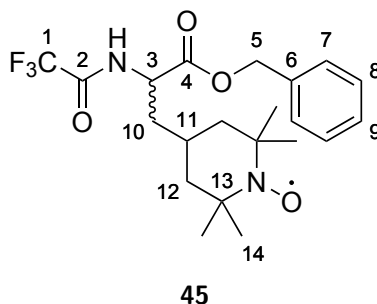
5.18 (1H, d,  $J = 11.9$  Hz, H5), 4.72 (1H, app dt,  $J = 8.9, 4.2$  Hz, H3), 1.90—1.76 (3H, m, H10, H12), 1.71—1.63 (1H, m, H11), 1.62 (3H, s, H13), 1.60 (3H, s, H13), 1.54—1.40 (3H, m, H10, H12), 1.35 (3H, s, H13), 1.34 (3H, s, H13)

$^{13}\text{C}$  NMR (100 MHz,  $\text{CDCl}_3$ )  $\delta\text{C}$  170.4 (C4), 156.6 (q,  $J = 37.6$  Hz, C2), 134.1 (C6), 128.6 (C9), 128.4 (C7), 128.2 (C8), 115.1 (q,  $J = 289.0$  Hz, C1), 67.7 (C5), 56.2 (C13), 56.0 (C13), 49.8 (C3), 41.6 (C12), 40.8 (C12), 38.4 (C10), 30.4 (C14), 24.8 (C14), 24.6 (C11), 24.5 (C14)

HRMS (EI) Calcd for  $\text{C}_{21}\text{H}_{30}\text{F}_3\text{N}_2\text{O}_3$   $[\text{M}]^{*+}$  414.2126, found 414.2130

**Benzyl 3-(1-oxyl-2,2,6,6-tetramethylpiperidin-4-yl)-2-(2,2,2-trifluoroacetamido)propanoate**

(45)



Compound **44** (1.06 g, 2.56 mmol, 1.0 equiv) was suspended in 24 mL of dry  $\text{Et}_2\text{O}$  under argon in a flame dried vial and cooled to 0 °C. A separate solution of mCPBA (0.88 g, 5.12 mmol, 2.0 equiv) in 12 mL of dry  $\text{Et}_2\text{O}$  was prepared under argon in a flame dried vial. This solution was then cannulated over to the first mixture. Upon addition of mCPBA, the reaction mixture turned from cloudy and colourless to intense orange and transparent. The reaction mixture was then removed from the ice bath and allowed to stir for 2 h. Afterwards, the reaction mixture was diluted with DCM and saturated  $\text{NaHCO}_3(\text{aq})$ . Additional extractions were made with DCM and the combined layers were dried over  $\text{Na}_2\text{SO}_4$  and concentrated to furnish a dark oil. Material was purified by flash chromatography on silica using an eluent of 20/80  $\text{EtOAc}/\text{Hexane}$ . Product elution was tracked by TLC using an eluent system of 30/70  $\text{EtOAc}/\text{Hexane}$  and  $\text{KMnO}_4$  staining ( $R_f = 0.32$ ). Concentration of

fractions yields an orange oil **45** (1.01 g, 2.35 mmol, 92%).

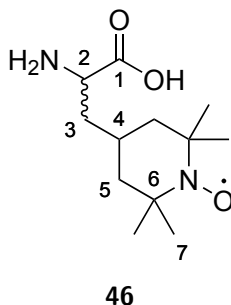
IR (thin film,  $\nu_{\max}$  /  $\text{cm}^{-1}$ ) 3282, 3073, 3036, 2977, 2933, 2867, 1747, 1724, 1555, 1499, 1457, 1211, 1175

$^1\text{H}$  NMR (700 MHz,  $\text{CDCl}_3$ )  $\delta$ H 7.37—7.35 (3H, m, Ar-H), 7.34—7.31 (2H, m, Ar-H), 5.22 (1H, d,  $J = 12.6$  Hz, H5), 5.16 (1H, d,  $J = 12.6$  Hz, H5), 4.60 (1H, dd,  $J = 10.2, 5.7$  Hz, H3), 1.86—1.77 (1H, m, H11), 1.77—1.66 (2H, m, H10), 1.62 (2H, 2 overlapping app t,  $J = 12.7$  Hz, H12), 1.25 (1H, app t,  $J = 12.7$  Hz, H12), 1.17 (1H, app t,  $J = 12.7$  Hz, H12), 1.16 (6H, s, H14), 1.09 (3H, s, H14), 1.06 (3H, s, H14)

$^{13}\text{C}$  NMR (125 MHz,  $\text{CDCl}_3$ )  $\delta$ C 172.1 (C4), 169.6 (C2), 129.6 (C7), 129.5 (C9), 129.4 (C8), 129.3 (C6), 90.2 (C1), 68.3 (C5), 61.4 (C13, assigned by HMBC), 51.8 (C3), 46.5 (C12), 45.3 (C12), 38.0 (C10), 31.8 (C14), 25.9 (C11), 20.3 (C14), 20.2 (C14)

HRMS (ESI) Calcd for  $\text{C}_{21}\text{H}_{28}\text{F}_3\text{N}_2\text{O}_4$   $[\text{M}]^{*+}$  429.2001, found 429.2003

## 2-Amino-3-(1-oxyl-2,2,6,6-tetramethylpiperidin-4-yl)propanoic acid (**46**)



Compound **45** (0.978 g, 2.278 mmol, 1.0 equiv) was dissolved in 10.0 mL each of acetone and 10%  $\text{K}_2\text{CO}_3(\text{aq})$ . The reaction mixture was then capped and stirred for 48 h at 60 °C. Afterwards, the sample was concentrated and solvent removed to yield a crude mixture. Purification was undertaken by flash chromatography on silica using and eluent gradient of 3/97  $\rightarrow$  20/80  $\text{NH}_4\text{OH}/i\text{PrOH}$ . Product elution was monitored by TLC and ninhydrin staining ( $R_f = 0.38$ ). Concentration of fractions yields an orange solid **46** (0.518 g, 2.130 mmol, 94%).

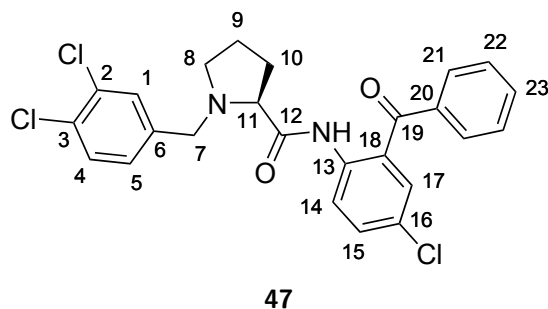
IR (thin film,  $\nu_{\max}$  /  $\text{cm}^{-1}$ ) 3415, 3074, 2974, 2937, 1633, 1610, 1555, 1365

$^1\text{H}$  NMR (700 MHz,  $\text{CDCl}_3$ )  $\delta$ H 3.52 (1H, t,  $J = 7.4$  Hz, H2), 2.03—1.95 (1H, m, H4), 1.80—1.70 (2H, m, H3, H5), 1.66 (1H, app dt,  $J = 13.0, 2.9$  Hz, H5), 1.57—1.51 (1H, m, H3), 1.18 (2H, app q,  $J = 12.6$  Hz, H5), 1.16 (6H, s, H7), 1.15 (6H, s, H7)

$^{13}\text{C}$  NMR (175 MHz,  $\text{CDCl}_3$ )  $\delta$ C 174.7 (C1), 60.0 (C6), 54.1 (C2), 46.9 (C5), 46.7 (C5), 39.7 (C3), 32.6 (C7), 32.6 (C7), 26.1 (C4), 20.4 (C7), 20.3 (C7)

HRMS (ESI) Calcd for  $\text{C}_{12}\text{H}_{22}\text{N}_2\text{O}_3$   $[\text{M}]^{*+}$  243.1709, found 243.1709

### Soloshonok Ligand (47)



This known compound<sup>58</sup> was synthesized via an alternative route. *N*-Boc-L-Proline (20.0 g, 93.0 mmol, 1.0 equiv) was dissolved in 200 mL of dry DMF. To this solution was added *N*-methylimidazole (19.2 mL, 241.4 mmol, 2.6 equiv) at 0 °C and left to stir for 10 min. The reaction mixture was then cooled to -10 °C and methanesulfonyl chloride (7.2 mL, 93.0 mmol, 1.0 equiv) was added. The mixture was left to stir for an additional 20 min before 2-amino-5-chlorobenzophenone (19.4 g, 83.6 mmol, 0.9 equiv) was added. Finally, the reaction mixture was allowed to warm to room temperature overnight. The reaction was subsequently quenched by addition of 1 L of  $\text{H}_2\text{O}$  and diluted with 500 mL of ethyl acetate. The layers were separated and the organic layer was additionally washed with  $\text{H}_2\text{O}$  (2 x 1 L) and brine (1 x 1 L). The organic layer was then dried over  $\text{Na}_2\text{SO}_4$ , filtered, and concentrated *in vacuo* to yield a thick yellow oil. This material was then dissolved in 200 mL of dichloromethane and to this was added 100 mL of trifluoroacetic acid. Gas evolution occurred and the reaction mixture was allowed to stir at room temperature for 45 min until gas evolution had ceased. The reaction mixture was then quenched and washed with 4 x 250 mL of aqueous saturated

NaHCO<sub>3</sub> solution. The organic layer was then dried over NaHCO<sub>3</sub> and concentrated to yield a thick yellow oil. This crude material was then deposited in a round-bottom flask along with KI (22.2 g, 133.7 mmol, 1.5 equiv) and K<sub>2</sub>CO<sub>3</sub> (18.5 g, 133.7 mmol, 1.5 equiv), to which 500 mL of dry DMF was added under an argon atmosphere and heated to 90 °C. After the solid material had completely dissolved, 3,4-dichlorobenzyl chloride (18.5 mL, 133.7 mmol, 1.5 equiv) was added and the reaction mixture was allowed to stir at 90 °C for 20 h. The mixture was subsequently diluted with 500 mL of ethyl acetate and washed with H<sub>2</sub>O (3 x 1L). The organic layer was then dried over Na<sub>2</sub>SO<sub>4</sub> and concentrated to yield a very dark oil. This crude material was then purified by flash chromatography on silica using an eluent system of 25/75 of EtOAc/Hexane (R<sub>f</sub> = 0.31). Concentration of fractions yielded a pale yellow foam **47** (31.9 g, 488 mmol, 78%).

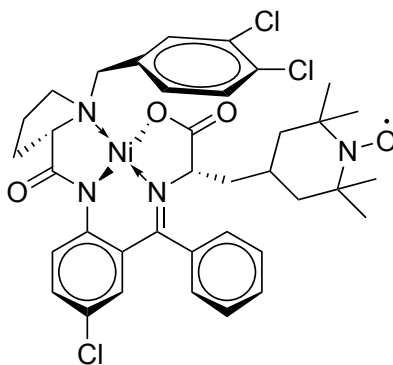
IR (thin film,  $\nu_{\max}$  / cm<sup>-1</sup>) 3255, 3065, 2969, 2882, 2821, 1692, 1648, 1596, 1568, 1501, 1473  
<sup>1</sup>H NMR (600 MHz, CDCl<sub>3</sub>)  $\delta$ H 8.65—8.62 (1H, s, Ar-H), 7.82—7.77 (2H, m, Ar-H), 7.71 (1H, d,  $J$  = 1.8 Hz, Ar-H), 7.65, (1H, tt,  $J$  = 7.5, 1.3 Hz, Ar-H), 7.56—7.50 (4H, m, Ar-H), 7.24 (1H, td,  $J$  = 8.3, 2.1 Hz, Ar-H), 7.22 (1H, t,  $J$  = 8.2 Hz, Ar-H), 3.91 (1H, d,  $J$  = 13.2 Hz, H7), 3.54 (1H, d,  $J$  = 13.2 Hz, H7), 3.32 (1H, dd,  $J$  = 10.2, 5.2 Hz, H11), 3.25—3.19 (1H, m, H8), 2.42—2.35 (1H, m, H8), 2.35—2.25 (1H, m, H10), 2.04—1.96 (1H, m, H10), 1.88—1.78 (2H, m, H9)

<sup>13</sup>C NMR (125 MHz, CDCl<sub>3</sub>)  $\delta$ C 197.1 (C19), 174.2 (C12), 138.3 (Ar-C), 138.0 (Ar-C), 138.8 (Ar-C), 133.4 (Ar-C), 133.1 (Ar-C), 132.4 (Ar-C), 132.1 (Ar-C), 131.1 (Ar-C), 131.0 (Ar-C), 130.1 (Ar-C), 130.1 (Ar-C), 128.6 (Ar-C), 128.3 (Ar-C), 127.4 (Ar-C), 125.9 (Ar-C), 122.8 (Ar-C), 68.7 (C11), 59.1 (C7), 54.0 (C8), 31.0 (C10), 24.1 (C9)

OR:  $[\alpha]_{\text{D}}^{26} = -24.64$  ( $c = 0.34$ , DCM)

HRMS (EI) Calcd for C<sub>25</sub>H<sub>22</sub>Cl<sub>3</sub>N<sub>2</sub>O<sub>2</sub> [M]<sup>\*+</sup> 486.0669, found 486.0671

### Extended 6-Membered Ring Nickle Complex (**53**)



**53**

**46** (0.010 g, 0.041 mmol, 1.0 equiv), **47** (0.022 g, 0.045 mmol, 1.1 equiv), Ni(OAc)<sub>2</sub> · 4 H<sub>2</sub>O (0.011 g, 0.045 mmol, 1.1 equiv), and K<sub>2</sub>CO<sub>3</sub> (0.028 g, 0.205 mmol, 5.0 equiv) were dissolved in 2.0 mL of MeOH and heated to 60 °C, stirring for 24 h. The reaction mixture turned from green to red shortly after heating. After 24 h, compound was diluted with H<sub>2</sub>O (6.0 mL) and DCM (6.0 mL). Three further extractions were made with DCM (6.0 mL) and the combined organic layers dried over Na<sub>2</sub>SO<sub>4</sub>, yielding a red solid crude upon concentration. The material was purified by flash column chromatography on silica, with an initial flush of 50/50 EtOAc/Hexane to elute excess ligand followed by 5/95 MeOH/EtOAc to elute the product as a visible red band. Product elution was monitored by TLC and KMnO<sub>4</sub> staining using an eluent system of 10/90 MeOH/EtOAc (R<sub>f</sub> = 0.41). Concentration of fractions yields a red solid **53** as the product (0.031g, 0.040 mmol, 98%).

IR (thin film,  $\nu_{\max}$  / cm<sup>-1</sup>) 3054, 2974, 2936, 2874, 1673, 1641, 1589, 1535, 1465, 1397, 1337, 1248

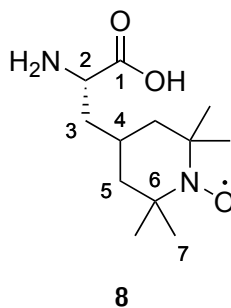
<sup>1</sup>H NMR Due to product decomposition upon phenylhydrazine-mediated quenching of the radical, NMR data was not obtained.

<sup>13</sup>C NMR Due to product decomposition upon phenylhydrazine-mediated quenching of the radical, NMR data was not obtained.

OR:  $[\alpha]_D^{26} = 1434.48$  (c = 1.47, DCM)

HRMS (EI) Calcd for C<sub>37</sub>H<sub>40</sub>Cl<sub>3</sub>NaN<sub>4</sub>O<sub>4</sub> [M]<sup>+</sup> 767.1469, found 767.1468

**(S)-2-Amino-3-(1-oxyl-2,2,6,6-tetramethylpiperidin-4-yl)propanoic acid (8)**



**53** (1.198 g, 1.557 mmol, 1.0 equiv) and  $\text{H}_2\text{N}-\text{OH} \cdot \text{HCl}$  (0.433 g, 6.227 mmol, 4.0 equiv) was dissolved in 6.25 mL of pyridine and allowed to stir at 60 °C for 2 h. Subsequently, the material was concentrated by rotary evaporation and pyridine removed by coevaporation with toluene. The crude material was then dissolved in 30 mL AcOH, 30 mL  $\text{H}_2\text{O}$ , 60 mL Hexane, and 30 mL DCM. The aqueous layer was then separated and the remaining organic layer washed with 5% AcOH solution (2 x 25 mL). The aqueous solution was then concentrated to furnish a crude material. Purification was performed by silica column with an eluent gradient of 3/97  $\rightarrow$  20/80  $\text{NH}_4\text{OH}/i\text{PrOH}$ . Product elution was checked by TLC and staining with ninhydrin, found to be 2 coeluting spots with  $R_f = 0.23$  and 0.34 in an eluent of 20/80  $\text{NH}_4\text{OH}/i\text{PrOH}$  and corresponds to the quenched and unquenched oxy-radicals respectively. Fractions were then concentrated, redissolved in 1/1  $\text{NH}_4\text{OH}/i\text{PrOH}$  and allowed to stir overnight to regenerate the radical. Concentration of the material furnished an orange solid **8** (0.379 g, 1.557 mmol, 100%).

IR (thin film,  $\nu_{\text{max}} / \text{cm}^{-1}$ ) 3421, 3005, 2975, 2935, 1602, 1458, 1405, 1365, 1302, 1245

$^1\text{H}$  NMR (700 MHz,  $\text{CDCl}_3$ )  $\delta$  3.52 (1H, t,  $J = 6.9$  Hz, H2), 2.05—1.97 (1H, m, H4), 1.79—1.72 (2H, m, H3, H5), 1.66 (1H, app dd,  $J = 13.4, 2.5$  Hz, H5), 1.57—1.51 (1H, m, H3), 1.20 (2H, app q,  $J = 13.3$  Hz, H5), 1.17 (6H, s, H7), 1.16 (6H, s, H7)

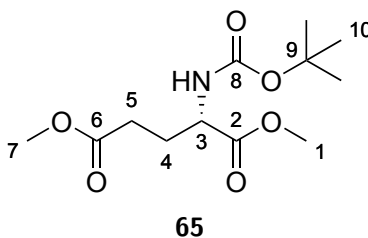
$^{13}\text{C}$  NMR (175 MHz,  $\text{CDCl}_3$ )  $\delta$  174.7 (C1), 60.8 (C6), 54.1 (C2), 46.6 (C5), 46.5 (C5), 39.6 (C3), 32.2 (C7), 32.1 (C7), 26.1 (C4), 20.4 (C7), 20.3 (C7)

OR:  $[\alpha]_{\text{D}}^{26} = 10.86$  ( $c = 0.230$ , MeOH)

HRMS (EI) Calcd for C<sub>12</sub>H<sub>22</sub>N<sub>2</sub>O<sub>3</sub> [M]<sup>+</sup> 243.1709, found 243.1708

## 7.8 Chapter 3 Synthetic Procedures

### Dimethyl (*tert*-butoxycarbonyl)-L-glutamate (65)



This known compound was synthesized based on a literature procedure.<sup>33</sup> L-Glutamic acid (30.00 g, 202.5 mmol, 1.0 equiv) was added to a flame-dried RBF under Ar, followed by the addition of dry MeOH (506.0 mL). The stirred suspension was then cooled to 0 °C, and TMS-Cl (113.1 mL, 891.7 mmol, 4.4 equiv) was added slowly over 15 minutes. The reaction mixture was stirred at 0 °C for 1.5 h, and then stirred overnight at room temperature. Triethylamine (182.5 mL, 1316 mmol, 6.5 equiv) was added to the reaction mixture slowly over 15 minutes. Next, Boc<sub>2</sub>O (48.62 g, 222.3 mmol, 1.1 equiv) was added in one portion, and then the reaction mixture was capped with pressure-equalizing Ar and stirred at room temperature for 3 h. The reaction mixture was then concentrated under reduced pressure to produce a white solid. The solid was triturated by suspension in Et<sub>2</sub>O (500 mL), and collected by filtration. The solid was washed with additional volumes of Et<sub>2</sub>O (3 × 250 mL), and then concentrated *in vacuo* to produce a crude oil. The crude product was purified using silica column chromatography (50/50 EtOAc/ Hexanes), and yielded a clear, yellow oil (50.44 g, 183.2 mmol, 91%): R<sub>f</sub> = 0.61 on SiO<sub>2</sub>, 50% EtOAc in hexanes;

IR (DCM cast film,  $\nu_{\max}$  / cm<sup>-1</sup>) 3369, 2979, 2956, 1742, 1717, 1518, 1439, 1392, 1368, 1252, 1212, 1167

<sup>1</sup>H NMR (500 MHz, CDCl<sub>3</sub>)  $\delta$ H 5.13 (1H, d, *J* = 6.8 Hz, NH), 4.30 (1H, app d, *J* = 5.0 Hz, H3) 3.71 (3H, s, H1), 3.65 (3H, s, H7), 2.31 (2H, m, H5), 2.15 (1H, app td, *J* = 13.0, 7.3,

H4), 1.92 (1H, app dtd,  $J = 14.0, 8.3, 6.5$ , H4), 1.40 (9H, s, H10)

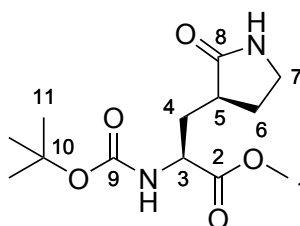
$^{13}\text{C}$  NMR (125 MHz,  $\text{CDCl}_3$ )  $\delta\text{C}$  173.3 (C6), 172.6 (C2), 155.3 (C8), 80.0 (C9), 52.8 (C3), 52.4 (C1), 51.7 (C7), 30.0 (C5), 28.3 (C10), 27.8 (C4)

OR:  $[\alpha]_{\text{D}}^{26} = 7.20$  ( $c = 1.35$ , DCM)

HRMS: (ESI) Calcd for  $\text{C}_{12}\text{H}_{21}\text{NNaO}_6$   $[\text{M} + \text{Na}]^+$  298.1261, found 298.1260

## Methyl

(*S*)-2-((*tert*-butoxycarbonyl)amino)-3-((*S*)-2-oxopyrrolidin-3-yl)propanoate  
(66)



66

This known compound was synthesized based on a modified literature procedure.<sup>33</sup> **65** (1.00 g, 3.62 mmol, 1.00 equiv) was deposited in a flame-dried round-bottom flask under argon, to which 10.34 mL of freshly distilled THF was added. The oily starting material was dissolved at room temperature before LiHMDS (1.0 M in THF, 7.82 mL, 7.82 mmol, 2.16 equiv) was added over a period of 2 min at  $-78^\circ\text{C}$ . The reaction mixture went from clear and nearly colourless to light yellow, and was allowed to stir at  $-78^\circ\text{C}$  for 1 h. Next  $\text{BrCH}_2\text{CN}$  (0.270 mL, 3.88 mmol, 1.07 equiv) was slowly added over a period of 1 h (addition rate of *ca.* 0.02 mL / 5 min), while maintaining reaction temperature at  $-78^\circ\text{C}$ . The reaction mixture was then stirred at  $-78^\circ\text{C}$  over a period of 2 h. After 2 h, some starting material remained but the reaction mixture was quenched by addition of 5.2 mL of HCl at  $-78^\circ\text{C}$ . The reaction mixture was then removed from the cooling bath to allow the ice in the flask to melt, stirring for 50 min. The mixture was then extracted with EtOAc ( $3 \times 30$  mL). The combined EtOAc layers were washed with  $\text{H}_2\text{O}$  ( $2 \times 30$  mL) and brine ( $1 \times 30$  mL). Drying



over  $\text{MgSO}_4$  and concentration by rotovap furnishes a dark brown oil. This oil was then dissolved in 5.0 mL of DCM, to which activated charcoal (0.35 g) and silica (1.40 g) was added. The slurry was spun on a rotovap without heat or vacuum for 1 h. Afterwards, the charcoal and silica was filtered through a celite pad and the filtrate washed with additional volumes of DCM. Concentration of the filtrate furnishes a yellow oil. This oil was then transferred to a flame-dried round-bottom flask under argon, to which  $\text{CoCl}_2 \cdot 6 \text{H}_2\text{O}$  (0.314 g, 2.42 mmol, 0.67 equiv) was added. The material was then dissolved in 20.0 mL of freshly distilled MeOH. The solution was then cooled to 0 °C and  $\text{NaBH}_4$  (0.917 g, 24.20 mmol, 6.74 equiv) was added in multiple portions over a period of 30 min. Upon addition of  $\text{NaBH}_4$ , the reaction mixture immediately turned black and started bubbling. Once addition was finished and bubbling slowed, the reaction mixture was capped under a blanket of pressure-equalizing argon, removed from the ice bath, and allowed to warm to room temperature, stirring for 24 h. After 24 h, the reaction mixture was concentrated on the rotovap to a minimal volume. To the obtained residue was then added 1 M of citric acid at 0 °C. The mixture was further diluted with EtOAc and extracted with EtOAc (3x). The combined EtOAc layers were then washed with sat.  $\text{NaHCO}_3$  (2x) and brine (1x). Drying over  $\text{Na}_2\text{SO}_4$  and removal of solvent furnishes a very pale yellow oil as crude. This material was then purified via flash column chromatography using an eluent system of EtOAc. Elution of product was monitored by  $\text{KMnO}_4$  staining ( $R_f = 0.16$ , EtOAc). Concentration of product fractions and co-evaporation with  $\text{Et}_2\text{O}$  furnished the desired product as a white solid (0.280 g, 0.973 mmol, 54%).

IR (DCM cast film,  $\nu_{\text{max}} / \text{cm}^{-1}$ ) 3290, 2977, 1745, 1698, 1523, 1440, 1392, 1367, 1276, 1213, 1168

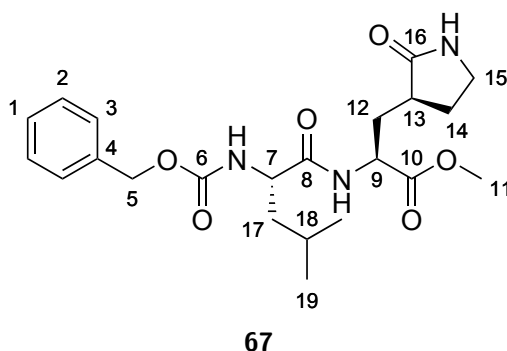
$^1\text{H}$  NMR (500 MHz,  $\text{CDCl}_3$ )  $\delta$  6.62 (1H, s, NH), 5.55 (1H, d,  $J = 7.8$  Hz, NH), 4.29 (1H, m, H3), 3.72 (3H, s, H1), 3.36–3.31 (2H, m, H7), 2.48–2.40 (2H, m, H5, H6), 2.11 (1H, ddd,  $J = 14.3, 10.8, 3.7$  Hz, H4), 1.88–1.40 (2H, m, H4, H6), 1.41 (9H, s, H11)

$^{13}\text{C}$  NMR (125 MHz,  $\text{CDCl}_3$ )  $\delta$  179.8 (C8), 172.9 (C2), 155.8 (C9), 79.9 (C10), 52.4 (C1), 52.3 (C3), 40.4 (C7), 38.2 (C5), 34.1 (C4), 28.3 (C11), 28.1 (C6)

OR:  $[\alpha]_D^{26} = 3.65$  ( $c = 0.57$ , DCM)

HRMS: (ESI) Calcd for  $C_{13}H_{22}N_2NaO_5$   $[M + Na]^+$  309.1421, found 309.1423

**Methyl (*S*)-2-((*S*)-2-(((benzyloxy)carbonyl)amino)-4-methylpentanamido)-3-((*S*)-2-oxopyrrolidin-3-yl)propanoate**  
**(67)**



This known compound was synthesized via an alternative procedure.<sup>83</sup> **66**, (4.00 g, 13.97 mmol, 1.0 equiv) was dissolved in 140 mL of 50/50 TFA/DCM and stirred for 1 h at room temperature, with gas evolution being observed. The solution was then concentrated on rotovap and co-evaporated with DCM (5 ×). In a separate flame-dried round-bottom flask under argon was deposited Cbz-Leu-OH (90% purity, 4.12 g, 13.97 mmol, 1.0 equiv), HATU (5.31 g, 13.97 mmol, 1.0 equiv). The material was then dissolved in 70 mL of DMF. Next, HOAt (0.6 M in DMF, 2.33 mL, 1.40 mmol, 0.1 equiv) was added, followed by DIPEA (7.30 mL, 41.91 mmol, 3.0 equiv). The reaction mixture turned bright yellow and was incubated for 5 min. The previously concentrated Boc-protected material was then dissolved in 70 mL of DCM and added dropwise to the incubating solution, with the bright yellow colour quickly fading. The reaction mixture was capped under a blanket of argon and allowed to react at room temperature for 1.5 h. Next, the reaction mixture was diluted with H<sub>2</sub>O and EtOAc. The layers were separated and the H<sub>2</sub>O layer was further extracted with EtOAc (3x). The combined EtOAc layers were then washed with sat. NaHCO<sub>3</sub> (2x), 1 M HCl (2x), and brine (1x). Drying over Na<sub>2</sub>SO<sub>4</sub> and concentrating on the rotovap furnishes a

crude yellow oil. This material was used without further purification but may be purified by flash column chromatography over silica, using an eluent system of pure EtOAc. Product elution was monitored by TLC and KMnO<sub>4</sub> staining ( $R_f = 0.43$ , 5/95 MeOH/EtOAc), and concentration of product fractions furnishes a transparent, slightly yellow oil as the desired product (6.056 g, 13.97 mmol, 100%).

IR (DCM cast film,  $\nu_{\max}$  /  $\text{cm}^{-1}$ ) 3275, 3063, 2955, 2871, 1688, 1538, 1455, 1439, 1385, 1268, 1176, 1134

<sup>1</sup>H NMR (700 MHz, CDCl<sub>3</sub>)  $\delta$ H 7.84 (1H, d,  $J = 5.3$  Hz, NH), 7.37—7.27 (5H, m, H1, H2, H3), 5.97 (1H, s, NH), 5.34 (1H, d,  $J = 7.0$  Hz, NH), 5.09 (2H, s, H5), 4.51—4.42 (1H, m, H9), 4.36—4.27 (1H, m, H7), 3.72 (3H, s, H11), 3.35—3.25 (2H, m, H15), 2.42—2.32 (2H, m, H13, H14), 2.21—2.10 (1H, m, H12), 1.95—1.88 (1H, m, H12), 1.86—1.78 (1H, m, H14), 1.78—1.71 (1H, m, H18), 1.71—1.65 (1H, m, H17), 1.56—1.47 (1H, m, H17), 0.99—0.91 (6H, m, H19)

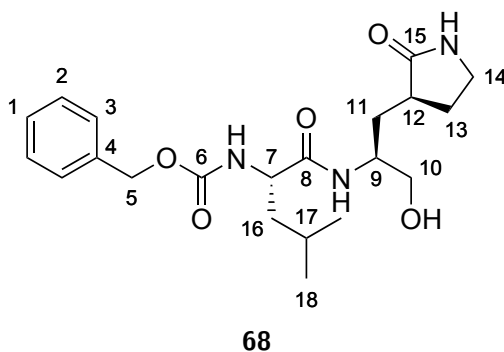
<sup>13</sup>C NMR (175 MHz, CDCl<sub>3</sub>)  $\delta$ C 179.7 (C16), 172.8 (C8), 172.1 (C10), 156.1 (C6), 136.4 (C4), 128.5 (C2), 128.1 (C3), 128.0 (C1), 66.9 (C5), 53.4 (C7), 52.4 (C11), 51.7 (C9), 42.3 (C17), 40.5 (C15), 38.4 (C13), 32.9 (C12), 28.6 (C14), 24.6 (C18), 22.9 (C19), 22.1 (C19)

OR:  $[\alpha]_D^{26} = -12.51$  ( $c = 0.78$ , DCM)

HRMS: (ESI) (ESI) Calcd for C<sub>22</sub>H<sub>31</sub>N<sub>3</sub>NaO<sub>6</sub> [M + Na]<sup>+</sup> 456.2105, found 456.2101

**Benzyl ((*S*)-1-(((*S*)-1-hydroxy-3-((*S*)-2-oxopyrrolidin-3-yl)propan-2-yl)amino)-4-methyl-1-oxopentan-2-yl)carbamate**

**(68)**



This compound was synthesized based on a literature procedure.<sup>83</sup> **67** (0.167 g, 0.385 mmol, 1.0 equiv) was deposited in a flame-dried round-bottom flask under argon and dissolved in 2.31 mL of dry THF. To the reaction mixture was then added LiBH<sub>4</sub> (2.0 M in THF, 0.578 mL, 1.156 mmol, 3.0 equiv) dropwise. Addition causes the reaction mixture to turn bright yellow in colour, with continued addition eventually resulting in fading of the yellow colour. Gas evolution also occurred during this process. After gas evolution ceased, 1.16 mL of dry MeOH was added dropwise. This was followed by a second gas evolution event. RM was allowed to stir at room temperature for 1.5 h under a blanket of argon. Reaction mixture was worked up by quenching with 1 M HCl until pH 1–2. The reaction mixture was then concentrated on rotovap and the resulting residue was dissolved in EtOAc and brine. The layers were separated and the EtOAc layer was dried over Na<sub>2</sub>SO<sub>4</sub>. Concentration and co-evaporation with Et<sub>2</sub>O furnished a white foam as the product (R<sub>f</sub> = 0.14, 5/95 MeOH/EtOAc) (0.14 g, 0.345 mmol, 90%) with no further purification required.

IR (DCM cast film,  $\nu_{\max}$  / cm<sup>-1</sup>) 3282, 3065, 2955, 2871, 1686, 1539, 1456, 1442, 1386, 1369, 1263, 1173

<sup>1</sup>H NMR (500 MHz, CDCl<sub>3</sub>)  $\delta$ H 7.79–7.63 (1H, m, NH), 7.40–7.27 (5H, m, H1, H2, H3), 6.51–6.00 (1H, m, NH), 5.74–5.41 (1H, m, NH), 5.09 (2H, s, H5), 4.32–4.16 (1H, m, H7),

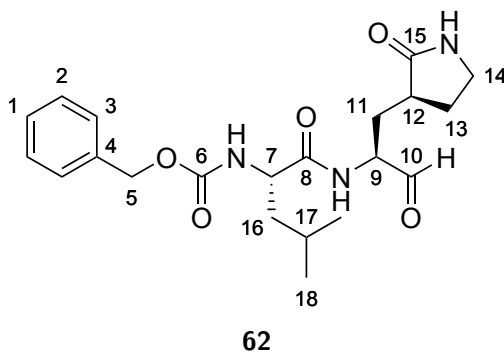
4.04—3.90 (1H, m, H9), 3.73—3.40 (3H, m, H10, OH), 3.34—3.18 (2H, m, H14), 2.55—2.25 (2H, m, H12, H13), 2.06—1.94 (1H, m, H11), 1.85—1.73 (1H, m, H13), 1.73—1.56 (3H, m, H11, H16, H17), 1.58—1.44 (1H, m, H16), 1.01—0.84 (6H, m, H18)

$^{13}\text{C}$  NMR (125 MHz,  $\text{CDCl}_3$ )  $\delta\text{C}$  181.0 (C15), 173.7(C8), 156.2 (C6), 136.4 (C4), 128.5 (C2), 128.1 (C3), 128.0 (C1), 66.9 (C5), 66.1 (C10), 53.9 (C7), 51.3 (C9), 42.3 (C16), 40.6 (C14), 38.6 (C12), 32.1 (C11), 28.9 (C13), 24.8 (C17), 23.0 (C18), 22.0 (C18)

OR:  $[\alpha]_{\text{D}}^{26} = -21.20$  ( $c = 1.05$ , DCM)

HRMS: (ESI) Calcd for  $\text{C}_{21}\text{H}_{32}\text{N}_3\text{O}_5$   $[\text{M} + \text{H}]^+$  406.2336, found 406.2234

### GC373 (62)



This compound was synthesized based on a literature procedure.<sup>83</sup> **68** (0.319 g, 0.786 mmol, 1.0 equiv) was dissolved in 0.8 mL of dry DCM under argon. Dess—Martin periodinane (0.500 g, 1.179 mmol, 1.5 equiv) was then added at 0 °C. The reaction mixture was capped under a blanket of argon and allowed to warm to room temperature. The reaction was then allowed to stir at room temperature for 3 h. Reaction mixture was then quenched with the addition of 3 mL of 10%  $\text{Na}_2\text{S}_2\text{O}_3$  followed with stirring for 15 min. The layers were then separated and the DCM layer was washed sequentially with 10%  $\text{Na}_2\text{S}_2\text{O}_3$  (1 x 3 mL), sat.  $\text{NaHCO}_3$  (2 x 3 mL),  $\text{H}_2\text{O}$  (2 x 3 mL), and brine (2 x 3 mL). The DCM layer was then dried over  $\text{Na}_2\text{SO}_4$  and concentrated to furnish a yellow residue. The TLC of this crude is very messy (extensive streaking) but the product was successfully purified via flash column chromatography on silica using an eluent system of 2.5/97.5 MeOH/EtOAc. Elution of

product was monitored by TLC and  $\text{KMnO}_4$  staining ( $R_f = 0.14$ , 2.5/97.5 MeOH/EtOAc). Concentration of product fractions furnished an oil that solidified to a light yellow foam upon co-evaporation with  $\text{Et}_2\text{O}$  (0.206 g, 0.511 mmol, 65%).

IR (DCM cast film,  $\nu_{\text{max}} / \text{cm}^{-1}$ ) 3287, 3064, 2957, 2871, 1691, 1535, 1456, 1440, 1386, 1369, 1265, 1119

Please note that this compound exists as a mixture of diastereomers due to rapid epimerization at the alpha carbon of alpha-amido aldehydes. Although the  $^1\text{H}$  NMR spectra does not appear to readily show this, some  $^{13}\text{C}$  NMR signals do appear separated and have been noted as pairs where appropriate.

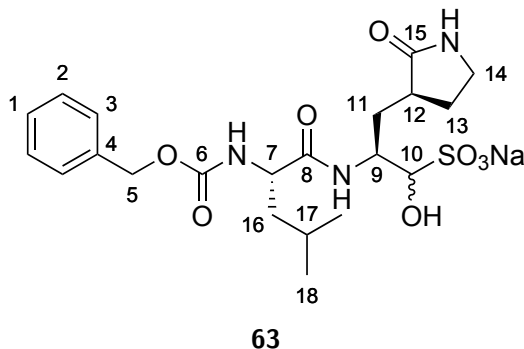
$^1\text{H}$  NMR (500 MHz,  $\text{CDCl}_3$ )  $\delta\text{H}$  9.58 (0.5H, br s, H10 of diastereomers), 9.44 (0.5H, br s, H10 of diastereomers), 8.57 (0.5H, d,  $J = 4.62$  Hz, NH of diastereomers), 8.27 (0.5H, d,  $J = 4.62$  Hz, NH of diastereomers), 7.42—7.27 (5H, m, H1, H2, H3), 6.33 (0.5H, br s, NH of diastereomers), 6.03 (0.5H, br s, NH of diastereomers), 5.52 (0.5H, d,  $J = 8.25$  Hz, NH of diastereomers), 5.38 (0.5H, d,  $J = 8.25$  Hz, NH of diastereomers), 5.08 (2H, d,  $J = 9.5$  Hz, H5), 4.55—4.07 (2H, m, H7, H9), 3.40—3.17 (2H, m, H14), 2.58—2.20 (2H, m, H12, H13), 2.14—2.00 (1H, m, H11), 2.00—1.88 (1H, m, H11), 1.88—1.80 (1H, m, H13), 1.79—1.62 (2H, m, H16, H17), 1.62—1.44 (1H, m, H16), 1.03—0.84 (6H, m, H18)

$^{13}\text{C}$  NMR (125 MHz,  $\text{CDCl}_3$ )  $\delta\text{C}$  200.8/199.7 (C10), 180.2/180.1 (C15), 173.7/173.4 (C8), 156.1 (C6), 136.4 (C4), 128.6/128.5 (C2), 128.2/128.1 (C3), 128.0 (C1), 67.0/66.9 (C5), 57.9/57.0 (C7), 53.7/53.6 (C9), 42.3/41.9 (C16), 40.6 (C14), 38.2/37.7 (C12), 29.7/29.1 (C11), 28.8/28.3 (C13), 24.8 (C17), 23.0/23.0 (C18), 22.0/21.9 (C18)

OR:  $[\alpha]_{\text{D}}^{26} = -2.93$  ( $c = 0.43$ , DCM)

HRMS: (ESI) Calcd for  $\text{C}_{21}\text{H}_{30}\text{N}_3\text{O}_5$   $[\text{M} + \text{H}]^+$  404.2180, found 404.2173

## GC376 (63)



This compound was synthesized based on a literature procedure.<sup>83</sup> GC373 (**62**) (0.030 g, 0.074 mmol, 1.0 equiv) was deposited in a vial and dissolved in 0.296 mL of dry EtOAc and 0.178 mL of absolute EtOH. To this was added 1 M NaHSO<sub>3</sub> (0.074 mL, 0.074 mmol, 1.0 equiv). The reaction vessel was then capped and stirred at 50 °C for 3 h. Afterwards, the mixture was filtered to remove solids and the solids were thoroughly washed with additional volumes of EtOH. The combined washings were dried over Na<sub>2</sub>SO<sub>4</sub> and filtered again. Concentration of the filtrate furnishes a yellow oil. To this oil was added 0.5 mL of Et<sub>2</sub>O, causing a white solid to crash out after mixing. The mixture was then centrifuged and the Et<sub>2</sub>O was removed. This step was repeated once more. The resultant white solid was then treated with Et<sub>2</sub>O (0.444 mL) and EtOAc (0.222 mL). Mixing for 5 min followed by centrifuge and removal of solvent furnishes the white bisulfite adduct as the product. The material was dried on hi-vac overnight to remove residual solvent. A check by LCMS shows the desired adduct as the major product (0.025 g, 0.050 mmol, 68%) and was used without further purification.

IR (H<sub>2</sub>O cast film,  $\nu_{\max}$  / cm<sup>-1</sup>) 3291, 3090, 3066, 3035, 2957, 2872, 1674, 1527, 1455, 1387, 1368, 1216

Please note that this compound exists as a mixture of diastereomers due to rapid epimerization at the alpha carbon of alpha-amido aldehydes. Although the <sup>1</sup>H NMR spectra does not appear to readily show this, some <sup>13</sup>C NMR signals do appear separated

and have been noted as pairs where appropriate.

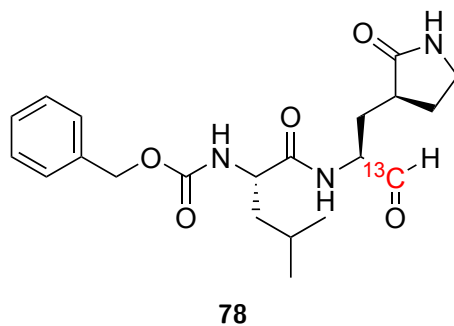
$^1\text{H}$  NMR (500 MHz, DMSO- $d_6$ )  $\delta$ H 7.65—7.56 (1H, m NH), 7.50—7.42 (1H, m NH), 7.39—7.31 (5H, m, H1, H2, H3), 5.38 (1H, d,  $J = 4.5$  Hz, NH), 5.24 (1H, d,  $J = 4.5$  Hz, OH), 5.07—4.96 (2H, m, H5), 4.25—3.79 (3H, m, H7, H9, H10), 3.14—3.07 (1H, m, H14), 3.04—2.98 (1H, m, H14), 2.22—2.04 (2H, m, H12, H13), 2.03—1.52 (4H, m, H11, H13, H17), 1.50—1.40 (2H, m, H16), 0.91-077 (6H, m, H18)

$^{13}\text{C}$  NMR (125 MHz, DMSO- $d_6$ )  $\delta$ C 179.0 (C15), 171.8 (C8), 156.0 (C6), 137.1 (C4), 128.2/128.2 (C2), 127.6 (C3), 127.6/127.6 (C1), 84.4/83.7 (C10), 65.3 (C5), 53.6/53.5 (C9), 49.1/48.6 (C7), 40.5 (C16), 40.7/40.4 (C14), 37.8/37.7 (C12), 31.8 (C11), 27.5/27.3 (C13), 24.2/24.2 (C17), 23.1/23.0 (C18), 21.4/21.3 (C18)

OR:  $[\alpha]_D^{26} = -37.38$  ( $c = 0.31$ ,  $\text{H}_2\text{O}$ )

HRMS: (ESI) Calcd for  $\text{C}_{21}\text{H}_{32}\text{N}_3\text{O}_8\text{S}$   $[\text{M} + \text{H}]^+$  486.1905, found 486.1896

### $^{13}\text{C}$ -GC373 (78)

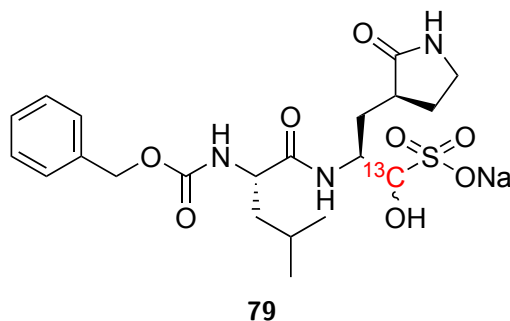


Synthesis of  $^{13}\text{C}$ -labelled GC373 was carried out using the method described for the synthesis of **62**. All characterization data was in agreement as described previously.

HRMS: (ESI) Calcd for  $\text{C}_{20}^{13}\text{CH}_{30}\text{N}_3\text{O}_5$   $[\text{M} + \text{H}]^+$  405.2214, found 405.2215



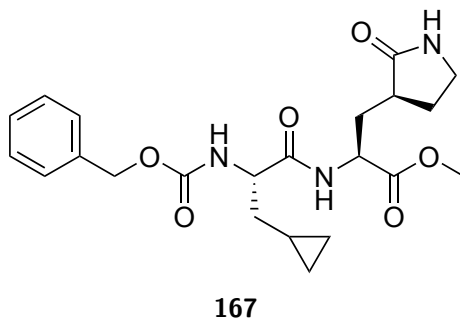
<sup>13</sup>C-GC376 (79)



Synthesis of <sup>13</sup>C-labelled GC376 was carried out using the method described for the synthesis of **63**. All characterization data was in agreement as described previously.

HRMS: (ESI) Calcd for C<sub>20</sub><sup>13</sup>CH<sub>32</sub>N<sub>3</sub>O<sub>8</sub>S [M + H]<sup>+</sup> 487.1938, found 487.1939

**Methyl (*S*)-2-((*S*)-2-(((benzyloxy)carbonyl)amino)-3-cyclopropylpropanamido)-3-((*S*)-2-oxopyrrolidin-3-yl)propanoate**  
(167)



**66** (synthesized according to a previously published procedure<sup>25</sup>) (0.200 g, 0.698 mmol, 1.0 equiv) was deposited in a vial and deprotected via addition of 7 mL of a 50/50 mixture of TFA/DCM. The solution was stirred for 1 h at room temperature, with gas evolution observed. The solution was then concentrated by rotary evaporation and co-evaporated DCM (5 ×). In a separate vessel was deposited Cbz-Cpa-OH (0.239 g, 0.907 mmol, 1.3 equiv), HATU (0.265 g, 0.698 mmol, 1.0 equiv), DMF (3.5 mL), HOAt (0.6 M solution in

DMF, 0.116 mL, 0.070 mmol, 0.1 equiv), and DIPEA (0.401 mL, 2.303 mmol, 3.3 equiv). The solution was then allowed to stir and incubate for 5 min at room temperature, turning bright yellow in colouration. The previously co-evaporated and deprotected **66**, was then dissolved in 3.5 mL of DCM and added dropwise to the incubating solution. Fading of the bright yellow colour was observed. The reaction mixture was then capped under a blanket of argon and allowed to react at room temperature for 1.5 h. Next, the reaction mixture was diluted with H<sub>2</sub>O (5 mL) and EtOAc (5 mL). The layers were separated and the H<sub>2</sub>O layer was subjected to additional extractions with EtOAc (3 × 5 mL). The EtOAc layers were then combined and washed with sat. NaHCO<sub>3</sub>(aq) (2 × 5 mL), 1 M HCl (2 × 5 mL), and brine (1 × 5 mL). Drying over Na<sub>2</sub>SO<sub>4</sub> and concentration by rotary evaporation furnished a crude yellow oil. This material was then subjected to purification by flash column chromatography over silica using an eluent system of 5/95 MeOH/EtOAc. Product elution was monitored by TLC and KMnO<sub>4</sub> staining (R<sub>f</sub> = 0.17, 5/95 MeOH/EtOAc). Concentration of product fractions furnished a clear oil that solidified to a white foam upon co-evaporation with Et<sub>2</sub>O (0.231 g, 0.535 mmol, 77%).

IR (DCM cast film,  $\nu_{\max}$  / cm<sup>-1</sup>) 3295, 3069, 3038, 3004, 2954, 1686, 1534, 1455, 1439, 1381, 1340, 1269, 1176, 1130, 1054

<sup>1</sup>H NMR (500 MHz, CDCl<sub>3</sub>)  $\delta$ H 7.79 (1H, d,  $J$  = 5.0 Hz), 7.35—7.30 (5H, m), 5.75 (1H, s), 5.54 (1H, d,  $J$  = 7.5 Hz), 5.10 (2H, s), 4.54—5.48 (1H, m), 4.35—4.28 (1H, m), 3.72 (3H, s), 3.32 (2H, d,  $J$  = 9.0 Hz), 2.45—2.39 (2H, m), 2.15 (1H, d,  $J$  = 7.0 Hz), 1.95 (1H, d,  $J$  = 7.0 Hz), 1.87—1.80 (1H, m), 1.76—1.71 (1H, m), 1.66—1.60 (1H, m), 0.82—0.78 (1H, m), 0.48 (2H, d,  $J$  = 7.0 Hz), 0.13 (2H, s)

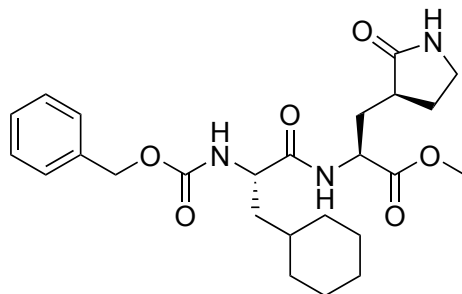
<sup>13</sup>C NMR (125 MHz, CDCl<sub>3</sub>)  $\delta$ C 179.6, 172.1, 155.9, 138.1, 136.4, 128.5, 128.1, 128.0, 66.8, 55.4, 52.4, 51.8, 40.4, 38.6, 38.4, 37.9, 32.9, 28.7, 7.1, 4.6, 4.1

OR:  $[\alpha]_{\text{D}}^{26} = 11.47$  ( $c = 0.19$ , MeOH)

HRMS: (ESI) Calcd for C<sub>22</sub>H<sub>29</sub>N<sub>3</sub>NaO<sub>6</sub> [M + Na]<sup>+</sup> 454.1948, found 454.1947

Methyl (*S*)-2-((*S*)-2-(((benzyloxy)carbonyl)amino)-3-cyclohexylpropanamido)-3-((*S*)-2-oxopyrrolidin-3-yl)propanoate

(168)



168

**168** was prepared from **66**, following the same general procedure as that of **167**, substituted with the appropriate building block and employing noncritical variations in procedure to furnish a crude product.

Purification: Flash column chromatography over silica, eluent system of pure EtOAc.

TLC:  $R_f = 0.28$ , EtOAc

Appearance: Transparent colourless oil.

Yield: 98%

IR (DCM cast film,  $\nu_{\max}$  /  $\text{cm}^{-1}$ ) 3288, 2924, 2851, 1690, 1537, 1447, 1264, 1217, 1044

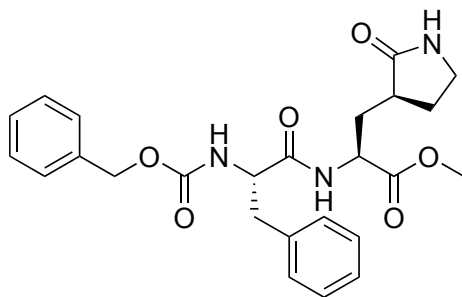
$^1\text{H}$  NMR (700 MHz,  $\text{CDCl}_3$ )  $\delta$  7.70 (1H, d,  $J = 6.2$  Hz), 7.35 (4H, d,  $J = 4.5$  Hz), 7.31 (1H, app sextet,  $J = 3.9$  Hz), 5.65 (1H, s), 5.34 (1H, d,  $J = 8.1$  Hz), 5.12 (1H, d,  $J = 12.2$  Hz), 5.09 (1H, d,  $J = 12.2$  Hz), 4.54—4.47 (1H, m), 4.33—4.26 (1H, m), 3.73 (3H, s), 3.36—3.25 (2H, m), 2.46—2.36 (2H, m), 2.19—2.10 (1H, m), 1.97—1.89 (1H, m), 1.88—1.78 (2H, m), 1.74—1.66 (4H, m), 1.66—1.60 (1H, m), 1.54—1.46 (1H, m), 1.44—1.34 (1H, m), 1.25—1.09 (3H, m), 1.02—0.86 (2H, m)

$^{13}\text{C}$  NMR (175 MHz,  $\text{CDCl}_3$ )  $\delta$  172.1, 171.1, 155.8, 136.7, 128.5, 128.1, 128.0, 66.9, 52.8, 52.4, 40.6, 40.4, 38.6, 33.9, 33.7, 32.9, 32.6, 28.8, 26.4, 26.2, 26.1, 19.9 (carbamate carbonyl not observed)

OR:  $[\alpha]_D^{26} = 0.50$  ( $c = 0.32$ , DCM)

HRMS: (ESI) Calcd for C<sub>25</sub>H<sub>35</sub>N<sub>3</sub>NaO<sub>6</sub> [M + Na]<sup>+</sup> 496.2418, found 496.2423

**Methyl (*S*)-2-((*S*)-2-(((benzyloxy)carbonyl)amino)-3-phenylpropanamido)-3-((*S*)-2-oxopyrrolidin-3-yl)propanoate**  
**(169)**



**169**

**169** was prepared from **66**, following the same general procedure as that of **167**, substituted with the appropriate building block and employing noncritical variations in procedure to furnish a crude product.

Purification: Flash column chromatography over silica, eluent system of 2/98 MeOH/EtOAc.

TLC: R<sub>f</sub> = 0.36, 5/95 MeOH/EtOAc

Appearance: White foam.

Yield: 91%

IR (DCM cast film,  $\nu_{\max}$  / cm<sup>-1</sup>) 3281, 3063, 2952, 2922, 2850, 1688.4, 1537, 1440, 1366, 1215, 1053

<sup>1</sup>H NMR (700 MHz, CDCl<sub>3</sub>)  $\delta$ H 7.64 (1H, d, *J* = 6.45 Hz), 7.35—7.31 (2H, m), 7.31—7.27 (3H, m), 7.25—7.22 (2H, m), 7.21—7.16 (3H, m), 5.91 (1H, s), 5.50 (1H, d, *J* = 9.17 Hz), 5.07 (1H, d, *J* = 12.4 Hz), 5.04 (1H, d, *J* = 12.4 Hz), 4.63—4.54 (1H, m), 4.50—4.41 (1H, m), 3.69 (3H, s), 3.30—3.21 (2H, m), 3.14—3.04 (2H, m), 2.38—2.28 (1H, m), 2.28—2.17 (1H, m), 2.13—2.04 (1H, m), 1.89—1.81 (1H, m), 1.81—1.73 (1H, m)

<sup>13</sup>C NMR (175 MHz, CDCl<sub>3</sub>)  $\delta$ C 179.7, 171.9, 171.3, 155.8, 136.4, 129.6, 128.5, 128.5, 128.1, 128.0, 126.9, 113.0, 66.9, 55.9, 52.5, 51.7, 40.5, 38.7, 38.3, 33.0, 28.5



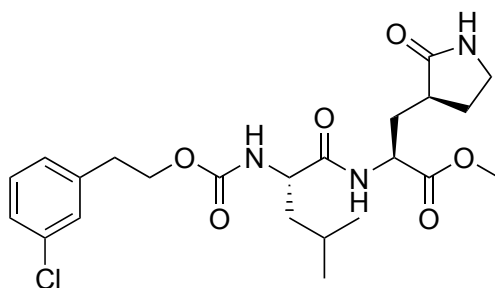
$^{13}\text{C}$  NMR (125 MHz,  $\text{CDCl}_3$ )  $\delta\text{C}$  179.8, 172.7, 172.0, 163.8, 161.8, 155.9, 130.1, 130.0, 123.2, 115.0, 114.8, 114.7, 114.5, 65.9, 53.5, 52.4, 52.0, 42.2, 40.5, 36.5, 32.8, 28.7, 24.6, 22.9, 22.0

OR:  $[\alpha]_{\text{D}}^{26} = -22.6$  ( $c = 0.12$ , DCM)

HRMS: (ESI) Calcd for  $\text{C}_{22}\text{H}_{31}\text{FN}_3\text{O}_6$   $[\text{M}^*]^+$  451.2119, found 451.2123

**Methyl (*S*)-2-((*S*)-2-(((3-chlorophenoxy)carbonyl)amino)-4-methylpentanamido)-3-((*S*)-2-oxopyrrolidin-3-yl)propanoate**

**(171)**



**171**

**171** was prepared from **66**, following the same general procedure as that of **167**, substituted with the appropriate building block and employing noncritical variations in procedure to furnish a crude product.

Purification: Flash column chromatography over silica, eluent system of pure EtOAc.

TLC:  $R_f = 0.26$ , 5/95 MeOH/EtOAc

Appearance: Clear transparent oil.

Yield: 83%

IR (DCM cast film,  $\nu_{\text{max}}$  /  $\text{cm}^{-1}$ ) 3288, 3063, 2955, 2924, 2870, 1750, 1690, 1538, 1437, 1267, 1245, 1059

$^1\text{H}$  NMR (700 MHz,  $\text{CDCl}_3$ )  $\delta\text{H}$  7.84 (1H, d,  $J = 5.9$  Hz), 7.24–7.18 (3H, m), 7.10 (1H, d,  $J = 6.9$  Hz), 5.84 (1H, s), 5.19 (1H, d,  $J = 8.6$  Hz), 4.47 (1H, ddd,  $J = 10.9, 6.6, 4.3$  Hz), 4.31–4.20 (3H, m), 3.73 (3H, s), 3.38–3.30 (2H, m), 2.90 (2H, app t,  $J = 6.7$  Hz), 2.46–2.38 (2H, m), 2.19–2.10 (1H, m), 1.96–1.90 (1H, m), 1.90–1.81 (1H, m), 1.76–1.63

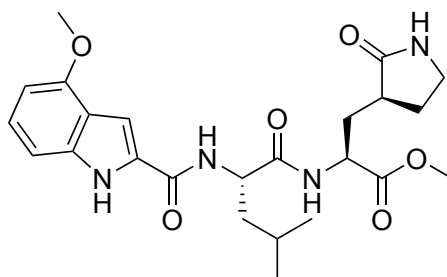
(2H, m), 1.54—1.46 (1H, m), 0.96 (6H, d,  $J = 6.2$  Hz)

$^{13}\text{C}$  NMR (175 MHz,  $\text{CDCl}_3$ )  $\delta\text{C}$  179.7, 172.8, 172.1, 140.1, 134.3, 129.8, 129.1, 127.2, 126.8, 65.1, 53.4, 52.5, 51.9, 42.3, 40.5, 28.5, 35.2, 32.9, 28.7, 24.7, 23.0, 22.0, 19.9

OR:  $[\alpha]_{\text{D}}^{26} = -13.07$  ( $c = 0.54$ , DCM)

HRMS: (ESI) Calcd for  $\text{C}_{23}\text{H}_{32}\text{ClN}_3\text{NaO}_6$   $[\text{M} + \text{Na}]^+$  504.1872, found 504.1870

**Methyl (*S*)-2-((*S*)-2-(4-methoxy-1*H*-indole-2-carboxamido)-4-methylpentanamido)-3-((*S*)-2-oxopyrrolidin-3-yl)propanoate**  
**(172)**



**172**

**172** was prepared from 7a following the same general procedure as that of **167**, substituted with the appropriate building block and employing noncritical variations in procedure to furnish a crude product.

Purification: Flash column chromatography over silica, eluent system of 5/95 MeOH/EtOAc.

TLC:  $R_f = 0.50$ , 5/95 MeOH/EtOAc

Appearance: Off-white powder.

Yield: 28%

IR (DCM cast film,  $\nu_{\text{max}} / \text{cm}^{-1}$ ) 3281, 3063, 2956, 2932, 2871, 1744, 1686, 1633, 1583, 1551, 1516, 1466, 1433, 1367, 1302, 1256, 1213, 1165, 1134, 1100, 1055

$^1\text{H}$  NMR (500 MHz,  $\text{CDCl}_3$ )  $\delta\text{H}$  9.35 (1H, s), 8.05 (1H, d,  $J = 6.5$  Hz), 7.20 (1H, t,  $J = 8$  Hz), 7.09 (1H, s), 7.01 (1H, d,  $J = 8$  Hz), 6.78 (1H, d,  $J = 8$  Hz), 6.50 (1H, d,  $J = 8$  Hz), 5.90 (1H, s), 4.81—4.77 (1H, m), 4.53—4.49 (1H, m), 3.95 (3H, s), 3.73 (3H, s), 3.30—3.25

(2H, m), 2.43—2.36 (2H, m), 2.20—2.15 (1H, m), 1.97—1.94 (1H, m), 1.85—1.77 (3H, m), 1.68—1.63 (1H, m), 1.00—0.98 (6H, m)

$^{13}\text{C}$  NMR (125 MHz,  $\text{CDCl}_3$ )  $\delta\text{C}$  179.7, 172.5, 172.1, 161.3, 154.2, 137.7, 128.9, 125.6, 118.9, 104.9, 100.6, 99.7, 65.8, 55.3, 52.4, 51.9, 51.7, 42.1, 40.4, 38.6, 38.5, 32.8, 28.6, 24.8, 22.2

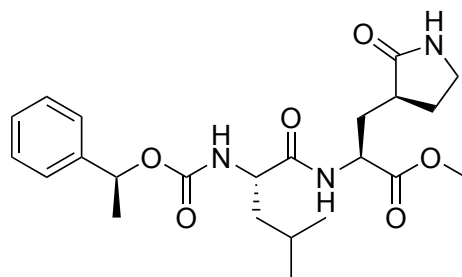
OR:  $[\alpha]_{\text{D}}^{26} = 6.70$  ( $c = 0.17$ , DCM)

HRMS: (ESI) Calcd for  $\text{C}_{24}\text{H}_{32}\text{N}_4\text{NaO}_6$   $[\text{M} + \text{Na}]^+$  495.2220, found 495.2214

## Methyl

**(*S*)-2-((*S*)-4-methyl-2-(((*S*)-1-phenylethoxy)carbonyl)amino)pentanamido)-3-((*S*)-2-oxopyrrolidin-3-yl)propanoate**

**(173)**



**173**

**173** was prepared from **66**, following the same general procedure as that of **167**, substituted with the appropriate building block and employing noncritical variations in procedure to furnish a crude product.

Purification: Flash column chromatography over silica, eluent system of 3/97 MeOH/EtOAc.

TLC:  $R_f = 0.32$ , 3/97 MeOH/EtOAc

Appearance: Clear oil.

Yield: 87%

IR (DCM cast film,  $\nu_{\text{max}}$  /  $\text{cm}^{-1}$ ) 3288, 3062, 2955, 2930, 2870, 1745, 1692, 1536, 1439, 1267, 1247, 1065

$^1\text{H}$  NMR (700 MHz,  $\text{CDCl}_3$ )  $\delta\text{H}$  7.79 (1H, d,  $J = 6.6$  Hz), 7.36—7.30 (4H, m), 7.30—7.25



(1H, m), 6.15 (1H, s), 5.76 (1H, q,  $J = 6.8$  Hz), 5.28 (1H, d,  $J = 8.5$  Hz), 4.53—4.47 (1H, m), 4.31—4.24 (1H, m), 3.73 (3H, s), 3.37—3.30 (2H, m), 2.48—2.38 (1H, m), 2.23—2.14 (1H, m), 1.94—1.88 (1H, m), 1.88—1.80 (1H, m), 1.72—1.61 (2H, m), 1.52 (3H, d,  $J = 6.8$  Hz), 1.51—1.44 (1H, m), 1.03 (1H, m), 0.92 (3H, d,  $J = 5.9$  Hz), 0.90 (3H, d,  $J = 5.9$  Hz)  
 $^{13}\text{C}$  NMR (175 MHz,  $\text{CDCl}_3$ )  $\delta$  179.8, 173.0, 172.2, 155.6, 142.1, 128.5, 127.8, 125.9, 73.2, 53.3, 52.4, 51.6, 42.3, 40.5, 38.7, 33.1, 28.5, 24.7, 22.9, 22.6, 22.1

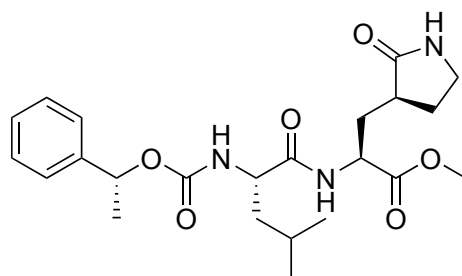
OR:  $[\alpha]_{\text{D}}^{26} = -34.28$  ( $c = 0.84$ , DCM)

HRMS: (ESI) Calcd for  $\text{C}_{23}\text{H}_{33}\text{N}_3\text{NaO}_6$   $[\text{M} + \text{Na}]^+$  470.2262, found 470.2264

### Methyl

**(*S*)-2-((*S*)-4-methyl-2-(((*R*)-1-phenylethoxy)carbonyl)amino)pentanamido)-3-((*S*)-2-oxopyrrolidin-3-yl)propanoate**

**(174)**



**174**

**174** was prepared from **66**, following the same general procedure as that of **167**, substituted with the appropriate building block and employing noncritical variations in procedure to furnish a crude product.

Purification: Flash column chromatography over silica, eluent system of 3/97 MeOH/EtOAc.

TLC:  $R_f = 0.37$ , 3/97 MeOH/EtOAc

Appearance: Clear oil.

Yield: 78%

IR (DCM cast film,  $\nu_{\text{max}}$  /  $\text{cm}^{-1}$ ) 3284, 3062, 2955, 2931, 2871, 1684, 1536, 1439, 1268, 1251,

1065

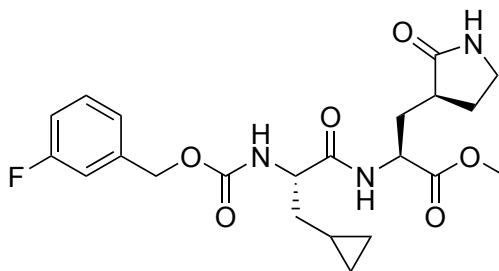
$^1\text{H}$  NMR (700 MHz,  $\text{CDCl}_3$ )  $\delta$  7.74 (1H, d,  $J = 6.6$  Hz), 7.35—7.29 (4H, m), 7.27—7.22 (1H, m), 6.10 (1H, s), 5.76 (1H, q,  $J = 6.3$  Hz), 5.33 (1H, d,  $J = 8.8$  Hz), 4.45—4.39 (1H, m), 4.33—4.27 (1H, m), 3.69 (3H, s), 3.24 (1H, t,  $J = 9.4$  Hz), 3.16 (1H, q,  $J = 9.4$  Hz), 2.35—2.24 (2H, m), 2.14 (1H, ddd,  $J = 14.1, 11.2, 5.3$  Hz), 1.88—1.81 (1H, m), 1.80—1.71 (2H, m), 1.71—1.63 (2H, m), 1.52 (3H, d,  $J = 6.8$  Hz), 0.97 (6H, d,  $J = 6.3$  Hz)

$^{13}\text{C}$  NMR (175 MHz,  $\text{CDCl}_3$ )  $\delta$  179.7, 172.8, 172.1, 155.6, 142.2, 128.4, 127.7, 125.9, 73.1, 53.2, 52.4, 51.6, 42.5, 40.4, 38.3, 32.8, 28.4, 24.7, 22.9, 22.7, 22.2

OR:  $[\alpha]_{\text{D}}^{26} = 6.55$  ( $c = 1.05$ , DCM)

HRMS: (ESI) Calcd for  $\text{C}_{23}\text{H}_{33}\text{N}_3\text{NaO}_6$   $[\text{M} + \text{Na}]^+$  470.2262, found 470.2266

**Methyl (*S*)-2-(((*S*)-3-cyclopropyl-2-(((3-fluorobenzyl)oxy)carbonyl)amino)propanamido)-3-((*S*)-2-oxopyrrolidin-3-yl)propanoate**  
(175)



**175**

**175** was prepared from **66**, following the same general procedure as that of **167**, substituted with the appropriate building block and employing noncritical variations in procedure to furnish a crude product.

Purification: Flash column chromatography over silica, eluent system of 3/97 MeOH/EtOAc.

TLC:  $R_f = 0.39$ , 5/95 MeOH/EtOAc

Appearance: Pale transparent solid.

Yield: 92%

IR (DCM cast film,  $\nu_{\max}$  /  $\text{cm}^{-1}$ ) 3290, 3078, 3001, 2952, 1684, 1619, 1529, 1538, 1490, 1259

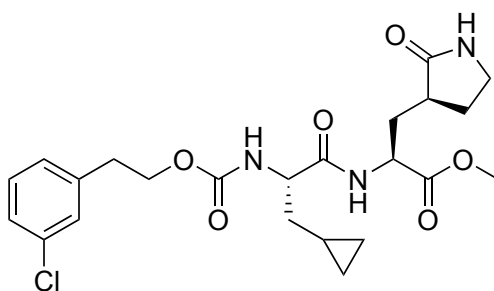
$^1\text{H}$  NMR (700 MHz,  $\text{CDCl}_3$ )  $\delta$ H 7.90 (1H, d,  $J = 6.4$  Hz), 7.31—7.26 (1H, m), 7.10 (1H, d,  $J = 7.63$  Hz), 7.06 (1H, t,  $J = 10.2$  Hz), 6.97 (1H, td,  $J = 8.5, 2.7$  Hz), 6.01 (1H, s), 5.65—5.57 (1H, m), 5.16—5.03 (2H, m), 4.52—4.44 (1H, m), 4.33 (1H, app q,  $J = 7.1$  Hz), 3.71 (3H, s), 3.35—3.27 (2H, m), 2.53—2.27 (2H, m), 2.17—2.08 (1H, m), 1.95—1.88 (1H, m), 1.88—1.80 (1H, m), 1.77—1.67 (1H, m), 1.67—1.60 (1H, m), 0.82—0.73 (1H, m), 0.51—0.41 (2H, m), 0.14—0.06 (2H, m)

$^{13}\text{C}$  NMR (175 MHz,  $\text{CDCl}_3$ )  $\delta$ C 179.8, 172.1, 163.2, 162.2, 155.7, 130.1, 123.3, 114.9, 114.7, 65.9, 55.4, 52.5, 51.9, 40.6, 38.7, 38.0, 33.0, 32.0, 28.7, 7.1, 4.6, 4.2

OR:  $[\alpha]_{\text{D}}^{26} = -4.04$  ( $c = 0.55$ , DCM)

HRMS: (ESI) Calcd for  $\text{C}_{22}\text{H}_{28}\text{FN}_3\text{NaO}_6$   $[\text{M} + \text{Na}]^+$  472.1854, found 472.1853

**Methyl (*S*)-2-((*S*)-2-(((3-chlorophenoxy)carbonyl)amino)-3-cyclopropylpropanamido)-3-((*S*)-2-oxopyrrolidin-3-yl)propanoate (176)**



**176**

**176** was prepared from **66**, following the same general procedure as that of **167**, substituted with the appropriate building block and employing noncritical variations in procedure to furnish a crude product.

Purification: Flash column chromatography over silica, eluent system of 3/97 MeOH/EtOAc.

TLC:  $R_f = 0.39$ , 5/95 MeOH/EtOAc

Appearance: Pale semi-solid.

Yield: 91%

IR (DCM cast film,  $\nu_{\max}$  /  $\text{cm}^{-1}$ ) 3291, 3076, 3000, 2953, 2925, 1687, 1599, 1538, 1476, 1460, 1269, 1247

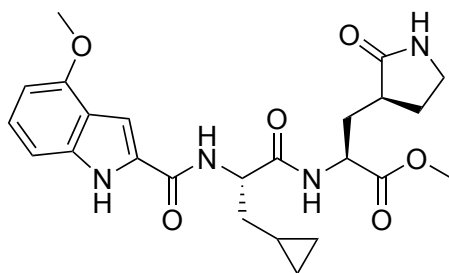
$^1\text{H}$  NMR (700 MHz,  $\text{CDCl}_3$ )  $\delta$ H 7.81 (1H, d,  $J = 6.2$  Hz), 7.24—7.18 (3H, m), 7.12—7.08 (1H, m), 5.75 (1H, d,  $J = 16.0$  Hz), 5.43 (1H, d,  $J = 9.5$  Hz), 4.53—4.47 (1H, m), 4.33—4.21 (3H, m), 3.73 (3H, s), 3.38—3.31 (2H, m), 2.91 (2H, t,  $J = 6.8$  Hz), 2.55—2.29 (2H, m), 2.18—2.10 (1H, m), 1.97—1.91 (1H, m), 1.91—1.83 (1H, m), 1.75—1.67 (1H, m), 1.67—1.56 (1H, m), 0.82—0.73 (1H, m), 0.52—0.43 (2H, m), 0.16—0.06 (2H, m)

$^{13}\text{C}$  NMR (175 MHz,  $\text{CDCl}_3$ )  $\delta$ C 179.7, 172.2, 165.3, 140.1, 134.2, 129.8, 129.1, 127.2, 126.8, 66.3, 65.1, 55.4, 52.5, 40.5, 38.6, 35.2, 33.0, 32.1, 28.8, 19.7, 7.1, 4.6, 4.2

OR:  $[\alpha]_{\text{D}}^{26} = 6.15$  ( $c = 0.13$ , DCM)

HRMS: (ESI) Calcd for  $\text{C}_{23}\text{H}_{30}\text{ClN}_3\text{NaO}_6$   $[\text{M} + \text{Na}]^+$  502.1715, found 502.1712

**Methyl (*S*)-2-((*S*)-3-cyclopropyl-2-(4-methoxy-1*H*-indole-2-carboxamido)propanamido)-3-((*S*)-2-oxopyrrolidin-3-yl)propanoate**  
(177)



**177**

**177** was prepared from 7b following the same general procedure as that of **167**, substituted with the appropriate building block and employing noncritical variations in procedure to furnish a crude product.

Purification: Flash column chromatography over silica, eluent system of 5/95 MeOH/EtOAc.

TLC:  $R_f$  0.45, 5/95 MeOH/EtOAc

Appearance: Off-white powder.

Yield: 31%

IR (DCM cast film,  $\nu_{\max}$  /  $\text{cm}^{-1}$ ) 3271, 3077, 3002, 2953, 2932, 1745, 1687, 1632, 1582, 1550, 1460, 1432, 1369, 1303, 1256, 1215, 1132, 1101

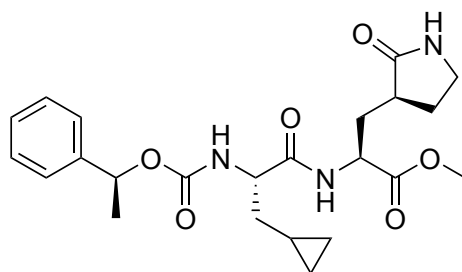
$^1\text{H}$  NMR (500 MHz,  $\text{CDCl}_3$ )  $\delta$  9.65 (1H, s), 8.14 (1H, s), 7.19 (1H, t,  $J = 8$  Hz), 7.10 (2H, m), 7.03 (d,  $J=8.5\text{Hz}$ ), 6.49 (1H, d,  $J = 8$  Hz), 6.02 (1H, s), 4.92—4.88 (1H, m), 4.59—4.55 (1H, m), 3.95 (3H, s), 3.74 (3H, s), 3.29—3.27 (2H, m), 2.50—2.45 (1H, m), 2.41—2.36 (1H, m), 2.22—2.17 (1H, m), 1.96—1.89 (1H, m), 1.84—1.78 (3H, m), 0.86—0.82 (1H, m), 0.50—0.46 (2H, m), 0.16—0.12 (2H, m)

$^{13}\text{C}$  NMR (125 MHz,  $\text{CDCl}_3$ )  $\delta$  179.9, 179.8, 172.2, 172.0, 161.2, 154.2, 137.9, 129.1, 125.5, 118.9, 105.1, 100.7, 99.6, 55.3, 53.5, 52.5, 51.8, 40.6, 38.6, 38.2, 37.8, 33.0, 28.6, 7.0, 4.6, 4.1

OR:  $[\alpha]_{\text{D}}^{26} = 6.17$  ( $c = 0.24$ , DCM)

HRMS: (ESI) Calcd for  $\text{C}_{24}\text{H}_{30}\text{N}_4\text{NaO}_6$   $[\text{M} + \text{Na}]^+$  493.2058, found 493.2051

**Methyl (*S*)-2-(((*S*)-3-cyclopropyl-2-(((*S*)-1-phenylethoxy)carbonyl)amino)propanamido)-3-((*S*)-2-oxopyrrolidin-3-yl)propanoate**  
(178)



**178**

**178** was prepared from **66**, following the same general procedure as that of **167**, substituted with the appropriate building block and employing noncritical variations in procedure

to furnish a crude product.

Purification: Flash column chromatography over silica, eluent system of 5/95 MeOH/EtOAc.

TLC:  $R_f$  0.41, 5/95 MeOH/EtOAc

Appearance: White powder.

Yield: 81%

IR (DCM cast film,  $\nu_{\max}$  /  $\text{cm}^{-1}$ ) 3290, 3064, 3035, 2981, 2952, 2933, 1746, 1690, 1537, 1440, 1377, 1269, 1253, 1210, 1177, 1129, 1066, 1030

$^1\text{H}$  NMR (500 MHz,  $\text{CDCl}_3$ )  $\delta$  7.73—7.68 (1H, m), 7.36—7.31 (5H, m), 5.80—5.76 (1H, m), 5.54 (1H, s), 5.45—5.39 (1H, m), 4.55—4.49 (1H, m), 4.28—4.25 (m, 1H), 3.73 (s, 3H), 3.37—3.33 (2H, m), 2.44—2.38 (2H, m), 2.15—2.08 (1H, m), 1.96—1.88 (2H, m), 1.71—1.68 (1H, m), 1.59—1.50 (3H, m), 0.76—0.70 (1H, m), 0.47—0.42 (1H, m), 0.09 (s, 2H)

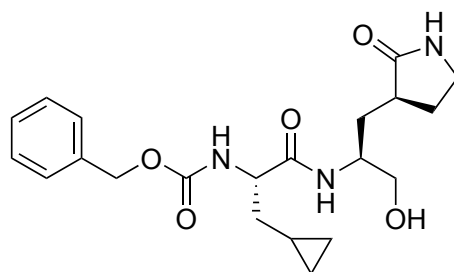
$^{13}\text{C}$  NMR (125 MHz,  $\text{CDCl}_3$ )  $\delta$  179.6, 172.2, 172.0, 155.4, 142.1, 128.4, 127.7, 125.9, 73.1, 65.8, 55.2, 52.4, 51.8, 51.0, 40.5, 40.4, 38.6, 38.4, 38.1, 38.8, 33.0, 28.2, 7.1, 4.6, 4.1

OR:  $[\alpha]_{\text{D}}^{26} = -27.38$  ( $c = 0.15$ , DCM)

HRMS: (ESI) Calcd for  $\text{C}_{23}\text{H}_{31}\text{N}_3\text{NaO}_6$   $[\text{M} + \text{Na}]^+$  468.2105, found 468.2107

**Benzyl ((*S*)-3-cyclopropyl-1-(((*S*)-1-hydroxy-3-((*S*)-2-oxopyrrolidin-3-yl)propan-2-yl)amino)-1-oxopropan-2-yl)carbamate**

(179)



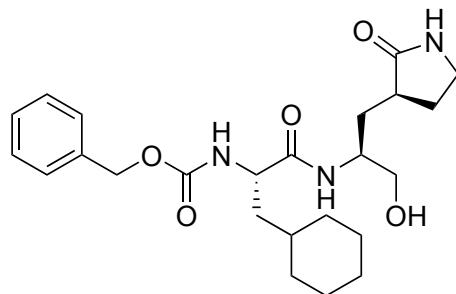
**179**

**167** (0.222 g, 0.514 mmol, 1.0 equiv) was dissolved in 3.4 mL of freshly distilled THF under an argon atmosphere. To the solution was added  $\text{LiBH}_4$  (2.0 M in THF, 0.772 mL,

1.543 mmol, 3.0 equiv) dropwise over a period of 5 min at room temperature. The reaction mixture was allowed to stir for an additional 5 min. Next, 1.7 mL of dry MeOH was added dropwise, and gas evolution was observed. The reaction mixture was then allowed to react at room temperature for 1.5 h. Afterwards, the mixture was quenched with 1 M HCl until a pH of 1-2 was reached. Concentration by rotary evaporation then yields a white residue. This residue was then dissolved in EtOAc and brine with sonication, then separated. The EtOAc layer was then dried over Na<sub>2</sub>SO<sub>4</sub> and concentrated to furnish a crude white solid. The crude material was then purified by flash column chromatography over silica using an eluent system of 10/90 MeOH/EtOAc. Product elution was monitored by TLC and KMnO<sub>4</sub> staining ( $R_f = 0.26$ , 10/90 MeOH/EtOAc). Concentration of product fractions then furnishes a white solid (0.173 g, 0.429 mmol, 83%). IR (DCM cast film,  $\nu_{\max}$  / cm<sup>-1</sup>) 3282, 3078, 3000, 2927, 2883, 1684, 1539, 1456, 1442, 1381, 1261, 1178, 1128, 1047 <sup>1</sup>H NMR (500 MHz, CDCl<sub>3</sub>)  $\delta$ H 7.80 (1H, s), 7.36—7.31 (5H, m), 5.80 (s, 1H), 5.58 (1H, d,  $J = 8.0$  Hz), 5.11 (2H, s), 4.30—4.24 (1H, m), 4.02—3.96 (1H, m), 3.63—3.57 (2H, m), 3.33 (2H, d,  $J = 9.0$  Hz), 2.45—2.38 (2H, m), 1.96—1.90 (1H, m), 1.85-1.80 (1H, m), 1.69—1.66 (3H, m), 0.73—0.68 (1H, m), 0.47 (2H, d,  $J = 7.5$  Hz), 0.12 (2H, d,  $J = 4.5$  Hz) <sup>13</sup>C NMR (125 MHz, CDCl<sub>3</sub>)  $\delta$ C 180.9, 173.0, 156.0, 136.4, 128.5, 128.1, 128.0, 66.9, 66.1, 55.8, 51.7, 40.6, 38.4, 37.8, 31.9, 29.7, 29.0, 7.2, 4.4, 4.3  
OR:  $[\alpha]_D^{26} = -14.24$  ( $c = 0.132$ , DCM)  
HRMS: (ESI) Calcd for C<sub>21</sub>H<sub>29</sub>N<sub>3</sub>NaO<sub>5</sub> [M + Na]<sup>+</sup> 426.1999, found 426.1999

**Benzyl ((*S*)-3-cyclohexyl-1-(((*S*)-1-hydroxy-3-((*S*)-2-oxopyrrolidin-3-yl)propan-2-yl)amino)-1-oxopropan-2-yl)carbamate**

**(180)**



**180**

**180** was prepared from **168** following the same general procedure as that of **179**, employing noncritical variations in procedure to furnish a crude product.

Purification: No purification required.

TLC:  $R_f = 0.11$ , 5/95 MeOH/EtOAc

Appearance: White solid.

Yield: 82%

IR (DCM cast film,  $\nu_{\max}$  /  $\text{cm}^{-1}$ ) 3278, 3091, 3064, 2923, 2851, 1686, 1538, 1448, 1261, 1045

$^1\text{H}$  NMR (700 MHz,  $\text{CDCl}_3$ )  $\delta$  7.70 (1H, s), 7.38—7.25 (5H, m), 5.98 (1H, s), 5.39 (1H, s), 5.10 (2H, app q,  $J = 12.8$  Hz), 4.26 (1H, dd,  $J = 13.6, 8.2$  Hz), 4.05—3.90 (1H, m), 3.70—3.50 (2H, m), 3.34—3.20 (2H, m), 2.49—2.30 (2H, m), 2.05—1.93 (1H, m), 1.86—1.74 (2H, m), 1.74—1.55 (6H, m), 1.54—1.44 (1H, m), 1.54—1.45 (1H, m), 1.40—1.27 (1H, m), 1.26—1.07 (3H, m), 0.99—0.83 (2H, m)

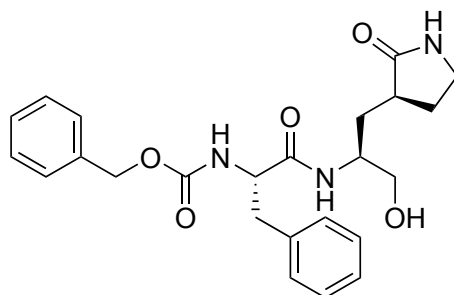
$^{13}\text{C}$  NMR (175 MHz,  $\text{CDCl}_3$ )  $\delta$  181.0, 173.8, 156.2, 136.5, 128.6, 128.5, 128.2, 128.0, 95.0, 67.0, 66.1, 53.3, 51.4, 40.5, 28.7, 34.2, 33.7, 32.6, 31.9, 29.0, 26.4, 26.3, 26.2, 26.1 OR:  $[\alpha]_{\text{D}}^{26} = -9.83$  ( $c = 0.36$ , DCM)

HRMS: (ESI) Calcd for  $\text{C}_{24}\text{H}_{36}\text{N}_3\text{O}_5$   $[\text{M} + \text{H}]^+$  446.2649, found 446.2656



**Benzyl ((*S*)-1-(((*S*)-1-hydroxy-3-((*S*)-2-oxopyrrolidin-3-yl)propan-2-yl)amino)-1-oxo-3-phenylpropan-2-yl)carbamate**

**(181)**



**181**

**181** was prepared from **169** following the same general procedure as that of **179**, employing noncritical variations in procedure to furnish a crude product.

Purification: No purification required.

TLC:  $R_f = 0.26$ , 10/90 MeOH/EtOAc

Appearance: White foam.

Yield: 86%

IR (DCM cast film,  $\nu_{\max}$  /  $\text{cm}^{-1}$ ) 3287, 3063, 2926, 1681, 1539, 1497, 1454, 1294, 1263, 1052

$^1\text{H}$  NMR (700 MHz,  $\text{CDCl}_3$ )  $\delta$  7.48 (1H, d,  $J = 5.3$  Hz), 7.36—7.29 (4H, m), 7.29—7.24 (2H, m), 7.24—7.16 (4H, m), 5.99 (1H, s), 5.62 (1H, d,  $J = 6.9$  Hz), 5.12—5.03 (2H, m), 4.51 (1H, q,  $J = 7.1$  Hz), 3.92—3.85 (1H, m), 1.68—3.39 (2H, m), 3.30 (3.19 (2H, m), 3.16—3.09 (1H, m), 3.09—2.98 (1H, m), 2.34—2.26 (1H, m), 2.24—2.16 (1H, m), 1.89—1.82 (1H, m), 1.78—1.70 (1H, m), 1.55—1.47 (1H, m), 1.29—1.22 (1H, m)

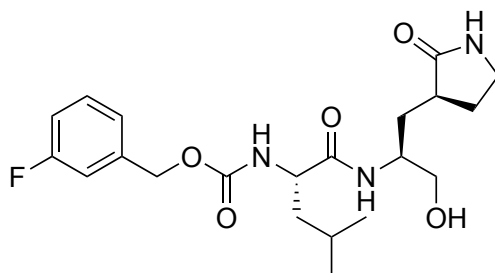
$^{13}\text{C}$  NMR (175 MHz,  $\text{CDCl}_3$ )  $\delta$  180.9, 171.9, 155.9, 136.6, 129.5, 128.6, 128.5, 128.4, 128.2, 128.0, 127.0, 67.0, 65.1, 56.4, 51.5, 40.6, 39.0, 38.3, 31.7, 28.9

OR:  $[\alpha]_{\text{D}}^{26} = -2.87$  ( $c = 1.03$ , DCM)

HRMS: (ESI) Calcd for  $\text{C}_{24}\text{H}_{29}\text{N}_3\text{NaO}_5$   $[\text{M} + \text{Na}]^+$  462.1999, found 462.1996

**3-Fluorobenzyl ((*S*)-1-(((*S*)-1-hydroxy-3-((*S*)-2-oxopyrrolidin-3-yl)propan-2-yl)amino)-4-methyl-1-oxopentan-2-yl)carbamate**

**(182)**



**182**

**182** was prepared from **170** following the same general procedure as that of **7a**, employing noncritical variations in procedure to furnish a crude product.

Purification: Flash column chromatography over silica, eluent system of 10/90 MeOH/EtOAc.

TLC:  $R_f = 0.25$ , 10/90 MeOH/EtOAc

Appearance: White foam.

Yield: 67%

IR (DCM cast film,  $\nu_{\max}$  /  $\text{cm}^{-1}$ ) 3281, 3068, 2956, 2872, 1686, 1592, 1536, 1490, 1450, 1259, 1050

$^1\text{H}$  NMR (700 MHz,  $\text{CDCl}_3$ )  $\delta$  7.92 (1H, d,  $J = 5.5$  Hz), 7.30 (1H, td,  $J = 7.8, 6.0$  Hz), 7.10 (1H, d,  $J = 7.8$  Hz), 7.07 (1H, d,  $J = 9.3$  Hz), 6.99 (1H, td,  $J = 8.3, 2.4$  Hz), 5.86 (1H, s), 5.41 (1H, d,  $J = 8.0$  Hz), 5.09 (2H, app q,  $J = 13.2$  Hz), 4.26—4.20 (1H, m), 4.00—3.92 (1H, m), 3.67—3.61 (1H, m), 3.60—3.55 (1H, m), 3.45 (1H, t,  $J = 6.1$  Hz), 3.36—3.30 (2H, m), 2.49—2.41 (1H, m), 2.41—2.34 (1H, m), 1.95 (1H, ddd,  $J = 14.5, 10.8, 6.9$  Hz), 1.84 (1H, ddd,  $J = 20.0, 12.5, 9.6$  Hz), 1.73—1.64 (3H, m), 1.52 (1H, ddd,  $J = 12.8, 9.2, 4.8$  Hz), 0.98—0.92 (6H, m)

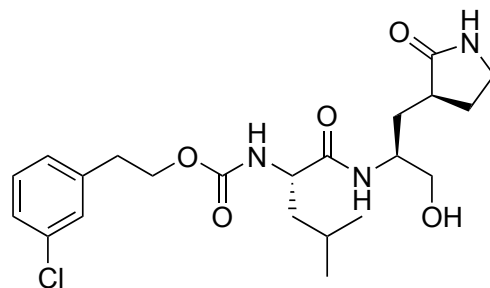
$^{13}\text{C}$  NMR (175 MHz,  $\text{CDCl}_3$ )  $\delta$  181.0, 173.8, 162.2, 156.0, 130.1, 123.2, 115.0, 114.9, 114.7, 114.6, 66.3, 54.0, 51.9, 42.3, 40.7, 38.6, 31.9, 29.1, 24.9, 23.0, 22.0

OR:  $[\alpha]_D^{26} = -29.33$  ( $c = 0.30$ , DCM)

HRMS: (ESI) Calcd for  $C_{21}H_{30}FN_3NaO_5$   $[M + Na]^+$  446.2062, found 446.2059

**3-Chlorophenethyl ((*S*)-1-(((*S*)-1-hydroxy-3-((*S*)-2-oxopyrrolidin-3-yl)propan-2-yl)amino)-4-methyl-1-oxopentan-2-yl)carbamate**

**(183)**



**183**

**183** was prepared from **171** following the same general procedure as that of **179**, employing noncritical variations in procedure to furnish a crude product.

Purification: Flash column chromatography over silica, eluent system of 5/95 MeOH/EtOAc.

TLC:  $R_f$  0.17, 5/95 MeOH/EtOAc.

Appearance: White powder.

Yield: 95%

IR (DCM cast film,  $\nu_{\max}$  /  $\text{cm}^{-1}$ ) 3286, 3066, 2956, 2927, 2871, 1689, 1599, 1540, 1469, 1438, 1387, 1368, 1342, 1264, 1172, 1122, 1056

$^1\text{H}$  NMR (500 MHz,  $\text{CDCl}_3$ )  $\delta$ H 7.86 (1H, s), 7.22—7.17 (3H, m), 7.09 (1H, d,  $J = 7$  Hz), 5.92 (1H, s), 5.28 (1H, d,  $J = 7.5$  Hz), 4.25 (2H, t,  $J = 7$  Hz), 4.23—4.18 (1H, m), 3.99—3.94 (1H, m), 3.70 (1H, d,  $J = 7$  Hz), 3.60 (2H, d,  $J = 7$  Hz), 3.35 (2H, d,  $J = 9.5$  Hz), 2.90 (2H, t,  $J = 7$  Hz), 2.43—2.47 (2H, m), 2.00—1.95 (1H, m), 1.87—1.83 (2H, m), 1.66—1.61 (2H, m), 1.53—1.48 (1H, m), 0.94 (6H, s)

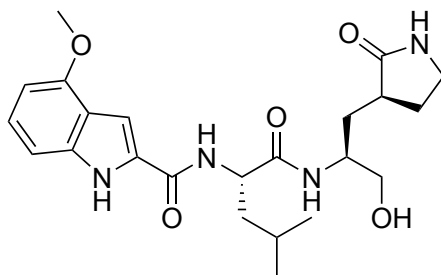
$^{13}\text{C}$  NMR (125 MHz,  $\text{CDCl}_3$ )  $\delta$ C 180.9, 173.8, 156.1, 140.0, 134.2, 129.7, 129.1, 127.1, 126.7, 66.1, 65.1, 64.3, 53.7, 51.7, 42.2, 41.9, 40.6, 38.5, 35.1, 31.9, 29.0, 28.1, 24.8, 23.0, 21.9

OR:  $[\alpha]_D^{26} = -24.88$  ( $c = 0.18$ , DCM)

HRMS: (ESI) Calcd for  $C_{22}H_{32}N_3NaO_5$   $[M + Na]^+$  476.1923, found 476.1923

*N*-((*S*)-1-(((*S*)-1-Hydroxy-3-((*S*)-2-oxopyrrolidin-3-yl)propan-2-yl)amino)-4-methyl-1-oxopentan-2-yl)-4-methoxy-1*H*-indole-2-carboxamide

(184)



**184**

**184** was prepared from **172** following the same general procedure as that of **179**, employing noncritical variations in procedure to furnish a crude product.

Purification: Flash column chromatography over silica, eluent system of 5/95 MeOH/EtOAc.

TLC:  $R_f$  0.19, 5/95 MeOH/EtOAc

Appearance: Off-white powder.

Yield: 77%

IR (DCM cast film,  $\nu_{\max}$  /  $\text{cm}^{-1}$ ) 3276, 2955, 2931, 2870, 1669, 1614, 1537, 1515, 1368, 1256, 1101

$^1\text{H}$  NMR (700 MHz,  $\text{CDCl}_3$ )  $\delta$  9.16 (1H, m), 8.05 (1H, d,  $J = 6.4$  Hz), 7.19 (1H, td,  $J = 8.1, 2.8$  Hz), 7.32 (1H, d,  $J = 7.4$  Hz), 7.14—7.10 (1H, m), 7.00 (1H, dd,  $J = 8.3, 2.9$  Hz), 6.71—6.62 (1H, m), 6.51—6.48 (1H, m), 5.62—5.55 (1H, m), 4.72—4.64 (1H, m), 4.01—3.95 (1H, m), 3.93 (3H, s), 3.74—3.58 (2H, m), 3.34—3.27 (2H, m), 2.56—2.42 (1H, m), 2.40—2.25 (1H, m), 1.97—1.86 (2H, m), 1.84—1.76 (1H, m), 1.76—1.66 (2H, m), 1.66—1.60 (1H, m), 0.97 (6H, app dt,  $J = 8.7, 6.2$  Hz)

$^{13}\text{C}$  NMR (175 MHz,  $\text{CDCl}_3$ )  $\delta$  172.0, 171.3, 165.7, 155.9, 136.6, 128.3, 128.0, 125.6, 105.1,

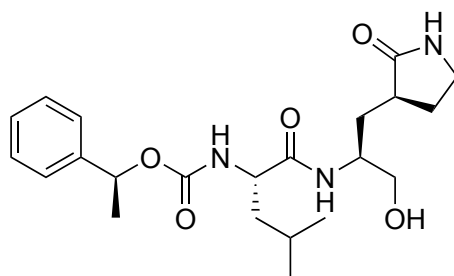
101.2, 99.7, 66.9, 60.3, 55.5, 40.6, 38.7, 33.6, 31.5, 31.0, 23.2, 22.2, 21.1, 14.3

OR:  $[\alpha]_D^{26} = 1364.56$  ( $c = 0.14$ , DCM)

HRMS: (ESI) Calcd for  $C_{23}H_{32}N_4NaO_5$   $[M + Na]^+$  467.2265, found 467.2265

**(*S*)-1-Phenylethyl ((*S*)-1-(((*S*)-1-hydroxy-3-((*S*)-2-oxopyrrolidin-3-yl)propan-2-yl)amino)-4-methyl-1-oxopentan-2-yl)carbamate**

**(185)**



**185**

**185** was prepared from **173** following the same general procedure as that of **179**, employing noncritical variations in procedure to furnish a crude product.

Purification: Flash column chromatography over silica, eluent system of 10/90 MeOH/EtOAc.

TLC:  $R_f = 0.29$ , 10/90 MeOH/EtOAc

Appearance: White foam.

Yield: 76%

IR (DCM cast film,  $\nu_{\max}$  /  $\text{cm}^{-1}$ ) 3248, 2955, 2930, 2780, 1689, 1237, 1448, 1285, 1262, 1066, 1032

$^1\text{H}$  NMR (700 MHz,  $\text{CDCl}_3$ )  $\delta$  7.72 (1H, d,  $J = 6.3$  Hz), 7.36—7.29 (4H, m), 7.29—7.25 (1H, m), 6.14 (1H, s), 5.75 (1H, app q,  $J = 6.5$  Hz), 5.35 (1H, d,  $J = 8.0$  Hz), 4.21—4.15 (1H, m), 4.04—3.96 (1H, m), 3.68—3.62 (1H, m), 3.62—3.56 (1H, m), 3.52 (1H, s), 3.36—3.30 (2H, m), 2.50—2.43 (1H, m), 2.43—2.36 (1H, m), 2.04—1.96 (1H, m), 1.87—1.79 (1H, m), 1.76 (1H, s), 1.69—1.57 (3H, m), 1.52 (3H, d,  $J = 6.6$  Hz), 1.51—1.44

(1H, m), 0.89 (6H, dd,  $J = 15.4, 5.7$  Hz)

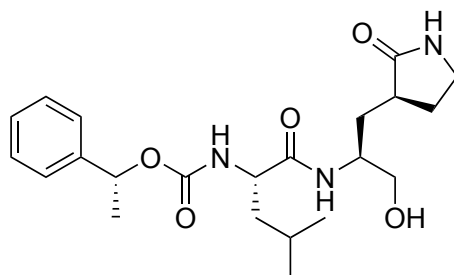
$^{13}\text{C}$  NMR (700 MHz,  $\text{CDCl}_3$ )  $\delta\text{C}$  181.0, 173.8, 155.8, 142.0, 128.5, 127.8, 125.9, 73.3, 66.1, 53.8, 51.3, 42.2, 40.6, 38.4, 32.0, 28.9, 24.8, 23.0, 22.6, 22.0

OR:  $[\alpha]_{\text{D}}^{26} = -34.33$  ( $c = 1.02$ , DCM)

HRMS: (ESI) Calcd for  $\text{C}_{22}\text{H}_{33}\text{N}_3\text{NaO}_5$   $[\text{M} + \text{Na}]^+$  442.2312, found 442.2309

**(*R*)-1-Phenylethyl ((*S*)-1-(((*S*)-1-hydroxy-3-((*S*)-2-oxopyrrolidin-3-yl)propan-2-yl)amino)-4-methyl-1-oxopentan-2-yl)carbamate**

**(186)**



**186**

**186** was prepared from **174** following the same general procedure as that of **179**, employing noncritical variations in procedure to furnish a crude product.

Purification: Flash column chromatography over silica, eluent system of 10/90 MeOH/EtOAc.

TLC:  $R_f = 0.32$ , 10/90 MeOH/EtOAc

Appearance: White foam.

Yield: 78%

IR (DCM cast film,  $\nu_{\text{max}}$  /  $\text{cm}^{-1}$ ) 3284, 3063, 3956, 3927, 2871, 1685, 1539, 1448, 1264, 1066

$^1\text{H}$  NMR (700 MHz,  $\text{CDCl}_3$ )  $\delta\text{H}$  7.72 (1H, d,  $J = 6.5$  Hz), 7.37–7.29 (4H, m), 7.29–7.25 (1H, m), 6.14 (1H, s), 5.75 (1H, app q,  $J = 5.8$  Hz), 5.35 (1H, d,  $J = 7.6$  Hz), 4.21–4.15 (1H, m), 4.04–3.96 (1H, m), 3.68–3.62 (1H, m), 3.62–3.56 (1H, m), 3.55–3.49 (1H, m), 3.36–3.29 (2H, m), 2.50–2.43 (1H, m), 2.43–2.36 (1H, m), 2.04–1.96 (1H, m),

1.87—1.79 (1H, m), 1.76 (1H, s), 1.69—1.58 (2H, m), 1.52 (3H, d,  $J = 6.7$  Hz), 1.50—1.44 (1H, m), 0.89 (6H, dd,  $J = 14.9, 5.3$  Hz)

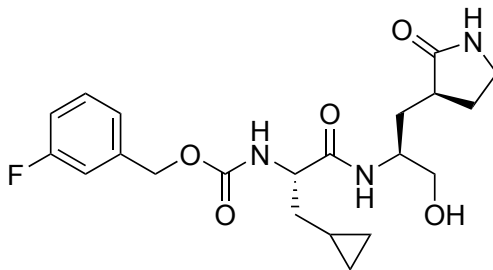
$^{13}\text{C}$  NMR (175 MHz,  $\text{CDCl}_3$ )  $\delta\text{C}$  180.7, 173.6, 155.7, 128.5, 127.7, 125.9, 112.9, 73.2, 66.1, 53.8, 51.3, 42.2, 40.5, 38.2, 31.9, 28.8, 24.9, 23.0, 22.7, 22.0

OR:  $[\alpha]_{\text{D}}^{26} = 6.49$  ( $c = 0.61$ , DCM)

HRMS: (ESI) Calcd for  $\text{C}_{22}\text{H}_{33}\text{N}_3\text{NaO}_5$   $[\text{M} + \text{Na}]^+$  442.2312, found 442.2311

**3-Fluorobenzyl ((*S*)-3-cyclopropyl-1-(((*S*)-1-hydroxy-3-((*S*)-2-oxopyrrolidin-3-yl)propan-2-yl)amino)-1-oxopropan-2-yl)carbamate**

**(187)**



**187**

**187** was prepared from **175** following the same general procedure as that of **179**, employing noncritical variations in procedure to furnish a crude product.

Purification: Flash column chromatography over silica, eluent system of 10/90 MeOH/EtOAc.

TLC:  $R_f = 0.26$ , 10/90 MeOH/EtOAc

Appearance: Transparent foamy solid.

Yield: 84%

IR (DCM cast film,  $\nu_{\text{max}}$  /  $\text{cm}^{-1}$ ) 3280, 3079, 2948, 2878, 1683, 1540, 1490, 1450, 1259, 1049

$^1\text{H}$  NMR (700 MHz,  $\text{CDCl}_3$ )  $\delta\text{H}$  7.92 (1H, d,  $J = 6.3$  Hz), 7.31 (1H, td,  $J = 7.9, 6.1$  Hz), 7.13—7.10 (1H, m), 7.08 (1H, d,  $J = 9.2$  Hz), 6.99 (1H, dd,  $J = 8.6, 2.0$  Hz), 5.96—5.86 (1H, m), 5.70—5.58 (1H, m), 5.14—5.04 (2H, m), 4.31—4.20 (1H, m), 4.10—3.95 (1H,

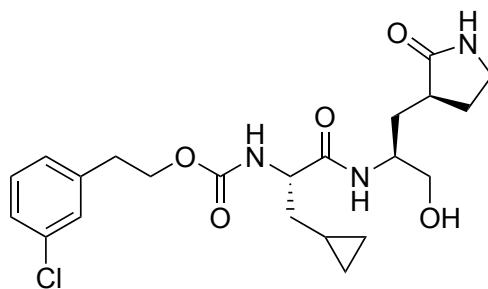
m), 3.67—3.61 (1H, m), 3.61—3.55 (1H, m), 3.37—3.28 (2H, m), 2.57—2.42 (1H, m), 2.42—2.27 (1H, m), 1.97 (1H, ddd,  $J = 14.4, 11.1, 6.8$  Hz), 1.94—1.80 (2H, m), 1.70—1.60 (3H, m), 0.76—0.67 (1H, m), 0.50—0.44 (2H, m), 0.14—0.07 (2H, m)

$^{13}\text{C}$  NMR (175 MHz,  $\text{CDCl}_3$ )  $\delta\text{C}$  181.0, 173.0, 163.6, 162.2, 155.8, 130.1, 123.3, 114.9, 112.9, 66.1, 55.8, 51.8, 40.7, 38.6, 37.9, 32.0, 29.1, 19.8, 7.2, 4.5, 4.3

OR:  $[\alpha]_{\text{D}}^{26} = -4.42$  ( $c = 0.33$ , DCM)

HRMS: (ESI) Calcd for  $\text{C}_{21}\text{H}_{28}\text{FN}_3\text{NaO}_5$   $[\text{M} + \text{Na}]^+$  444.1905, found 444.1898

**3-Chlorophenethyl ((*S*)-3-cyclopropyl-1-(((*S*)-1-hydroxy-3-((*S*)-2-oxopyrrolidin-3-yl)propan-2-yl)amino)-1-oxopropan-2-yl)carbamate (188)**



**188**

**188** was prepared from **176** following the same general procedure as that of **179**, employing noncritical variations in procedure to furnish a crude product.

Purification: Flash column chromatography over silica, eluent system of 10/90 MeOH/EtOAc.

TLC:  $R_f = 0.29$ , 10/90 MeOH/EtOAc

Appearance: Translucent semi-solid.

Yield: 81%

IR (DCM cast film,  $\nu_{\text{max}}$  /  $\text{cm}^{-1}$ ) 3286, 3078, 3002, 2923, 2878, 1688, 1538, 1439, 1264, 1175, 1069

$^1\text{H}$  NMR (700 MHz,  $\text{CDCl}_3$ )  $\delta\text{H}$  7.86 (1H, d,  $J = 5.7$  Hz), 7.24—7.18 (3H, m), 7.11—7.08

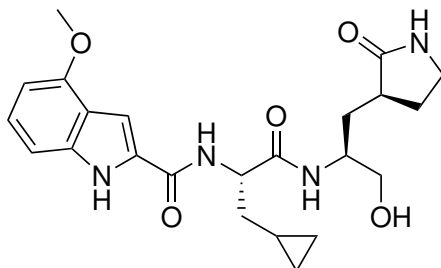


(1H, m), 5.99—5.85 (1H, m), 5.56—5.43 (1H, m), 4.32—4.22 (3H, m), 4.02—3.96 (1H, m), 3.68—3.62 (1H, m), 3.62—3.55 (1H, m), 3.37—3.30 (2H, m), 2.90 (2H, t,  $J = 7.0$  Hz), 2.56—2.42 (1H, m), 2.42—2.28 (1H, m), 2.02—1.95 (1H, m), 1.96—1.81 (2H, m), 1.70—1.60 (3H, m), 0.73—0.64 (1H, m), 0.47 (2H, d,  $J = 7.4$  Hz), 0.13—0.08 (2H, m)  
 $^{13}\text{C}$  NMR (175 MHz,  $\text{CDCl}_3$ )  $\delta\text{C}$  181.0, 173.1, 140.1, 134.2, 129.8, 129.1, 127.2, 126.8, 66.1, 65.2, 60.4, 55.7, 51.7, 40.7, 37.9, 35.2, 32.0, 29.1, 21.1, 14.2, 7.2, 4.5

OR:  $[\alpha]_{\text{D}}^{26} = -11.93$  ( $c = 0.95$ , DCM)

HRMS: (ESI) Calcd for  $\text{C}_{22}\text{H}_{30}\text{ClN}_3\text{NaO}_5$   $[\text{M} + \text{Na}]^+$  474.1766, found 474.1766

***N*-((*S*)-3-Cyclopropyl-1-(((*S*)-1-hydroxy-3-((*S*)-2-oxopyrrolidin-3-yl)propan-2-yl)amino)-1-oxopropan-2-yl)-4-methoxy-1*H*-indole-2-carboxamide**  
**(189)**



**189**

**189** was prepared from **177** following the same general procedure as that of **179**, employing noncritical variations in procedure to furnish a crude product.

Purification: Flash column chromatography over silica, eluent system of 5/95 MeOH/EtOAc.

TLC:  $R_f = 0.18$ , 5/95 MeOH/EtOAc

Appearance: White powder.

Yield: 95%

IR (DCM cast film,  $\nu_{\text{max}} / \text{cm}^{-1}$ ) 3285, 3080, 3001, 2937, 2884, 2842, 1670, 1633, 1583, 1549, 1516, 1462, 1429, 1362, 1303, 1257, 1164, 1101

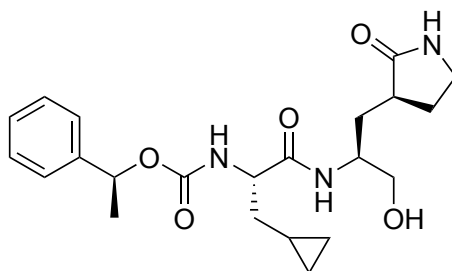
$^1\text{H}$  NMR (500 MHz,  $\text{CDCl}_3$ )  $\delta\text{H}$  9.61 (1H, s), 8.08 (1H, d,  $J = 7.0$  Hz), 7.19 (1H, t,  $J = 8.0$

Hz), 7.13 (1H, s), 7.09 (1H, d,  $J = 8.0$  Hz), 7.03 (1H, t,  $J = 7.8$  Hz), 6.49 (1H, d,  $J = 8.0$  Hz), 5.80 (1H, s), 4.82—4.80 (1H, m), 4.05—4.02 (1H, m), 3.95 (3H, s), 3.67—3.64 (2H, m), 3.30—3.27 (2H, m), 2.50—2.46 (1H, m), 2.41—2.36 (1H, m), 2.04—1.91 (2H, m), 1.83—1.76 (3H, m), 0.80—0.75 (1H, m), 0.51—0.47 (2H, m), 0.17—0.11 (2H, m)  
 $^{13}\text{C}$  NMR (125 MHz,  $\text{CDCl}_3$ )  $\delta\text{C}$  181.0, 172.8, 161.4, 154.2, 137.9, 129.1, 125.5, 118.9, 105.1, 100.9, 99.6, 66.0, 64.2, 55.3, 54.0, 53.8, 51.6, 50.2, 40.5, 38.5, 37.9, 31.9, 28.9, 28.0, 7.2, 4.5, 4.3

OR:  $[\alpha]_{\text{D}}^{26} = 0.21$  ( $c = 0.25$ , DCM)

HRMS: (ESI) Calcd for  $\text{C}_{23}\text{H}_{30}\text{N}_4\text{NaO}_5$   $[\text{M} + \text{Na}]^+$  465.2108, found 465.2109

**(*S*)-1-Phenylethyl ((*S*)-3-cyclopropyl-1-(((*S*)-1-hydroxy-3-((*S*)-2-oxopyrrolidin-3-yl)propan-2-yl)amino)-1-oxopropan-2-yl)carbamate**  
**(190)**



**190**

**190** was prepared from **178** following the same general procedure as that of **179**, employing noncritical variations in procedure to furnish a crude product.

Purification: Flash column chromatography over silica, eluent system of 10/90 MeOH/EtOAc.

TLC:  $R_f = 0.28$ , 10/90 MeOH/EtOAc

Appearance: Transparent semi-solid.

Yield: 70%

IR (DCM cast film,  $\nu_{\text{max}}$  /  $\text{cm}^{-1}$ ) 3293, 2979, 2928, 2870, 1691, 1537, 1442, 1377, 1265, 1066,

1030

$^1\text{H}$  NMR (700 MHz,  $\text{CDCl}_3$ )  $\delta$ H 7.77 (1H, d,  $J = 6.5$  Hz), 7.36—7.31 (4H, m), 7.30—7.25 (1H, m), 5.84 (1H, s), 5.80—5.73 (1H, m), 5.53—5.43 (1H, m), 4.26—4.15 (1H, m), 4.10—3.98 (1H, m), 3.69—3.63 (1H, m), 3.63—3.57 (1H, m), 3.38—3.30 (2H, m), 2.56—2.44 (1H, m), 2.44—2.28 (1H, m), 2.03—1.95 (1H, m), 1.95—1.81 (2H, m), 1.73—1.57 (3H, m), 1.53 (3H, d,  $J = 6.7$  Hz), 0.71—0.61 (1H, m), 0.46—0.40 (2H, m), 0.10—0.04 (2H, m)

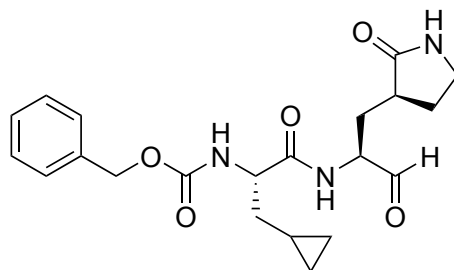
$^{13}\text{C}$  NMR (175 MHz,  $\text{CDCl}_3$ )  $\delta$ C 180.9, 173.1, 155.7, 142.1, 128.5, 127.8, 126.0, 73.2, 66.1, 55.7, 51.7, 40.6, 38.4, 37.8, 31.9, 29.1, 22.6, 7.2, 4.5, 4.3

OR:  $[\alpha]_{\text{D}}^{26} = -20.88$  ( $c = 0.09$ , DCM)

HRMS: (ESI) Calcd for  $\text{C}_{22}\text{H}_{31}\text{N}_3\text{NaO}_5$   $[\text{M} + \text{Na}]^+$  440.2156, found 440.2160

**Benzyl ((*S*)-3-cyclopropyl-1-oxo-1-(((*S*)-1-oxo-3-((*S*)-2-oxopyrrolidin-3-yl)propan-2-yl)amino)propan-2-yl)carbamate**

(80)



80

**179** (0.145 g, 0.359 mmol, 1.0 equiv) was dissolved in 3.6 mL of DCM. To this solution was added Dess-Martin periodinane (0.229 g, 0.539 mmol, 1.5 equiv) at room temperature. The reaction mixture was then stirred at room temperature, exposed to the atmosphere, for 4 h. Reaction progress was monitored by TLC, noting consumption of starting material. The reaction mixture was then worked up by addition of 1.2 mL of 10%  $\text{Na}_2\text{S}_2\text{O}_3(\text{aq})$  followed by stirring for 15 min. The layers were then separated and the DCM was washed with additional volumes of 10%  $\text{Na}_2\text{S}_2\text{O}_3(\text{aq})$  (1x1.2 mL), sat.  $\text{NaHCO}_3(\text{aq})$  (2x1.2 mL),  $\text{H}_2\text{O}$  (2x1.2

mL), and brine (2x1.2 mL). The DCM layer was then dried over Na<sub>2</sub>SO<sub>4</sub> and concentrated to furnish a crude yellow semi-solid. The crude material was then purified by flash column chromatography over silica using an eluent system of 4/96 MeOH/EtOAc. Product elution was monitored by TLC and KMnO<sub>4</sub> staining (R<sub>f</sub> = 0.42, 5/95 MeOH/EtOAc). Concentration of product fractions furnishes a white foam upon Et<sub>2</sub>O co-evaporation (0.078 g, 0.193 mmol, 54%).

IR (DCM cast film,  $\nu_{\max}$  / cm<sup>-1</sup>) 3293, 3064, 3031, 3006, 2935, 1689, 1535, 1456, 1442, 1384, 1266, 1119, 1054, 1029

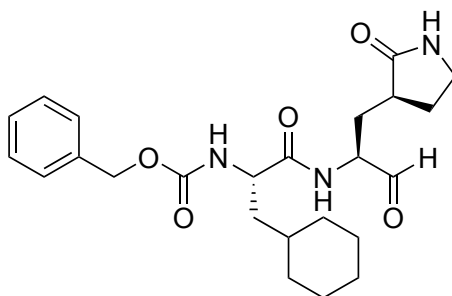
<sup>1</sup>H NMR (700 MHz, CDCl<sub>3</sub>)  $\delta$ H 9.51 (1H, s), 8.34 (1H, s), 7.36—7.30 (5H, m), 5.62 (1H, s), 5.50 (2H, d, *J* = 6.3 Hz), 5.12 (2H, s), 4.38—4.34 (1H, m), 4.34—4.32 (1H, m), 3.37—3.33 (2H, m), 2.48—2.44 (1H, m), 2.43—2.40 (1H, m), 1.99—1.94 (2H, m), 1.89—1.84 (1H, m), 1.74—1.69 (2H, m), 0.77—0.73 (1H, m), 0.49 (2H, d, *J* = 7.0 Hz), 0.13 (2H, d, *J* = 3.5 Hz)

<sup>13</sup>C NMR (125 MHz, CDCl<sub>3</sub>)  $\delta$ C 200.0, 179.9, 155.2, 136.5, 128.5, 128.1, 128.0, 66.9, 58.3, 55.5, 40.6, 38.3, 37.8, 29.6, 29.1, 7.2, 4.6, 2.3

OR:  $[\alpha]_{\text{D}}^{26} = -20.68$  (c=0.32, DCM)

HRMS: (ESI) Calcd for C<sub>21</sub>H<sub>27</sub>N<sub>3</sub>NaO<sub>5</sub> [M + Na]<sup>+</sup> 424.1843, found 424.1841

**Benzyl ((*S*)-3-cyclohexyl-1-oxo-1-(((*S*)-1-oxo-3-((*S*)-2-oxopyrrolidin-3-yl)propan-2-yl)amino)propan-2-yl)carbamate**  
(81)



**81**

**81** was prepared from **180** following the same general procedure as that of **80**, employing

noncritical variations in procedure to furnish a crude product.

Purification: Flash column chromatography over silica, eluent system of 3/97 MeOH/EtOAc.

TLC:  $R_f = 0.26$ , 5/95 MeOH/EtOAc

Appearance: White foam.

Yield: 45%

IR (DCM cast film,  $\nu_{\max}$  /  $\text{cm}^{-1}$ ) 3284, 3063, 2924, 2851, 1688, 1533, 1448, 1387, 1264, 1044, 1028

$^1\text{H}$  NMR (700 MHz,  $\text{CDCl}_3$ )  $\delta$ H 9.48 (1H, s), 8.26 (1H, d,  $J = 5.4$  Hz), 7.40—7.27 (5H, m), 5.87 (1H, s), 5.36—5.30 (1H, m), 5.15—5.06 (2H, m), 4.38—4.30 (2H, m), 3.38—3.28 (2H, m), 2.52—2.25 (2H, m), 2.01—1.91 (1H, m), 1.91—1.76 (2H, m), 1.76—1.56 (5H, m), 1.56—1.44 (1H, m), 1.42—1.30 (1H, m), 1.27—1.09 (4H, m), 1.01—0.82 (2H, m)

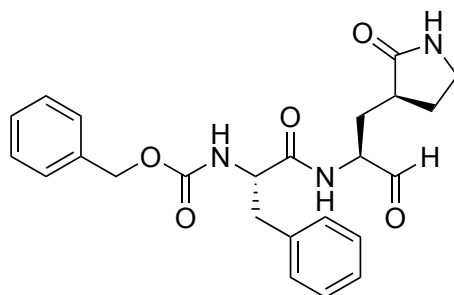
$^{13}\text{C}$  NMR (175 MHz,  $\text{CDCl}_3$ )  $\delta$ C 198.9, 180.1, 136.4, 128.6, 128.1, 128.0, 67.0, 58.1, 53.0, 40.8, 40.6, 38.3, 34.1, 33.7, 32.6, 29.7, 28.9, 26.4, 26.3, 26.1 (2 carbonyls not shown)

OR:  $[\alpha]_{\text{D}}^{26} = -11.14$  ( $c = 0.65$ , DCM)

HRMS: (ESI) Calcd for  $\text{C}_{24}\text{H}_{34}\text{N}_3\text{O}_5$   $[\text{M} + \text{H}]^+$  444.2493, found 444.2487

**Benzyl ((*S*)-1-oxo-1-(((*S*)-1-oxo-3-((*S*)-2-oxopyrrolidin-3-yl)propan-2-yl)amino)-3-phenylpropan-2-yl)carbamate**

**(82)**



**82**

**82** was prepared from **181** following the same general procedure as that of **80**, employing noncritical variations in procedure to furnish a crude product.

Purification: Flash column chromatography over silica, eluent system of 4/96 MeOH/EtOAc.

TLC:  $R_f = 0.31$ , 5/95 MeOH/EtOAc

Appearance: White foam.

Yield: 48%

IR (DCM cast film,  $\nu_{\max}$  /  $\text{cm}^{-1}$ ) 3288, 2063, 2950, 1684, 1535, 1497, 1455, 1364, 1053, 1028

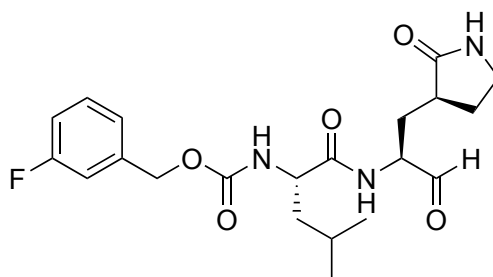
$^1\text{H}$  NMR (700 MHz,  $\text{CDCl}_3$ )  $\delta$  9.26 (1H, s), 8.14 (1H, d,  $J = 4.5$  Hz), 7.36—7.15 (10H, m), 5.59 (1H, s), 5.52 (1H, d,  $J = 7.5$  Hz), 5.13—5.06 (2H, m), 4.64—4.54 (1H, m), 4.24 (1H, app q,  $J = 7.1$  Hz), 3.34—3.23 (2H, m), 3.19—3.13 (1H, m), 3.13—3.04 (1H, m), 2.36—2.28 (1H, m), 2.28—2.21 (1H, m), 1.89—1.82 (2H, m), 1.82—1.73 (1H, m)

$^{13}\text{C}$  NMR (175 MHz,  $\text{CDCl}_3$ )  $\delta$  198.1, 180.0, 172.0, 155.8, 136.3, 129.5, 128.7, 128.6, 128.5, 128.2, 128.0, 127.0, 67.0, 58.0, 56.1, 40.6, 38.8, 38.1, 29.4, 28.7

OR:  $[\alpha]_{\text{D}}^{26} = -3.03$  ( $c = 0.74$ , DCM)

HRMS: (ESI) Calcd for  $\text{C}_{24}\text{H}_{27}\text{N}_3\text{NaO}_5$   $[\text{M} + \text{Na}]^+$  460.1843, found 460.1843

**3-Fluorobenzyl ((*S*)-4-methyl-1-oxo-1-(((*S*)-1-oxo-3-(((*S*)-2-oxopyrrolidin-3-yl)propan-2-yl)amino)pentan-2-yl)carbamate**  
**(83)**



**83**

**83** was prepared from **182** following the same general procedure as that of **80**, employing noncritical variations in procedure to furnish a crude product.

Purification: Flash column chromatography over silica, eluent system of 5/95 MeOH/EtOAc.

TLC:  $R_f = 0.26$ , 5/95 MeOH/EtOAc

Appearance: White foam.

Yield: 62%

IR (DCM cast film,  $\nu_{\max}$  /  $\text{cm}^{-1}$ ) 3296, 3066, 2957, 2871, 1688, 1533, 1490, 1451, 1260, 1052

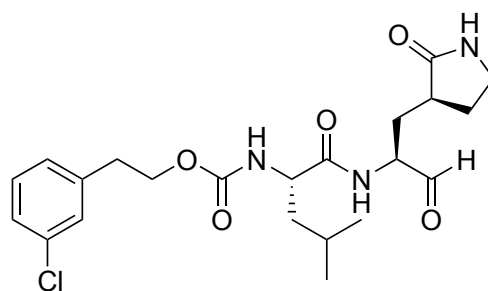
$^1\text{H}$  NMR (700 MHz,  $\text{CDCl}_3$ )  $\delta$  9.48 (1H, s), 8.43 (1H, d,  $J = 4.8$  Hz), 7.33—7.28 (1H, m), 7.12—7.01 (2H, m), 7.01—6.95 (1H, m), 6.05 (1H, s), 5.47—5.40 (1H, m), 5.14—5.00 (2H, m), 4.38—4.28 (2H, m), 3.39—3.28 (2H, m), 2.53—2.43 (1H, m), 2.43—2.28 (1H, m), 2.01—1.89 (2H, m), 1.89—1.81 (1H, m), 1.77—1.65 (2H, m), 1.60—1.50 (1H, m), 1.00—0.86 (6H, m)

$^{13}\text{C}$  NMR (175 MHz,  $\text{CDCl}_3$ )  $\delta$  198.6, 180.2, 173.6, 155.9, 130.1, 123.2, 115.0, 114.9, 114.7, 114.6, 66.0, 58.2, 53.6, 42.3, 40.7, 38.4, 29.7, 28.9, 24.9, 23.0, 22.0

OR:  $[\alpha]_{\text{D}}^{26} = -19.70$  ( $c = 0.88$ , DCM)

HRMS: (ESI) Calcd for  $\text{C}_{21}\text{H}_{28}\text{FN}_3\text{NaO}_5$   $[\text{M} + \text{Na}]^+$  444.1905, found 444.1903

**3-Chlorophenethyl ((*S*)-4-methyl-1-oxo-1-(((*S*)-1-oxo-3-((*S*)-2-oxopyrrolidin-3-yl)propan-2-yl)amino)pentan-2-yl)carbamate**  
(84)



84

**84** was prepared from **183** following the same general procedure as that of **80**, employing noncritical variations in procedure to furnish a crude product.

Purification: Flash column chromatography over silica, eluent system of 5/95 MeOH/EtOAc.

TLC:  $R_f = 0.24$ , 5/95 MeOH/EtOAc

Appearance: White foam.

Yield: 56%

IR (DCM cast film,  $\nu_{\max}$  /  $\text{cm}^{-1}$ ) 3293, 3067, 2957, 2932, 1689, 1533, 1436, 1265, 1173, 1115, 1058

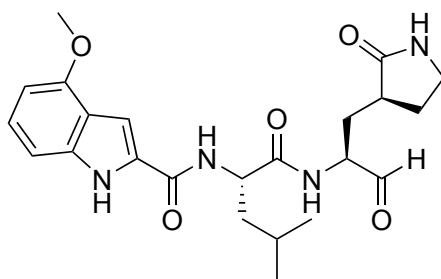
$^1\text{H}$  NMR (700 MHz,  $\text{CDCl}_3$ )  $\delta$  9.49 (1H, s), 8.35 (1H, d,  $J = 5.1$  Hz), 7.25—7.15 (3H, m), 7.09 (1H, app dt,  $J = 7.1, 1.8$  Hz), 6.11—5.97 (1H, m), 5.32—5.22 (1H, m), 4.56—3.89 (4H, m), 3.45—3.25 (2H, m), 2.95—2.80 (2H, m), 2.55—2.42 (1H, m), 2.42—2.30 (1H, m), 2.05—1.90 (2H, m), 1.90—1.79 (1H, m), 1.79—1.60 (2H, m), 1.59—1.44 (1H, m), 1.01—0.80 (6H, m)

$^{13}\text{C}$  NMR (175 MHz,  $\text{CDCl}_3$ )  $\delta$  199.3, 180.1, 173.7, 156.1, 140.0, 134.2, 129.8, 129.1, 127.2, 126.8, 65.2, 58.1, 53.4, 42.3, 40.7, 38.4, 35.2, 29.7, 28.9, 24.8, 23.0, 22.0

OR:  $[\alpha]_{\text{D}}^{26} = -21.77$  ( $c = 0.80$ , DCM)

HRMS: (ESI) Calcd for  $\text{C}_{22}\text{H}_{30}\text{ClN}_3\text{NaO}_5$   $[\text{M} + \text{Na}]^+$  474.1766, found 474.1767

**4-Methoxy-*N*-((*S*)-4-methyl-1-oxo-1-(((*S*)-1-oxo-3-((*S*)-2-oxopyrrolidin-3-yl)propan-2-yl)amino)pentan-2-yl)-1*H*-indole-2-carboxamide**  
(85)



**85**

**85** was prepared from **184** following the same general procedure as that of **80**, employing noncritical variations in procedure to furnish a crude product.

Purification: Flash column chromatography over silica, eluent system of 5/95 MeOH/EtOAc.

TLC:  $R_f = 0.22$ , 5/95 MeOH/EtOAc

Appearance: Off-white powder.



Yield: 37%

IR (DCM cast film,  $\nu_{\max}$  /  $\text{cm}^{-1}$ ) 3280, 3061, 2958, 2932, 2871, 1734, 1684, 1641, 1583, 1516, 1464, 1431, 1362, 1262, 1165, 1100

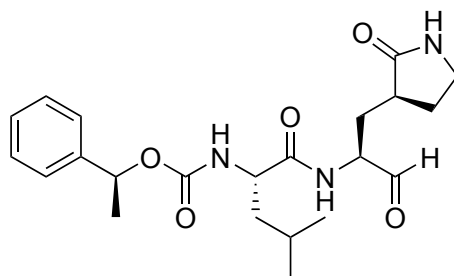
$^1\text{H}$  NMR (700 MHz,  $\text{CDCl}_3$ )  $\delta$  9.51 (1H, s), 8.52 (1H, m), 7.21—7.17 (1H, t,  $J = 8.0$  Hz), 7.14—7.10 (1H, m), 7.00 (1H, d,  $J = 8.4$  Hz), 6.75 (1H, d,  $J = 8.0$  Hz), 6.50 (1H, d,  $J = 8.0$  Hz), 5.87 (1H, m), 4.82 (1H, m), 4.34—4.31 (1H, m), 3.94 (3H, s), 3.32—3.28 (2H, m), 2.45—2.35 (2H, m), 1.97 (2H, t,  $J = 7.0$  Hz), 1.87—1.67 (6H, m), 1.02—0.98 (6H, m)

$^{13}\text{C}$  NMR (175 MHz,  $\text{CDCl}_3$ )  $\delta$  200.0, 180.0, 173.3, 160.5, 154.2, 137.8, 125.7, 118.9, 105.0, 100.8, 99.7, 58.3, 55.3, 51.8, 42.1, 40.6, 38.5, 29.5, 28.9, 25.0, 23.0, 22.1

OR:  $[\alpha]_{\text{D}}^{26} = -0.45$  ( $c = 0.11$ , DCM)

HRMS: (ESI) Calcd for  $\text{C}_{23}\text{H}_{30}\text{N}_4\text{NaO}_5$   $[\text{M} + \text{Na}]^+$  465.2108, found 465.2106

**(*S*)-1-Phenylethyl ((*S*)-4-methyl-1-oxo-1-(((*S*)-1-oxo-3-((*S*)-2-oxopyrrolidin-3-yl)propan-2-yl)amino)pentan-2-yl)carbamate**  
**(86)**



**86**

**86** was prepared from **185** following the same general procedure as that of **80**, employing noncritical variations in procedure to furnish a crude product.

Purification: Flash column chromatography over silica, eluent system of 4/96 MeOH/EtOAc.

TLC:  $R_f = 0.30$ , 5/95 MeOH/EtOAc

Appearance: White foam.

Yield: 51%

IR (DCM cast film,  $\nu_{\max}$  /  $\text{cm}^{-1}$ ) 3287, 3063, 2957, 2934, 2871, 1690, 1532, 1449, 1385, 1265, 1065

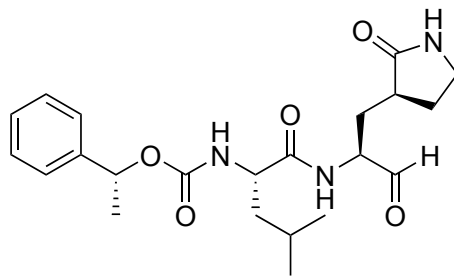
$^1\text{H}$  NMR (700 MHz,  $\text{CDCl}_3$ )  $\delta$  9.50 (1H, s), 8.27 (1H, d,  $J = 6.2$  Hz), 7.37—7.23 (5H, m), 6.21—5.96 (1H, m), 5.81—5.63 (1H, m), 5.29 (1H, s), 4.41—4.32 (1H, m), 4.32—4.23 (1H, m), 3.40—3.24 (2H, m), 2.52—2.45 (1H, m), 2.45—2.36 (1H, m), 2.05—1.97 (1H, m), 1.97—1.90 (1H, m), 1.90—1.80 (1H, m), 1.74—1.62 (2H, m), 1.57—1.43 (4H, m), 1.01—0.81 (6H, m)

$^{13}\text{C}$  NMR (175 MHz,  $\text{CDCl}_3$ )  $\delta$  198.9, 180.0, 173.7, 155.7, 142.1, 128.5, 127.8, 125.9, 73.3, 58.0, 53.4, 42.3, 40.6, 38.2, 29.8, 28.8, 24.8, 22.9, 22.6, 22.0

OR:  $[\alpha]_{\text{D}}^{26} = -37.24$  ( $c = 1.01$ , DCM)

HRMS: (ESI) Calcd for  $\text{C}_{22}\text{H}_{31}\text{N}_3\text{NaO}_5$   $[\text{M} + \text{Na}]^+$  440.2156, found 440.2154

**(*R*)-1-Phenylethyl ((*S*)-4-methyl-1-oxo-1-(((*S*)-1-oxo-3-((*S*)-2-oxopyrrolidin-3-yl)propan-2-yl)amino)pentan-2-yl)carbamate**  
**(87)**



**87**

**87** was prepared from **186** following the same general procedure as that of **80**, employing noncritical variations in procedure to furnish a crude product.

Purification: Flash column chromatography over silica, eluent system of 5/95 MeOH/EtOAc.

TLC:  $R_f = 0.41$ , 5/95 MeOH/EtOAc

Appearance: White powder.

Yield: 72%

IR (DCM cast film,  $\nu_{\max}$  /  $\text{cm}^{-1}$ ) 3302, 3059, 3034, 2958, 2935, 2872, 1692, 1534, 1449, 1386, 1265, 1173, 1118, 1065, 1030  $^1\text{H}$  NMR (700 MHz,  $\text{CDCl}_3$ )  $\delta$ H 9.42 (1H, s), 8.15 (1H, s), 7.34—7.31 (5H, m), 5.77 (1H, d,  $J = 6.3$  Hz), 5.73 (1H, s), 4.30—4.24 (2H, m), 3.29—3.24 (2H, m), 2.38—2.34 (1H, m), 2.30—2.26 (1H, m), 1.93—1.88 (2H, m), 1.79—1.75 (1H, m), 1.75—1.73 (1H, m), 1.70—1.64 (1H, m), 1.59—1.56 (1H, m), 1.55—1.52 (3H, d,  $J = 6.3$  Hz), 0.99 (3H, s), 0.98 (3H, s)

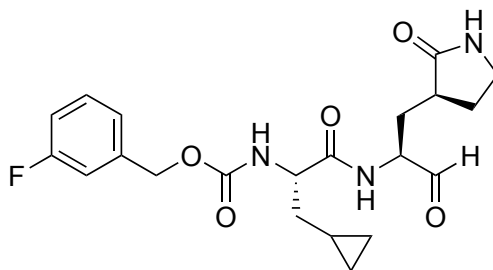
$^{13}\text{C}$  NMR (125 MHz,  $\text{CDCl}_3$ )  $\delta$ C 199.6, 179.9, 173.6, 155.6, 128.4, 127.6, 126.0, 125.9, 73.2, 58.0, 53.4, 42.3, 40.5, 38.1, 29.5, 28.8, 24.8, 22.9, 22.6, 22.0

OR:  $[\alpha]_{\text{D}}^{26} = -14.85$  ( $c = 0.28$ , DCM)

HRMS: (ESI) Calcd for  $\text{C}_{22}\text{H}_{31}\text{N}_3\text{NaO}_5$   $[\text{M} + \text{Na}]^+$  440.2156, found 440.2155

**3-Fluorobenzyl ((*S*)-3-cyclopropyl-1-oxo-1-(((*S*)-1-oxo-3-((*S*)-2-oxopyrrolidin-3-yl)propan-2-yl)amino)propan-2-yl)carbamate**

(**88**)



**88**

**88** was prepared from **187** following the same general procedure as that of **80**, employing noncritical variations in procedure to furnish a crude product.

Purification: Flash column chromatography over silica, eluent system of 5/95 MeOH/EtOAc.

TLC:  $R_f = 0.41$ , 5/95 MeOH/EtOAc

Appearance: White powder.

Yield: 92%

IR (DCM cast film,  $\nu_{\max}$  /  $\text{cm}^{-1}$ ) 3290, 3078, 300, 2945, 1683, 1592, 1536, 1491, 1451, 1382,

1334, 1261, 1143, 1054

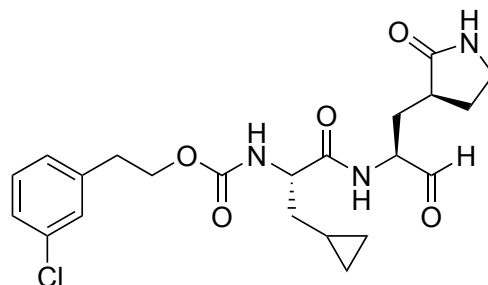
$^1\text{H}$  NMR (500 MHz,  $\text{CDCl}_3$ )  $\delta$  9.50 (1H, s), 8.50—8.46 (1H, m), 7.33—7.30 (1H, m), 7.12—7.09 (2H, m), 6.99 (1H, t,  $J = 8.1$  Hz), 5.69 (1H, s), 5.55 (1H, d,  $J = 8.2$  Hz), 5.15—5.09 (2H, m), 4.37—4.28 (2H, m), 3.38—3.32 (2H, m), 2.48—2.40 (2H, m), 1.97—1.86 (3H, m), 1.73—1.70 (2H, m), 0.77—0.74 (1H, m), 0.52—0.49 (2H, m), 0.15—0.13 (2H, m)

$^{13}\text{C}$  NMR (125 MHz,  $\text{CDCl}_3$ )  $\delta$  199.5, 180.0, 172.8, 172.4, 163.8, 163.6, 155.2, 130.0, 123.2, 115.0, 114.8, 114.6, 114.5, 110.1, 65.9, 58.4, 57.0, 55.5, 40.6, 38.4, 37.8, 29.6, 29.1, 7.2, 4.6, 4.3

OR:  $[\alpha]_{\text{D}}^{26} = -22.68$  ( $c = 0.12$ , DCM)

HRMS: (ESI) Calcd for  $\text{C}_{21}\text{H}_{26}\text{FN}_3\text{NaO}_5$   $[\text{M} + \text{Na}]^+$  442.1749, found 442.1751

**3-Chlorophenethyl ((*S*)-3-cyclopropyl-1-oxo-1-(((*S*)-1-oxo-3-((*S*)-2-oxopyrrolidin-3-yl)propan-2-yl)amino)propan-2-yl)carbamate**  
**(89)**



**89**

**89** was prepared from **188** following the same general procedure as that of **80**, employing noncritical variations in procedure to furnish a crude product.

Purification: Flash column chromatography over silica, eluent system of 5/95 MeOH/EtOAc.

TLC:  $R_f = 0.25$ , 5/95 MeOH/EtOAc

Appearance: White foam.

Yield: 42%

IR (DCM cast film,  $\nu_{\text{max}}$  /  $\text{cm}^{-1}$ ) 3300, 3079, 2998, 2925, 1687, 1534, 1429, 1307, 1270, 1079

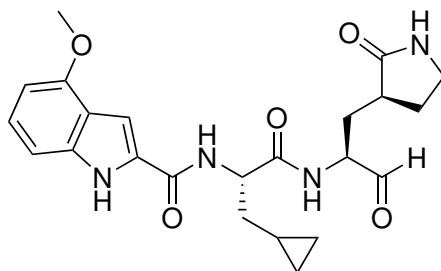
$^1\text{H}$  NMR (700 MHz,  $\text{CDCl}_3$ )  $\delta$  9.62—9.48 (1H, m), 8.54—8.33 (1H, m), 7.25—7.19 (3H, m), 7.12—7.08 (1H, m), 5.82—5.72 (1H, m), 5.47—5.39 (1H, m), 4.38—4.31 (2H, m), 4.31—4.24 (2H, m), 3.40—3.31 (2H, m), 2.93—2.88 (2H, m), 2.55—2.45 (1H, m), 2.45—2.39 (1H, m), 2.00—1.93 (1H, m), 1.92—1.82 (1H, m), 1.75—1.66 (2H, m), 1.29—1.22 (1H, m), 0.78—0.67 (1H, m), 0.52—0.43 (2H, m), 0.17—0.06 (2H, m)

$^{13}\text{C}$  NMR (175 MHz,  $\text{CDCl}_3$ )  $\delta$  198.7, 180.2, 172.9, 139.5, 156.1, 134.2, 129.8, 129.1, 127.2, 126.8, 65.2, 58.3, 55.5, 40.7, 38.4, 37.8, 35.2, 29.8, 29.1, 7.2, 4.6, 4.3

OR:  $[\alpha]_{\text{D}}^{26} = 4.79$  ( $c = 0.48$ , DCM)

HRMS: (ESI) Calcd for  $\text{C}_{22}\text{H}_{28}\text{ClN}_3\text{NaO}_5$   $[\text{M} + \text{Na}]^+$  472.1610, found 472.1609

***N*-((*S*)-3-Cyclopropyl-1-oxo-1-(((*S*)-1-oxo-3-((*S*)-2-oxopyrrolidin-3-yl)propan-2-yl)amino)propan-2-yl)-4-methoxy-1*H*-indole-2-carboxamide**  
(90)



90

90 was prepared from 189 following the same general procedure as that of 80, employing noncritical variations in procedure to furnish a crude product.

Purification: Flash column chromatography over silica, eluent system of 5/95 MeOH/EtOAc.

TLC:  $R_f = 0.48$ , 5/95 MeOH/EtOAc

Appearance: Off-white powder.

Yield: 27%

IR (DCM cast film,  $\nu_{\text{max}}$  /  $\text{cm}^{-1}$ ) 3308, 3122, 3078, 2999, 2925, 1730, 1669, 1617, 1541, 1462, 1428, 1379, 1362, 1303, 1259, 1223, 1165, 1102

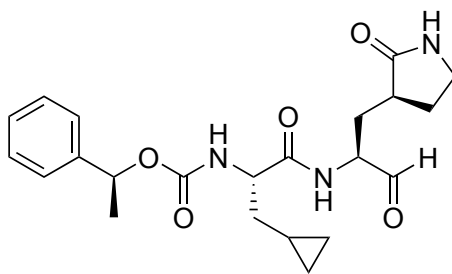
<sup>1</sup>H NMR (500 MHz, CDCl<sub>3</sub>) δH 9.54 (1H, s), 9.41 (1H, s), 8.54 (1H, m), 7.21—7.18 (1H, t, *J* = 8.0 Hz), 7.15—7.12 (1H, m), 7.03—7.01 (2H, m), 6.50 (1H, d, *J* = 8.3 Hz), 5.83 (1H, s), 4.91—4.88 (1H, m), 4.37—4.34 (1H, m), 3.95 (3H, s), 3.27—3.22 (2H, m), 2.48—2.40 (2H, m), 2.09—2.05 (1H, m), 1.99—1.97 (1H, m), 1.88—1.80 (3H, m), 0.82—0.79 (1H, m), 0.52—0.50 (2H, m), 0.19—0.16 (2H, m)

<sup>13</sup>C NMR (125 MHz, CDCl<sub>3</sub>) δC 199.4, 172.7, 154.3, 137.8, 129.0, 125.7, 119.0, 105.0, 100.8, 99.7, 58.4, 55.3, 53.7, 40.6, 38.5, 37.7, 29.6, 29.0, 7.2, 4.6, 4.3

OR: [α]<sub>D</sub><sup>26</sup> = 7.78 (c = 0.18, DCM)

HRMS: (ESI) Calcd for C<sub>23</sub>H<sub>28</sub>N<sub>4</sub>NaO<sub>5</sub> [M + Na]<sup>+</sup> 463.1952, found 463.1945

**(*S*)-1-Phenylethyl ((*S*)-3-cyclopropyl-1-oxo-1-(((*S*)-1-oxo-3-((*S*)-2-oxopyrrolidin-3-yl)propan-2-yl)amino)propan-2-yl)carbamate**  
**(91)**



**91**

**91** was prepared from **190** following the same general procedure as that of **80**, employing noncritical variations in procedure to furnish a crude product.

Purification: Flash column chromatography over silica, eluent system of 5/95 MeOH/EtOAc.

TLC: R<sub>f</sub> = 0.25, 5/95 MeOH/EtOAc

Appearance: White foam.

Yield: 46%

IR (DCM cast film, ν<sub>max</sub> / cm<sup>-1</sup>) 3298, 3077, 2980, 2929, 1687, 1531, 1495, 1267, 1064

<sup>1</sup>H NMR (700 MHz, CDCl<sub>3</sub>) δH 9.66—9.44 (1H, m), 8.43—8.21 (1H, m), 7.36—7.31 (4H, m),

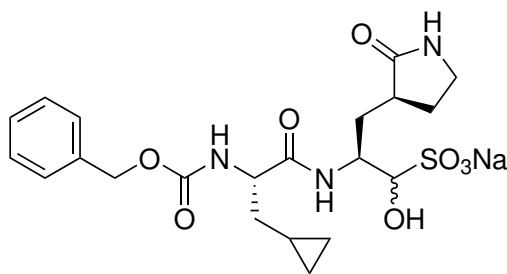
7.29—7.26 (1H, m), 5.81—5.75 (1H, m), 5.67—5.61 (1H, m), 5.47—5.41 (1H, m), 4.40—4.35 (1H, m), 4.35—4.29 (1H, m), 3.40—3.31 (2H, m), 2.57—2.47 (1H, m), 2.47—2.32 (1H, m), 2.02—1.95 (1H, m), 1.93—1.84 (1H, m), 1.74—1.63 (2H, m), 1.54 (3H, d,  $J = 6.4$  Hz), 1.28—1.23 (1H, m), 0.75—0.66 (1H, m), 0.49—0.39 (2H, m), 0.14—0.04 (2H, m)  
 $^{13}\text{C}$  NMR (175 MHz,  $\text{CDCl}_3$ )  $\delta\text{C}$  199.9, 180.5, 173.5, 155.1, 140.0, 134.0, 128.6, 127.9, 126.8, 126.0, 73.3, 58.2, 55.5, 40.7, 38.2, 37.8, 29.7, 29.1, 22.6, 7.4, 4.2, 4.1

OR:  $[\alpha]_{\text{D}}^{26} = -6.69$  ( $c = 0.26$ , DCM)

HRMS: (ESI) Calcd for  $\text{C}_{22}\text{H}_{29}\text{N}_3\text{NaO}_5$   $[\text{M} + \text{Na}]^+$  438.1999, found 438.1997

## Sodium

**(2*S*)-2-((*S*)-2-(((benzyloxy)carbonyl)amino)-3-cyclopropylpropanamido)-1-hydroxy-3-((*S*)-2-oxopyrrolidin-3-yl)propane-1-sulfonate**  
**(92)**



**92**

**80** (0.010 g, 0.025 mmol, 1.0 equiv) was dissolved in 0.1 mL of dry EtOAc and 0.06 mL of absolute EtOH. Next, a solution of  $\text{NaHSO}_3(\text{aq})$  (1 M in  $\text{H}_2\text{O}$ , 0.025 mL, 0.025 mmol, 1.0 equiv) was added. The reaction vessel was then sealed and stirred at 50 °C for 3 h. Afterwards, the reaction mixture was filtered in order to remove any solids. This was followed by additional washings with anhydrous EtOH. The combined EtOH filtrate and washings were then concentrated *in vacuo*, followed by co-evaporation with *i*PrOH (3  $\times$ ) to remove any residual  $\text{H}_2\text{O}$ , furnishing a crude.  $\text{Et}_2\text{O}$  (0.2 mL) was then added in order to precipitate out a white solid after mixing and sonication. The dispersion was then centrifuged and the

Et<sub>2</sub>O supernatant decanted, with the process repeated with an identical additional volume of Et<sub>2</sub>O (1 ×). The resultant white solid was then resuspended in a mixture of Et<sub>2</sub>O (0.15 mL) and EtOAc (0.7 mL) and mixed for 5 min. This was followed by a final centrifugation step and decanting of the supernatant. Drying of the pellet overnight then furnishes a white powder as the product (0.013 g, 0.017 mmol, 68%)

IR (DCM cast film,  $\nu_{\max}$  / cm<sup>-1</sup>) 3290, 3092, 3069, 3034, 2958, 2872, 1674, 1528, 1455, 1387, 1370, 1215

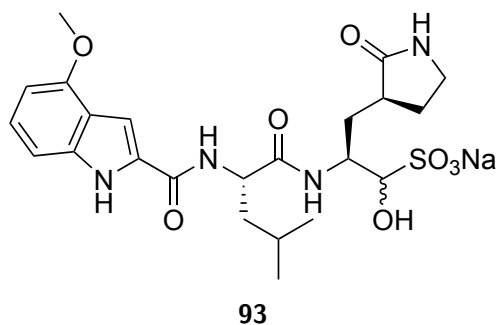
<sup>1</sup>H NMR (700 MHz, DMSO-d<sub>6</sub>)  $\delta$ H 9.40, 8.47, 7.61—7.55 (1H, m) (mixture of diastereomers), 7.49—7.42 (1H, m), 7.40—7.30 (5H, m), 6.07, 5.33, 5.22 (1H, m) (mixture of diastereomers), 5.03—5.00 (2H, m), 4.22—3.62 (2H, m), 3.14—3.01 (2H, m), 2.21—1.74 (3H, m), 1.63—1.39 (3H, m), 0.76—0.73 (1H, m), 0.37—0.30 (2H, m), 0.14—0.00 (m, 2H)

<sup>13</sup>C NMR (175 MHz, DMSO-d<sub>6</sub>)  $\delta$ C 178.4, 170.0, 156.0, 137.0, 128.3, 128.2, 127.7, 127.6, 95.5, 84.4, 65.3, 56.3, 55.3, 48.6, 40.0, 37.7, 37.2, 36.6, 29.3, 27.3, 7.9, 4.6, 3.7

OR:  $[\alpha]_{\text{D}}^{26} = -31.18$  (c = 0.21, H<sub>2</sub>O)

HRMS: (ESI) Calcd for C<sub>21</sub>H<sub>28</sub>N<sub>3</sub>O<sub>8</sub>S [M - H]<sup>-</sup> 482.1603, found 482.1604

**Sodium (2*S*)-1-hydroxy-2-((*S*)-2-(4-methoxy-1*H*-indole-2-carboxamido)-4-methylpentanamido)-3-((*S*)-2-oxopyrrolidin-3-yl)propane-1-sulfonate**  
**(93)**



**93** was prepared from **85** following the same general procedure as that of **92**, employing noncritical variations in procedure to furnish a crude product.



Purification: Precipitation in Et<sub>2</sub>O.

TLC: N/A

Appearance: Off-white powder.

Yield: 96%

IR (H<sub>2</sub>O cast film,  $\nu_{\max}$  / cm<sup>-1</sup>) 3381, 3292, 3091, 3068, 3033, 2957, 2872, 1730, 1674, 1527, 1455, 1387, 1368, 1216

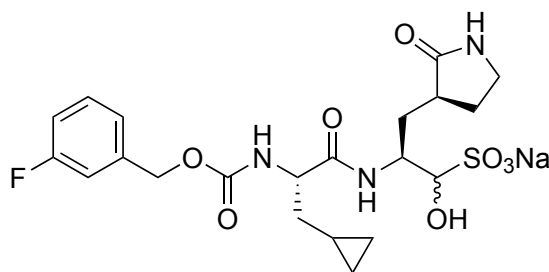
<sup>1</sup>H NMR (500 MHz, DMSO-d<sub>6</sub>)  $\delta$ H 8.41—8.33 (1H, m), 7.69—7.61 (1H, m), 7.42 (1H, s), 7.33—7.30 (1H, m), 7.09—7.07 (1H, m), 7.02—6.99 (1H, m), 6.52—6.49 (1H, m), 5.32—5.23 (1H, m), 4.46—3.82 (3H, m), 3.89 (3H, s), 3.10—3.00 (2H, m), 2.20—2.10 (3H, m), 1.67—1.56 (4H, m), 0.92—0.89 (3H, m), 0.88—0.86 (3H, m)

<sup>13</sup>C NMR (125 MHz, DMSO-d<sub>6</sub>)  $\delta$ C 179.1, 171.6, 160.6, 153.6, 137.7, 130.0, 124.2, 118.0, 105.3, 101.0, 99.1, 84.5, 83.8, 59.0, 55.0, 51.7, 49.2, 41.5, 37.9, 37.7, 24.4, 23.1, 21.4

OR:  $[\alpha]_{\text{D}}^{26} = -4.82$  (c = 0.21, H<sub>2</sub>O)

HRMS: (ESI) Calcd for C<sub>23</sub>H<sub>31</sub>N<sub>4</sub>O<sub>8</sub>S [M - H]<sup>-</sup> 523.1868, found 523.1868

**Sodium (2*S*)-2-((*S*)-3-cyclopropyl-2-(((3-fluorobenzyl)oxy)carbonyl)amino)propanamido)-1-hydroxy-3-((*S*)-2-oxopyrrolidin-3-yl)propane-1-sulfonate**  
(94)



**94**

**94** was prepared from **88** following the same general procedure as that of **92**, employing noncritical variations in procedure to furnish a crude product.

Purification: Precipitation in Et<sub>2</sub>O.

TLC: N/A

Appearance: White powder.

Yield: 73%

IR (H<sub>2</sub>O cast film,  $\nu_{\max}$  / cm<sup>-1</sup>) 3291, 3091, 3068, 3031, 2957, 2872, 1675, 1528, 1455, 1386, 1368, 1217

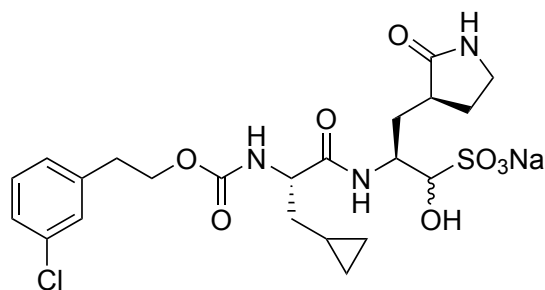
<sup>1</sup>H NMR (500 MHz, DMSO-d<sub>6</sub>)  $\delta$ H 7.64—7.12 (6H, m), 5.65 and 5.36 and 5.23 and 5.18 (1H, d,  $J$  = 8.0 Hz), 5.06—5.00 (2H, m), 4.23—4.20 (1H, m), 4.00—3.84 (2H, m), 3.08—2.96 (2H, m), 2.18—2.11 (3H, m), 1.73—1.36 (5H, m), 0.77—0.74 (1H, m), 0.36—0.34 (2H, m), 0.13—0.10 (1H, m), 0.04—0.02 (1H, m)

<sup>13</sup>C NMR (125 MHz, DMSO-d<sub>6</sub>)  $\delta$ C 179.2, 179.1, 171.3, 163.0, 161.1, 155.9, 155.8, 140.2, 140.1, 130.3, 130.2, 123.5, 123.4, 114.4, 114.2, 113.9, 84.3, 83.7, 64.4, 56.0, 55.9, 55.6, 49.2, 48.6, 37.6, 36.6, 36.3, 31.8, 29.9, 27.5, 27.3, 8.0, 7.9, 4.7, 3.7

OR:  $[\alpha]_{\text{D}}^{26} = -30.4$  ( $c = 0.23$ , H<sub>2</sub>O)

HRMS: (ESI) Calcd for C<sub>21</sub>H<sub>27</sub>FN<sub>3</sub>O<sub>8</sub>S [M - H]<sup>-</sup> 500.1508, found 500.1505

**Sodium (2*S*)-2-((*S*)-2-(((3-chlorophenoxy)carbonyl)amino)-3-cyclopropylpropanamido)-1-hydroxy-3-((*S*)-2-oxopyrrolidin-3-yl)propane-1-sulfonate**  
(95)



95

95 was prepared from 89 following the same general procedure as that of 92, employing

noncritical variations in procedure to furnish a crude product.

Purification: Precipitation in Et<sub>2</sub>O.

TLC: N/A

Appearance: White powder.

Yield: 85%

IR (H<sub>2</sub>O cast film,  $\nu_{\max}$  / cm<sup>-1</sup>) 3293, 3090, 3068, 3033, 2957, 2872, 1674, 1528, 1455, 1386, 1368, 1216.

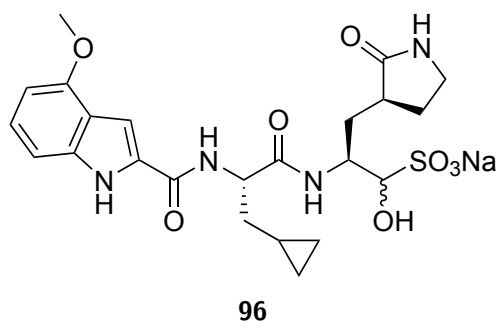
<sup>1</sup>H NMR (500 MHz, CDCl<sub>3</sub>)  $\delta$ H 7.57—7.50 (2H, m), 7.44—7.41 (1H, m), 7.34—7.27 (4H, m), 5.33 and 5.22 (1H, d,  $J$  = 8.0 Hz), 5.21—5.15 (2H, m), 3.97—3.87 (2H, m), 3.16—3.04 (2H, m), 2.89—2.87 (2H, m), 2.18—2.12 (3H, m), 1.65—1.36 (3H, m), 0.72—0.69 (1H, m), 0.35—0.32 (2H, m), 0.11—0.08 (1H, m), 0.03—0.00 (1H, m)

<sup>13</sup>C NMR (125 MHz, CDCl<sub>3</sub>)  $\delta$ C 179.2, 171.3, 155.9, 140.9, 132.8, 130.1, 128.3, 128.0, 126.2, 84.2, 83.7, 64.0, 50.4, 49.5, 37.0, 34.4, 27.3, 7.8, 4.6, 3.9

OR:  $[\alpha]_{\text{D}}^{26} = -27.6$  ( $c = 0.24$ , H<sub>2</sub>O)

HRMS: (ESI) Calcd for C<sub>22</sub>H<sub>29</sub>ClN<sub>3</sub>O<sub>8</sub>S [M - H]<sup>-</sup> 530.1360, found 530.1360

**Sodium (2*S*)-2-((*S*)-3-cyclopropyl-2-(4-methoxy-1*H*-indole-2-carboxamido)propanamido)-1-hydroxy-3-((*S*)-2-oxopyrrolidin-3-yl)propane-1-sulfonate**  
**(96)**



**96** was prepared from **90** following the same general procedure as that of **92**, employing

noncritical variations in procedure to furnish a crude product.

Purification: Precipitation in Et<sub>2</sub>O.

TLC: N/A

Appearance: Off-white powder.

Yield: 79%

IR (H<sub>2</sub>O cast film,  $\nu_{\max}$  / cm<sup>-1</sup>) 3384, 3292, 3091, 3068, 3033, 2957, 2872, 1715, 1674, 1527, 1455, 1387, 1368, 1216

<sup>1</sup>H NMR (500 MHz, DMSO-d<sub>6</sub>)  $\delta$ H (mixture of diastereomers) 8.41 and 8.36 (1H, d,  $J = 8.0$  Hz), 7.81 and 7.67 and 7.61 and 7.50 (1H, d,  $J = 8.0$  Hz), 7.43—7.40 (1H, m), 7.33—7.31 (1H, m), 7.09 (1H, t,  $J = 8.0$  Hz), 7.01 (1H, d,  $J = 8.0$  Hz), 6.50 (1H, d,  $J = 8.0$  Hz), 5.34 and 5.25 (1H, d,  $J = 8.0$  Hz), 4.49—4.42 (1H, m), 4.24—3.94 (1H, m), 3.89 (3H, s), 3.10—2.99 (2H, m), 2.17—2.14 (3H, m), 1.67—1.57 (4H, m), 0.80—0.77 (1H, m), 0.38—0.36 (2H, m), 0.20—0.18 (1H, m), 0.08—0.06 (1H, m)

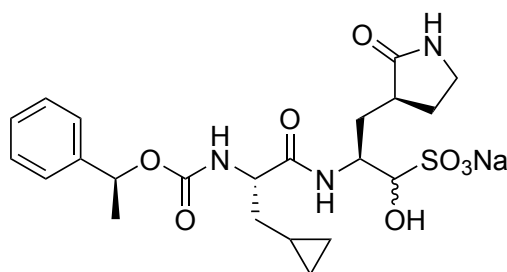
<sup>13</sup>C NMR (125 MHz, DMSO-d<sub>6</sub>)  $\delta$ C (mixture of diastereomers) 179.1, 171.2, 171.1, 160.9, 160.8, 153.6, 137.7, 130.1, 124.2, 118.0, 105.3, 100.8, 99.1, 84.5, 83.8, 64.9, 55.0, 54.4, 54.0, 49.2, 48.6, 37.8, 37.7, 36.7, 33.0, 29.7, 28.0, 27.9, 8.3, 8.1, 4.6, 3.8

OR:  $[\alpha]_{\text{D}}^{26} = 7.68$  ( $c = 0.26$ , H<sub>2</sub>O)

HRMS: (ESI) Calcd for C<sub>23</sub>H<sub>29</sub>N<sub>4</sub>O<sub>8</sub>S [M - H]<sup>-</sup> 521.1712, found 521.1728

**Sodium (2*S*)-2-((*S*)-3-cyclopropyl-2-(((*S*)-1-phenylethoxy)carbonyl)amino)propanamido)-1-hydroxy-3-((*S*)-2-oxopyrrolidin-3-yl)propane-1-sulfonate**

**(97)**



**97**

**97** was prepared from **91** following the same general procedure as that of **92**, employing noncritical variations in procedure to furnish a crude product.

Purification: Precipitation in Et<sub>2</sub>O.

TLC: N/A

Appearance: White powder.

Yield: 57%

IR (H<sub>2</sub>O cast film,  $\nu_{\max}$  / cm<sup>-1</sup>) 3290, 3092, 3068, 3031, 2957, 2873, 1675, 1528, 1455, 1386, 1368, 1215

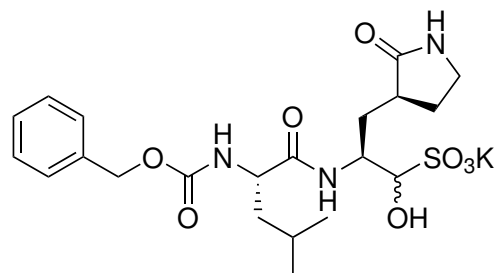
<sup>1</sup>H NMR (700 MHz, DMSO-d<sub>6</sub>)  $\delta$ H 9.37—9.34 (1H, m), 8.43—8.39 (1H, m), 7.59—7.57 (1H, m), 7.42—7.26 (5H, m), 5.69—5.67 (1H, m), 4.18—4.06 (1H, m), 3.06—2.94 (2H, m), 2.22—2.00 (2H, m), 1.61—1.50 (3H, m), 1.46—1.43 (3H, m), 0.78 (1H, s), 0.41—0.35 (2H, m), 0.13—0.05 (2H, m)

<sup>13</sup>C NMR (175 MHz, DMSO-d<sub>6</sub>)  $\delta$ C 178.3, 172.7, 154.0, 142.5, 133.5, 128.2, 127.3, 125.6, 94.5, 71.3, 56.2, 55.3, 40.0, 37.5, 37.1, 36.6, 29.3, 27.2, 22.6, 7.9, 4.6, 3.8

OR:  $[\alpha]_D^{26} = -9.20$  ( $c = 0.16$ , H<sub>2</sub>O)

HRMS: (ESI) Calcd for C<sub>22</sub>H<sub>30</sub>N<sub>3</sub>O<sub>8</sub>S [M - H]<sup>-</sup> 496.1759, found 496.1765

**Potassium (2*S*)-2-((*S*)-2-(((benzyloxy)carbonyl)amino)-4-methylpentanamido)-1-hydroxy-3-((*S*)-2-oxopyrrolidin-3-yl)propane-1-sulfonate**  
(98)



98

GC373 (**62**) (0.050 g, 0.124 mmol, 1.0 equiv) was dissolved in anhydrous EtOAc (0.52 mL) and absolute EtOH (0.31 mL). To this solution was then added a solution of potassium bisulfite (1 M in H<sub>2</sub>O, 0.124 mL, 0.124 mmol, 1.0 equiv). The reaction vessel was then capped and heated to 50 °C, stirring for 3 h. Afterwards, the reaction mixture was filtered to remove any solids and the filtrate further flushed with anhydrous EtOH. The combined filtrate and flow-through was dried in vacuo. The remaining residue was then redissolved in *i*PrOH and co-evaporated (3 ×) to remove any residual water. Trituration by addition with Et<sub>2</sub>O followed by sonication furnishes a white precipitate. The suspension was then centrifuged (*ca.* 1000 × *g*) and the supernatant decanted, and further repeated once more. The white precipitate was resuspended once more in a solution of 1/2 EtOAc/Et<sub>2</sub>O, followed by mixing for 5 min and subsequent centrifugation (*ca.* 1000 × *g*). Decanting of the supernatant and drying overnight furnished the product as a white solid (0.058 g, 0.112 mmol, 90%) with no further purification required.

IR (DCM cast film,  $\nu_{\max}$  / cm<sup>-1</sup>) 3291, 2956, 2934, 2870, 1673, 1523, 1454, 1255, 1213, 1189, 1038

<sup>1</sup>H NMR (700 MHz, DMSO-*d*<sub>6</sub>)  $\delta$ H 7.65—7.53 (1H, m), 7.49—7.41 (1H, m), 7.38—7.26 (5H, m), 5.41 (1H, d, *J* = 6.3 Hz), 5.25 (1H, d, *J* = 6.1 Hz), 5.06—4.94 (2H, m), 4.25—3.80 (3H, m), 3.15—3.05 (1H, m), 3.03—2.96 (1H, m), 2.23—2.04 (2H, m), 2.02—1.51 (4H, m),

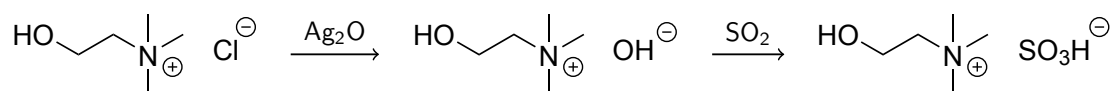
1.50—1.39 (2H, m), 0.84 (6H, app dt,  $J = 17.1, 6.3$  Hz)

$^{13}\text{C}$  NMR (175 MHz, DMSO- $d_6$ )  $\delta$ C 179.2, 171.8, 156.0, 137.1, 128.2, 127.6, 127.6, 83.7, 65.3, 53.6, 48.6, 40.7, 40.4, 37.8, 32.0, 27.5, 24.2, 23.1, 21.5

OR:  $[\alpha]_{\text{D}}^{26} = -10.15$  ( $c = 0.63$ ,  $\text{H}_2\text{O}$ )

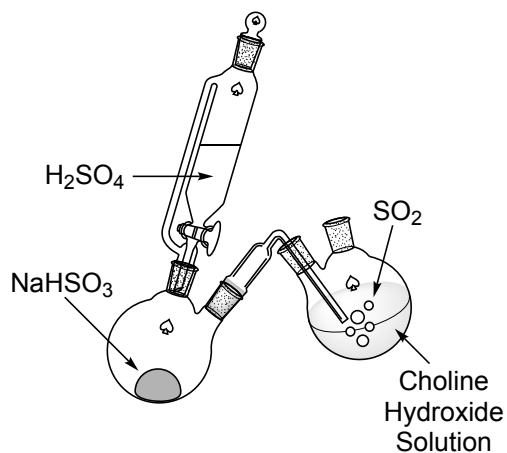
HRMS: (ESI) Calcd for  $\text{C}_{21}\text{H}_{30}\text{N}_3\text{O}_8\text{S}$   $[\text{M}^*]^-$  484.1759, found 484.1758

### Production of Choline Bisulfite



To a solution of choline chloride (1 M in  $\text{H}_2\text{O}$ , 1.00 mL, 1 mmol, 1.0 equiv) was deposited  $\text{Ag}_2\text{O}$  (0.116 g, 0.5 mmol, 0.5 equiv). The mixture was then stirred at room temperature for 1 h. Subsequently, the mixture was filtered to remove the silver precipitate, and the pH of the filtrate checked ( $>10$ ). Gaseous  $\text{SO}_2$  was then bubbled through the solution until a neutral pH was observed ( $\leq 7$ ). This freshly prepared 1 M solution of choline bisulfite was then used with no further refinement needed.

### Production of $\text{SO}_2$ Gas

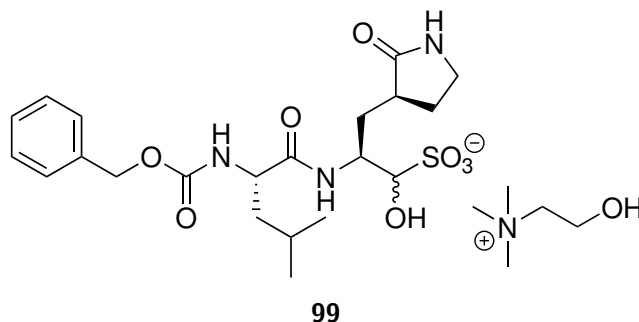


In a 2-neck round bottom flask was deposited solid  $\text{NaHSO}_3$ , and attached to it was an addition funnel containing concentrated  $\text{H}_2\text{SO}_4$ . Dropwise addition of  $\text{H}_2\text{SO}_4$  to solid

NaHSO<sub>3</sub> then resulted in rapid liberation and evolution of SO<sub>2</sub> gas. This gas was captured and bubbled through tubing into a solution of choline hydroxide to furnish choline bisulfite.

**Choline (2*S*)-2-((*S*)-2-(((benzyloxy)carbonyl)amino)-4-methylpentanamido)-1-hydroxy-3-((*S*)-2-oxopyrrolidin-3-yl)propane-1-sulfonate**

(99)



GC373 (**62**) (0.100 g, 0.248 mmol, 1.0 equiv) was dissolved in 1.03 mL of anhydrous EtOAc and 0.62 mL of absolute EtOH. To this solution was then added a solution of choline bisulfite (1 M in H<sub>2</sub>O, 0.248 mL, 0.248 mmol, 1.0 equiv). The reaction vessel was then capped and heated to 50 °C, stirring for 3 h. Afterwards, the reaction mixture was filtered to remove any solids and the filtrate further flushed with anhydrous EtOH. The combined filtrate and flow-through was dried *in vacuo*. The remaining residue was then redissolved in *i*PrOH and co-evaporated (3 ×) to remove any residual water. Trituration by addition with Et<sub>2</sub>O followed by sonication furnishes a white precipitate. The suspension was then centrifuged (*ca.* 1000 × *g*) and the supernatant decanted, and further repeated once more. The white precipitate was resuspended once more in a solution of 1/2 EtOAc/Et<sub>2</sub>O, followed by mixing for 5 min and subsequent centrifugation (*ca.* 1000 × *g*). Decanting of the supernatant and drying overnight furnishes the product as a white solid (0.108 g, 0.183 mmol, 74%) with no further purification required.

IR (DCM cast film,  $\nu_{\max}$  / cm<sup>-1</sup>) 3289, 3037, 2956, 2871, 1675, 1528, 1496, 1469, 1455, 1386, 1368, 1336, 1245, 1203, 1172, 1116, 1086, 1033



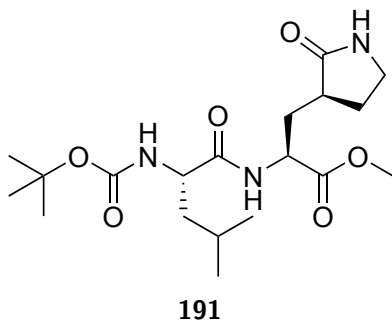
<sup>1</sup>H NMR (700 MHz, DMSO-d<sub>6</sub>) δH 7.64—7.54 (1H, m), 7.50—7.41 (1H, m), 7.38—7.24 (5H, m), 5.32 (1H, d, *J* = 6.4 Hz), 5.29 (1H, s), 5.20 (1H, d, *J* = 5.8 Hz), 5.06—4.94 (2H, m), 4.25—3.85 (3H, m), 3.85—3.79 (2H, m), 3.41—3.36 (2H, m), 3.09 (10H, app s), 3.03—2.96 (1H, m), 2.22—2.03 (2H, m), 2.03—1.51 (4H, m), 1.51—1.38 (2H, m), 0.84 (6H, app dt, *J* = 17.4, 6.2 Hz)

<sup>13</sup>C NMR (175 MHz, DMSO-d<sub>6</sub>) δC 156.0, 137.1, 128.2, 127.6, 84.5, 67.0, 65.3, 55.1, 53.5, 53.1, 48.6, 40.7, 37.7, 32.0, 30.0, 27.5, 24.2, 23.0, 21.5 (2 carbonyls and 1 aromatic quaternary carbon not observed)

OR: [α]<sub>D</sub><sup>26</sup> = -34.64 (c = 0.28, H<sub>2</sub>O)

HRMS: (ESI) Calcd for C<sub>21</sub>H<sub>30</sub>N<sub>3</sub>O<sub>8</sub> [M<sub>a</sub>]<sup>-</sup> 484.1759, found 484.1752; Calcd for C<sub>5</sub>H<sub>14</sub>NO [M<sub>c</sub>]<sup>+</sup> 104.1070, found 104.1070

**Methyl (*S*)-2-((*S*)-2-((*tert*-butoxycarbonyl)amino)-4-methylpentanamido)-3-((*S*)-2-oxopyrrolidin-3-yl)propanoate**  
**(191)**



**191** was prepared from **66**, following the same general procedure as that of **167**, substituted with the appropriate building block and employing noncritical variations in procedure to furnish a crude product.

Purification: Flash column chromatography over silica, eluent system of 3/97 MeOH/EtOAc

TLC: R<sub>f</sub> = 0.38, 4/96 MeOH/EtOAc

Appearance: White foam.

Yield: 87%

IR (DCM cast film,  $\nu_{\max}$  /  $\text{cm}^{-1}$ ) 3287, 2956, 2936, 1749, 1659, 1527, 1438, 1366, 1269, 1171, 1046

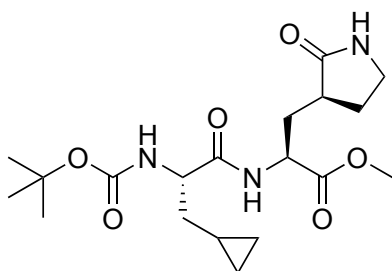
$^1\text{H}$  NMR (700 MHz,  $\text{CDCl}_3$ )  $\delta$ H 7.64 (1H, d,  $J = 6.5$  Hz), 6.44 (1H, s), 5.05 (1H, d,  $J = 8.0$  Hz), 4.54—4.47 (1H, m), 4.29—4.21 (1H, m), 3.71 (3H, s), 3.37—3.27 (2H, m), 2.47—2.36 (2H, m), 2.24—2.15 (1H, m), 1.90—1.78 (2H, m), 1.76—1.68 (1H, m), 1.68—1.61 (1H, m), 1.50—1.45 (1H, m), 1.42 (9H, s), 0.95 (6H, app t,  $J = 5.8$  Hz)

$^{13}\text{C}$  NMR (175 MHz,  $\text{CDCl}_3$ )  $\delta$ C 179.7, 173.2, 172.2, 155.6, 113.0, 79.8?, 53.0, 52.4, 51.2, 42.2, 40.4, 38.6, 38.3, 33.2, 28.3, 28.3, 24.7, 22.9, 22.2

OR:  $[\alpha]_{\text{D}}^{26} = -11.91$  ( $c = 0.92$ , DCM)

HRMS: (ESI) Calcd for  $\text{C}_{19}\text{H}_{33}\text{N}_3\text{NaO}_6$   $[\text{M} + \text{Na}]^+$  422.2262, found 422.2261

**Methyl (*S*)-2-((*S*)-2-((*tert*-butoxycarbonyl)amino)-3-cyclopropylpropanamido)-3-((*S*)-2-oxopyrrolidin-3-yl)propanoate**  
**(192)**



**192**

**192** was prepared from **66**, following the same general procedure as that of **167**, substituted with the appropriate building block and employing noncritical variations in procedure to furnish a crude product.

Purification: Flash column chromatography over silica, eluent system of pure EtOAc.

TLC:  $R_f = 0.43$ , 5/95 MeOH/EtOAc

Appearance: White foam.

Yield: 98%

IR (DCM cast film,  $\nu_{\max}$  /  $\text{cm}^{-1}$ ) 3405, 3295, 3004, 2978, 2935, 2864, 1742, 1685, 1524, 1271, 1170

$^1\text{H}$  NMR (400 MHz,  $\text{CDCl}_3$ )  $\delta$ H 7.56—7.41 (1H, m), 6.80 (1H, s), 5.34—5.13 (1H, m), 4.77—4.49 (1H, m), 4.26—4.05 (1H, m), 3.73 (3H, s), 3.42—3.27 (2H, m), 2.56—2.26 (2H, m), 2.24—2.10 (1H, m), 1.96—1.78 (2H, m), 1.76—1.65 (1H, m), 1.65—1.52 (1H, m), 1.44 (9H, s), 0.84—0.67 (1H, m), 0.54—0.42 (2H, m), 0.17—0.07 (2H, m)

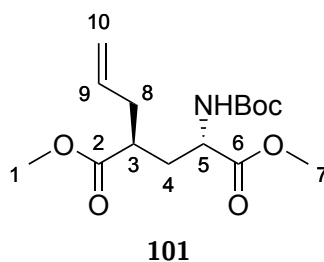
$^{13}\text{C}$  NMR (100 MHz,  $\text{CDCl}_3$ )  $\delta$ C 172.1, 79.4, 55.1, 52.2, 40.3, 37.1, 32.7, 29.1, 28.5, 27.9, 27.8, 24.5, 7.2, 4.8, 3.5 (some carbonyls not shown)

OR:  $[\alpha]_{\text{D}}^{26} = -6.53$  ( $c = 0.19$ , DCM)

HRMS: (ESI) Calcd for  $\text{C}_{19}\text{H}_{31}\text{N}_3\text{NaO}_6$   $[\text{M} + \text{Na}]^+$  420.2105, found 420.2106

## 7.9 Chapter 4 Synthetic Procedures

### Dimethyl (2*S*,4*S*)-2-allyl-4-((*tert*-butoxycarbonyl)-amino)pentanedioate (101)



**Small Scale.** This procedure was adapted from the literature.<sup>86</sup> Commercially available Boc-L-glutamate dimethyl ester (0.750 g, 2.74 mmol, 1.0 equiv) was dissolved in 11.0 mL of freshly distilled THF in a flame-dried 50 mL round-bottom flask under an argon atmosphere. The solution was then cooled to  $-78\text{ }^\circ\text{C}$ , and LiHMDS (1 M in THF, 5.92 mL, 5.92 mmol, 2.16 equiv) was added dropwise over 5 min. The reaction mixture was then allowed to incubate at  $-78\text{ }^\circ\text{C}$  for an additional 1 h. Allyl bromide (0.710 mL, 8.22 mmol, 3.0 equiv) was then added dropwise over a period of 30 min, and the reaction mixture became a light

yellow colour. The reaction mixture was checked by TLC after 2 h, and the starting material was found to be fully consumed. The reaction was quenched via addition of HCl (1 M, 7.5 mL) and subsequently extracted with EtOAc ( $3 \times 35$  mL). The combined EtOAc layers were washed with H<sub>2</sub>O ( $2 \times 35$  mL) and brine ( $1 \times 35$  mL). The organic layer was then dried over MgSO<sub>4</sub>, filtered, and concentrated to furnish a light yellow oil as a crude. The material was then purified by flash chromatography over silica, using an eluent system of 15/85 EtOAc/Hexane. Product elution was monitored by KMnO<sub>4</sub> staining ( $R_f = 0.44$ , 30/70 EtOAc/Hexane). Concentration of product fractions furnished a clear, slightly yellow oil as the desired compound (0.830 g, 2.63 mmol, 96% yield).

**Large Scale.** Commercially available Boc-L-glutamate dimethyl ester (10.00 g, 36.32 mmol, 1.0 equiv) was dissolved in freshly distilled THF (134.5 mL) under an argon atmosphere in a flame-dried 500 mL round-bottom flask. The reaction mixture was then cooled to -78 °C, and LiHMDS (1 M in THF, 79.90 mL, 79.90 mmol, 2.2 equiv) was added dropwise. The reaction mixture was then allowed to stir at -78 °C for 1 h. Next, allyl bromide (9.42 mL, 109 mmol, 3.0 equiv) was added dropwise over a period of 15 min. The reaction mixture was then stirred at -78 °C for 4 h, and a check by TLC showed minimal starting material remaining at the end of this period. The reaction mixture was then diluted with sat. NH<sub>4</sub>Cl(aq) (75 mL) to quench the reaction. The reaction mixture was then warmed to room temperature and diluted with EtOAc (75 mL). The layers were separated, and the aqueous layer was then extracted with additional EtOAc ( $2 \times 75$  mL). The combined EtOAc layers were washed with H<sub>2</sub>O ( $2 \times 75$  mL) and brine ( $1 \times 75$  mL), then dried over MgSO<sub>4</sub>. Filtration and subsequent concentration of the organic layer then furnished a yellow oil as a crude product. The material was purified by flash chromatography over silica using an eluent system of 15/85 EtOAc/Hexane. Product elution was monitored by KMnO<sub>4</sub> ( $R_f = 0.15$ , 15/85 EtOAc/Hexane). Concentration of product fractions furnished a light yellow oil as the desired product (10.34 g, 32.78 mmol, 90% yield).

IR (DCM cast film,  $\nu_{\max}$  / cm<sup>-1</sup>) 3370, 3080, 2979, 2954, 1739, 1718, 1516, 1440, 1169.

<sup>1</sup>H NMR (700 MHz, CDCl<sub>3</sub>)  $\delta$ H 5.75—5.65 (1H, m, H9), 5.115.02 (2H, m, H10), 4.95 (1H,

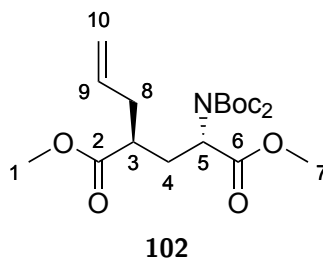
d,  $J = 9.8$  Hz, NH), 4.41–4.29 (1H, m, H5), 3.72 (3H, s, H7), 3.66 (3H, s, H1), 2.57 (1H, app quint,  $J = 6.9$  Hz, H3), 2.41–2.27 (2H, m, H4), 2.00 (2H, app t,  $J = 7.1$  Hz, H8), 1.44 (9H, s,  $3 \times \text{Boc-CH}_3$ ).

$^{13}\text{C}$  NMR (175 MHz,  $\text{CDCl}_3$ )  $\delta\text{C}$  175.5 (C2), 172.9 (C6), 155.4 (Boc-C=O), 134.4 (C9), 117.7 (C10), 80.1 (Boc-4° C), 52.4 (C7), 52.2 (C5), 51.8 (C1), 41.9 (C3), 36.5 (C4), 33.8 (C8), 28.3 (Boc-CH<sub>3</sub>).

OR  $[\alpha]_{\text{D}}^{26} = +74.42$  ( $c = 0.23$ , DCM).

HRMS (ESI) Calcd for  $\text{C}_{15}\text{H}_{25}\text{NNaO}_6$   $[\text{M} + \text{Na}]^+$  338.1574, found 338.1570.

### Dimethyl (2*S*,4*S*)-2-allyl-4-(bis(*tert*-butoxycarbonyl)amino)pentanedioate (**102**)



**Small Scale.** This procedure was adapted from the literature.<sup>102,160</sup> Compound **101** (3.00 g, 9.51 mmol, 1.0 equiv) was dissolved in MeCN (31.7 mL) in a flame-dried 100 mL round-bottom flask. To this were successively added DMAP (0.230 g, 1.90 mmol, 0.2 equiv) and  $\text{Boc}_2\text{O}$  (8.30 g, 38.1 mmol, 4.0 equiv). The reaction mixture then quickly changed colour to a light orange and was allowed to stir at room temperature. A check by TLC at 94 h showed near total consumption of starting material. The reaction mixture was then concentrated *in vacuo* to *ca.* 10 mL to remove the MeCN. After concentration to a minimal volume, the material was partitioned between *ca.* 75 mL each of EtOAc and 1 M citric acid, then separated. The EtOAc layer was washed once more with  $\text{H}_2\text{O}$  (75 mL), then once with brine (75 mL). The EtOAc layer was then dried over  $\text{Na}_2\text{SO}_4$  and concentrated to furnish a crude, dark orange oil. This material was purified by flash chromatography using an eluent system of 15/85 EtOAc/Hexane. Product elution was monitored by TLC

and  $\text{KMnO}_4$  staining ( $R_f = 0.29$ , 15/85 EtOAc/Hexane). Concentration of product fractions furnishes a yellow oil as the desired product (3.63 g, 8.74 mmol, 92% yield).

**Large Scale.** Compound **101** (9.500 g, 30.12 mmol, 1.0 equiv) was deposited in a flame-dried 250 mL round-bottom flask and dissolved in freshly distilled MeCN (100 mL). DMAP (0.740 g, 6.02 mmol, 0.2 equiv) and  $\text{Boc}_2\text{O}$  (26.30 g, 120.5 mmol, 4.0 equiv) were then sequentially added under an argon atmosphere. The reaction mixture was then capped under an argon atmosphere and allowed to stir at room temperature, changing to a yellow colour. After 99 h, a TLC check of the reaction mixture showed total consumption of starting material. The MeCN was removed by concentrating the reaction mixture *in vacuo* to a minimal volume (ca. 30 mL) and was then partitioned between ca. 250 mL each of EtOAc and 1 M citric acid. The layers were separated, and the aqueous layer was then extracted with additional EtOAc ( $2 \times 250$  mL). The combined EtOAc layers were then washed with  $\text{H}_2\text{O}$  ( $1 \times 250$  mL) and brine ( $1 \times 250$  mL), then dried over  $\text{Na}_2\text{SO}_4$ . Concentration *in vacuo* then furnishes a dark yellow oil. A TLC of this crude material showed only product ( $R_f = 0.29$ , 15/85 EtOAc/Hexane,  $\text{KMnO}_4$  staining), along with a spot on the baseline. The crude oil (crude mass ca. 15 g) was deposited onto a silica plug (silica mass ca. 135 g) and eluted with 1.25 L of eluent (15/85 EtOAc/Hexane). Total elution was monitored by TLC. Concentration of product fractions furnished a yellow oil as the desired product (12.51 g, 30.12 mmol, >99% yield).

IR (DCM cast film,  $\nu_{\text{max}} / \text{cm}^{-1}$ ) 3079, 2981, 2953, 1715, 1717, 1703, 1369, 1167, 1145.

$^1\text{H}$  NMR (700 MHz,  $\text{CDCl}_3$ )  $\delta$ H 5.73 (1H, ddt,  $J = 16.9, 9.9, 7.0$  Hz, H9), 5.07 (1H, dq,  $J = 17.2, 1.6$  Hz, H10), 5.05—5.01 (1H, m, H10), 4.96 (1H, dd,  $J = 8.9, 5.5$  Hz, H5), 3.71 (3H, s, H7), 3.65 (3H, s, H1), 2.59 (1H, ttt,  $J = 14.1, 8.26, 5.9$  Hz, H3), 2.39—2.33 (1H, m, H4), 2.31—2.23 (3H, m, H4, H8), 1.50 (18H, s,  $6 \times \text{Boc-CH}_3$ ).

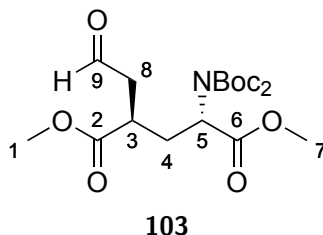
$^{13}\text{C}$  NMR (175 MHz,  $\text{CDCl}_3$ )  $\delta$ C 175.4 (C2), 171.1 (C6), 151.8 (Boc-C=O), 134.9 (C9), 117.4 (C10), 83.3 (Boc-4° C), 56.6 (C5), 52.3 (C7), 51.7 (C1), 42.8 (C3), 36.7 (C4), 32.2 (C8), 28.0 (Boc- $\text{CH}_3$ ).

OR  $[\alpha]_{\text{D}}^{26} = -21.81$  ( $c = 0.54$ , DCM).

HRMS (ESI) Calcd for C<sub>20</sub>H<sub>33</sub>NNaO<sub>8</sub> [M + Na]<sup>+</sup> 438.2098, found 438.2091.

## Dimethyl

### (2*S*,4*R*)-2-(bis(*tert*-butoxycarbonyl)amino)-4-(2-oxoethyl)-pentanedioate (**103**)



**Small Scale.** This procedure was adapted from the literature.<sup>161</sup> Compound **102** (0.166 g, 0.400 mmol, 1.0 equiv) was dissolved in a mixture of dioxane/H<sub>2</sub>O (3:1, 4.00 mL) in a 25 mL round-bottom flask. To this solution were added 2,6-lutidine (0.093 mL, 0.800 mmol, 2.0 equiv), OsO<sub>4</sub> (0.002 g, 0.008 mmol, 0.02 equiv), and NaIO<sub>4</sub> (0.342 g, 1.60 mmol, 4.0 equiv) in succession. The reaction mixture was then capped with a septa and allowed to stir at room temperature, quickly turning into a slurry. After 2 h, the reaction mixture was checked by TLC (30/70 EtOAc/Hexane), showing consumption of all starting material. The reaction mixture was then diluted with *ca.* 25 mL each of DCM and H<sub>2</sub>O, then separated. The H<sub>2</sub>O layer was further extracted with DCM (2 × 25 mL), and the combined DCM layers were washed with brine (1 × 25 mL). The DCM layer was dried over Na<sub>2</sub>SO<sub>4</sub> and concentrated to furnish a crude that turned black in colouration. The crude material was purified via flash chromatography using an eluent system of 20/80 EtOAc/Hexane. The black impurity was found to stick to the baseline of the silica. Product elution was monitored by TLC and KMnO<sub>4</sub> staining (R<sub>f</sub> = 0.29, 30/70 EtOAc/Hexane). Concentration of product fractions and co-evaporation with Et<sub>2</sub>O furnishes an oil (0.167 g, 0.400 mmol, >99% yield).

**Large Scale.** Compound **102** (12.00 g, 28.88 mmol, 1.0 equiv) was dissolved in a mixture of dioxane/H<sub>2</sub>O (3:1, 290 mL) in a 500 mL round-bottom flask. To this solution were added 2,6-lutidine (6.69 mL, 57.8 mmol, 2.0 equiv), OsO<sub>4</sub> (0.147 g, 0.578 mmol, 0.02 equiv), and NaIO<sub>4</sub> (24.71 g, 115.5 mmol, 4.0 equiv) in succession, and the reaction mixture was

capped with a septa. A check by TLC (30/70 EtOAc/Hexane) after 3 h showed complete consumption of starting material. The reaction mixture was then diluted with *ca.* 1 L each of DCM and H<sub>2</sub>O, and the layers were separated. The H<sub>2</sub>O layer was further extracted with DCM (2 × 1 L), and the combined DCM layers were washed with brine (1 × 1L). Drying over Na<sub>2</sub>SO<sub>4</sub> and concentration furnished a crude dark brown oil. The crude material (crude mass *ca.* 25 g) was loaded onto a silica plug (silica mass *ca.* 130 g) and eluted using 1.4 L of 15/85 EtOAc/Hexane, with elution completion being confirmed by TLC (R<sub>f</sub> = 0.29, 30/70 EtOAc/Hexane). Concentration of product solution furnishes a brown-black oil after co-evaporation with Et<sub>2</sub>O (11.57 g, 27.71 mmol, 96% yield).

IR (DCM cast film,  $\nu_{\max}$  / cm<sup>-1</sup>) 2981, 2945, 1795, 1743, 1703, 1437, 1369, 1251, 1170, 1146, 1122.

<sup>1</sup>H NMR (700 MHz, CDCl<sub>3</sub>)  $\delta$ H 9.74 (1H, s, H9), 4.99 (1H, dd, *J* = 9.3, 5.5 Hz, H5), 3.71 (3H, s, H7), 3.69 (3H, s, H1), 2.99—2.94 (1H, m, H3), 2.88 (1H, ddd, *J* = 18.1, 9.1, 1.1 Hz, H8), 2.71 (1H, dd, *J* = 18.1, 4.4 Hz, H8), 2.36—2.30 (1H, m, H4), 2.29—2.24 (1H, m, H4), 1.49 (18H, s, 6 × Boc-CH<sub>3</sub>).

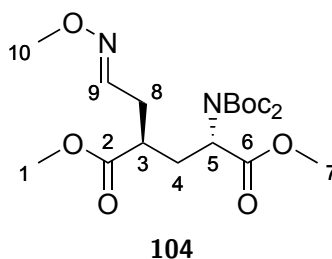
<sup>13</sup>C NMR (175 MHz, CDCl<sub>3</sub>)  $\delta$ C 199.0 (by HSQC, C9), 174.7 (C2), 170.8 (C6), 151.9 (Boc-C=O), 83.6 (Boc-4° C), 55.9 (C5), 52.4 (C7), 52.2 (C1), 45.1 (C8), 36.4 (C3), 32.0 (C4), 28.0 (Boc-CH<sub>3</sub>).

OR  $[\alpha]_{\text{D}}^{26} = -25.54$  (*c* = 0.40, DCM).

HRMS (ESI) Calcd for C<sub>19</sub>H<sub>31</sub>NNaO<sub>9</sub> [M + Na]<sup>+</sup> 440.1891, found 440.1888.



**Dimethyl (2*S*,4*R*)-2-(bis(*tert*-butoxycarbonyl)amino)-4-(2-(methoxyimino)ethyl)pentanedioate**  
**(104)**



**Small Scale.** Compound **103** (0.050 g, 0.120 mmol, 1.0 equiv), MeONH<sub>2</sub> · HCl (0.012 g, 0.144 mmol, 1.2 equiv), and NaOAc (0.020 g, 0.240 mmol, 2.0 equiv) were charged into a 5 mL round-bottom flask, to which dry DCM (0.3 mL) was added. The flask was capped and stirred at room temperature for 16 h. A check by TLC (25/75 EtOAc/Hexane) at this point showed total consumption of starting material. The reaction mixture was then quenched by addition of *ca.* 5 mL of sat. NaHCO<sub>3</sub>, followed by dilution with *ca.* 5 mL of EtOAc. The layers were then separated, and the aqueous layer was further extracted with EtOAc (2 × 5 mL). The combined EtOAc layers were washed sequentially with sat. NaHCO<sub>3</sub> (2 × 5 mL), H<sub>2</sub>O (2 × 5 mL), and brine (1 × 5 mL), then dried over Na<sub>2</sub>SO<sub>4</sub>. Concentration of the EtOAc solution then furnishes a yellow oil as a crude. The material was found to not require further purification (R<sub>f</sub> = 0.28, 25/75 EtOAc/Hexane). Concentration of product fractions furnishes a clear, colourless oil as the desired product (mixture of imine isomers, 0.054 g, 0.120 mmol, >99% yield).

**Large Scale.** Compound **103** (4.18 g, 10.00 mmol, 1.0 equiv), MeONH<sub>2</sub> · HCl (1.00 g, 12.00 mmol, 1.2 equiv), and NaOAc (1.64 g, 20.00 mmol, 2.0 equiv) were added to a 50 mL round-bottom flask and dissolved with freshly distilled DCM (11.7 mL). The vessel was then capped with a septa and stirred at room temperature for 16 h. A check by TLC (25/75 EtOAc/Hexane) showed total consumption of starting material, so the reaction mixture was diluted with *ca.* 150 mL each of EtOAc and sat. NaHCO<sub>3</sub>, then separated. The aqueous

layer was further extracted with EtOAc ( $2 \times 150$  mL). The combined EtOAc layers were then washed with sat.  $\text{NaHCO}_3$  ( $2 \times 150$  mL),  $\text{H}_2\text{O}$  ( $2 \times 150$  mL), and brine ( $1 \times 150$  mL). The EtOAc layer was then dried over  $\text{Na}_2\text{SO}_4$  and concentrated to furnish a yellow oil (4.47 g, 10.00 mmol, >99% yield). A check of this crude material by NMR showed that it was clean and suitable for subsequent use without further purification.

IR (DCM cast film,  $\nu_{\text{max}} / \text{cm}^{-1}$ ) 2981, 2953, 1797, 1744, 1437, 1369, 1274, 1169, 1146.

$^1\text{H}$  NMR (700 MHz,  $\text{CDCl}_3$ )  $\delta$ H 7.33 (0.6H, app t,  $J = 6.0$  Hz, H9, Isomer A), 6.67 (0.4H, app t,  $J = 5.4$  Hz, H9, Isomer B), 5.02-4.97 (1H, m, H5), 3.86 (1.3H, s, H10, Isomer B), 3.78 (1.7H, s, H10, Isomer A), 3.71 (3H, s, H7), 3.68 (1.3H, s, H1, Isomer B), 3.67 (1.7H, s, H1, Isomer A), 2.78—2.69 (1H, m, H3), 2.68—2.39 (2H, m, H8), 2.36—2.23 (2H, m, H4), 1.50 (18H, s,  $6 \times \text{Boc-CH}_3$ ).

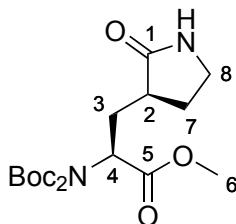
$^{13}\text{C}$  NMR (175 MHz,  $\text{CDCl}_3$ )  $\delta$ C 174.7 (C2, Isomer B), 174.7 (C2, Isomer A), 170.9 (C6, Isomer B), 170.9 (C6, Isomer A), 151.7 (Boc-C=O), 148.0 (C9, Isomer B), 147.4 (C9, Isomer A), 83.6 (Boc- $4^\circ$  C), 61.8 (C10, Isomer B), 61.5 (C10, Isomer A), 56.4 (C5, Isomer B), 56.3 (C5 Isomer A), 52.3 (C7), 52.1 (C1, Isomer B), 52.0 (C1, Isomer A), 40.6 (C3, Isomer A), 40.2 (C3, Isomer B), 32.3 (C4, Isomer B), 32.2 (C4, Isomer A), 31.9 (C8, Isomer A), 28.1 (C8, Isomer B), 28.0 (Boc- $\text{CH}_3$ ).

OR  $[\alpha]_{\text{D}}^{26} = -20.24$  ( $c = 0.99$ , DCM).

HRMS (ESI) Calcd for  $\text{C}_{20}\text{H}_{34}\text{N}_2\text{NaO}_9$   $[\text{M} + \text{Na}]^+$  469.2157, found 469.2153.

Methyl

(*S*)-2-(bis(*tert*-butoxycarbonyl)amino)-3-((*S*)-2-oxopyrrolidin-3-yl)propanoate  
(105)



**Small Scale.** This procedure was adapted from the literature.<sup>162,163</sup> Compound **104** (0.080 g, 0.179 mmol, 1.0 equiv), Raney Nickel (W.R. Grace and Co. Raney 2800, *ca.* 0.080 g), NaHCO<sub>3</sub> (saturated solution at 21 °C, 0.16 mL, *ca.* 1 equiv), 15-crown-5 ether (0.036 mL, 0.179 mmol, 1.0 equiv), and MeOH (7.0 mL) were added to a vial (Chemglass CG4907-02) with a stir bar and custom cap equipped with a glass frit. The mixture was then placed in a high pressure reaction vessel (Parr Series 4750, 200 mL), stirred, and subjected to purge-charge cycles (3 ×) with H<sub>2</sub>. The reaction mixture was then subjected to H<sub>2</sub> (800 psi, 41372 Torr) for 17.5 h. A check of the reaction mixture at this point by LCMS showed consumption of starting material. The catalyst was removed using a magnetic source (computer hard-drive magnet), and the reaction mixture was then partitioned between EtOAc (21 mL) and H<sub>2</sub>O (21 mL), and the layers separated. The H<sub>2</sub>O layer was further extracted with EtOAc (2 × 21 mL), and the combined EtOAc layers were washed with brine (1 × 21 mL). Drying over Na<sub>2</sub>SO<sub>4</sub> and removal of solvent furnish a yellow crude. This material was purified by flash chromatography, using an eluent system of 85/15 EtOAc/Hexane. Product elution was monitored by TLC and KMnO<sub>4</sub> staining (R<sub>f</sub> = 0.21, 85/15 EtOAc/Hexane, requires prolonged heating to visualize with KMnO<sub>4</sub>). Concentration of product fractions furnishes a clear, colourless oil (0.069 g, 0.179 mmol, >99% yield).

**Large Scale.** Compound **104** (6.00 g, 13.4 mmol, 1.0 equiv), Raney Nickel (W.R. Grace and Co. Raney 2800, *ca.* 6.00 g), NaHCO<sub>3</sub> (saturated solution at 21 °C, 12.0 mL, *ca.* 1 equiv),

and MeOH (538 mL) were added to a glass bottle equipped with a fritted cap. This mixture was then placed within a high pressure reaction vessel, stirred, and subjected to purge-charge cycles with H<sub>2</sub> (3 ×). The reaction mixture was then subjected to high pressure H<sub>2</sub> (800 psi, 41372 Torr). A check of the reaction mixture at 40 h by LCMS indicated the presence of fully reduced, but uncyclized, material. More NaHCO<sub>3</sub> (0.79 g, 9.41 mmol, 0.7 equiv) was added to the reaction, at which point intramolecular cyclization was found to proceed. The cyclization event was found to be sluggish at times, possibly as a result of localized effects, but the cyclization rate can be increased by addition of NaHCO<sub>3</sub> (up to 2.5 equiv) or by heating to 60 °C with no detrimental effects. The reaction was continually monitored by LCMS, and upon completion, the Raney Nickel was removed using a magnetic source (computer hard-drive magnet) and the solution was diluted with EtOAc (1.5 L) and H<sub>2</sub>O (1.5 L). The layers were separated, and the aqueous layer was further extracted using EtOAc (2 × 1 L). The combined organic layers were then washed with brine (1 × 1 L) and dried over Na<sub>2</sub>SO<sub>4</sub>. Concentration of the organic extracts then furnishes a yellow oil as a crude. The oil was then subjected to flash chromatography, using an eluent system of 85/15 EtOAc/Hexane. Product elution was monitored by TLC and KMnO<sub>4</sub> staining (R<sub>f</sub> = 0.21, 85/15 EtOAc/Hexane, prolonged heating required for visualization). Concentration of product fractions furnishes an oil (4.72 g, 12.20 mmol, 91% yield).

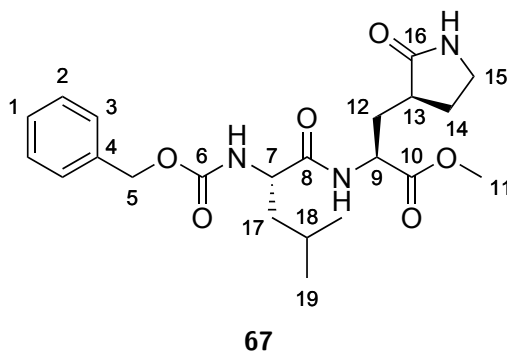
IR (DCM cast film,  $\nu_{\max}$  / cm<sup>-1</sup>) 3227, 2980, 2935, 1791, 1749, 1703, 1369, 1274, 1148, 1124. <sup>1</sup>H NMR (700 MHz, CDCl<sub>3</sub>)  $\delta$ H 5.54 (1H, s, NH), 5.04 (1H, dd,  $J$  = 10.1, 4.8 Hz, H4), 3.72 (3H, s, H6), 3.38—3.26 (2H, m, diastereotopic H8), 2.50 (1H, ddd,  $J$  = 14.7, 10.1, 3.7 Hz, diastereotopic H3), 2.41—2.32 (2H, m, H2, diastereotopic H7), 2.10 (1H, ddd,  $J$  = 14.7, 11.0, 4.8 Hz, diastereotopic H3), 1.88—1.78 (1H, m, diastereotopic H7), 1.51 (18H, s, 6 × Boc-CH<sub>3</sub>).

<sup>13</sup>C NMR (175 MHz, CDCl<sub>3</sub>)  $\delta$ C 179.2 (C1), 171.2 (C5), 152.1 (Boc-C=O), 83.5 (Boc-4° C), 56.2 (C4), 52.3 (C6), 40.5 (C8), 37.9 (C2), 31.8 (C3), 28.1 (C7), 28.0 (Boc-CH<sub>3</sub>).

OR  $[\alpha]_{\text{D}}^{26} = -30.29$  ( $c = 0.27$ , DCM).

HRMS (ESI) Calcd for C<sub>18</sub>H<sub>30</sub>N<sub>2</sub>NaO<sub>7</sub> [M + Na]<sup>+</sup> 409.1945, found 409.1943.

### Test reaction utilizing 105 - formation of compound (67)



Compound **105** (0.030 g, 0.078 mmol, 1.0 equiv) was dissolved in 2.0 mL of 50/50 DCM/TFA and allowed to deprotect for 1.5 h. The mixture was then concentrated *in vacuo* and co-evaporated with DCM (5 ×) to remove residual TFA. This oily material was then dissolved in 0.35 mL of DCM to furnish Solution 1. Cbz-Leu-OH (90% pure, 0.023 g, 0.078 mmol, 1.0 equiv) and HATU (0.030 g, 0.078 mmol, 1.0 equiv) were dissolved in 0.35 mL of DMF. To this were added HOAt (0.6 M solution in DMF, 0.013 mL, 0.008 mmol, 0.1 equiv) and finally DIPEA (0.041 mL, 0.233 mmol, 3.0 equiv). The mixture turned yellow at this point, forming Solution 2, and was allowed to incubate at room temperature for 5 min. Solution 1 was then added to Solution 2, and the reaction mixture was allowed to stir at room temperature for 1.5 h. The reaction mixture was then diluted with 7.5 mL each of EtOAc and H<sub>2</sub>O. The layers were separated, and the aqueous layer was further extracted with EtOAc (2 × 7.5 mL). The combined EtOAc layers were washed sequentially with sat. NaHCO<sub>3</sub> (2 × 7.5 mL), 1 M HCl (2 × 7.5 mL), and brine (1 × 7.5 mL). Drying over Na<sub>2</sub>SO<sub>4</sub>, followed by filtration and concentration, furnishes a crude yellow oil. The material was then purified by flash chromatography using EtOAc as the eluent. Product elution was monitored by TLC and KMnO<sub>4</sub> staining ( $R_f = 0.47$ , 5/95 MeOH/EtOAc). Concentration of product fractions furnishes a transparent oily film as the product (0.030 g, 0.069 mmol, 89%). All characterization data were found to match previously reported values.<sup>25</sup>

IR (DCM cast film,  $\nu_{\max}$  / cm<sup>-1</sup>) 3286, 2956, 2926, 2689, 1537, 1439, 1268.

$^1\text{H}$  NMR (700 MHz,  $\text{CDCl}_3$ )  $\delta$ H 7.88 (1H, d,  $J = 6.6$  Hz, NH), 7.37—7.27 (5H, m, H1, H2, H3), 6.31 (1H, s, NH), 5.44 (1H, d,  $J = 8.3$  Hz, NH), 5.09 (2H, s, H5), 4.50—4.42 (1H, m, H9), 4.39—4.31 (1H, m, H7), 3.72 (3H, s, H11), 3.35—3.23 (2H, m, H15), 2.47—2.30 (2H, m, H13, H14), 2.23—2.14 (1H, m, H12), 1.93—1.85 (1H, m, H12), 1.85—1.77 (1H, m, H14), 1.77—1.70 (1H, m, H18), 1.70—1.63 (1H, m, H17), 1.56—1.47 (1H, m, H17), 1.0—0.91 (6H, m, H19).

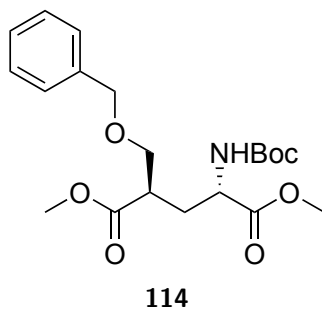
$^{13}\text{C}$  NMR (175 MHz,  $\text{CDCl}_3$ )  $\delta$ C 179.8 (C16), 171.9 (C8), 172.1 (C10), 152.1 (C6), 136.4 (C4), 128.5 (C2), 128.1 (C3), 128.0 (C1), 66.9 (C5), 53.4 (C7), 52.4 (C11), 51.6 (C9), 42.4 (C17), 40.5 (C15), 38.4 (C13), 32.9 (C12), 28.4 (C14), 24.7 (C18), 22.9 (H19), 22.1 (H19).

OR  $[\alpha]_{\text{D}}^{26} = -9.89$  ( $c = 0.38$ , DCM).

HRMS (ESI) Calcd for  $\text{C}_{22}\text{H}_{31}\text{N}_3\text{NaO}_6$   $[\text{M} + \text{Na}]^+$  456.2105, found 456.2102.

## 7.10 Chapter 5 Synthetic Procedures

Dimethyl (2*R*,4*S*)-2-((benzyloxy)methyl)-4-((*tert*-butoxycarbonyl)amino)pentanedioate (114)



Compound **99** (2.00 g, 7.26 mmol, 1.0 equiv) was deposited in a flame-dried round-bottom flask under argon and dissolved in dry THF (19.6 mL). The solution was cooled to  $-78$  °C and LiHMDS (1.0 M in THF, 15.25 mL, 15.26 mmol, 2.1 equiv) was added dropwise over 20 min. The reaction was then left to stir at  $-78$  °C for 30 min. Next, BOM-Cl (2.02 mL, 14.53 mmol, 2.0 equiv) was added over 20 min, and the reaction mixture was allowed to stir at  $-78$  °C for 3 h. The reaction mixture was then quenched

with 1 M HCl (60 mL) and diluted with EtOAc (60 mL). The layers were separated and the aqueous phase was further extracted with EtOAc (2 × 60 mL). The combined organic layers were washed sequentially with 1 M HCl (1 × 60 mL), H<sub>2</sub>O (1 × 60 mL), and brine (1 × 60 mL). The organic layers were then dried over Na<sub>2</sub>SO<sub>4</sub>, filtered, and concentrated *in vacuo* to furnish a crude yellow oil. This material was then purified by FCC using an eluent system of 15/85 EtOAc/Hexane, with product elution monitored by KMnO<sub>4</sub> staining (R<sub>f</sub> = 0.22, 25/75 EtOAc/Hexane). Concentration of product fractions furnished a clear, colourless oil as the desired product (1.69 g, 4.27 mmol, 58.8%).

IR (DCM cast film,  $\nu_{(\max)}$  / cm<sup>-1</sup>) 3369, 2978, 2954, 2874, 1740, 1716, 1514, 1438, 1367, 1250, 1216, 1167

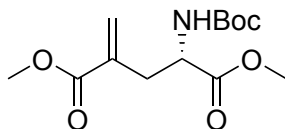
<sup>1</sup>H NMR (700 MHz, CDCl<sub>3</sub>)  $\delta$ H 7.40—7.27 (5H, m), 5.06 (1H, br s), 4.51 (2H, s), 4.35 (1H, br s), 3.76—3.67 (6H, m), 3.67—3.58 (1H, m), 2.83—2.77 (1H, m) 2.22—1.91 (3H, m), 1.43 (9H, s)

<sup>13</sup>C NMR (175 MHz, CDCl<sub>3</sub>)  $\delta$ C 174.1, 172.8, 155.4, 137.9, 128.4, 127.7, 127.6, 80.1, 73.2, 70.2, 52.4, 52.0, 51.8, 42.7, 31.8, 28.3

OR:  $[\alpha]_D^{26} = 4.97$  (c = 1.03, DCM)

HRMS (ESI) Calcd for C<sub>13</sub>H<sub>21</sub>NNaO<sub>6</sub> [M + Na]<sup>+</sup> 310.1261, found 310.1257.

### Dimethyl (*S*)-2-((*tert*-butoxycarbonyl)amino)-4-methylenepentanedioate (**119**)



**119**

**115** (0.077 g, 0.253 mmol, 1.0 equiv), *N*-hydroxyphthalimide (0.045 g, 0.278 mmol, 1.1 equiv), and PPh<sub>3</sub> (0.073 g, 0.278 mmol, 1.1 equiv) was dissolved in dry THF (2.5 mL) under argon and cooled to 0 °C. To this solution was added diethyl azodicarboxylate (0.044 mL, 0.278 mmol, 1.1 equiv). The solution was stirred at 0 °C for 1 h, then warmed to room

temperature and stirred for a further 3 h. The reaction mixture was then diluted with EtOAc (7.5 mL) and sat. NaHCO<sub>3</sub>. The layers were separated and the EtOAc layer was washed with NaHCO<sub>3</sub> (3 × 7.5 mL), then dried over Na<sub>2</sub>SO<sub>4</sub>. Concentration then furnishes a crude yellow oil. This material was then purified by flash column chromatography using an eluent system of 20/80 EtOAc/Hexane. Product elution was monitored by TLC and KMnO<sub>4</sub> staining (*R<sub>f</sub>* = 0.20, 20/80 EtOAc/Hexane). Concentration of product fractions furnished a colourless oil (0.056 g, 0.195 mmol, 77%).

IR (DCM cast film,  $\nu_{\text{max}}$  / cm<sup>-1</sup>) 3375, 2979, 2955, 1719, 1632, 1513, 1439, 1367, 1252, 1217, 1165, 1056, 1024

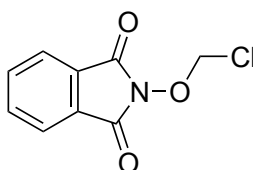
<sup>1</sup>H NMR (700 MHz, CDCl<sub>3</sub>)  $\delta$ H 6.27 (1H, s), 5.66 (1H, s), 5.17 (1H, d, *J* = 7.0 Hz), 4.52–4.44 (1H, m), 3.77 (3H, s), 3.73 (3H, s), 2.83 (1H, dd, *J* = 14.1, 5.6 Hz), 2.69 (1H, dd, *J* = 14.1, 8.1 Hz), 1.42 (9H, s)

<sup>13</sup>C NMR (175 MHz, CDCl<sub>3</sub>)  $\delta$ C 172.4, 166.2, 135.7, 128.7, 79.9, 53.0, 52.3, 52.2, 35.0, 28.3, 27.9

OR:  $[\alpha]_{\text{D}}^{26} = 11.50$  (*c* = 0.16, DCM)

HRMS (ESI) Calcd for C<sub>13</sub>H<sub>21</sub>NNaO<sub>6</sub> [M + Na]<sup>+</sup> 310.1261, found 310.1257.

## 2-(Chloromethoxy)isoindoline-1,3-dione (122)



**122**

This known compound was prepared according to a literature procedure.<sup>164</sup> *N*-hydroxyphthalimide (4.24 g, 26.00 mmol, 3.0 equiv) was suspended in CHCl<sub>3</sub> (200 mL). Next, CH<sub>2</sub>ClBr (17.35 mL, 258.80 mmol, 30.0 equiv) was added and the reaction mixture was heated at reflux for 30 min. Next Ag<sub>2</sub>O (2.00 g, 8.63 mmol, 1.0 equiv) was added and



the reaction was kept dark and refluxed with vigorous stirring for 16 h. Afterwards, the reaction mixture was filtered over celite and concentrated to furnish a crude white solid. This material was then loaded onto a silica column using DCM and purified by flash column chromatography using an eluent gradient of 10/90 → 20/80 EtOAc/Hexane. Product elution was monitored by TLC and KMnO<sub>4</sub> staining (*R<sub>f</sub>* = 0.25, 20/80 EtOAc/Hexane). Concentration of product fractions furnished a white solid (2.01 g, 9.50 mmol, 37%).

IR (DCM cast film,  $\nu_{\text{max}}$  / cm<sup>-1</sup>) 3497, 3102, 3048, 2978, 1789, 1739, 1609, 1467, 1373, 1327, 1267, 1186, 1126

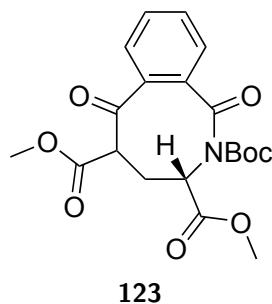
<sup>1</sup>H NMR (700 MHz, CDCl<sub>3</sub>)  $\delta$ H 7.92—7.85 (2H, m), 7.82-7.77 (2H, m), 5.88 (2H, s)

<sup>13</sup>C NMR (175 MHz, CDCl<sub>3</sub>)  $\delta$ C 162.9, 135.0, 128.8, 124.0, 83.7

HRMS (ESI) Calcd for C<sub>9</sub>H<sub>6</sub>ClNNaO<sub>3</sub> [M + Na]<sup>+</sup> 233.9928, found 233.9931.

## 2-(*tert*-Butyl) 3,5-dimethyl

### (3*S*)-1,6-dioxo-3,4,5,6-tetrahydrobenzo[*c*]azocine-2,3,5(1*H*)-tricarboxylate (123)



Compound **65** (0.050 g, 0.182 mmol, 1.0 equiv) was dissolved in freshly distilled THF (1.8 mL) in a flame-dried round bottom flask under an argon atmosphere. The solution was then cooled to -78 °C. LiHMDS (1.0 M in THF, 0.381 mL, 0.381 mmol, 2.1 equiv) was then added dropwise and the reaction mixture was allowed to incubate at -78 °C for 1 h. Next, a solution of **122** (0.076 g, 0.363, 2.0 equiv) in dry THF (0.2 mL) was added dropwise and the reaction mixture was allowed to stir for an additional 3 h at -78 °C. The

reaction mixture was then quenched with sat.  $\text{NH}_4\text{Cl}$  (*ca.* 4.0 mL) at  $-78\text{ }^\circ\text{C}$  and allowed to warm to room temperature. The reaction mixture was further diluted with EtOAc (6.0 mL) and the layers were separated. The aqueous layer was further extracted with EtOAc ( $2 \times 6$  mL) and the combined organic layers were then sequentially washed with sat.  $\text{NH}_4\text{Cl}$  ( $1 \times 6$  mL),  $\text{H}_2\text{O}$  ( $1 \times 6$  mL), and brine ( $1 \times 6$  mL). The organic layer was then dried over  $\text{Na}_2\text{SO}_4$  and concentrated to furnish a crude yellow material. The crude material was then purified by flash column chromatography using an eluent system of 25/75 EtOAc/Hexane. Product elution was monitored by TLC and  $\text{KMnO}_4$  staining ( $R_f = 0.16$ , 25/75 EtOAc/Hexane). Concentration of product fractions furnished a white solid (0.027 g, 0.066 mmol, 36%).

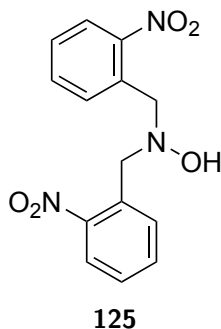
IR (DCM cast film,  $\nu_{(\text{max})}$  /  $\text{cm}^{-1}$ ) 3477, 2957, 2925, 2851, 1778, 1746, 1709, 1467, 1437, 1388, 1368, 1348, 1293, 1257, 1217, 1154, 1089

$^1\text{H}$  NMR (700 MHz,  $\text{CDCl}_3$ )  $\delta$ H 7.90 (1H, d,  $J = 8.2$  Hz), 7.85 (1H, d,  $J = 8.2$  Hz), 7.73 (1H, t,  $J = 7.4$  Hz), 7.57 (1H, t,  $J = 7.4$  Hz), 4.70 (1H, app d,  $J = 9.3$  Hz), 3.84 (3H, s), 3.81—3.75 (1H, m), 3.50 (3H, s), 2.92—2.81 (1H, m), 2.33 (1H, dd,  $J = 13.7, 7.1$  Hz), 0.96 (9H, s)

$^{13}\text{C}$  NMR (175 MHz,  $\text{CDCl}_3$ )  $\delta$ C 173.1, 168.2, 167.4, 151.7, 148.8, 134.4, 129.9, 128.6, 124.8, 122.2, 97.1, 82.3, 58.8, 53.3, 52.7, 52.3, 28.2, 27.5

HRMS (ESI) Calcd for  $\text{C}_{21}\text{H}_{26}\text{N}_2\text{NaO}_9$   $[\text{M} + \text{Na}]^+$  428.1316, found 428.1317.

### *N,N*-Bis(2-nitrobenzyl)hydroxylamine (125)



This known compound was synthesized using a method modified from literature.<sup>165</sup> Hydroxylamine hydrochloride (1.00 g, 14.39 mmol, 1.0 equiv) was dissolved in a minimal volume of H<sub>2</sub>O (*ca.* 2.0 mL) to form Solution 1. *O*-Nitrobenzylchloride (2.47 g, 14.39 mmol, 1.0 equiv) was dissolved in a minimal amount of absolute EtOH (*ca.* 40 mL) and K<sub>2</sub>CO<sub>3</sub> (1.00 g, 7.20 mmol, 0.5 equiv) was added, forming Solution 2. Solution 1 was then added to Solution 2 and the mixture was refluxed overnight. The reaction mixture was then cooled to room temperature and concentrated to a minimal volume *in vacuo* (*ca.* 5 mL). Next, the mixture was diluted with EtOAc (120 mL) and H<sub>2</sub>O (120 mL). The layers were separated and the aqueous layer was further extracted with EtOAc (2 × 120 mL). The combined organic layers were dried over Na<sub>2</sub>SO<sub>4</sub> and concentrated to furnish a crude yellow oil. This crude material was then purified by flash column chromatography using an eluent system of 25/75 EtOAc/Hexane. Product elution was monitored by TLC and KMnO<sub>4</sub> staining (*R*<sub>f</sub> = 0.32, 30/70 EtOAc/Hexane). Concentration of product fractions furnished a yellow solid as the desired product (1.00 g, 3.28 mmol, 46%).

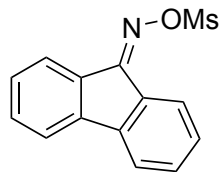
IR (DCM cast film,  $\nu_{(\max)}$  / cm<sup>-1</sup>) 3493, 3071, 2877, 1610, 1578, 1525, 1445, 1351, 1305, 1076, 1041

<sup>1</sup>H NMR (500 MHz, CDCl<sub>3</sub>)  $\delta$ H 7.88 (1H, d, *J* = 8.0 Hz), 7.60—7.56 (2H, m), 7.46—7.40 (1H, m), 4.68 (1H, br s), 4.30 (2H, s)

<sup>13</sup>C NMR (125 MHz, CDCl<sub>3</sub>)  $\delta$ C 149.7, 132.8, 132.3, 161.6, 128.4, 124.5, 61.0

HRMS (ESI) Calcd for C<sub>14</sub>H<sub>13</sub>N<sub>3</sub>NaO<sub>5</sub> [M + Na]<sup>+</sup> 326.0747, found 326.0749.

**9*H*-Fluoren-9-one *O*-methylsulfonyl oxime (127)**



**127**

This known compound was prepared according to a literature procedure.<sup>112</sup> 9-Fluorenone oxime (2.00 g, 10.24 mmol, 1.0 equiv) was dissolved in dry THF (51.2 mL) under argon in a flame-dried round-bottom flask. The solution was then cooled to 0 °C and Et<sub>3</sub>N (1.72 mL, 12.29 mmol, 1.2 equiv) was added. Next MsCl (0.95 mL, 12.29 mmol, 1.2 equiv) was added dropwise over the course of 5 min. The reaction mixture was then allowed to stir at 0 °C for 40 min, followed by removal from the ice bath and continued stirring for an additional 30 min, warming to room temperature over this period of time. Next, the reaction mixture was diluted with H<sub>2</sub>O (150 mL) and EtOAc (150 mL). The layers were separated and the aqueous layer was further extracted with EtOAc (2 × 75 mL). The combined organic layers were then washed with brine (150 mL) and dried over Na<sub>2</sub>SO<sub>4</sub>. Concentration of the organic layer furnishes a dark yellow solid (2.80 g, 10.24 mmol, >99%, R<sub>f</sub> = 0.33, 20/80 EtOAc/Hexane) that did not require further purification.

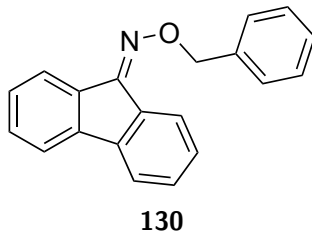
IR (DCM cast film,  $\nu(\text{max})$  / cm<sup>-1</sup>) 3060, 3040, 2947, 1644, 1607, 1597, 1449, 1368, 1185, 1153, 968

<sup>1</sup>H NMR (500 MHz, CDCl<sub>3</sub>)  $\delta$ H 8.27 (1H, d, *J* = 8.0 Hz), 7.79 (1H, d, *J* = 8.0 Hz), 7.61 (1H, d, *J* = 7.7 Hz), 7.58 (1H, d, *J* = 7.7 Hz), 7.49 (1H, td, *J* = 7.5, 1.0 Hz), 7.45 (1H, td, *J* = 7.5, 1.0 Hz), 7.35–7.27 (2H, m), 3.33 (3H, s)

<sup>13</sup>C NMR (125 MHz, CDCl<sub>3</sub>)  $\delta$ C 159.4, 142.7, 141.5, 133.6, 133.4, 132.3, 131.0, 129.7, 129.0, 128.5, 123.2, 120.4, 30.6

HRMS (ESI) Calcd for C<sub>14</sub>H<sub>11</sub>NNaO<sub>3</sub>S [M + Na]<sup>+</sup> 296.0352, found 296.0356.

**9*H*-Fluoren-9-one *O*-benzyl oxime (130)**



This known compound was prepared according to a literature procedure.<sup>112</sup> In a flame-dried round-bottom flask under an argon atmosphere was deposited NaH (60% dispersion in mineral oil, 0.08 g, 2.00 mmol, 1.0 equiv) and dry THF (15 mL). To this was added BnOH (0.212 mL, 2.03 mmol, 1.0 equiv). This mixture was then allowed to stir at room temperature for 30 min. Next, a solution of **127** (0.55 g, 2.01 mmol, 1.0 equiv) in THF (930 mL) was added dropwise to the reaction mixture at room temperature. The reaction mixture turned a bright yellow colour, eventually becoming dark orange in colouration. After 3 h, the reaction mixture was concentrated in vacuo and redissolved in EtOAc (60 mL) and H<sub>2</sub>O (60 mL). The layers were separated and the aqueous layer was extracted with additional volumes of EtOAc (2 × 60 mL). The combined organic layers were dried over Na<sub>2</sub>SO<sub>4</sub> and concentrated to furnish an orange crude. This material was then loaded onto a column using DCM and purified by flash column chromatography using an eluent system of 5/95 EtOAc/Hexane. Product elution was monitored by TLC and KMnO<sub>4</sub> staining (*R<sub>f</sub>* = 0.65, 5/95 EtOAc/Hexane). Concentration of product fractions furnished a yellow-orange oil (0.311 g, 1.09 mmol, 54%).

IR (DCM cast film,  $\nu_{(\max)}$  / cm<sup>-1</sup>) 3061, 3032, 2925, 2870, 1622, 1607, 1496, 1450, 1364, 1322, 1164, 1091, 1016, 962

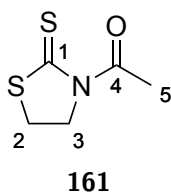
<sup>1</sup>H NMR (500 MHz, CDCl<sub>3</sub>)  $\delta$ H 8.29 (1H, dt, *J* = 7.6, 0.9 Hz), 7.78 (1H, dt, *J* = 7.6, 0.9 Hz), 7.65 (1H, dt, *J* = 7.6, 0.9 Hz), 7.61 (1H, dt, *J* = 7.6, 0.9 Hz), 7.44–7.32 (5H, m), 7.28 (2H, tdd, *J* = 7.6, 2.7, 1.0 Hz), 5.46 (2H, s)

$^{13}\text{C}$  NMR (125 MHz,  $\text{CDCl}_3$ )  $\delta\text{C}$  152.5, 141.4, 140.3, 137.5, 135.6, 130.9, 130.7, 129.9, 129.4, 128.5, 128.3, 128.2, 128.1, 127.9, 121.8, 119.9, 119.8, 77.9

HRMS (ESI) Calcd for  $\text{C}_{20}\text{H}_{16}\text{NO}$   $[\text{M} + \text{H}]^+$  286.1226, found 286.1228.

## 7.11 Chapter 6 Synthetic Procedures

### 1-(2-Thioxothiazolidin-3-yl)ethan-1-one (161)



This known compound was synthesized based on a literature procedure.<sup>166</sup> 2-Thiazoline-2-thione (10.0 g, 83.9 mmol, 1.0 eq) was dissolved in pyridine (40.5 mL, 503 mmol, 6.0 eq). To this mixture was added acetic anhydride (39.7 mL, 419.4 mmol, 5.0 eq). The reaction vessel was affixed with a reflux condenser and refluxed at 135 °C for 1 h. The reaction mixture was then concentrated *in vacuo* to furnish a yellow oil as a crude. The material was then dissolved with EtOAc (250 mL) and washed with 10% aq  $\text{K}_2\text{CO}_3$  (3  $\times$  100 mL), 1 M HCl (1  $\times$  100 mL), and brine (1  $\times$  100 mL). The organic layer was then dried over  $\text{Na}_2\text{SO}_4$  and concentrated to furnish a crude yellow oil. The crude material was then subjected to purification by flash column chromatography on silica, using an eluent system of  $\text{CHCl}_3$ . Elution of the product was monitored by UV on TLC and  $\text{KMnO}_4$  staining ( $R_f = 0.33$ ,  $\text{CHCl}_3$ ). Concentration of product fractions furnished a yellow solid (13.5g, 83.9 mmol, >99%).

IR (DCM cast film,  $\nu_{\text{max}}$  /  $\text{cm}^{-1}$ ) 3381, 3001, 2940, 2889, 1698, 1465, 1409, 1361, 1278, 1228, 1197, 1086, 1049, 998

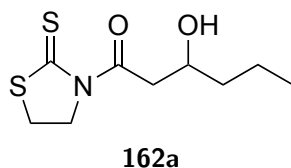
$^1\text{H}$  NMR (700 MHz,  $\text{CDCl}_3$ )  $\delta\text{H}$  4.57 (2H, t,  $J = 6.4$  Hz, H3), 3.29 (2H, t,  $J = 6.4$  Hz, H2),

2.77 (3H, s, H5)

$^{13}\text{C}$  NMR (175 MHz,  $\text{CDCl}_3$ )  $\delta\text{C}$  202.1 (C1), 171.6 (C4), 55.8 (C3), 28.3 (C2), 27.1 (C5)

HRMS (ESI) Calcd for  $\text{C}_5\text{H}_8\text{NOS}_2$   $[\text{M} + \text{H}]^+$  162.0042, found 162.0046

### 3-Hydroxy-1-(2-thioxothiazolidin-3-yl)hexan-1-one (162a)



The synthesis of this novel compound was adapted from a literature procedure.<sup>139</sup> **161** (1.00 g, 6.20 mmol, 1.0 eq) was dissolved in dry DCM (62 mL) under argon in a flame-dried round-bottom flask at  $-78\text{ }^\circ\text{C}$ . To the solution was then added  $\text{TiCl}_4$  as a 1 M solution in DCM (6.82 mL, 6.82 mmol, 1.1 eq). The reaction mixture was then allowed to stir for 10 min. DIPEA (1.40 mL, 8.06 mmol, 1.3 eq) was then added. The reaction mixture turned from yellow to dark brown and was allowed to stir for 1 h. Butanal (0.56 mL, 6.20 mmol, 1.0 eq) was then added and the reaction mixture was allowed to stir for an additional 1 h. The reaction mixture was then quenched by the addition of saturated  $\text{NH}_4\text{Cl}$  (15 mL). The organic and aqueous layers were then separated and the aqueous layer was further extracted with EtOAc ( $3 \times 30$  mL). The combined organic layers were dried over  $\text{Na}_2\text{SO}_4$  and concentrated to furnish a thick yellow oil as a crude. The material was then purified by flash column chromatography on silica using an eluent system of 20/80 EtOAc/Hexane. Product elution was monitored by TLC using UV and  $\text{KMnO}_4$  staining ( $R_f = 0.35$ , 50/50 EtOAc/Hexane). Concentration of product fractions furnishes a yellow solid as the desired product (0.99 g, 4.22 mmol, 68%).

IR (DCM cast film,  $\nu_{\text{max}}$  /  $\text{cm}^{-1}$ ) 3439, 2956, 2931, 2870, 1694, 1366, 1280, 1223, 1157

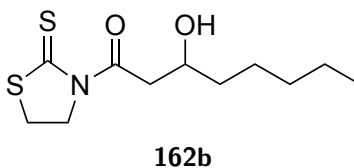
$^1\text{H}$  NMR (700 MHz,  $\text{CDCl}_3$ )  $\delta\text{H}$  4.65—4.53 (2H, m), 4.16—4.07 (1H, m), 3.51 (1H, dd,  $J = 17.6, 2.4$  Hz), 3.35—3.24 (3H, m), 2.85 (1H, d,  $J = 4.3$  Hz), 1.61—1.53 (1H, m), 1.51—1.43

(2H, m), 1.43—1.35 (1H, m), 0.94 (3H, t,  $J = 7.1$  Hz)

$^{13}\text{C}$  NMR (175 MHz,  $\text{CDCl}_3$ )  $\delta\text{C}$  174.4, 67.9, 55.7, 45.9, 38.7, 28.4, 18.8, 14.0 (thione carbon not observed)

HRMS: (ESI) Calcd for  $\text{C}_9\text{H}_{15}\text{NNaO}_2\text{S}_2$   $[\text{M} + \text{Na}]^+$  256.0435, found 256.0436

### 3-Hydroxy-1-(2-thioxothiazolidin-3-yl)octan-1-one (**162b**)



Compound **162b** was synthesized from **161** via the method employed for the synthesis of **162a**.

Purification: Flash column chromatography over silica, eluent system of 50/50 EtOAc/Hexane.

TLC:  $R_f = 0.40$ , 50/50 EtOAc/Hexane

Appearance: Yellow solid.

Yield: 66%

IR (DCM cast film,  $\nu_{\text{max}}$  /  $\text{cm}^{-1}$ ) 3439, 2953, 2930, 2858, 1697, 1367, 1281, 1224, 1157

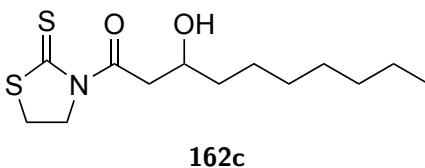
$^1\text{H}$  NMR (700 MHz,  $\text{CDCl}_3$ )  $\delta\text{H}$  4.65—4.55 (2H, m), 4.14—4.06 (1H, m), 3.51 (1H, dd,  $J = 17.6, 2.4$  Hz), 3.35—3.24 (3H, m), 2.95—2.75 (1H, m), 1.61—1.52 (1H, m), 1.52—1.41 (2H, m), 1.43v1.22 (5H, m), 0.89 (3H, t,  $J = 6.8$  Hz)

$^{13}\text{C}$  NMR (175 MHz,  $\text{CDCl}_3$ )  $\delta\text{C}$  174.4, 68.2, 55.7, 45.9, 36.5, 31.8, 28.4, 25.2, 22.6, 14.1 (thione carbon not observed)

HRMS: (ESI) Calcd for  $\text{C}_{11}\text{H}_{19}\text{NNaO}_2\text{S}_2$   $[\text{M} + \text{Na}]^+$  284.0749, found 284.0747



### 3-Hydroxy-1-(2-thioxothiazolidin-3-yl)decan-1-one (162c)



Compound **162c** was synthesized from **161** via the method employed for the synthesis of **162a**.

Purification: Flash column chromatography over silica, eluent system of 50/50 EtOAc/Hexane.

TLC:  $R_f = 0.41$ , 50/50 EtOAc/Hexane

Appearance: Yellow solid.

Yield: 52%

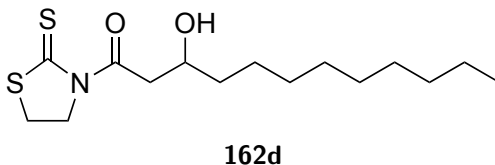
IR (DCM cast film,  $\nu_{\max}$  /  $\text{cm}^{-1}$ ) 3435, 2957, 2927, 2855, 1696, 1366, 1280, 1223, 1156

$^1\text{H}$  NMR (500 MHz,  $\text{CDCl}_3$ )  $\delta$ H 4.67—4.54 (2H, m), 4.14—4.06 (1H, m), 3.51 (1H, dd,  $J = 17.6, 2.6$  Hz), 3.36—3.23 (3H, m), 2.85 (1H, d,  $J = 3.9$  Hz), 1.64—1.54 (1H, m), 1.54—1.40 (2H, m), 1.40—1.20 (9H, m), 0.88 (3H, t,  $J = 7.1$  Hz)

$^{13}\text{C}$  NMR (125 MHz,  $\text{CDCl}_3$ )  $\delta$ C 201.9, 174.4, 68.2, 55.7, 45.9, 36.6, 31.9, 29.6, 29.3, 28.4, 25.6, 22.7, 14.1

HRMS: (ESI) Calcd for  $\text{C}_{13}\text{H}_{23}\text{NNaO}_2\text{S}_2$   $[\text{M} + \text{Na}]^+$  312.1062, found 312.1063

### 3-Hydroxy-1-(2-thioxothiazolidin-3-yl)dodecan-1-one (162d)



Compound **162d** was synthesized from **161** via the method employed for the synthesis of **162a**.

Purification: Flash column chromatography over silica, eluent system of 50/50 EtOAc/Hexane.

TLC:  $R_f = 0.47$ , 50/50 EtOAc/Hexane

Appearance: Yellow solid.

Yield: 45%

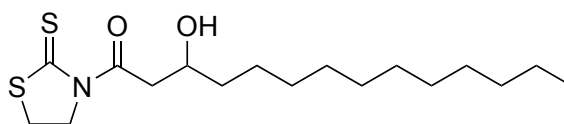
IR (DCM cast film,  $\nu_{\max}$  /  $\text{cm}^{-1}$ ) 3424, 2924, 2854, 1697, 1465, 1366, 1280, 1224, 1156

$^1\text{H}$  NMR (500 MHz,  $\text{CDCl}_3$ )  $\delta$ H 4.65—4.54 (2H, m), 4.16—4.05 (1H, m), 3.52 (1H, dd,  $J = 17.6, 2.5$  Hz), 3.35—3.23 (3H, m), 2.85 (1H, d,  $J = 4.1$  Hz), 1.64—1.53 (1H, m), 1.53—1.34 (2H, m), 1.34—1.20 (13H, m), 0.88 (3H, t,  $J = 6.9$  Hz)

$^{13}\text{C}$  NMR (125 MHz,  $\text{CDCl}_3$ )  $\delta$ C 201.9, 174.4, 68.2, 55.7, 45.9, 36.6, 31.9, 29.6, 29.4, 28.4, 25.6, 22.7, 14.1 (overlapping carbon signals observed)

HRMS: (ESI) Calcd for  $\text{C}_{15}\text{H}_{27}\text{NNaO}_2\text{S}_2$   $[\text{M} + \text{Na}]^+$  340.1375, found 340.1378

### 3-Hydroxy-1-(2-thioxothiazolidin-3-yl)tetradecan-1-one (162e)



**162e**

Compound **162e** was synthesized from **161** via the method employed for the synthesis of **162a**.

Purification: Flash column chromatography over silica, eluent system of 50/50 EtOAc/Hexane.

TLC:  $R_f = 0.49$ , 50/50 EtOAc/Hexane

Appearance: Yellow solid.

Yield: 66%

IR (DCM cast film,  $\nu_{\max}$  /  $\text{cm}^{-1}$ ) 3574, 2954, 2918, 2852, 1684, 1469, 1402, 1384, 1280, 1196

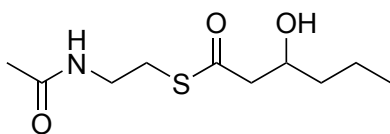
$^1\text{H}$  NMR (500 MHz,  $\text{CDCl}_3$ )  $\delta$ H 4.67—4.53 (2H, m), 4.14—4.04 (1H, m), 3.51 (1H, dd,  $J =$

17.6, 2.5 Hz), 3.35—3.22 (3H, m), 2.85 (1H, s), 1.64—1.53 (1H, m), 1.53—1.40 (2H, m), 1.40—1.20 (17H, m), 0.88 (3H, t,  $J = 6.9$  Hz)

$^{13}\text{C}$  NMR (125 MHz,  $\text{CDCl}_3$ )  $\delta\text{C}$  201.9, 174.4, 68.2, 55.7, 45.9, 36.6, 32.0, 29.7, 29.7, 29.6, 29.6, 29.6, 29.4, 28.4, 25.6, 22.7, 14.2

HRMS: (ESI) Calcd for  $\text{C}_{17}\text{H}_{31}\text{NNaO}_2\text{S}_2$   $[\text{M} + \text{Na}]^+$  368.1688, found 368.1686

### ***S*-(2-Acetamidoethyl) 3-hydroxyhexanethioate (164a)**



**164a**

This known compound was synthesized via an adapted procedure.<sup>140</sup> **162a** (0.100 g, 0.428 mmol, 1.05 eq) and  $\text{K}_2\text{CO}_3$  (0.206 g, 1.490 mmol, 3.65 eq) was deposited in a round-bottom flask to which MeCN (10.0 mL) was added and the resultant mixture stirred. This was followed by the addition of *N*-acetylcysteamine (0.043 mL, 0.408 mmol, 1.00 eq). The reaction mixture was then stirred until the yellow colouration disappeared (*ca.* 10-15 min). The reaction mixture was then quenched using a sat.  $\text{NH}_4\text{Cl}$  solution (10.0 mL) and diluted with EtOAc (10.0 mL). The layers were separated and the aqueous layer was further extracted with EtOAc ( $3 \times 10.0$  mL). The combined organic layers were dried over  $\text{Na}_2\text{SO}_4$  and concentrated to furnish a white crude material. This was then purified by flash column chromatography on silica using EtOAc as the eluent. Elution of the product was monitored on TLC using UV and  $\text{KMnO}_4$  staining ( $R_f = 0.17$ , EtOAc). Concentration of product fractions furnished a white solid (0.093 g, 0.400 mmol, 98%).

IR (DCM cast film,  $\nu_{\text{max}}$  /  $\text{cm}^{-1}$ ) 3303, 3084, 2958, 2933, 2872, 1688, 1658, 1552, 1435, 1374, 1291

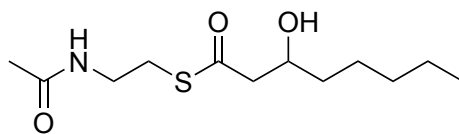
$^1\text{H}$  NMR (500 MHz,  $\text{CDCl}_3$ )  $\delta\text{H}$  5.85 (1H, br s), 4.11—4.03 (1H, m), 3.52—3.39 (2H, m), 3.10—2.98 (2H, m), 2.79—2.57 (3H, m), 1.96 (3H, s), 1.56—1.31 (4H, m), 0.93 (3H, t,  $J =$

6.92 Hz)

$^{13}\text{C}$  NMR (125 MHz,  $\text{CDCl}_3$ )  $\delta\text{C}$  199.6, 170.5, 68.6, 51.1, 39.3, 38.9, 28.9, 23.3, 18.7, 13.9

HRMS: (ESI) Calcd for  $\text{C}_{10}\text{H}_{19}\text{NNaO}_3\text{S}$   $[\text{M} + \text{Na}]^+$  256.0978, found 256.0977

### *S*-(2-Acetamidoethyl) 3-hydroxyoctanethioate (**164b**)



**164b**

Compound **164b** was synthesized from **162b** via the method employed for the synthesis of **164a**.

Purification: Flash column chromatography over silica, eluent system of EtOAc.

TLC:  $R_f$  = 0.26, EtOAc

Appearance: White solid.

Yield: 97%

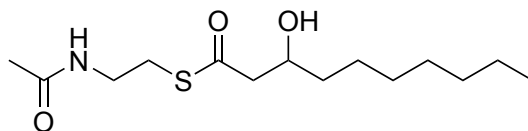
IR (DCM cast film,  $\nu_{\text{max}}$  /  $\text{cm}^{-1}$ ) 3390, 3312, 3080, 2952, 2926, 2857, 1683, 1643, 1555, 1437, 1374, 1295

$^1\text{H}$  NMR (500 MHz,  $\text{CDCl}_3$ )  $\delta\text{H}$  5.82 (1H, br s), 4.11—4.00 (1H, m), 3.52—3.37 (2H, m), 3.11—2.98 (2H, m), 2.80—2.58 (3H, m), 1.97 (3H, s), 1.56—1.38 (3H, m), 1.38—1.22 (5H, m), 0.89 (3H, t,  $J$  = 7.1 Hz)

$^{13}\text{C}$  NMR (125 MHz,  $\text{CDCl}_3$ )  $\delta\text{C}$  199.6, 170.4, 68.9, 51.1, 39.3, 36.7, 31.7, 28.9, 25.1, 23.3, 22.6, 14.0

HRMS: (ESI) Calcd for  $\text{C}_{12}\text{H}_{23}\text{NNaO}_3\text{S}$   $[\text{M} + \text{Na}]^+$  284.1291, found 284.1291

***S*-(2-Acetamidoethyl) 3-hydroxydecanethioate (164c)**



**164c**

Compound **164c** was synthesized from **162c** via the method employed for the synthesis of **164a**.

Purification: Flash column chromatography over silica, eluent system of EtOAc.

TLC:  $R_f = 0.34$ , EtOAc

Appearance: White solid.

Yield: >99%

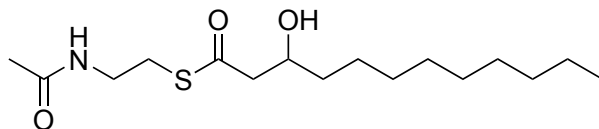
IR (DCM cast film,  $\nu_{\max}$  /  $\text{cm}^{-1}$ ) 3398, 3303, 3078, 2952, 2921, 2849, 1686, 1643, 1554, 1467, 1396, 1358, 1295

$^1\text{H}$  NMR (500 MHz,  $\text{CDCl}_3$ )  $\delta$  5.80 (1H, br s), 4.10—4.01 (1H, m), 3.52—3.40 (2H, m), 3.11—2.98 (2H, m), 2.80—2.57 (3H, m), 1.97 (3H, s), 1.58—1.38 (3H, m), 1.38—1.20 (9H, m), 0.88 (3H, t,  $J = 6.8$  Hz)

$^{13}\text{C}$  NMR (125 MHz,  $\text{CDCl}_3$ )  $\delta$  199.6, 170.4, 68.9, 51.1, 39.4, 36.8, 31.8, 29.5, 29.3, 28.9, 25.5, 23.3, 22.7, 14.1

HRMS: (ESI) Calcd for  $\text{C}_{14}\text{H}_{27}\text{NNaO}_3\text{S}$   $[\text{M} + \text{Na}]^+$  312.1604, found 312.1603

***S*-(2-Acetamidoethyl) 3-hydroxydodecanethioate (164d)**



**164d**

Compound **164d** was synthesized from **162d** via the method employed for the synthesis

of **164a**.

Purification: Flash column chromatography over silica, eluent system of EtOAc.

TLC:  $R_f = 0.33$ , EtOAc

Appearance: White solid.

Yield: 83%

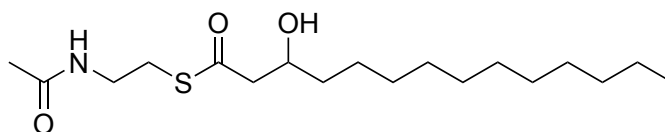
IR (DCM cast film,  $\nu_{\max}$  /  $\text{cm}^{-1}$ ) 3402, 3302, 3055, 2953, 2919, 2849, 1686, 1643, 1554, 1466, 1265

$^1\text{H}$  NMR (500 MHz,  $\text{CDCl}_3$ )  $\delta$  5.80 (1H, br s), 4.12—4.00 (1H, m), 3.52—3.39 (2H, m), 3.13—2.99 (2H, m), 2.79—2.55 (3H, m), 1.97 (3H, s), 1.57—1.37 (3H, m), 1.37—1.19 (13H, m), 0.88 (3H, t,  $J = 7.1$  Hz)

$^{13}\text{C}$  NMR (125 MHz,  $\text{CDCl}_3$ )  $\delta$  199.7, 170.4, 68.9, 51.1, 39.4, 36.8, 31.9, 29.6, 29.6, 29.5, 29.3, 28.9, 25.5, 23.3, 22.7, 14.2

HRMS: (ESI) Calcd for  $\text{C}_{16}\text{H}_{31}\text{NNaO}_3\text{S}$   $[\text{M} + \text{Na}]^+$  340.1917, found 340.1916

### *S*-(2-Acetamidoethyl) 3-hydroxytetradecanethioate (**164e**)



**164e**

Compound **164e** was synthesized from **162e** via the method employed for the synthesis of **164a**.

Purification: Flash column chromatography over silica, eluent system of EtOAc.

TLC:  $R_f = 0.22$ , EtOAc

Appearance: White solid.

Yield: 84%

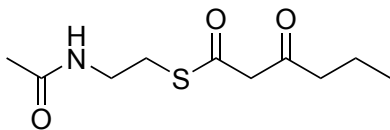
IR (DCM cast film,  $\nu_{\max}$  /  $\text{cm}^{-1}$ ) 3392, 3298, 3079, 2952, 2916, 2849, 1696, 1642, 1555, 1465, 1396, 1358, 1296

$^1\text{H}$  NMR (500 MHz,  $\text{CDCl}_3$ )  $\delta$  5.77 (1H, br s), 4.10—4.00 (1H, m), 3.53—3.39 (2H, m), 3.11—2.99 (2H, m), 2.76 (1H, dd,  $J = 15.3, 3.1$  Hz), 2.68 (1H, dd,  $J = 15.3, 8.7$  Hz), 2.58 (1H, d,  $J = 4.5$  Hz), 1.97 (3H, s), 1.56—1.37 (3H, m), 1.37—1.19 (17H, m), 0.88 (3H, t,  $J = 6.8$  Hz)

$^{13}\text{C}$  NMR (125 MHz,  $\text{CDCl}_3$ )  $\delta$  199.7, 170.4, 68.9, 51.1, 39.4, 36.8, 32.0, 29.7, 29.7, 29.6, 29.6, 29.5, 29.4, 28.9, 25.5, 23.3, 22.7, 14.2

HRMS: (ESI) Calcd for  $\text{C}_{18}\text{H}_{35}\text{NNaO}_3\text{S}$   $[\text{M} + \text{Na}]^+$  368.2230, found 368.2230

### *S*-(2-Acetamidoethyl) 3-oxohexanethioate (**165a**)



**165a**

The synthesis of this known compound was carried out via modified literature procedures.<sup>139,140</sup> **164a** (0.080 g, 0.343 mmol, 1.0 eq) was dissolved in 3.5 mL of DCM at room temperature. To this was added a solution of Dess-Martin periodinane (0.160 g, 0.377 mmol, 1.1 eq) in DCM (3.5 mL). The reaction mixture was then allowed to stir at room temperature, exposed to the atmosphere. Reaction progress was monitored by TLC (EtOAc) and starting material was found to be quickly consumed (*ca.* 15 min). The reaction mixture was then quenched by the addition of an aqueous 1/1 sat.  $\text{NaHCO}_3$ /sat.  $\text{Na}_2\text{S}_2\text{O}_3$  solution (10.0 mL). The mixture was further diluted with EtOAc (10 mL) and the layers were separated. The aqueous layer was further extracted using EtOAc ( $3 \times 10$  mL). The combined organic layers were dried over  $\text{Na}_2\text{SO}_4$  and concentrated to furnish a crude material. The material was then purified by flash column chromatography on silica using an eluent system of EtOAc. Elution of product was monitored by TLC using UV and  $\text{KMnO}_4$  staining ( $R_f = 0.28$ , EtOAc). Concentration of product fractions furnished a white solid (0.058 g, 0.249 mmol, 73%).

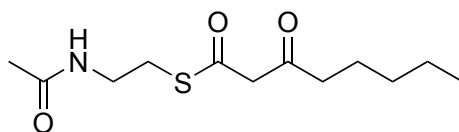
IR (DCM cast film,  $\nu_{\max}$  /  $\text{cm}^{-1}$ ) 3284, 3103, 2958, 2933, 2874, 1716, 1684, 1651, 1562, 14444, 1408, 1372, 1306

$^1\text{H}$  NMR (500 MHz,  $\text{CDCl}_3$ )  $\delta\text{H}$  (mixture of tautomers) 5.87 (1H, br s), 3.69 (1.5H, s), 3.47 (2H, q,  $J = 6.2$  Hz), 3.09 (2H, t,  $J = 6.2$  Hz), 2.51 (1.5H, t,  $J = 7.2$  Hz), 1.98 (3H, s), 1.73—1.52 (3H, m), 0.99—0.90 (3H, m)

$^{13}\text{C}$  NMR (125 MHz,  $\text{CDCl}_3$ )  $\delta\text{C}$  (mixture of tautomers) 202.2, 192.4, 170.4, 99.3, 57.3, 45.3, 39.3, 29.3, 23.2, 17.0, 13.6

HRMS: (ESI) Calcd for  $\text{C}_{10}\text{H}_{17}\text{NNaO}_3\text{S}$   $[\text{M} + \text{Na}]^+$  254.0281, found 254.0281

### ***S*-(2-Acetamidoethyl) 3-oxooctanethioate (165b)**



**165b**

Compound **165b** was synthesized from **164b** via the method employed for the synthesis of **165a**.

Purification: Flash column chromatography over silica, eluent system of EtOAc.

TLC:  $R_f = 0.33$ , EtOAc

Appearance: White solid.

Yield: 81%

IR (DCM cast film,  $\nu_{\max}$  /  $\text{cm}^{-1}$ ) 3283, 3104, 2951, 2926, 2868, 1716, 1686, 1637, 1563, 1445, 1408, 1371

$^1\text{H}$  NMR (500 MHz,  $\text{CDCl}_3$ )  $\delta\text{H}$  (mixture of tautomers) 5.89 (1H, br s), 3.71 (1.5H, s), 3.49 (2H, q,  $J = 6.4$  Hz), 3.12 (2H, t,  $J = 5.7$  Hz), 2.51 (1.5H, t,  $J = 7.6$  Hz), 2.00 (3H, s), 1.68—1.56 (3H, m), 1.41—1.24 (4H, m), 0.97—0.88 (3H, m)

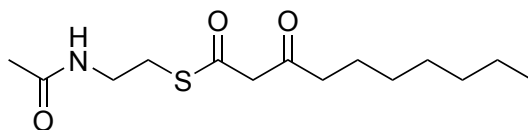
$^{13}\text{C}$  NMR (125 MHz,  $\text{CDCl}_3$ )  $\delta\text{C}$  (mixture of tautomers) 202.3, 194.4, 192.5, 177.8, 170.4, 99.2, 77.8, 57.2, 43.5, 40.0, 39.3, 34.9, 31.3, 31.2, 29.3, 27.9, 26.0, 23.3, 23.2, 23.2, 22.4,



22.4, 13.9, 13.9

HRMS: (ESI) Calcd for C<sub>12</sub>H<sub>21</sub>NNaO<sub>3</sub>S [M + Na]<sup>+</sup> 282.1134, found 282.1134

***S*-(2-Acetamidoethyl) 3-oxodecanethioate (165c)**



**165c**

Compound **165c** was synthesized from **164c** via the method employed for the synthesis of **165a**.

Purification: Flash column chromatography over silica, eluent system of EtOAc.

TLC: R<sub>f</sub> = 0.35, EtOAc

Appearance: White solid.

Yield: 53%

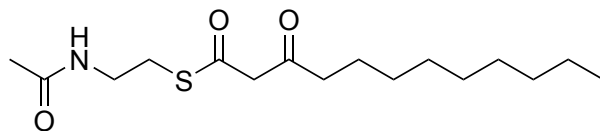
IR (DCM cast film,  $\nu_{\max}$  / cm<sup>-1</sup>) 3281, 3105, 2948, 2923, 2856, 1717, 1686, 1637, 1564, 1469, 1444, 1408, 1296, 1265

<sup>1</sup>H NMR (500 MHz, CDCl<sub>3</sub>)  $\delta$ H (mixture of tautomers) 5.88 (1H, br s), 3.69 (1.5H, s), 3.46 (2H, q, *J* = 6.1 Hz), 3.09 (2H, t, *J* = 6.5 Hz), 2.52 (1.5H, t, *J* = 7.5 Hz), 1.98 (3H, s), 1.63—1.51 (3H, m), 1.36—1.20 (8H, m), 0.92—0.85 (3H, m)

<sup>13</sup>C NMR (125 MHz, CDCl<sub>3</sub>)  $\delta$ C (mixture of tautomers) 202.4, 194.4, 192.5, 177.8, 170.4, 99.2, 27.2, 43.5, 40.0, 39.3, 35.0, 31.7, 31.7, 29.3, 29.1, 29.0, 29.0, 27.9, 26.3, 23.5, 23.3, 23.2, 22.6, 14.1

HRMS: (ESI) Calcd for C<sub>14</sub>H<sub>25</sub>NNaO<sub>3</sub>S [M + Na]<sup>+</sup> 310.1447, found 310.1449

***S*-(2-Acetamidoethyl) 3-oxododecanethioate (165d)**



**165d**

Compound **165d** was synthesized from **164d** via the method employed for the synthesis of **165a**.

Purification: Flash column chromatography over silica, eluent system of EtOAc.

TLC:  $R_f = 0.37$ , EtOAc

Appearance: White solid.

Yield: 75%

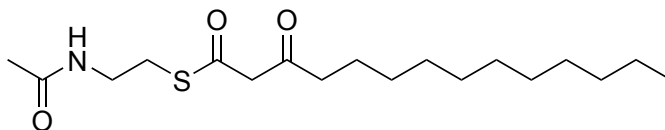
IR (DCM cast film,  $\nu_{\max}$  /  $\text{cm}^{-1}$ ) 3280, 2948, 2922, 2849, 1717, 1686, 1637, 1563, 1469, 1444, 1407, 1304, 1265

$^1\text{H}$  NMR (500 MHz,  $\text{CDCl}_3$ )  $\delta\text{H}$  (mixture of tautomers) 5.87 (1H, br s), 3.69 (1.5H, s), 3.46 (2H, q,  $J = 6.1$  Hz), 3.09 (2H, t,  $J = 5.9$  Hz), 2.52 (1.5H, t,  $J = 7.3$  Hz), 1.98 (3H, s), 1.64—1.52 (3H, m), 1.35—1.19 (12H, m), 0.88 (3H, t,  $J = 7.5$  Hz)

$^{13}\text{C}$  NMR (125 MHz,  $\text{CDCl}_3$ )  $\delta\text{C}$  (mixture of tautomers) 202.3, 192.5, 177.8, 170.4, 99.2, 57.2, 43.5, 40.0, 39.3, 35.0, 31.9, 29.4, 29.4, 29.3, 29.3, 29.1, 29.0, 27.9, 26.3, 23.5, 23.3, 23.2, 22.7, 14.1

HRMS: (ESI) Calcd for  $\text{C}_{16}\text{H}_{29}\text{NNaO}_3\text{S}$   $[\text{M} + \text{Na}]^+$  338.1760, found 338.1759

***S*-(2-Acetamidoethyl) 3-oxotetradecanethioate (165e)**



**165e**

Compound **165e** was synthesized from **164e** via the method employed for the synthesis of **165a**.

Purification: Flash column chromatography over silica, eluent system of EtOAc.

TLC:  $R_f = 0.37$ , EtOAc

Appearance: White solid.

Yield: 77%

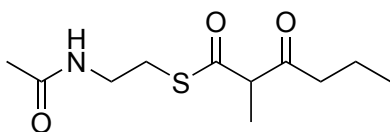
IR (DCM cast film,  $\nu_{\max}$  /  $\text{cm}^{-1}$ ) 3280, 2948, 2918, 1848, 1716, 1686, 1637, 1564, 1469, 1444, 1408, 1372, 1305

$^1\text{H}$  NMR (500 MHz,  $\text{CDCl}_3$ )  $\delta$ H 5.89 (1H, br s), 3.72 (1.5H, s), 3.46 (2H, q,  $J = 6.2$  Hz), 3.12 (2H, t,  $J = 6.1$  Hz), 2.55 (1.5H, t,  $J = 8.0$  Hz), 2.00 (3H, s), 1.66—1.53 (3H, m), 1.38—1.22 (16H, m), 0.91 (3H, t,  $J = 7.1$  Hz)

$^{13}\text{C}$  NMR (125 MHz,  $\text{CDCl}_3$ )  $\delta$ C (mixture of tautomers) 202.3, 192.5, 177.8, 170.4, 99.2, 57.2, 43.5, 40.0, 39.3, 35.0, 31.9, 29.6, 29.5, 29.4, 29.4, 29.3, 29.2, 29.0, 27.9, 26.3, 23.5, 23.3, 23.2, 22.7, 14.2

HRMS: (ESI) Calcd for  $\text{C}_{18}\text{H}_{23}\text{NNaO}_3\text{S}$   $[\text{M} + \text{Na}]^+$  366.2073, found 366.2071

### *S*-(2-Acetamidoethyl) 2-methyl-3-oxohexanethioate (**166a**)



**166a**

In a flame-dried round-bottom flask under argon was deposited **165a** (0.0150 g, 0.065 mmol, 1.00 equiv) and  $\text{KOtBu}$  (0.0084 g, 0.075 mmol, 1.15 equiv). To this was added dry THF (2.2 mL) at 0 °C. The reaction mixture was then allowed to stir at 0 °C for 30 min. Subsequently, MeI (0.024 mL, 0.389 mmol, 6.00 equiv) was added and stirring was allowed to continue at 0 °C for 1 h. The reaction mixture was then removed from the ice bath and allowed to warm to room temperature over a period of 16 h with continued stirring.

Next, the reaction mixture was quenched with the addition of 0.1 M HCl (2.5 mL), then diluted with EtOAc (2.5 mL). The layers were separated and additional extractions were performed with EtOAc (3 × 2.5 mL). The combined organic fractions were then dried over Na<sub>2</sub>SO<sub>4</sub> and concentrated to furnish a crude yellow oil. This crude material was then purified by flash column chromatography using an eluent system of pure EtOAc. Product elution was monitored by TLC and KMnO<sub>4</sub> staining (R<sub>f</sub> = 0.25, EtOAc). Concentration of product fractions furnished a clear oil as a mixture of mono- and di-alkylated products (0.0123 g, 0.050 mmol, 77% combined yield).

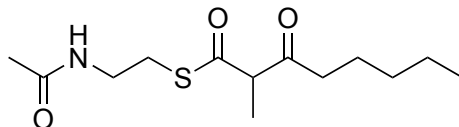
IR (DCM cast film,  $\nu_{\text{max}}$  / cm<sup>-1</sup>) 3368, 3097, 2959, 2925, 2878, 2853, 1721, 1672, 1555, 1458, 1377, 1205, 1174

<sup>1</sup>H NMR (500 MHz, CDCl<sub>3</sub>)  $\delta$ H (mixture of tautomers and mono/di-alkylated products) 5.83 (1H, br s), 3.78 (1H, q,  $J$  = 7.2 Hz), 3.52–3.36 (2H, m), 3.14–3.00 (2H, m), 2.60–2.40 (2H, m), 1.96 (3H, s), 1.67–1.55 (2H, m), 1.45–1.35 (3H, m), 0.91 (3H, t,  $J$  = 7.4 Hz)

<sup>13</sup>C NMR (125 MHz, CDCl<sub>3</sub>)  $\delta$ C (mixture of tautomers and mono-/di-alkylated products) 204.9, 197.0, 170.3, 61.3, 43.5, 39.4, 28.9, 23.2, 17.0, 13.6, 13.6

HRMS: (ESI) Calcd for C<sub>13</sub>H<sub>23</sub>NNaO<sub>3</sub>S [M + Na]<sup>+</sup> 268.0978, found 268.0974

### ***S*-(2-Acetamidoethyl) 2-methyl-3-oxooctanethioate (166b)**



**166b**

Compound **166b** was synthesized from **165b** via the method employed for the synthesis of **166a**.

Purification: Flash column chromatography over silica, eluent system of EtOAc.

TLC: R<sub>f</sub> = 0.33, EtOAc

Appearance: White solid.

Yield: 94% (combined yield)

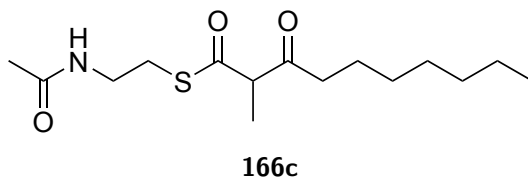
IR (DCM cast film,  $\nu_{\max}$  /  $\text{cm}^{-1}$ ) 3379, 3290, 3095, 2958, 2935, 2873, 1721, 1670, 1548, 1454, 1373, 1202, 1171

$^1\text{H}$  NMR (500 MHz,  $\text{CDCl}_3$ )  $\delta\text{H}$  (mixture of tautomers and mono/di-alkylated products) 5.80 (1H, br s), 3.78 (1H, q,  $J = 7.1$  Hz), 3.53—3.37 (2H, m), 3.14—3.00 (2H, m), 2.60—2.42 (2H, m), 1.97 (3H, s), 1.63—1.53 (2H, m), 1.45—1.36 (3H, m), 1.36—1.18 (4H, m), 0.89 (3H, t,  $J = 7.2$  Hz)

$^{13}\text{C}$  NMR (125 MHz,  $\text{CDCl}_3$ )  $\delta\text{C}$  (mixture of tautomers and mono-/di-alkylated products) 205.0, 197.0, 170.3, 61.3, 41.6, 39.4, 31.2, 29.0, 23.3, 23.2, 22.5, 13.9, 13.7

HRMS: (ESI) Calcd for  $\text{C}_{13}\text{H}_{23}\text{NNaO}_3\text{S}$   $[\text{M} + \text{Na}]^+$  296.1291, found 296.1287

### *S*-(2-Acetamidoethyl) 2-methyl-3-oxodecanethioate (**166c**)



Compound **166c** was synthesized from **165c** via the method employed for the synthesis of **166a**.

Purification: Flash column chromatography over silica, eluent system of EtOAc.

TLC:  $R_f = 0.33$ , EtOAc

Appearance: White solid.

Yield: 78% (combined yield)

IR (DCM cast film,  $\nu_{\max}$  /  $\text{cm}^{-1}$ ) 3379, 3290, 3083, 2955, 2930, 2857, 1723, 1675, 1550, 1453, 1374, 1202, 1174

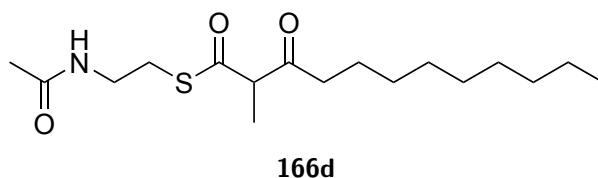
$^1\text{H}$  NMR (500 MHz,  $\text{CDCl}_3$ )  $\delta\text{H}$  (mixture of tautomers and mono/di-alkylated products) 5.80 (1H, br s), 3.78 (1H, q,  $J = 7.2$  Hz), 3.53—3.37 (2H, m), 3.14—3.00 (2H, m),

2.60—2.41 (2H, m), 1.97 (3H, s), 1.63—1.51 (2H, m), 1.45—1.35 (3H, m), 1.34—1.19 (8H, m), 0.87 (3H, t,  $J = 7.1$  Hz)

$^{13}\text{C}$  NMR (125 MHz,  $\text{CDCl}_3$ )  $\delta\text{C}$  (mixture of tautomers and mono-/di-alkylated products)  
205.1, 197.1, 170.3, 61.3, 41.7, 39.4, 31.7, 29.1, 29.0, 29.0, 23.6, 23.2, 22.6, 14.1, 13.7

HRMS: (ESI) Calcd for  $\text{C}_{15}\text{H}_{27}\text{NNaO}_3\text{S}$   $[\text{M} + \text{Na}]^+$  324.1604, found 324.1599

### ***S*-(2-Acetamidoethyl) 2-methyl-3-oxododecanethioate (166d)**



Compound **166d** was synthesized from **165d** via the method employed for the synthesis of **166a**.

Purification: Flash column chromatography over silica, eluent system of EtOAc.

TLC:  $R_f = 0.46$ , EtOAc

Appearance: White solid.

Yield: 79% (combined yield)

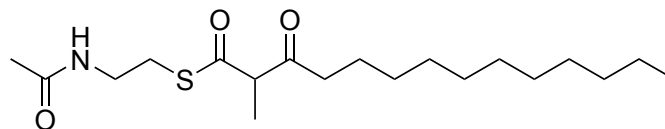
IR (DCM cast film,  $\nu_{\text{max}}$  /  $\text{cm}^{-1}$ ) 3396, 3288, 3080, 2927, 2855, 1724, 1677, 1550, 1454, 1374, 1201, 1177

$^1\text{H}$  NMR (500 MHz,  $\text{CDCl}_3$ )  $\delta\text{H}$  (mixture of tautomers and mono/di-alkylated products)  
5.80 (1H, br s), 3.78 (1H, q,  $J = 7.1$  Hz), 3.53—3.37 (2H, m), 3.14—3.00 (2H, m), 2.60—2.42 (2H, m), 1.97 (3H, s), 1.63—1.51 (2H, m), 1.45-1.36 (3H, m), 1.34—1.19 (12H, m), 0.88 (3H, t,  $J = 7.0$  Hz)

$^{13}\text{C}$  NMR (125 MHz,  $\text{CDCl}_3$ )  $\delta\text{C}$  (mixture of tautomers and mono-/di-alkylated products)  
205.1, 197.1, 170.3, 61.3, 41.7, 39.4, 31.9, 29.4, 29.4, 29.3, 29.1, 29.0, 23.6, 23.2, 22.7, 14.1, 13.7

HRMS: (ESI) Calcd for  $\text{C}_{17}\text{H}_{31}\text{NNaO}_3\text{S}$   $[\text{M} + \text{Na}]^+$  352.1917, found 352.1916

***S*-(2-Acetamidoethyl) 2-methyl-3-oxotetradecanethioate (166e)**



**166e**

Compound **166e** was synthesized from **165e** via the method employed for the synthesis of **166a**.

Purification: Flash column chromatography over silica, eluent system of EtOAc.

TLC:  $R_f = 0.39$ , EtOAc

Appearance: White solid.

Yield: 68% (combined yield)

IR (DCM cast film,  $\nu_{\max}$  /  $\text{cm}^{-1}$ ) 3392, 3286, 3076, 2925, 2854, 1723, 1676, 1548, 1454, 1373, 1288

$^1\text{H}$  NMR (500 MHz,  $\text{CDCl}_3$ )  $\delta\text{H}$  (mixture of tautomers and mono/di-alkylated products) 5.78 (1H, br s), 3.78 (1H, q,  $J = 7.0$  Hz), 3.53—3.37 (2H, m), 3.14—3.01 (2H, m), 2.60—2.41 (2H, m), 1.97 (3H, s), 1.63—1.51 (2H, m), 1.45-1.36 (3H, m), 1.33—1.19 (16H, m), 0.88 (3H, t,  $J = 7.0$  Hz)

$^{13}\text{C}$  NMR (125 MHz,  $\text{CDCl}_3$ )  $\delta\text{C}$  (mixture of tautomers and mono-/di-alkylated products) 205.1, 197.1, 170.3, 61.3, 41.7, 39.4, 31.9, 29.6 (2C), 29.5, 29.4, 29.4, 29.4, 29.1, 29.0, 23.6, 23.2, 22.7, 14.2, 13.7

HRMS: (ESI) Calcd for  $\text{C}_{19}\text{H}_{35}\text{NNaO}_3\text{S}$   $[\text{M} + \text{Na}]^+$  380.2230, found 380.2226

## References

- (1) Shoulders, M. D.; Raines, R. T. Collagen Structure and Stability. *Annu. Rev. Biochem.* **2009**, *78*, 929–958.
- (2) Mirabeau, O.; Perlas, E.; Severini, C.; Audero, E.; Gascuel, O.; Possenti, R.; Birney, E.; Rosenthal, N.; Gross, C. Identification of novel peptide hormones in the human proteome by hidden Markov model screening. *Genome Res.* **2007**, *17*, 320–327.
- (3) Kraut, J. How Do Enzymes Work? *Science* **1988**, *242*, 533–540.
- (4) Lohans, C. T.; Vederas, J. C. Development of Class IIa Bacteriocins as Therapeutic Agents. *Int. J. Microbiol.* **2011**, *2012*, e386410.
- (5) Norton, R. S. Enhancing the therapeutic potential of peptide toxins. *Expert Opin. Drug Discovery* **2017**, *12*, 611–623.
- (6) King, G. F. Venoms as a platform for human drugs: translating toxins into therapeutics. *Expert Opin. Biol. Ther.* **2011**, *11*, 1469–1484.
- (7) Drucker, D. J. Advances in oral peptide therapeutics. *Nat. Rev. Drug Discovery* **2020**, *19*, 277–289.
- (8) Drag, M.; Salvesen, G. S. Emerging principles in protease-based drug discovery. *Nat. Rev. Drug Discovery* **2010**, *9*, 690–701.
- (9) Fosgerau, K.; Hoffmann, T. Peptide therapeutics: current status and future directions. *Drug Discovery Today* **2015**, *20*, 122–128.



- (10) Klare, J. P.; Steinhoff, H.-J. Spin labeling EPR. *Photosynthesis Research* **2009**, *102*, 377–390.
- (11) Chiesa, M.; Giamello, E. In *Encyclopedia of Analytical Chemistry*; John Wiley & Sons, Ltd: 2014, pp 1–34.
- (12) Salikhov, K. M.; Zavoiskaya, N. E. Zavoisky and the discovery of EPR. *Resonance* **2015**, *20*, 963–968.
- (13) Jeschke, G. The contribution of modern EPR to structural biology. *Emerging Top. Life Sci.* **2018**, *2*, 9–18.
- (14) Martin, R. E.; Pannier, M.; Diederich, F.; Gramlich, V.; Hubrich, M.; Spiess, H. W. Determination of End-to-End Distances in a Series of TEMPO Diradicals of up to 2.8 nm Length with a New Four-Pulse Double Electron Electron Resonance Experiment. *Angew. Chem. Int. Ed.* **1998**, *37*, 2833–2837.
- (15) Pannier, M.; Veit, S.; Godt, A.; Jeschke, G.; Spiess, H. W. Dead-Time Free Measurement of Dipole–Dipole Interactions between Electron Spins. *J. Magn. Reson.* **2000**, *142*, 331–340.
- (16) Jeschke, G. DEER Distance Measurements on Proteins. *Annu. Rev. Phys. Chem.* **2012**, *63*, eprint: <https://doi.org/10.1146/annurev-physchem-032511-143716>, 419–446.
- (17) Stone, T. J.; Buckman, T.; Nordio, P. L.; McConnell, H. M. Spin-labeled biomolecules. *Proc. Natl. Acad. Sci. U. S. A.* **1965**, *54*, 1010–1017.
- (18) Schreier, S.; Bozelli, J. C.; Marín, N.; Vieira, R. F. F.; Nakaie, C. R. The spin label amino acid TOAC and its uses in studies of peptides: chemical, physicochemical, spectroscopic, and conformational aspects. *Biophys. Rev.* **2012**, *4*, 45–66.
- (19) V'kovski, P.; Kratzel, A.; Steiner, S.; Stalder, H.; Thiel, V. Coronavirus biology and replication: implications for SARS-CoV-2. *Nat. Rev. Microbiol.* **2021**, *19*, 155–170.

- (20) Pillaiyar, T.; Manickam, M.; Namasivayam, V.; Hayashi, Y.; Jung, S.-H. An Overview of Severe Acute Respiratory Syndrome–Coronavirus (SARS-CoV) 3CL Protease Inhibitors: Peptidomimetics and Small Molecule Chemotherapy. *J. Med. Chem.* **2016**, *59*, 6595–6628.
- (21) Kim, Y.; Liu, H.; Galasiti Kankanamalage, A. C.; Weerasekara, S.; Hua, D. H.; Groutas, W. C.; Chang, K.-O.; Pedersen, N. C. Reversal of the Progression of Fatal Coronavirus Infection in Cats by a Broad-Spectrum Coronavirus Protease Inhibitor. *PLoS Pathog.* **2016**, *12*, ed. by Perlman, S., e1005531.
- (22) Pedersen, N. C.; Kim, Y.; Liu, H.; Galasiti Kankanamalage, A. C.; Eckstrand, C.; Groutas, W. C.; Bannasch, M.; Meadows, J. M.; Chang, K.-O. Efficacy of a 3C-like protease inhibitor in treating various forms of acquired feline infectious peritonitis. *J. Feline Med. Surg.* **2018**, *20*, 378–392.
- (23) Hoffman, R. L. et al. Discovery of Ketone-Based Covalent Inhibitors of Coronavirus 3CL Proteases for the Potential Therapeutic Treatment of COVID-19. *J. Med. Chem.* **2020**, *63*, 12725–12747.
- (24) Zhang, L.; Lin, D.; Kusov, Y.; Nian, Y.; Ma, Q.; Wang, J.; von Brunn, A.; Leyssen, P.; Lanko, K.; Neyts, J.; de Wilde, A.; Snijder, E. J.; Liu, H.; Hilgenfeld, R.  $\alpha$ -Ketoamides as Broad-Spectrum Inhibitors of Coronavirus and Enterovirus Replication: Structure-Based Design, Synthesis, and Activity Assessment. *J. Med. Chem.* **2020**, *63*, 4562–4578.
- (25) Vuong, W.; Khan, M. B.; Fischer, C.; Arutyunova, E.; Lamer, T.; Shields, J.; Saffran, H. A.; McKay, R. T.; van Belkum, M. J.; Joyce, M. A.; Young, H. S.; Tyrrell, D. L.; Vederas, J. C.; Lemieux, M. J. Feline coronavirus drug inhibits the main protease of SARS-CoV-2 and blocks virus replication. *Nat. Commun.* **2020**, *11*, 4282.

- (26) Vuong, W.; Vederas, J. C. Improved Synthesis of a Cyclic Glutamine Analogue Used in Antiviral Agents Targeting 3C and 3CL Proteases Including SARS-CoV-2 M<sup>pro</sup>. *J. Org. Chem.* **2021**, *86*, 13104–13110.
- (27) Dai, W. et al. Structure-based design of antiviral drug candidates targeting the SARS-CoV-2 main protease. *Science* **2020**, *368*, 1331–1335.
- (28) Rathnayake, A. D.; Zheng, J.; Kim, Y.; Perera, K. D.; Mackin, S.; Meyerholz, D. K.; Kashipathy, M. M.; Battaile, K. P.; Lovell, S.; Perlman, S.; Groutas, W. C.; Chang, K.-O. 3C-like protease inhibitors block coronavirus replication in vitro and improve survival in MERS-CoV-infected mice. *Sci. Transl. Med.* **2020**, *12*, eabc5332.
- (29) Rathnayake, A. D.; Kim, Y.; Dampalla, C. S.; Nguyen, H. N.; Jesri, A.-R. M.; Kashipathy, M. M.; Lushington, G. H.; Battaile, K. P.; Lovell, S.; Chang, K.-O.; Groutas, W. C. Structure-Guided Optimization of Dipeptidyl Inhibitors of Norovirus 3CL Protease. *J. Med. Chem.* **2020**, *63*, 11945–11963.
- (30) Chemical & Engineering News. Pfizer unveils its oral SARS-CoV-2 inhibitor. <https://cen.acs.org/acs-news/acs-meeting-news/Pfizer-unveils-oral-SARS-CoV/99/i13>, 2021.
- (31) Chemical & Engineering News. Pfizer's novel COVID-19 antiviral heads to clinical trials. <https://cen.acs.org/pharmaceuticals/drug-discovery/Pfizers-novel-COVID-19-antiviral/98/web/2020/09>, 2020.
- (32) Tian, Q.; Nayyar, N. K.; Babu, S.; Chen, L.; Tao, J.; Lee, S.; Tibbetts, A.; Moran, T.; Liou, J.; Guo, M.; Kennedy, T. P. An efficient synthesis of a key intermediate for the preparation of the rhinovirus protease inhibitor AG7088 via asymmetric dianionic cyanomethylation of N-Boc-L-(+)-glutamic acid dimethyl ester. *Tetrahedron Lett.* **2001**, *42*, 6807–6809.
- (33) Kim, Y.; Lovell, S.; Tiew, K.-C.; Mandadapu, S. R.; Alliston, K. R.; Battaile, K. P.; Groutas, W. C.; Chang, K.-O. Broad-Spectrum Antivirals against 3C or 3C-Like Pro-

- teases of Picornaviruses, Noroviruses, and Coronaviruses. *J. Virol.* **2012**, *86*, 11754–11762.
- (34) Fung, T. S.; Liu, D. X. Human Coronavirus: Host-Pathogen Interaction. *Annu. Rev. Microbiol.* **2019**, *73*, 529–557.
- (35) Cui, J.; Li, F.; Shi, Z.-L. Origin and evolution of pathogenic coronaviruses. *Nat. Rev. Microbiol.* **2019**, *17*, 181–192.
- (36) Snijder, E. J.; Decroly, E.; Ziebuhr, J. In *Advances in Virus Research*, Ziebuhr, J., Ed.; Coronaviruses, Vol. 96; Academic Press: 2016, pp 59–126.
- (37) Meunier, B.; de Visser, S. P.; Shaik, S. Mechanism of Oxidation Reactions Catalyzed by Cytochrome P450 Enzymes. *Chem. Rev.* **2004**, *104*, 3947–3980.
- (38) Huang, X.; Groves, J. T. Beyond ferryl-mediated hydroxylation: 40 years of the rebound mechanism and C–H activation. *JBIC, J. Biol. Inorg. Chem.* **2017**, *22*, 185–207.
- (39) Owen, D. R. et al. An oral SARS-CoV-2 Mpro inhibitor clinical candidate for the treatment of COVID-19. *Science* **2021**, *374*, 1586–1593.
- (40) Staunton, J.; Weissman, K. J. Polyketide biosynthesis: a millennium review. *Nat. Prod. Rep.* **2001**, *18*, 380–416.
- (41) Sahu, I. D.; Lorigan, G. A. Site-Directed Spin Labeling EPR for Studying Membrane Proteins. *BioMed Res. Int.* **2018**, *2018*, e3248289.
- (42) Hubbell, W. L.; López, C. J.; Altenbach, C.; Yang, Z. Technological advances in site-directed spin labeling of proteins. *Curr. Opin. Struct. Biol.* **2013**, *23*, 725–733.
- (43) Bonucci, A.; Ouari, O.; Guigliarelli, B.; Belle, V.; Mileo, E. In-Cell EPR: Progress towards Structural Studies Inside Cells. *ChemBioChem* **2020**, *21*, 451–460.

- (44) Todd, A. P.; Cong, J.; Levinthal, F.; Levinthal, C.; Hubell, W. L. Site-directed mutagenesis of colicin E1 provides specific attachment sites for spin labels whose spectra are sensitive to local conformation. *Proteins: Struct., Funct., Bioinf.* **1989**, *6*, 294–305.
- (45) Savitsky, A.; Dubinskii, A. A.; Zimmermann, H.; Lubitz, W.; Möbius, K. High-Field Dipolar Electron Paramagnetic Resonance (EPR) Spectroscopy of Nitroxide Biradicals for Determining Three-Dimensional Structures of Biomacromolecules in Disordered Solids. *J. Phys. Chem. B* **2011**, *115*, 11950–11963.
- (46) Joseph, B.; Tormyshev, V. M.; Rogozhnikova, O. Y.; Akhmetzyanov, D.; Bagryan-skaya, E. G.; Prisner, T. F. Selective High-Resolution Detection of Membrane Protein–Ligand Interaction in Native Membranes Using Trityl–Nitroxide PELDOR. *Angew. Chem. Int. Ed.* **2016**, *55*, 11538–11542.
- (47) Reichenwallner, J.; Hauenschild, T.; Schmelzer, C. E. H.; Hülsmann, M.; Godt, A.; Hinderberger, D. Fatty Acid Triangulation in Albumins Using a Landmark Spin Label. *Isr. J. Chem.* **2019**, *59*, 1059–1074.
- (48) Hauenschild, T.; Reichenwallner, J.; Enkelmann, V.; Hinderberger, D. Characterizing Active Pharmaceutical Ingredient Binding to Human Serum Albumin by Spin-Labeling and EPR Spectroscopy. *Chem. - Eur. J.* **2016**, *22*, 12825–12838.
- (49) Haugland, M. M.; Anderson, E. A.; Lovett, J. E. In *Electron Paramagnetic Resonance*, 2016, pp 1–34.
- (50) Wang, L.; Brock, A.; Herberich, B.; Schultz, P. G. Expanding the Genetic Code of *Escherichia coli*. *Science* **2001**, *292*, 498–500.
- (51) Wang, L.; Schultz, P. G. Expanding the Genetic Code. *Angew. Chem. Int. Ed.* **2005**, *44*, 34–66.
- (52) Liu, C. C.; Schultz, P. G. Adding New Chemistries to the Genetic Code. *Annu. Rev. Biochem.* **2010**, *79*, 413–444.

- (53) Schmidt, M. J.; Borbas, J.; Drescher, M.; Summerer, D. A Genetically Encoded Spin Label for Electron Paramagnetic Resonance Distance Measurements. *J. Am. Chem. Soc.* **2014**, *136*, 1238–1241.
- (54) Zhu, Z.; Xiao, L.; Xie, Z.; Le, Z. Recent Advances in the  $\alpha$ -C(sp<sup>3</sup>)-H Bond Functionalization of Glycine Derivatives. *Chinese J. Org. Chem.* **2019**, *39*, 2345.
- (55) Vogt, H.; Bräse, S. Recent approaches towards the asymmetric synthesis of  $\alpha,\alpha$ -disubstituted  $\alpha$ -amino acids. *Org. Biomol. Chem.* **2007**, *5*, 406–430.
- (56) Wang, Y.; Song, X.; Wang, J.; Moriwaki, H.; Soloshonok, V. A.; Liu, H. Recent approaches for asymmetric synthesis of  $\alpha$ -amino acids via homologation of Ni(II) complexes. *Amino Acids* **2017**, *49*, 1487–1520.
- (57) Bhushan, R.; Brückner, H. Marfey's reagent for chiral amino acid analysis: A review. *Amino Acids* **2004**, *27*, 231–247.
- (58) Nian, Y.; Wang, J.; Zhou, S.; Wang, S.; Moriwaki, H.; Kawashima, A.; Soloshonok, V. A.; Liu, H. Recyclable Ligands for the Non-Enzymatic Dynamic Kinetic Resolution of Challenging  $\alpha$ -Amino Acids. *Angew. Chem. Int. Ed.* **2015**, *54*, 12918–12922.
- (59) Wuts, P. G. M.; Greene, T. W., *Greene's Protective Groups in Organic Synthesis*, 4th ed.; John Wiley & Sons, Ltd: 2006.
- (60) Parmeggiani, F.; Lovelock, S. L.; Weise, N. J.; Ahmed, S. T.; Turner, N. J. Synthesis of D- and L-Phenylalanine Derivatives by Phenylalanine Ammonia Lyases: A Multienzymatic Cascade Process. *Angew. Chem. Int. Ed.* **2015**, *54*, 4608–4611.
- (61) Bernardo-García, N.; Sánchez-Murcia, P. A.; Espaillet, A.; Martínez-Caballero, S.; Cava, F.; Hermoso, J. A.; Gago, F. Cold-induced aldimine bond cleavage by Tris in *Bacillus subtilis* alanine racemase. *Org. Biomol. Chem.* **2019**, *17*, 4350–4358.

- (62) World Health Organization. Coronavirus Disease (COVID-19) Situation Reports. <http://www.who.int/emergencies/diseases/novel-coronavirus-2019/situation-reports>.
- (63) World Health Organization. Summary of probable SARS cases with onset of illness from 1 November 2002 to 31 July 2003. <https://www.who.int/publications/m/item/summary-of-probable-sars-cases-with-onset-of-illness-from-1-november-2002-to-31-july-2003>, 2015.
- (64) Fan, Y.; Zhao, K.; Shi, Z.-L.; Zhou, P. Bat Coronaviruses in China. *Viruses* **2019**, *11*, 210.
- (65) Tirotta, E.; Carbajal, K. S.; Schaumburg, C. S.; Whitman, L.; Lane, T. E. Cell replacement therapies to promote remyelination in a viral model of demyelination. *Journal of Neuroimmunology* **2010**, *224*, 101–107.
- (66) Perera, K. D.; Galasiti Kankanamalage, A. C.; Rathnayake, A. D.; Honeyfield, A.; Groutas, W.; Chang, K.-O.; Kim, Y. Protease inhibitors broadly effective against feline, ferret and mink coronaviruses. *Antiviral Res.* **2018**, *160*, 79–86.
- (67) Zhang, L.; Lin, D.; Sun, X.; Curth, U.; Drosten, C.; Sauerhering, L.; Becker, S.; Rox, K.; Hilgenfeld, R. Crystal structure of SARS-CoV-2 main protease provides a basis for design of improved a-ketoamide inhibitors. *Science* **2020**, *368*, 409–412.
- (68) Anand, K.; Ziebuhr, J.; Wadhwani, P.; Mesters, J. R.; Hilgenfeld, R. Coronavirus Main Proteinase (3CLpro) Structure: Basis for Design of Anti-SARS Drugs. *Science* **2003**, *300*, 6.
- (69) Sheahan, T. P. et al. An orally bioavailable broad-spectrum antiviral inhibits SARS-CoV-2 in human airway epithelial cell cultures and multiple coronaviruses in mice. *Sci Transl Med* **2020**, *12*, eabb5883.

- (70) Harapan, H.; Itoh, N.; Yufika, A.; Winardi, W.; Kean, S.; Te, H.; Megawati, D.; Hayati, Z.; Wagner, A. L.; Mudatsir, M. Coronavirus disease 2019 (COVID-19): A literature review. *J. Infect. Public Health* **2020**, *13*, 667–673.
- (71) Woo, P. C. Y.; Huang, Y.; Lau, S. K. P.; Yuen, K.-Y. Coronavirus Genomics and Bioinformatics Analysis. *Viruses* **2010**, *2*, 1804–1820.
- (72) Yin, J.; Niu, C.; Cherney, M. M.; Zhang, J.; Huitema, C.; Eltis, L. D.; Vederas, J. C.; James, M. N. G. A Mechanistic View of Enzyme Inhibition and Peptide Hydrolysis in the Active Site of the SARS-CoV 3C-like Peptidase. *Journal of Molecular Biology* **2007**, *371*, 1060–1074.
- (73) Malcolm, B. A.; Lowe, C.; Shechosky, S.; McKay, R. T.; Yang, C. C.; Shah, V. J.; Simon, R. J.; Vederas, J. C.; Santi, D. V. Peptide aldehyde inhibitors of hepatitis A virus 3C proteinase. *Biochemistry* **1995**, *34*, 8172–8179.
- (74) Patick, A. K.; Binford, S. L.; Brothers, M. A.; Jackson, R. L.; Ford, C. E.; Diem, M. D.; Maldonado, F.; Dragovich, P. S.; Zhou, R.; Prins, T. J.; Fuhrman, S. A.; Meador, J. W.; Zalman, L. S.; Matthews, D. A.; Worland, S. T. In Vitro Antiviral Activity of AG7088, a Potent Inhibitor of Human Rhinovirus 3C Protease. *Antimicrob. Agents Chemother.* **1999**, *43*, 2444–2450.
- (75) Zhong, N.; Zhang, S.; Xue, F.; Kang, X.; Zou, P.; Chen, J.; Liang, C.; Rao, Z.; Jin, C.; Lou, Z.; Xia, B. C-terminal domain of SARS-CoV main protease can form a 3D domain-swapped dimer. *Protein Sci.* **2009**, *18*, 839–844.
- (76) Chang, K.-O.; Kim, Y.; Lovell, S.; Rathnayake, A. D.; Groutas, W. C. Antiviral Drug Discovery: Norovirus Proteases and Development of Inhibitors. *Viruses* **2019**, *11*, 197.
- (77) Panda, P. K.; Arul, M. N.; Patel, P.; Verma, S. K.; Luo, W.; Rubahn, H.-G.; Mishra, Y. K.; Suar, M.; Ahuja, R. Structure-based drug designing and immunoinformatics approach for SARS-CoV-2. *Sci. Adv.* **2020**, *6*, eabb8097.



- (78) Otto, H.-H.; Schirmeister, T. Cysteine Proteases and Their Inhibitors. *Chem. Rev.* **1997**, *97*, 133–172.
- (79) Flexner, C.; Bate, G.; Kirkpatrick, P. Tipranavir. *Nat. Rev. Drug Discovery* **2005**, *4*, 955–956.
- (80) Njoroge, F. G.; Chen, K. X.; Shih, N.-Y.; Piwinski, J. J. Challenges in Modern Drug Discovery: A Case Study of Boceprevir, an HCV Protease Inhibitor for the Treatment of Hepatitis C Virus Infection. *Acc. Chem. Res.* **2008**, *41*, 50–59.
- (81) Leung, D.; Abbenante, G.; Fairlie, D. P. Protease Inhibitors: Current Status and Future Prospects. *J. Med. Chem.* **2000**, *43*, 305–341.
- (82) Abbenante, G.; Fairlie, D. P. Protease Inhibitors in the Clinic. *Med. Chem.* **2005**, *1*, 71–104.
- (83) Kim, Y.; Shivanna, V.; Narayanan, S.; Prior, A. M.; Weerasekara, S.; Hua, D. H.; Kankanamalage, A. C. G.; Groutas, W. C.; Chang, K.-O. Broad-Spectrum Inhibitors against 3C-Like Proteases of Feline Coronaviruses and Feline Caliciviruses. *J. Virol.* **2015**, *89*, 4942–4950.
- (84) Galasiti Kankanamalage, A. C.; Kim, Y.; Damalanka, V. C.; Rathnayake, A. D.; Fehr, A. R.; Mehzabeen, N.; Battaile, K. P.; Lovell, S.; Lushington, G. H.; Perlman, S.; Chang, K.-O.; Groutas, W. C. Structure-guided design of potent and permeable inhibitors of MERS coronavirus 3CL protease that utilize a piperidine moiety as a novel design element. *Eur. J. Med. Chem.* **2018**, *150*, 334–346.
- (85) Hanessian, S.; Schaum, R. 1,3-Asymmetric Induction in Enolate Alkylation Reactions of N-Protected 7-Amino Acid Derivatives. *Tetrahedron Lett.* **1997**, *38*, 163–166.
- (86) Hanessian, S.; Margarita, R. 1,3-Asymmetric Induction in Dianionic Allylation – Reactions of Amino Acid Derivatives-Synthesis of Functionally Useful Enantiopure Glutamates, Pipecolates and Pyroglutamates. *Tetrahedron Lett.* **1998**, *39*, 5887–5890.

- (87) Schneckenburger, H. Förster resonance energy transfer—what can we learn and how can we use it? *Methods Appl. Fluoresc.* **2019**, *8*, 013001.
- (88) Blanchard, J. E.; Elowe, N. H.; Huitema, C.; Fortin, P. D.; Cechetto, J. D.; Eltis, L. D.; Brown, E. D. High-Throughput Screening Identifies Inhibitors of the SARS Coronavirus Main Proteinase. *Chem. Biol.* **2004**, *11*, 1445–1453.
- (89) Jin, Z. et al. Structure of M pro from SARS-CoV-2 and discovery of its inhibitors. *Nature* **2020**, *582*, 289–293.
- (90) Ganneau, C.; Moulin, A.; Demange, L.; Martinez, J.; Fehrentz, J.-A. The epimerization of peptide aldehydes—a systematic study. *J. Pept. Sci.* **2006**, *12*, 497–501.
- (91) Boras, B. et al. Discovery of a Novel Inhibitor of Coronavirus 3CL Protease for the Potential Treatment of COVID-19. *bioRxiv* **2021**, Section: New Results Type: article, 2020.09.12.293498.
- (92) Bakkour, Y.; Darcos, V.; Li, S.; Coudane, J. Diffusion ordered spectroscopy (DOSY) as a powerful tool for amphiphilic block copolymer characterization and for critical micelle concentration (CMC) determination. *Polym. Chem.* **2012**, *3*, 2006–2010.
- (93) Costigliola, L.; Heyes, D. M.; Schröder, T. B.; Dyre, J. C. Revisiting the Stokes-Einstein relation without a hydrodynamic diameter. *J. Chem. Phys.* **2019**, *150*, 021101.
- (94) Sikorska, E.; Wyrzykowski, D.; Szutkowski, K.; Greber, K.; Lubecka, E. A.; Zhukov, I. Thermodynamics, size, and dynamics of zwitterionic dodecylphosphocholine and anionic sodium dodecyl sulfate mixed micelles. *J. Therm. Anal. Calorim.* **2016**, *123*, 511–523.
- (95) Mathaes, R.; Koulov, A.; Joerg, S.; Mahler, H.-C. Subcutaneous Injection Volume of Biopharmaceuticals—Pushing the Boundaries. *J. Pharm. Sci.* **2016**, *105*, 2255–2259.
- (96) Fu, L. et al. Both Boceprevir and GC376 efficaciously inhibit SARS-CoV-2 by targeting its main protease. *Nat. Commun.* **2020**, *11*, 4417.

- (97) Arutyunova, E.; Khan, M. B.; Fischer, C.; Lu, J.; Lamer, T.; Vuong, W.; Belkum, M. J. v.; McKay, R. T.; Tyrrell, D. L.; Vederas, J. C.; Young, H. S.; Lemieux, M. J. N-Terminal finger stabilizes the reversible feline drug GC376 in SARS-CoV-2 M<sup>pro</sup>. *bioRxiv* **2021**, 2021.02.16.431021.
- (98) Yang, S. et al. Synthesis, Crystal Structure, Structure-Activity Relationships, and Antiviral Activity of a Potent SARS Coronavirus 3CL Protease Inhibitor. *J. Med. Chem.* **2006**, *49*, 4971–4980.
- (99) Ghosh, A. K.; Xi, K.; Ratia, K.; Santarsiero, B. D.; Fu, W.; Harcourt, B. H.; Rota, P. A.; Baker, S. C.; Johnson, M. E.; Mesecar, A. D. Design and Synthesis of Peptidomimetic Severe Acute Respiratory Syndrome Chymotrypsin-like Protease Inhibitors. *J. Med. Chem.* **2005**, *48*, 6767–6771.
- (100) Zhai, Y.; Zhao, X.; Cui, Z.; Wang, M.; Wang, Y.; Li, L.; Sun, Q.; Yang, X.; Zeng, D.; Liu, Y.; Sun, Y.; Lou, Z.; Shang, L.; Yin, Z. Cyanohydrin as an Anchoring Group for Potent and Selective Inhibitors of Enterovirus 71 3C Protease. *J. Med. Chem.* **2015**, *58*, 9414–9420.
- (101) Shie, J.-J.; Fang, J.-M.; Kuo, T.-H.; Kuo, C.-J.; Liang, P.-H.; Huang, H.-J.; Wu, Y.-T.; Jan, J.-T.; Cheng, Y.-S. E.; Wong, C.-H. Inhibition of the severe acute respiratory syndrome 3CL protease by peptidomimetic  $\alpha,\beta$ -unsaturated esters. *Bioorg. Med. Chem.* **2005**, *13*, 5240–5252.
- (102) Sutherland, A.; Vederas, J. C. The first isolation of an alkoxy-N,N-dialkylaminodifluorosulfane from the reaction of an alcohol and DAST: an efficient synthesis of (2S,3R,6S)-3-fluoro-2,6-diaminopimelic acid. *Chem. Commun.* **1999**, 1739–1740.
- (103) Zhang, Z.; Tang, W. Drug metabolism in drug discovery and development. *Acta Pharm. Sin. B* **2018**, *8*, 721–732.

- (104) Zhao, M.; Ma, J.; Li, M.; Zhang, Y.; Jiang, B.; Zhao, X.; Huai, C.; Shen, L.; Zhang, N.; He, L.; Qin, S. Cytochrome P450 Enzymes and Drug Metabolism in Humans. *Int. J. Mol. Sci.* **2021**, *22*, 12808.
- (105) Gonzalez, F. J.; Gelboin, H. V. Human cytochromes P450: evolution and cDNA-directed expression. *Environ. Health Perspect.* **1992**, *98*, 81–85.
- (106) Danielson, P. B. The Cytochrome P450 Superfamily: Biochemistry, Evolution and Drug Metabolism in Humans. *Curr. Drug Metab.* **2002**, *3*, 561–597.
- (107) Shah, P.; Westwell, A. D. The role of fluorine in medicinal chemistry. *J. Enzyme Inhib. Med. Chem.* **2007**, *22*, 527–540.
- (108) Srinivasan, B. A guide to the Michaelis–Menten equation: steady state and beyond. *FEBS J.* **2021**, *n/a*, DOI: 10.1111/febs.16124.
- (109) Tredwell, M.; Gouverneur, V. In *Comprehensive Chirality*, Carreira, E. M., Yamamoto, H., Eds.; Elsevier: Amsterdam, 2012, pp 70–85.
- (110) Zhao, L.; Wang, Z.; Zhang, H.; Li, W.; Yue, Q.; Jin, Y. Design, Preparation of 3-Hydroxy Isoindolinone Cyclotriptides, and the In Vitro Antitumor Activities Against Cervical Carcinoma HeLa Cells. *J. Heterocycl. Chem.* **2018**, *55*, 1205–1218.
- (111) Zhao, L.; Zhang, H.; Tan, G.; Wang, Z.; Jin, Y. Photo-induced synthesis and in vitro biological activity of a Sansalvamide A analog. *Tetrahedron Lett.* **2017**, *58*, 1669–1672.
- (112) Hassner, A.; Patchornik, G.; Pradhan, T. K.; Kumareswaran, R. Intermolecular Electrophilic O-Amination of Alcohols. *J. Org. Chem.* **2007**, *72*, 658–661.
- (113) Quan, N.; Shi, X.-X.; Nie, L.-D.; Dong, J.; Zhu, R.-H. A Green Chemistry Method for the Regeneration of Carbonyl Compounds from Oximes by Using Cupric Chloride Dihydrate as a Recoverable Promoter for Hydrolysis. *Synlett* **2011**, *2011*, 1028–1032.

- (114) Legault, C.; Charette, A. B. Highly Efficient Synthesis of O-(2,4-Dinitrophenyl)hydroxylamine. Application to the Synthesis of Substituted N-Benzoyliminopyridinium Ylides. *J. Org. Chem.* **2003**, *68*, 7119–7122.
- (115) Möller, D.; Kling, R. C.; Skultety, M.; Leuner, K.; Hübner, H.; Gmeiner, P. Functionally Selective Dopamine D2, D3 Receptor Partial Agonists. *J. Med. Chem.* **2014**, *57*, 4861–4875.
- (116) Laus, G.; Kahlenberg, V.; Wurst, K.; Müller, T.; Kopacka, H.; Schottenberger, H. Synthesis and Crystal Structures of New 1,3-Disubstituted Imidazoline-2-thiones. *Z. Naturforsch. B* **2013**, *68*, 1239–1252.
- (117) Angelini, L.; Sanz, L. M.; Leonori, D. Divergent Nickel-Catalysed Ring-Opening–Functionalisation of Cyclobutanone Oximes with Organozincs. *Synlett* **2020**, *31*, 37–40.
- (118) Yamawaki, K.; Nomura, T.; Yasukata, T.; Uotani, K.; Miwa, H.; Takeda, K.; Nishitani, Y. A novel series of parenteral cephalosporins exhibiting potent activities against *Pseudomonas aeruginosa* and other Gram-negative pathogens: Synthesis and structure–activity relationships. *Bioorg. Med. Chem.* **2007**, *15*, 6716–6732.
- (119) Li, J. W.-H.; Vederas, J. C. Drug Discovery and Natural Products: End of an Era or an Endless Frontier? *Science* **2009**, *325*, 161–165.
- (120) Hertweck, C. The Biosynthetic Logic of Polyketide Diversity. *Angew. Chem. Int. Ed.* **2009**, *48*, 4688–4716.
- (121) Weissman, K. J.; Leadlay, P. F. Combinatorial biosynthesis of reduced polyketides. *Nat. Rev. Microbiol.* **2005**, *3*, 925–936.
- (122) Zhu, G.; LaGier, M. J.; Stejskal, F.; Millership, J. J.; Cai, X.; Keithly, J. S. *Cryptosporidium parvum*: the first protist known to encode a putative polyketide synthase. *Gene* **2002**, *298*, 79–89.

- (123) Chen, M.; Liu, Q.; Gao, S.-S.; Young, A. E.; Jacobsen, S. E.; Tang, Y. Genome mining and biosynthesis of a polyketide from a biofertilizer fungus that can facilitate reductive iron assimilation in plant. *Proc. Natl. Acad. Sci. U. S. A.* **2019**, *116*, 5499–5504.
- (124) Wang, W.-G.; Du, L.-Q.; Sheng, S.-L.; Li, A.; Li, Y.-P.; Cheng, G.-G.; Li, G.-P.; Sun, G.; Hu, Q.-F.; Matsuda, Y. Genome mining for fungal polyketide-diterpenoid hybrids: discovery of key terpene cyclases and multifunctional P450s for structural diversification. *Org. Chem. Front.* **2019**, *6*, 571–578.
- (125) Hoepfner, D. et al. Selective and Specific Inhibition of the Plasmodium falciparum Lysyl-tRNA Synthetase by the Fungal Secondary Metabolite Cladosporin. *Cell Host Microbe* **2012**, *11*, 654–663.
- (126) Sims, J. W.; Fillmore, J. P.; Warner, D. D.; Schmidt, E. W. Equisetin biosynthesis in *Fusarium heterosporum*. *Chem. Commun.* **2005**, 186–188.
- (127) Moore, R. N.; Bigam, G.; Chan, J. K.; Hogg, A. M.; Nakashima, T. T.; Vederas, J. C. Biosynthesis of the hypocholesterolemic agent mevinolin by *Aspergillus terreus*. Determination of the origin of carbon, hydrogen, and oxygen atoms by carbon-13 NMR and mass spectrometry. *J. Am. Chem. Soc.* **1985**, *107*, 3694–3701.
- (128) Kennedy, J.; Auclair, K.; Kendrew, S. G.; Park, C.; Vederas, J. C.; Hutchinson, C. R. Modulation of Polyketide Synthase Activity by Accessory Proteins During Lovastatin Biosynthesis. *Science* **1999**, *284*, 1368–1372.
- (129) Ma, S. M.; Li, J. W.-H.; Choi, J. W.; Zhou, H.; Lee, K. K. M.; Moorthie, V. A.; Xie, X.; Kealey, J. T.; Da Silva, N. A.; Vederas, J. C.; Tang, Y. Complete Reconstitution of a Highly Reducing Iterative Polyketide Synthase. *Science* **2009**, *326*, 589–592.
- (130) Cox, R. J. Polyketides, proteins and genes in fungi: programmed nano-machines begin to reveal their secrets. *Org. Biomol. Chem.* **2007**, *5*, 2010–2026.

- (131) Kao, C. M.; Luo, G.; Katz, L.; Cane, D. E.; Khosla, C. Manipulation of macrolide ring size by directed mutagenesis of a modular polyketide synthase. *J. Am. Chem. Soc.* **1995**, *117*, 9105–9106.
- (132) Rawlings, B. J. Type I polyketide biosynthesis in bacteria (Part B). *Nat. Prod. Rep.* **2001**, *18*, 231–281.
- (133) Hutchinson, C. R.; Fujii, I. Polyketide synthase gene manipulation: a structure-function approach in engineering novel antibiotics. *Annu. Rev. Microbiol.* **1995**, *49*, 201–238.
- (134) Austin, M. B.; Noel, J. P. The chalcone synthase superfamily of type III polyketide synthases. *Nat. Prod. Rep.* **2003**, *20*, 79–110.
- (135) Zhang, W.; Li, Y.; Tang, Y. Engineered biosynthesis of bacterial aromatic polyketides in *Escherichia coli*. *Proc. Natl. Acad. Sci. U. S. A.* **2008**, *105*, 20683–20688.
- (136) Baerson, S. R.; Rimando, A. M. In *Polyketides*; ACS Symposium Series 955, Vol. 955, Section: 1; American Chemical Society: 2007, pp 2–14.
- (137) Schröder, J. Probing plant polyketide biosynthesis. *Nat. Struct. Biol.* **1999**, *6*, 714–716.
- (138) Funai, N.; Ohnishi, Y.; Fujii, I.; Shibuya, M.; Ebizuka, Y.; Horinouchi, S. A new pathway for polyketide synthesis in microorganisms. *Nature* **1999**, *400*, 897–899.
- (139) Cacho, R. A.; Thuss, J.; Xu, W.; Sanichar, R.; Gao, Z.; Nguyen, A.; Vederas, J. C.; Tang, Y. Understanding Programming of Fungal Iterative Polyketide Synthases: The Biochemical Basis for Regioselectivity by the Methyltransferase Domain in the Lovastatin Megasyntase. *J. Am. Chem. Soc.* **2015**, *137*, 15688–15691.
- (140) Zhou, H.; Gao, Z.; Qiao, K.; Wang, J.; Vederas, J. C.; Tang, Y. A fungal ketoreductase domain that displays substrate-dependent stereospecificity. *Nat. Chem. Biol.* **2012**, *8*, 331–333.

- (141) Vuong, W.; Mosquera-Guagua, F.; Sanichar, R.; McDonald, T. R.; Ernst, O. P.; Wang, L.; Vederas, J. C. Synthesis of Chiral Spin-Labeled Amino Acids. *Org. Lett.* **2019**, *21*, 10149–10153.
- (142) Vuong, W. et al. Improved SARS-CoV-2 M<sup>Pro</sup> inhibitors based on feline antiviral drug GC376: structural enhancements, increased solubility, and micellar studies. *Eur. J. Med. Chem.* **2021**, 113584.
- (143) Raiford, D. S.; Fisk, C. L.; Becker, E. D. Calibration of methanol and ethylene glycol nuclear magnetic resonance thermometers. *Anal. Chem.* **1979**, *51*, 2050–2051.
- (144) Wishart, D. S.; Bigam, C. G.; Yao, J.; Abildgaard, F.; Dyson, H. J.; Oldfield, E.; Markley, J. L.; Sykes, B. D. <sup>1</sup>H, <sup>13</sup>C and <sup>15</sup>N chemical shift referencing in biomolecular NMR. *J. Biomol. NMR* **1995**, *6*, 135–140.
- (145) Hoult, D. I. Solvent peak saturation with single phase and quadrature fourier transformation. *J. Magn. Reson. (1969-1992)* **1976**, *21*, 337–347.
- (146) Campbell, I.; Dobson, C.; Jeminet, G.; Williams, R. Pulsed NMR methods for the observation and assignment of exchangeable hydrogens: Application to bacitracin. *FEBS Lett.* **1974**, *49*, 115–119.
- (147) Mao, X.-a.; Chen, J.-h. Radiation damping effects in solvent preirradiation experiments in NMR. *Chem. Phys.* **1996**, *202*, 357–366.
- (148) Wu, P. S. C.; Otting, G. Rapid pulse length determination in high-resolution NMR. *J. Magn. Reson.* **2005**, *176*, 115–119.
- (149) Bodenhausen, G.; Ruben, D. J. Natural abundance nitrogen-15 NMR by enhanced heteronuclear spectroscopy. *Chem. Phys. Lett.* **1980**, *69*, 185–189.
- (150) Kong, X. M.; Sze, K. H.; Zhu, G. Gradient and sensitivity enhanced multiple-quantum coherence in heteronuclear multidimensional NMR experiments. *J. Biomol. NMR* **1999**, *14*, 133–140.



- (151) Stonehouse, J.; Shaw, G. L.; Keeler, J.; Laue, E. D. Minimizing Sensitivity Losses in Gradient-Selected  $^{15}\text{N}$ - $^1\text{H}$  HSQC Spectra of Proteins. *J. Magn. Reson., Ser. A* **1994**, *107*, 178–184.
- (152) Markley, J. L.; Bax, A.; Arata, Y.; Hilbers, C. W.; Kaptein, R.; Sykes, B. D.; Wright, P. E.; Wüthrich, K. Recommendations for the presentation of NMR structures of proteins and nucleic acids – IUPAC-IUBMB-IUPAB Inter-Union Task Group on the Standardization of Data Bases of Protein and Nucleic Acid Structures Determined by NMR Spectroscopy. *J. Biomol. NMR* **1998**, *12*, 1–23.
- (153) Pelta, M. D.; Morris, G. A.; Stchedroff, M. J.; Hammond, S. J. A one-shot sequence for high-resolution diffusion-ordered spectroscopy. *Magn. Reson. Chem.* **2002**, *40*, S147–S152.
- (154) Botana, A.; Aguilar, J. A.; Nilsson, M.; Morris, G. A. J-modulation effects in DOSY experiments and their suppression: the Oneshot45 experiment. *J. Magn. Reson.* **2011**, *208*, 270–278.
- (155) Belokon', Y. N.; Tararov, V. I.; Maleev, V. I.; Savel'eva, T. F.; Ryzhov, M. G. Improved procedures for the synthesis of (S)-2-[N-(N'-benzylpropyl)amino]benzophenone (BPB) and Ni(II) complexes of Schiff's bases derived from BPB and amino acids. *Tetrahedron: Asymmetry* **1998**, *9*, 4249–4252.
- (156) Haugland, M. M.; El-Sagheer, A. H.; Porter, R. J.; Peña, J.; Brown, T.; Anderson, E. A.; Lovett, J. E. 2'-Alkynynucleotides: A Sequence- and Spin Label-Flexible Strategy for EPR Spectroscopy in DNA. *J. Am. Chem. Soc.* **2016**, *138*, 9069–9072.
- (157) Aggarwal, V. K.; Gültekin, Z.; Grainger, R. S.; Adams, H.; Spargo, P. L. (1R,3R)-2-Methylene-1,3-dithiolane 1,3-dioxide: a highly reactive and highly selective chiral ketene equivalent in cycloaddition reactions with a broad range of dienes. *J. Chem. Soc., Perkin Trans. 1* **1998**, 2771–2782.

- (158) Hubbs, J. L.; Heathcock, C. H. A Second-Generation Synthesis of the C1-C28 Portion of the Althohyrins (Spongistatins). *J. Am. Chem. Soc.* **2003**, *125*, 12836–12843.
- (159) Pfefferkorn, J. A. et al. Discovery of novel hepatoselective HMG-CoA reductase inhibitors for treating hypercholesterolemia: A bench-to-bedside case study on tissue selective drug distribution. *Bioorg. Med. Chem. Lett.* **2011**, *21*, 2725–2731.
- (160) Kokotos, G.; Padrón, J. M.; Martín, T.; Gibbons, W. A.; Martín, V. S. A General Approach to the Asymmetric Synthesis of Unsaturated Lipidic  $\alpha$ -Amino Acids. The First Synthesis of  $\alpha$ -Aminoarachidonic Acid. *J. Org. Chem.* **1998**, *63*, 3741–3744.
- (161) Yu, W.; Mei, Y.; Kang, Y.; Hua, Z.; Jin, Z. Improved Procedure for the Oxidative Cleavage of Olefins by OsO<sub>4</sub>-NaIO<sub>4</sub>. *Org. Lett.* **2004**, *6*, 3217–3219.
- (162) Zhao, H.; Hu, X.-G.; Xu, M.-J.; Cai, Q.-X.; Liu, Y.-J.; Su, D.-M.; Chen, S.-J.; Wang, K.; Gong, Z.-N. Six-step synthesis of Leonurine and toxicity study on zebrafish. *Chin. Chem. Lett.* **2017**, *28*, 1172–1175.
- (163) Atkinson, S. J.; Demont, E. H.; Harrison, L. A.; Hayhow, T. G. C.; House, D.; Lindon, M. J.; Preston, A. G.; Seal, J. T.; Wall, I. D.; Watson, R. J.; Woolven, J. M. Pyridinone Dicarboxamide for Use as Bromodomain Inhibitors, WO2017050714 (A1), 2017.
- (164) Numajiri, Y.; Jiménez-Osés, G.; Wang, B.; Houk, K. N.; Stoltz, B. M. Enantioselective Synthesis of Dialkylated N-Heterocycles by Palladium-Catalyzed Allylic Alkylation. *Org. Lett.* **2015**, *17*, Publisher: American Chemical Society, 1082–1085.
- (165) Paal, C.; Poller, H. Ueber die Einwirkung des o- Nitrobenzylchlorids auf Hydroxylamin. *Ber. Dtsch. Chem. Ges.* **1897**, *30*, 58–60.
- (166) Yang, S.-C.; Wang, H.-M.; Chen, L.-C. A Mild and Efficient Method for Selective Acetylation of Amines. *J. Chin. Chem. Soc.* **1995**, *42*, 585–587.